Integration of Electricity, Natural Gas and Heat Systems With Market-based Coordination.

Schwele, Anna

Publication date:
2020

Document Version
Publisher's PDF, also known as Version of record

Technical University of Denmark

Anna Schwele

Integration of Electricity, Natural Gas and Heat Systems With Market-based Coordination

Ph.D. Thesis, September 2020

Kgs. Lyngby, Denmark

Center for Electric Power and Energy
Department of Electrical Engineering

DANMARKS TEKNISKE UNIVERSITET
Center for Electric Power and Energy (CEE)
DTU Electrical Engineering

Integration of Electricity, Natural Gas and Heat Systems With Market-based Coordination

Ph.D. Thesis, by Anna Schwele

Supervisors:
Associate Professor Jalal Kazempour, Technical University of Denmark
Professor Pierre Pinson, Technical University of Denmark

DTU - Technical University of Denmark, Kgs. Lyngby - September 2020

Integration of Electricity, Natural Gas and Heat Systems With Market-based Coordination

This thesis was prepared by:
Anna Schwele

Supervisors:
Associate Professor Jalal Kazempour, Technical University of Denmark
Professor Pierre Pinson, Technical University of Denmark

Dissertation Examination Committee:
Associate Professor Qiuwei Wu
Department of Electrical Engineering, Technical University of Denmark, Denmark

Associate Professor Trine Krogh Boomsma
Department of Mathematical Sciences, University of Copenhagen, Denmark

Professor Ramteen Sioshansi
Department of Integrated Systems Engineering, The Ohio State University, USA

Center for Electric Power and Energy (CEE)
DTU Electrical Engineering
Elektrovej, Building 325
DK-2800 Kgs. Lyngby
Denmark

Tel: (+45) 4525 3500
Fax: (+45) 4588 6111
E-mail: cee@elektro.dtu.dk

Release date: September 2020

Edition: 1.0

Class: Internal

Field: Electrical Engineering

Remarks: The dissertation is presented to the Department of Electrical Engineering of the Technical University of Denmark in partial fulfillment of the requirements for the degree of Doctor of Philosophy.

ISBN: 000-00-00000-00-0

Preface

This thesis is prepared at the Center for Electric Power and Energy (CEE) within the Department of Electrical Engineering of the Technical University of Denmark in partial fulfillment of the requirements for acquiring the degree of Doctor of Philosophy in Engineering.

The Ph.D. studies were funded by the Danish EUD Programme through the 'Coordinated Operation of Integrated Energy Systems (CORE)' project under the grant 64017-0005. This dissertation summarizes the work carried out by the author during her Ph.D. project, which started on 1st September 2017 and was completed on 31st August 2020.

The thesis consists of a summary of the four attached scientific papers, of which three have been peer-reviewed and published, and the remaining one is currently under review. While the research details are left to the specific publications in appendix, the main body of the thesis is conceived as a guide on how these scientific papers can be contextualized in the bigger picture of coordination of integrated energy systems.

Anna Schwele
September 2020

Acknowledgements

The journey of pursuing a PhD was challenging and I would not have been able to complete this project without the guidance and encouragement of numerous people, all of whom I would like to sincerely thank.

First and foremost, I wish to thank my PhD supervisors Assoc. Prof. Jalal Kazempour and Prof. Pierre Pinson for giving me the opportunity to work under their guidance. They have provided me with great support and encouragement throughout my PhD studies. I appreciate the time they have devoted to advising me, their valuable insights and enthusiasm for research that they shared with me.

I am also thankful to my advisor Assoc. Prof. Eilyan Bitar for hosting me during my external stay at Cornell University and for embracing me into his research group. Moreover, I would like to thank Prof. Kameshwar Poolla and his team for hosting me at UC Berkeley.

Next, I would like to thank all current and former colleagues and friends at the ELMA group for creating a friendly and supportive working environment. In particular, I would like to thank Christos and Anubhav for the fruitful collaborations and Fabio, Lesia, Anubhav, Andrea, and Liyang for their valuable feedback on this manuscript.

Last but not least, I would like to thank my family for their understanding and support, especially my parents for their encouragement.

Anna

Kgs. Lyngby, Denmark, 2020

Table of Contents

List of Figures

List of Tables

Abstract

Higher shares of uncertain and variable renewable energy sources challenge the way energy systems are currently operated and increase the need for system-wide flexibility. Energy infrastructures are becoming more interdependent with growing physical, operational and economic interactions across multiple energy sectors. Increased couplings among power, natural gas and heat systems provide untapped sources of cross-carrier synergies, while uncertainty and variability of renewables will eventually affect the operation of all systems. In order to facilitate the transition towards a renewable-based energy system, revealing and exploiting potential flexibility from energy system integration is key.

In this context, the objective of this thesis is to improve coordination of power, heat and natural gas systems with a particular attention to "market-based" coordination schemes by defining new market products and mechanisms. Enhanced coordination aims at unveiling potential synergies and harvesting flexible assets in a way that benefits the overall energy system. This work aims to quantify potential flexibility from multi-energy coordination and investigates how markets can facilitate the utilization of available synergies. The new concepts introduced in this thesis span different degrees of coordination for power, natural gas and heat systems and awareness of the uncertainty introduced by renewable energy sources such as wind power production.

Full coordination schemes, which assume that energy systems are operated centrally, help to reveal and quantify the amount of available operational flexibility. Comprehensive models with accurate representation of energy flow dynamics and flexible assets, which link energy sectors together, are proposed to unlock the potential of energy storage from gas and heat grids to cope with uncertainty and variability. The propagation of uncertainty between sectors is studied and tools that reveal and harvest existing synergies are developed to mitigate this uncertainty. Policy-based reserves are introduced as new products for the coordinated response of flexible assets interfacing multiple sectors to uncertainty. Full coordination highlights the importance of proper modeling of complex multi-carrier flexibility in short-term operations, but is incompatible with current market designs.

Soft coordination approaches, which respect the sequential order of energy markets, provide independent, yet coordinated frameworks for energy systems in view of uncertainty. Market-based mechanisms, that create soft links via increased information exchange and financial interactions, are proposed to support coordination in interdependent electricity and natural gas systems. These market-based mechanisms focus on increasing awareness among sectors and trading floors such that each sector dispatches flexible assets in a way that benefits the overall energy system. Specifically, financial instruments in the form of virtual bidders are introduced to improve the coordination between separate and sequential electricity and natural gas markets under uncertainty without the need for major updates of current market setups and rules.

Finally, this thesis motivates more coordination of power, natural gas and heat systems and outlines future challenges from technical, computational and economic perspectives.

Resumé

En højere andel af usikkerhed og variation i vedvarende energikilder skaber udfordringer i driften af de nuværende energiinfrastrukturer og øger behovet for fleksibilitet over hele netværket. De forskellige energiinfrastrukturer bliver i en øget grad mere sammenknyttet hvor der er en stigning i både fysiske, driftsmæssige og økonomiske forbindelser. Øgede koblinger mellem strøm, naturgas og fjernvarme giver uudnyttede kilder til tværsbærer synergier, mens usikkerheden og variationen i vedvarende energikilder vil påvirke driften af alle energisystemer. Til at facilitere overgangen imod en energiinfrastruktur bygget på vedvarende energikilder, bliver det vigtigt at udnytte den mulige fleksibilitet ved integration af de forskellige energisystemer.

I denne sammenhæng er formålet med denne afhandling at forbedre koordinering af strøm, naturgas og fjernvarme med særlig fokus på "markedsbaseret" koordineringsordninger ved at definere nye markedsprodukter og mekanismer. Forbedret koordinering sigter mod at identificere potentielle synergier og udnytte fleksible aktiver på en måde, der gavner den samlede energiinfrastruktur. Dette arbejde sigter mod at kvantificere potentiel fleksibilitet fra koordinering af flere energisystemer og undersøger, hvordan markeder kan lette anvendelsen af tilgængelige synergier. De nye koncepter, der introduceres i denne afhandling, spænder over forskellige grader af koordination for strøm-, naturgas- og varmesystemer og påpeger den usikkerhed, der er introduceret af vedvarende energikilder såsom vindenergi.

Fulde koordineringsordninger, der antager, at energisystemer drives centralt, hjælper med at afsløre og kvantificere mængden af tilgængelig operationel fleksibilitet. Omfattende modeller med præcis repræsentation af energistrømningsdynamik og fleksible aktiver, der forbinder energisektorer sammen, foreslås for at skabe et potentiale for energilagring i gas- og varmesystemer for at klare usikkerhed og variation. Udbredelsen af usikkerhed mellem sektorer undersøges, og værktøjer, der afslører og høster eksisterende synergier, udvikles for at mindske denne usikkerhed. Politiskbaserede reserver introduceres som nye produkter til den koordinerede reaktion på fleksible aktiver, der forbinder flere sektorer til usikkerhed. Fuld koordinering understreger vigtigheden af korrekt modellering af kompleks flerudbyder energiinfrastruktur fleksibilitet i kortvarig drift, men er uforenelig med nuværende markedsdesign.

Blød koordinationsmetoder, som respekterer den sekventielle rækkefølge af energimarkeder, giver uafhængige, men alligevel koordinerede rammer for energisystemer i lyset af usikkerhed. Markedsbaserede mekanismer, der skaber bløde forbindelser via øget informationsudveksling og finansielle interaktioner, foreslås for at understøtte koordinering i indbyrdes afhængige elektricitets- og naturgassystemer. Disse markedsbaserede mekanismer fokuserer på at øge bevidstheden blandt sektorer og handel, således at hver sektor benytter fleksible aktiver på en måde, der gavner det samlede energisystem. Specifikt introduceres finansielle instrumenter i form af virtuelle byder, for at forbedre koordineringen mellem separate og sekventielle elektricitets- og naturgasmarkeder under usikkerhed uden behov for større opdateringer af de nuværende markedsopsætninger og regler.

Endelig motiverer denne afhandling yderligere koordinering af strøm-, naturgas- og varmesystemer og beskriver fremtidige udfordringer ud fra tekniske, beregningsmæssige og økonomiske perspektiver.

CHAPTER 1

Introduction

1.1 Energy sector coordination as a multidisciplinary challenge

Increasing penetration of variable and intermittent renewables is pushing energy infrastructures to become more interdependent. Physical, operational and economic interactions exist not only across geographically interconnected energy systems [4], but also across multiple energy carriers [5–8]. However, in the current energy system perspective, each energy sector operates separately and as if independent from other sectors. Growing interactions among energy sectors, on the one hand, challenge this operational paradigm, on the other hand, they provide opportunities for *cross-carrier synergies*.

Exploiting potential synergies among energy systems is a key solution to achieve flexibility and security of supply in a modern and sustainable energy system. Classic flexibility options, e.g., flexible dispatchable thermal plants, storage, and expanding transmission grids, require significant investments. A broader view of the overall energy system encouraging interactions among multiple energy carriers is able to achieve additional flexibility to further accommodate the variability and uncertainty of demand and supply balance in a cost-effective manner.

Increased coupling and synergies can be identified across multiple sectors and infrastructures, e.g., power, heat, cooling, gas, hydrogen, transportation, and water. Energy system integration is most valuable at the interfaces where the coupling and interactions between energy vectors are strong. In particular, the coupling among the three main energy grid infrastructures, i.e., electricity, district heating and natural gas, is increasing with higher shares of renewable energy penetrations. Several units operate at the interfaces of the three systems, e.g., gas-fired generators, power-to-gas (P2G) and power-to-heat (P2H) units, and combined heat and power (CHP) plants, intensifying the technical and economic interactions among sectors. As flexible technologies these units typically provide electricity generation- and demand-side flexibility. Furthermore, heat and gas grids can deliver network energy storage capacities for balancing the generation from renewables. Thus, integrating the electricity, heat and gas networks and leveraging this energy storage can unlock flexibility using the existing infrastructure when their interdependencies are properly accounted for.

Planning and operations of integrated energy systems are demanding tasks from modeling, optimization, and computational perspectives. Hybrid models accounting for the power system as well as the gas and heat systems require detailed modeling in order to optimize energy systems across multiple domains and scales. The dimension and complexity of decision-making problems for multi-energy systems are challenging. Uncertainty arising from increasing penetration of intermittent and variable renewables adds to this challenge requiring more advanced optimization techniques [9, 10]. In such a complex interconnected system with uncertainties, decision-makers including system operators, suppliers and load entities require advanced mathematical tools to be able to make informed decisions. Game-theoretic models are needed to develop and analyse

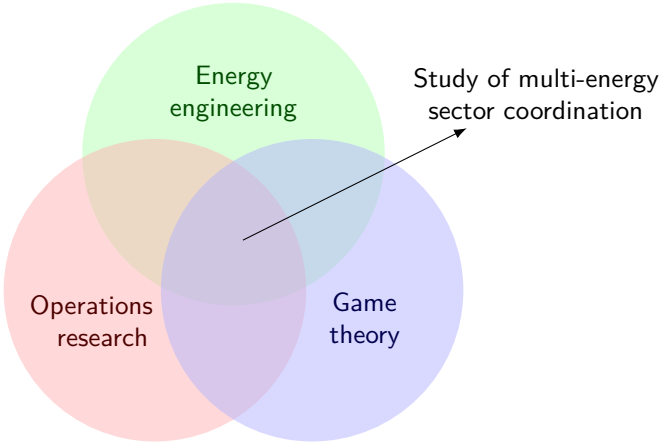

Figure 1.1: Multidisciplinary nature of energy sector coordination problem

coupling behaviours and coordination mechanisms in a more complex environment with several stakeholders, each with their distinct objectives, incentives, and information. Holistic approaches to design and operate such an integrated energy system in a cost efficient and secure way are needed. This multi-energy coordination problem poses *technical*, *operational* and *economic* challenges, that can be addressed by combining tools from operations research and game theory. Thus, building upon tools not only from energy engineering [11], but also using operations research [12] and game-theoretic concepts [13, 14], energy sector coordination becomes a *multi-disciplinary* challenge, see Figure 1.1.

In particular, this thesis studies the coordination problem arising in multi-energy systems. In this regard, different levels of coordination for integrated energy systems are proposed with a focus on power, gas and heat infrastructures. The main focus of this work is to connect optimization frameworks in the context of multi-energy systems with efficient solution methods while accounting for uncertainty, regulatory frameworks, and interactions of agents. For this purpose, optimization models that allow efficient modeling for complex interconnected systems are proposed and equilibrium models are used as market simulation tools. The integrated operation strategies and market frameworks developed in this thesis shall help to maximize social welfare and performance for better cost efficiency and reliability of the whole energy system.

1.2 From ideal to practical coordination schemes

1.2.1 How can the coordination of multi-energy systems be improved?

High shares of power production from renewable sources like wind and solar units increase the need for operational flexibility to cope with variability and uncertainty. Flexibility describes the concept that supply and demand have to be balanced by providing the capability of a system to modify its output or state in response to a change in net load, i.e., total demand minus renewable generation [15]. Flexible units that provide generation- or demand-side adaptability like gas-fired generators, CHP units, and heat pumps often operate at the interface of several energy systems. Recent studies aim at dispatching these units in a smarter way highlighting both the potential advantages and the current lack of coordination [16–22]. Additionally, the natural gas and heating networks can provide flexibility through stored energy in the pipelines, the so-called linepack

[17, 23] and delayed heat propagation [24, 25]. The idea of multi-energy hubs was proposed for the first time in [26] as poly-fuel systems with multiple inputs and multiple outputs. Unlocking these existing sources of flexibility propagates demand fluctuations and uncertainty from the electricity side into the gas and heat systems and markets. This can already be seen in the trend towards increasing volumes in gas trading in short-term spot markets like Gaspoint Nordic [27] and wind curtailment due to naive dispatch of CHPs [28]. In most countries, energy markets are cleared separately and sequentially [29] and dispatch decisions are made unaware of influences to and from other sectors. However, the increasing coupling of energy systems on the physical layer requires stronger coordination among market layers as well. How each system is operated and how markets are cleared need an update. *Full coordination* of integrated energy systems ranges from allowing interactions with other sectors to be adequately reflected in the scheduling process of each sector, to strengthening the flow of shared information, and to matching the timing of decisions and market clearings. However, full coordination cannot directly be applied to current market structures and operational setups, since independent system operators are in charge of individual energy sectors with limited information exchange, privacy requirements, potentially competing objectives, and asynchronous timing of market clearing. In contrast, *soft coordination* describes any mechanism or process that increases the efficiency of the overall system, adhering to the current setup and regulations. These *non-disruptive* coordination mechanisms can be of financial, operational or communicative nature.

In order to evolve from current separate and oblivious sectors to integrated energy systems, different levels of coordination need to be evaluated focusing on quantification of flexibility, the impact of uncertainty and compatibility with regulatory frameworks. Important issues to be addressed are how to quantify the potential flexibility from multi-energy coordination and how market designs, policies, and regulations affect or facilitate exploiting potential synergies and flexibility options. To this extent, different levels of coordination and the impact of uncertainty shall be investigated on operations and dispatch decisions as well as market design options for the multi-energy system.

1.2.2 Research questions

The objective to improve coordination in multi-energy systems leads to the following two main research questions which touch upon different levels of coordination and adherence to current regulations.

I) How much value can be derived through coordination of integrated energy systems?

Potential synergies and available flexibility arising from multi-energy coordination need to be properly defined and quantified. The monetary value can be deduced in terms of reduced total system cost under perfect coordination compared to the (current) uncoordinated setup. Furthermore, economic dispatch and scheduling tools need to be updated with more detailed information about gas and heat grids, energy flows and interactions among the systems to incorporate all potential flexibility for valuation. The physics of the multi-energy system and uncertainty from renewable generation are identified as key challenges for determining the value of coordination that can be unlocked. Based on the case of full coordination assuming energy carriers are operated centrally, synergies and operational flexibility shall be investigated, specifically: (i) how much flexibility can be derived and (ii) how can these synergies be revealed and harvested when accounting for uncertainty. Full coordination results in optimizing electricity, gas, and heat

networks as one comprehensive *co-optimization* problem. This requires advanced optimization models for detailed and accurate representation of complex energy systems, their dynamics and interactions [23, 30, 31]. The flexibility derived from accurate representation of energy flow dynamics can help mitigate variability inherent in renewable energies. As uncertainty from renewables propagates among the energy systems, the stochastic nature of renewable energy sources needs to be considered by means of probabilistic methods [32]. Concepts from energy engineering and physics as well as operations research tools are necessary to determine the value of multi-energy coordination. Through comparison of the ideal benchmark, i.e., the perfect case of full coordination, with other implemented setups the value of coordination can be quantified while accounting for energy flows, network flexibility and uncertainty.

However, this ideal benchmark of fully coordinated energy systems with a single central system coordinator or perfect information exchange and timing among systems is not implementable in current practice, which motivates the second conceptual question.

II) How can the value of multi-energy coordination be harvested while respecting the current regulatory framework?

While full coordination in an integrated energy system can be viewed as the ideal benchmark of a perfectly cooperative game [33], game-theoretic considerations are required to move towards more realistic and implementable mechanisms that adhere to the current regulation and organisation of energy markets. As opposed to the disruptive re-design of a fully coordinated integrated energy system, soft, market-based coordination mechanisms can be realized by increasing awareness among the sectors [18, 34–37] and by introducing new market products [38–40], new bidding formats [41–44] or new market players. These market mechanisms act as coordinator at the interface of different sectors and can enable flexibility provision from multi-carrier resources. Creating and analysing coordination mechanisms require proper understanding of the different agents involved, along with their motivations and incentives, operational constraints, the information each agent has access to, and the sequence of decision-making. For this purpose, optimization and equilibrium models need to be developed to support decision-making of various agents in the energy market environment. Complementarity models and variational inequalities [45–47] are used for in-depth analysis of energy markets with the concept of Nash equilibria as solutions of non-cooperative games involving multiple decision-makers [48]. These non-cooperative games in which each player solves a separate but related optimization problem can be more effective towards compatibility and real-life implementation. Furthermore, the impacts of soft coordination mechanisms on energy sector integration need to be evaluated in terms of harnessed flexibility, market efficiency, and social welfare.

1.3 Contributions

This thesis answers the two main research questions in Section 1.2.2 by developing tools applying concepts from the fields of energy system engineering, operations research and game theory. The main contribution of this thesis is improving the coordination of multi-energy systems through updated operational strategies and market design. For that purpose, this thesis develops new notions and methods for better coordination of multi-energy systems and concludes with several policy recommendations.

1.3.1 Conceptual contributions

The scientific contributions of this thesis span the aspects of different levels of coordination for heat, natural gas and electricity systems. The new concepts introduced in this thesis range from full to soft coordination. The proposed full coordination approaches focus on unlocking energy storage from gas and heat grids to cope with variability and responding to uncertainty from the power side. For this purpose, [**Paper A**] and [**Paper B**] account for energy flow dynamics and storage effects of multi-energy networks, quantifying the value of the revealed network flexibility. While [**Paper A**] is the first work that comprises all three energy systems accounting for heat and gas grid dynamics, [**Paper B**] focuses on the added power system flexibility from natural gas networks when accounting for both linepack and bidirectional gas flow. [**Paper C**] extends the valuation of the natural gas network as a provider of short-term flexibility to power systems under uncertainty. Specifically, [**Paper C**] investigates how affine policies can bring linepack flexibility from the gas network to the day-ahead power scheduling stage. This work for the first time in the literature extends response actions based on linear decision rules from the power side to include gas sector flexibility mitigating renewable forecast uncertainty. The uncertainty propagation between energy sectors is studied. Policy-based reserve products for coordinated response of flexible multi-energy assets to uncertainty are introduced as flexibility-oriented products to represent operational flexibility of market participants across various energy carriers.

Although full coordination violates existing market regulations, the approaches in [**Paper A**], [**Paper B**] and [**Paper C**] motivate the need to develop mechanisms to unlock and exploit the revealed flexibility within the current regulatory framework. The proposed representation of multi-energy synergies opens up various directions for exploiting the available flexibility in a market environment. Additionally, these works provide a basis to evaluate the efficiency of market-based mechanisms enabling power, gas and heat system agents and the respective energy networks to actively contribute to providing flexibility. The foundation is laid for a comprehensive market design evaluation to improve sector coordination. This translates in a novel market-based approach that aims at coordinating the operation of multi-energy systems and exploiting the revealed flexibility. For that purpose, a soft coordination approach via financial instruments is proposed to improve coordination between energy sectors under uncertainty in [**Paper D**]. In view of real-life implementation, an investigation is conducted of utilizing the concept of virtual bidding in two-settlement markets to enhance coordination. Virtual bidders perform financial arbitrage between two trading floors in energy markets. By taking advantage of price differences, these virtual bidders are defined to improve efficiency in two-settlement wholesale markets [49–51]. Thus, the role of market participants who perform arbitrage can be expected to bring value to the overall system. These virtual bidders can be players without physical assets or players at the interface of multiple energy sectors. Allowing key players to extend their bidding capabilities to virtual bids does not require major changes for market setup and rules. For the first time, [**Paper D**] proposes the introduction of virtual bidders specifically in natural gas markets. Furthermore, the capability of units at the interface of energy sectors, e.g., gas-fired generators, to improve coordination by performing arbitrage is investigated. Simultaneously, the impact of virtual bidding on coordination of electricity and natural gas markets is analysed.

1.3.2 Methodological contributions and applications

The methodological contributions of this thesis include the development of new efficient optimization and equilibrium models enabling the coordination of electricity, natural gas and heat

infrastructures and markets. One methodological contribution is to develop optimal dispatch algorithms for the integrated energy system accounting for inter-sectoral synergies and interactions with a focus on potential network flexibility from gas and thermal storage systems. Another contribution is to investigate the impact of uncertainty and probabilistic modeling on coordination efforts and revealed flexibility. For this purpose, two different techniques based on stochastic optimization are used to account for the effects of uncertainty propagation among energy systems: distributionally robust chance-constrained optimization [52, 53] and scenario-based programming [54]. The last methodological contribution is to develop equilibrium models as market simulation tools to evaluate coordination mechanisms.

Based on the view that energy carriers are operated centrally, this work starts by investigating the potential synergies and available flexibility in [**Paper A**] and [**Paper B**]. Full coordination of electricity, heat and natural gas systems is proposed in the form of a deterministic benchmark model for the combined power, heat and gas dispatch that accounts for sector interactions and network flexibility in [**Paper A**]. This work addresses the challenge of energy flow dynamics from both natural gas and district heating. For this purpose, the work incorporates the efficient, convexified heat flow modeling technique from [24] and the gas flow modeling technique from [55] to extend the concept of energy-hubs [26]. Quadratic relaxation, linearization, and McCormick relaxation techniques are used to include detailed physical flow dynamics while maintaining tractability of the problem along with preserving convexity, thereby ensuring global optimality is reached within reasonable computation times. The resulting combined integrated energy dispatch model is formulated as a mixed-integer second-order cone program (MISOCP) and allows to quantify the potential flexibility that can be unlocked from multi-energy coordination. In order to address the complexity of modeling natural gas flow dynamics, [**Paper B**] proposes a novel convexification method based on quadratic relaxation, McCormick relaxation and the Big-M method. The deterministic combined power and gas dispatch model proposes a convexified natural gas flow model, that allows efficient modeling of both bi-directional gas flow and linepack flexibility. The resulting MISOCP is compared to a mixed-integer linear program (MILP) which uses the outer linear approximation from [17]. Finally, [**Paper C**] proposes the first tractable reformulation of the distributionally robust chance-constrained power and gas co-optimization accounting for linepack. Distributionally robust optimization and affine response policies are used to account for forecast uncertainty in the day-ahead stage. First an ambiguity set is defined to represent uncertainty arising from wind power production forecasts and then affine policies are derived for flexibility providers, especially those interfacing gas and electricity sectors. The recourse actions in both systems are based on linear decision rules and allow scheduling adjustments when the uncertainty is revealed. Once the chance-constrained power flow has been generalized to include natural gas flow dynamics, the resulting second order cone program (SOCP) enables to study how uncertainty propagates from the power to the gas side and how the short-term gas storage in pipelines, i.e., linepack flexibility, can help mitigate this uncertainty.

While the distributionally robust method with affine policies in [**Paper C**] focuses on the day-ahead stage and adjusting dispatch decisions according to participation factors as forecast uncertainty is resolved, [**Paper D**] uses scenario-based stochastic market clearing in day-ahead to deal with uncertainty from real-time operations. The real-time recourse actions in the stochastic setup are less rigid than participation factors. A soft market-based mechanism for improving the coordination of existing energy infrastructures with a focus on natural gas and power systems is proposed in [**Paper D**]. The set of market participants is extended to include virtual bidders and self-schedulers,

where these financial market agents act as coordinators between energy sectors and trading floors. While the full coordination model is used as a benchmark based on stochastic market clearing, this work proposes a less disruptive solution that preserves the current regulatory framework with separate and sequential clearing of markets. Multi-period complementarity models are build for identifying the equilibria. These mixed complementarity programs (MCP) simulate the market behavior of all market agents, i.e., market operators, market participants and virtual bidders, and can be characterized as generalized Nash equilibrium problems [47, 56]. These equilibria are analyzed under different levels of coordination. Our results show that virtual bidders help reveal and exploit the existing flexibility in the systems while preserving the current sequential and separated market setup. Finally, policy recommendations are derived for regulators to improve coordination among energy infrastructures.

1.4 Thesis structure

The Ph.D. thesis is structured as a report introducing the main concepts that are at the core of this study and summarizing the contributions of the papers developed during this Ph.D. project. Chapter 2 provides an overview of power, heat and natural gas markets with a focus on the Danish case along with an overview of electricity, district heating and natural gas network modeling methods and different levels of coordination among energy systems. The contributions, main methodologies and summary of the results obtained in the papers included in this thesis are given in Chapters 3-5, while the scientific publications are attached in an appendix. Chapters 3 and 4 investigate full coordination of energy sectors, while Chapter 5 moves towards non-disruptive, soft coordination mechanisms. In particular, Chapter 3 focuses on efficient modeling of the combined integrated energy dispatch, with an emphasis on storage capabilities of natural gas and district heating networks. Building on this work, Chapter 4 explores the coordination of power and gas systems under uncertainty introduced by renewables. Chapter 5 presents a new soft, market-based coordination mechanism introducing financial players, i.e., virtual bidders, to enhance the efficiency of electricity and natural gas markets under the current regulatory framework. Finally, Chapter 6 concludes and discusses possible directions for future work.

1.5 List of publications

The relevant publications which are the core of this thesis are collected in the appendix attached and listed as follows:

[Paper A] A. Schwele, A. Arrigo, C. Vervaeren, J. Kazempour and F. Vallée, "Coordination of Electricity, Heat, and Natural Gas Systems Accounting for Network Flexibility", in *Proceedings of 21st Power Systems Computation Conference (PSCC)*, Porto, Portugal, June 2020. Published in special issue of *Electric Power Systems Research (EPSR)*, Volume 189, Article No: 106776, December 2020.

[Paper B] A. Schwele, C. Ordoudis, J. Kazempour and P. Pinson, "Coordination of power and natural gas systems: Convexification approaches for linepack modeling", in *Proceedings of IEEE PowerTech Conference*, Milan, Italy, June 2019. Recipient of Basil C. Papadias - Second Best Student Paper Award.

[Paper C] A. Ratha, A. Schwele, J. Kazempour, P. Pinson, S. Torbaghan and A. Virag, "Affine Policies for Flexibility Provision by Natural Gas Networks to Power Systems", in *Proceedings of 21st Power Systems Computation Conference (PSCC)*, Porto, Portugal, June 2020. Published in special issue of *Electric Power Systems Research (EPSR)*, Volume 189, Article No: 106565, December 2020.

[Paper D] A. Schwele, C. Ordoudis, P. Pinson and J. Kazempour, "Coordination of Electricity and Natural Gas Markets via Financial Instruments", submitted to *Computational Management Science*, (under review), 2020.

The following publication has also been prepared during the course of the Ph.D. study, but has been omitted from the thesis:

[Paper E] A. Schwele, J. Kazempour and P. Pinson, "Do unit commitment constraints affect generation expansion planning? A scalable stochastic model", in *Energy Systems*, vol. 11, pp. 247-282, May 2020.

CHAPTER 2

Coordination Schemes for Multi-Energy Systems

The energy sectors are experiencing fundamental changes leading to tighter techno-economic interdependencies among them. As markets interface physical and economic aspects of energy systems, market-based coordination mechanisms supported by accurate physical modeling shall be used to enhance the overall efficiency of energy systems[1]. The objective of this chapter is to provide context for this work and introduce essential concepts and tools that will be required in future chapters. The transition towards renewable-based energy systems is outlined in Section 2.1 and the general organization of electricity, gas and heat markets is discussed in Section 2.2. Section 2.3 describes the physical modeling of energy flows. Finally, Section 2.4 addresses various degrees of coordination and options to improve the coordination of power, gas and heat systems. Since Denmark has an extensive district heating system, a nationwide natural gas system, and broad experience in handling a high share of wind power penetration, most examples are drawn from the Danish energy system.

2.1 Towards renewable-based energy systems

The share of power production from renewable energy sources is steadily increasing, reaching 27.5% of installed electricity capacity in the European Union (EU) in 2017 [57] and covering 50% of total electricity consumption in Denmark in 2019 [1]. Especially wind power generation has been growing rapidly, hence 47% of the Danish power consumption were generated by wind in 2019 [1], see Figure 2.1. In addition, 3% came from solar units. The intermittency, variability and uncertainty of renewable energy production require more operational flexibility system-wide. In order to provide supply-demand balance across spatial and temporal scales, various flexible assets exist to be leveraged for operational flexibility in the power system including controllable power generation, transmission via international interconnectors, storage, and demand response [58]. A broader definition of power system flexibility to multi-energy system flexibility in [59] accounts for the fact that smart interactions among power, gas, and heating systems have the potential to provide new services for storage and balancing of electricity. Ultimately, flexible assets at the interface with other energy systems, e.g., gas-fired generators, combined heat and power (CHP) units, heat pumps, power-to-gas units, as well as solutions for more efficient interactions among power, gas and heat sectors strengthen the flexibility of the overall energy system.

At the same time, natural gas and heat systems are undergoing revolutionary changes, too. Natural gas is considered as a transition fuel towards energy systems based on higher shares of renewable energy. Other gaseous fuels, which are produced from biomass and waste by thermal gasification

[1] Throughout this thesis, the term coupling describes physical and economic interactions and links resulting in interdependencies of systems for given setups, while efforts to optimize these interactions are referred to as coordination.

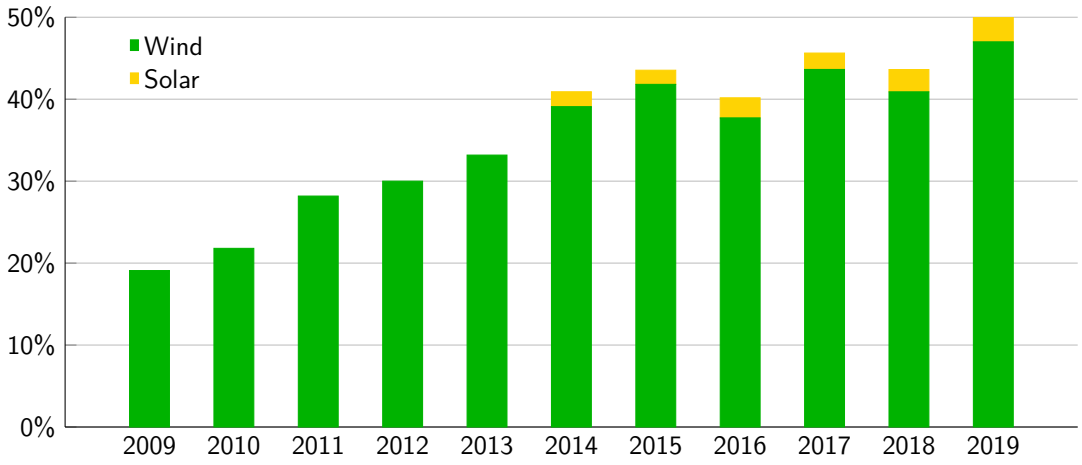

Figure 2.1: Trend of electricity production from wind and solar as a share of Danish electricity consumption (Figure reproduced from [1]).

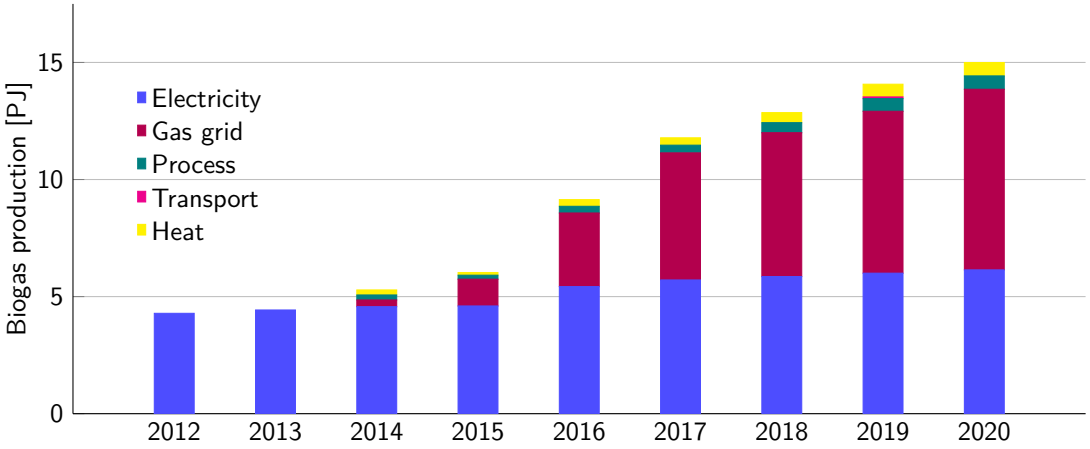

Figure 2.2: Historical and the expected future biogas production and its use in Denmark (Figure reproduced from [2]).

or from electricity via electrolysis, based on renewable energy, e.g., biogas, biomethane, hydrogen or synthetic gases, are expected to gain importance in the future energy mix [27, 60, 61]. In Denmark, production and consumption of biogas are on the rise, as is its injection into the gas grid, see Figure 2.2. Furthermore, natural and renewable gases can serve as seasonal storage and buffers in periods in which production of renewable energy from uncertain sources is low. Indeed, there has been significant growth of gas as fuel for electricity production, since gas is typically used to produce electricity in peak load situations and to mitigate real-time deviations [8, 62, 63].

The heat sector, which used to be dominated by fossil fuels, is also experiencing an increase in renewable energy production, mostly via bio-fuels and electrification. Heating in buildings and industry is the largest energy demand representing roughly half of all energy consumption in the EU [5]. Energy-efficient and cost-effective heating is key for sustainable energy systems. In particular, Denmark has heavily relied on district heating for heat consumption covering approximately 60% of the heat supply [61]. CHP plants produce a large share of both heat and thermal electricity production in Denmark [5]. Since heat and power output of CHP units are

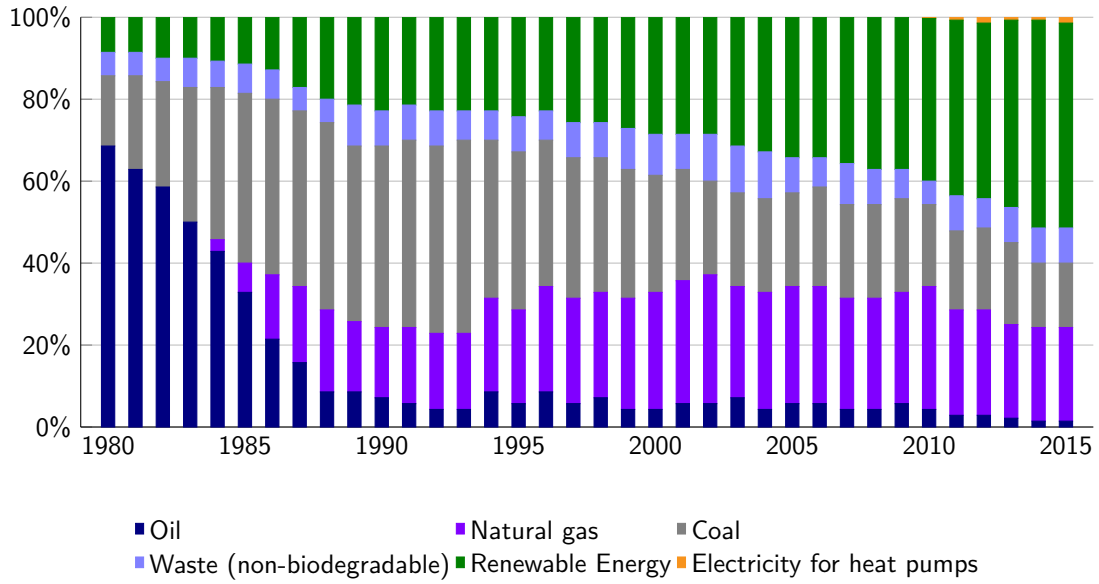

Figure 2.3: Heat sector energy mix in Denmark, as a percentage of the total consumption (Figure reproduced from [3]).

linked, these units induce strong physical and economic couplings between heat and electricity systems. Additionally, heat pumps are starting to leverage on excess wind production and low electricity prices for heat production, see Figure 2.3.

Increased coupling of energy sectors is identified as one of the main opportunities for a sustainable energy future [64]. This recognizes the potential to exploit untapped synergies and flexibility from existing infrastructures yielding possibly advantageous technical and economic interactions. At the same time, the interdependencies among energy carriers are amplified under extreme situations. For example, in winter 2014 North American system operators faced difficulties in operating the power system during periods of high heat and electricity demand because of the reliance on natural gas for both heating and peak electricity load [65]. In China, the heat-driven dispatch of CHP units caused a significant wind curtailment due to minimum power production requirements [28]. In Nordic countries, where CHPs cover a large share of both heat demand and thermal electricity capacity [5], issues regarding market power and competitiveness arise in both electricity and heat markets [66, 67].

Without appropriate market structures, these uncoordinated couplings may not only fail to optimally exploit existing synergies but even be damaging for the overall energy system. However, despite their interdependencies the three energy systems are typically operated separately, sequentially, and as if independent. In Denmark, the heat system is dispatched prior to the electricity system based on estimated electricity prices. The power system is dispatched prior to the gas system based on estimations of natural gas price and availability. This potentially leads to suboptimal dispatch decisions, particularly for CHPs, heat pumps and natural gas-fired generators at the interface between different systems.

The interested reader is referred to [11, 68, 69] for a detailed overview of electricity markets and power system economics, while [35, 70, 71] provide an overview of heat systems and markets. In addition, a comprehensive overview of natural gas markets can be found in [72, 73].

2.2 On the sequence of energy market clearings

Energy markets organize physical and economic aspects of energy via proper trading mechanisms to ensure security of supply and competitiveness. Energy products are traded as commodities at different time scales in wholesale markets. Trading takes place in various time spans and settlements from long-term financial contracts to real-time operations. Long-term financial products are traded via bilateral agreements and contracts or in futures markets, which allow the market participants to hedge against volatile prices. This thesis focuses on short-term trading floors only, i.e., within a day to actual delivery. Since spot markets are cleared 12 to 36 hours before the actual delivery of electricity, they are also referred to as day-ahead markets. The amount of heat and gas traded in dedicated day-ahead markets is also becoming more prominent [27]. After the day-ahead market is cleared, market participants can adjust their positions or dispatch in intra-day markets to mitigate possible deviations from the day-ahead schedule. The liquidity of these intra-day markets differs and they are country- and design-specific. Closer to real-time operations, deviations are balanced in the real-time market by transmission system operators. Note that energy and reserve markets are cleared separately in European markets [74], and the latter is not the focus of this thesis.

In European countries, electricity, natural gas and heat systems are operated by competitive auction-based markets that interface the physical, technical and economic aspects of each system. These wholesale markets are typically cleared in several settlements including day-ahead, intra-day and real-time balancing clearings. These energy markets operate as energy exchanges in which market participants submit bids and offers which implicitly embed their techno-economic characteristics. In day-ahead markets, each market participant submits bids for each hour of the following day. These bids are dispatched by heat, electricity and gas market operators based on a merit-order and least-cost principle. Note that electricity, gas and heat market operators are not necessarily the same entities. Energy markets usually operate heat, power and gas systems in the day-ahead stage sequentially and separately [8, 29]. For instance, in Denmark, the day-ahead heat market is cleared by Varmelast.dk before the electricity market Nordpool [75]. Moreover, the timing of electricity and natural gas day-ahead markets is not aligned [8, 29, 76]. Due to the asynchronous timing, physical and economic couplings are not properly accounted for. For instance, heat pumps are dispatched based on estimated production costs which depend on electricity prices. Similarly, gas-fired power plants face uncertainty about fuel price and natural gas availability which determine their production cost. CHP units need to decide both heat and electricity production with regards to opportunity cost and operational limitations.

The greater Copenhagen area was the first region in Denmark that implemented a wholesale heat market. The heat market operator, Varmelast.dk, which is owned by the three major heat distribution companies VEKS, CTR, and HOFOR, prepares a day-ahead heat dispatch based on a least-cost principle [75]. Because of limited competition on both supply and retail sides, heat market prices are still highly regulated. Heat producers compete on production costs since retail heat prices are predetermined and fixed [75]. CHP plants make up the largest share of total installed heating capacity in the Danish system. Electricity prices and opportunity cost impact the heat production cost of these CHP units that subsequently participate in the electricity market.

Once the heat market has been cleared, each electricity market participant, including CHPs and heat pumps, submits offers and bids for each hour of the following day, which are dispatched based on the merit order principle. Merit order describes the ranking of power plants with an ascending

order of price-bids, i.e., marginal production costs. This economic dispatch does not explicitly describe the techno-economic characteristic of power plants or physical networks. However, the bids submitted can range from simple hourly price-quantity bids to more complex bids, e.g., block orders [44]. These bids can implicitly embed technical characteristics such as minimum production levels. Congestion management mechanisms complement these auctions. The market is cleared by intersection of aggregate supply and demand curves and uniform market-clearing prices are derived for the case of no congestion in transmission lines. In case of congestion, zonal prices are derived with different market prices for zones linked by congested lines [77]. Thus, uniform prices are obtained as the marginal prices in each market zone and physical flows in each market zone are managed a posteriori by the transmission system operators. Alternative to this zonal market scheme is power pools that takes techno-economic characteristics and physical network directly into account. Thus, locational marginal prices are derived for each node of the network based on centralized market-clearing algorithms and these nodal prices are used for settlements and payments [78]. Note that the production cost of the marginal technology, which is often combined-cycle gas turbine [63], sets the price. The production costs of gas-fired units directly depend on the spot market-clearing price for natural gas.

PEGAS, now comprising the former Gaspoint Nordic, is the primary trading platform of the Danish gas spot market [79]. Trading natural gas takes place according to the entry-exit model [80, 81], which assumes virtual trading hubs with entry and exit points, i.e., large trading areas fragmented into zones with limited interconnection capacities, while network and technical characteristics are allocated implicitly. Thus, all injections and withdrawals bought and sold through shippers are considered to have the same price, compared to a point-to-point trading [63] representing the actual physical characteristics of each trade. Energinet.dk controls not only the Danish power transmission system but also the natural gas system, managing required scheduling adjustments and ensuring operational feasibility.

Disadvantages of the sequential market clearings arise from limited information exchange among the systems and markets potentially resulting in misrepresentation of actual operational cost, merit-order shift, or unavailability of flexible multi-energy assets. These issues may cause potential lack of flexibility in the systems, hinder the increasing penetration of renewable energy sources, eventually leading to loss of social welfare. Moreover, current energy markets clear several sequential trading floors, e.g., day-ahead and real-time stages, with deterministic description of uncertain supply and demand [82], see Figure 2.4. The changes mentioned in Section 2.1 towards increasing renewables in energy systems pose challenges for the current design paradigm. The deterministic forecast of stochastic renewable energy sources used for the day-ahead clearing is unaware of real-time deviations and resulting balancing costs, which may lead to inefficient dispatch decisions [83]. Tools from decision-making under uncertainty and probabilistic market clearings [84, 85] have been proposed to overcome the shortcomings of the current deterministic clearings and improve the coordination between trading floors.

Furthermore, the simple economic dispatch based on least-cost and merit order principles does not consider any network flows or network constraints and assumes lossless and unrestricted flow of energy. In order to better represent the underlying physics and improve the efficiency of market clearing and dispatch decisions, the economic dispatch can be extended to incorporate unit commitment decisions [66, 86], optimal power flow models [77], as well as gas and heat flow models [17, 24]. Accurate representation of the physical characteristics of technical operations and

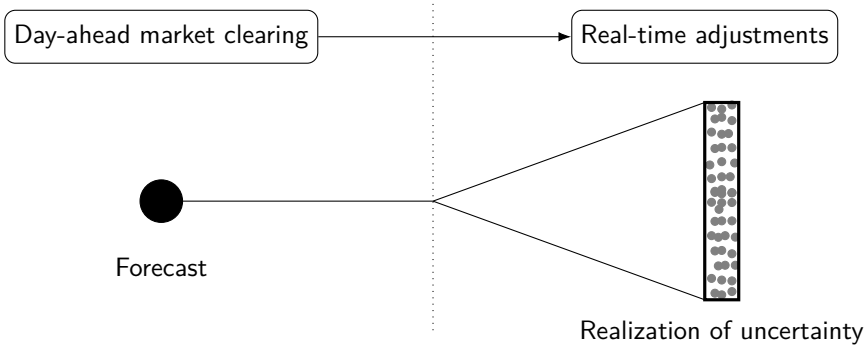

Figure 2.4: Temporal dimension of two-stage trading floors in short run.

networks of each energy carrier inside clearing models can help efficient and accurate pricing, especially for flexibility products. However, the non-convexities introduced in these optimization problems give rise to another challenge, specifically for convergence, solution quality guarantees and pricing non-convexities [87].

2.3 Energy flow modeling

The physical representation of energy flows can be described by mathematical models presented in the following.

2.3.1 Power flow modeling

The power flow in electricity networks is given by alternating current (AC) power flow equations which describe active and reactive power, losses along lines, and voltages at nodes according to Kirchhoff's laws [9]. However, these non-linear and non-convex equations pose computational and optimality challenges. Several works have addressed this challenge proposing convex relaxations of the original formulation [9, 88, 89]. In this thesis, the original AC power flow equations are approximated by the linearized lossless DC power flow equations, which neglect losses and reactive power flows, under the following three assumptions. Firstly, voltage magnitudes are close to their nominal values at all nodes. Secondly, differences between voltage angles θ_n and θ_r at adjacent nodes n and r are small. Thirdly, line resistances are negligible compared to line reactances, so transmission lines are assumed to be lossless. Under these assumptions flow $f_{n,r}$ along transmission line $(n,r) \in \mathcal{L}$ is described as a linear equation, i.e.,

$$f_{n,r} = B_{n,r}(\theta_n - \theta_r), \quad \forall (n,r) \in \mathcal{L}, \tag{2.1}$$

where $B_{n,r}$ denotes the line susceptance.

Alternatively, Power Transfer Distribution Factor (PTDF) matrix $PTDF_{(n,r),n}$ which describes the linear relation between power injections at node n and active power flows through transmission lines (n,r) can represent DC power flows [90]. PTDFs are linear sensitivities derived from the reactances of power transmission lines and relate line flows to nodal power injections p_n according to

$$f_{n,r} = PTDF_{(n,r),n}\, p_n, \quad \forall (n,r) \in \mathcal{L}. \tag{2.2}$$

While power flow dynamics are fast (microseconds to seconds) such that supply and demand need to be balanced instantaneously, gas and heat flows have slower time dynamics (minutes to hours) leading to longer transmission times but also to potential storage capacity of pipelines.

2.3.2 Natural gas flow modeling

Because of slow gas flow dynamics and the ability of pipelines to store a substantial mass of gas internally, gas networks provide short-term storage. Dynamic models are needed to capture this ability to accumulate and then release gas in a pipeline. The compressible gas flow through a network of pipelines in the ideal gas regime is governed by three conservation laws: conservation of mass, momentum and energy [73]. Assuming slow transients that do not excite shocks or waves, the temporal and spatial dimensions of natural gas flow are described by partial differential equations that model the dynamics of flow and pressure. Optimization of the physical operation based on the transient approach can be solved by spatial and temporal discretization [16, 36, 91–94]. However, these models are highly non-linear yielding challenges for computational tractability.

In this thesis, we refer to the stationary model of gas flow assuming isothermal flow in horizontal pipelines. The Weymouth equation describes the steady-state gas flow along pipeline $(m,u) \in \mathcal{Z}$ by

$$q_{m,u}|q_{m,u}| = K_{m,u}^2(pr_m^2 - pr_u^2), \forall (m,u) \in \mathcal{Z}, \tag{2.3}$$

which relates flow $q_{m,u}$ to the difference of squared pressure pr_m and pr_u at both ends of the pipeline. Weymouth equation (2.3) is piecewise quadratic, non-linear and non-convex. Parameter $K_{m,u}$ is the Weymouth constant that describes pipeline characteristics including pipeline length, diameter, and compressibility factor [95]. Hence, constant flow along a pipeline depends on pressure at adjacent nodes and physical pipeline properties. The gas flow is also defined as the arithmetic mean of pipeline in- and outflow ($q_{m,u}^{\text{in}}$ and $q_{m,u}^{\text{out}}$) according to

$$q_{m,u} = \frac{q_{m,u}^{\text{in}} + q_{m,u}^{\text{out}}}{2}, \forall (m,u) \in \mathcal{Z}. \tag{2.4}$$

Because of friction, the pressure of gas flowing through a pipeline gradually decreases, and is boosted by compressors so that it exceeds the minimum for delivery to customers [73]. These gas compressors are used to control the flow of gas and maintain pressure throughout a pipeline. Compressor action is modeled in a simplified manner as a multiplicative change in pressure at fixed compression factors. Hence, exit pressure should be at least equal to inlet pressure and can be as high as inlet pressure times compression ratio $\Gamma_{m,u}$ according to

$$pr_u \leq \Gamma_{m,u}\, pr_m, \forall (m,u) \in \mathcal{Z}. \tag{2.5}$$

Similarly, valves can be used for pressure reduction.

Because natural gas is compressible, injection and withdrawal rates can be unbalanced and the amount of gas stored in the network in short term is variable [17, 23, 73, 95, 96]. Pressures at both ends of a pipeline can be varied maintaining the same level of flow while accumulating or releasing gas inside the pipeline. The concept of storage of natural gas in pipelines due to available slack in pressure drop is called linepack. Linepack flexibility means that the total injection does not need to match the total consumption at each time step [95]. This storage capability enables gas-fired generators to withdraw gas in excess of the scheduled rate for a limited duration without violating pipeline operating limits [97]. Balance of injection and withdrawal is achieved over longer time periods, e.g., a day. Linepack mass $h_{m,u}$ is proportional to average pressure at both ends of a pipeline, given by

$$h_{m,u} = S_{m,u}\frac{pr_m + pr_u}{2}, \forall (m,u) \in \mathcal{Z}, \tag{2.6}$$

where the proportionality factor $S_{m,u}$ depends on pipeline and gas flow characteristics. The amount of gas contained in a pipeline is tracked through time and discretized over hourly time steps t as follows

$$h_{m,u,t} = h_{m,u,(t-1)} + q^{\text{in}}_{m,u,t} - q^{\text{out}}_{m,u,t}, \forall (m,u) \in \mathcal{Z}, t. \tag{2.7}$$

2.3.3 Heat flow modeling

District heating is distributed via water as the heat medium flowing through parallel supply and return pipelines that are connected by heat exchange stations. Control variables for the district heating network are inlet temperatures and mass flow rates. While in China control strategies typically use varying temperature levels keeping mass flow rates constant [98], Danish district heating networks are operated at constant temperature levels with adjustable mass flow rates [75]. Modeling of district heating includes hydraulic and thermal equations [99].

The hydraulic constraints represent continuity of mass flow at all nodes and the relation between pressure drop and mass flow rate in pipelines. Since water is incompressible, the sum of incoming flow is equal to the total outflow at each node and heat is distributed from high to low pressure nodes. The Darcy-Weisbach equation (2.8) relates pressure losses ($pr_o - pr_v$) due to friction inside the supply and return pipelines $(o,v) \in \mathcal{P}$ to mass flow rates $mf_{o,v}$ via pressure loss coefficient $L_{o,v}$ according to

$$L_{o,v}(mf_{o,v})^2 = pr_o - pr_v, \forall (o,v) \in \mathcal{P}, \tag{2.8}$$

which is a non-convex equality constraint.

Thermal equations characterize the changes in temperature levels within the district heating network including heat balance in heat sources and heat exchange station, mass flow and temperature mixing at nodes, and time delay of heat propagation. Heat Q_o generated at node o is transferred to the heating network at heat sources and delivered to consumers at heat-exchange stations according to the product of mass flow and temperatures differences $T^{\text{S}}_o - T^{\text{R}}_o$ with the specific heat capacity of water c given as

$$Q_o = c\, mf_o(T^{\text{S}}_o - T^{\text{R}}_o), \forall o. \tag{2.9}$$

The energy extracted from heat exchangers is proportional to the difference of temperatures between supply and return pipelines at the station. All incoming water flow is fully mixed at each node described by temperature mixing equations that determine the temperature at each node of supply and return networks to be a mix of mass flow-weighted outlet temperatures from pipelines arriving at that node.

In the dynamic model, the working fluid temperature is a function of time and position, which is expressed as a spatio-temporal partial differential equation. Assuming laminar flows in well insulated pipelines neglecting thermal losses due to exchange with the outside, in [100] a solution for the partial differential equations of heat propagation is given, which can be approximated and linearized using first order Taylor series expansion [24]. For discretized time steps t, the outlet temperature of a pipeline is defined as a nonlinear function of the inlet temperature at previous time slots according to

$$T^{\text{out}}_{o,v,t} = T^{\text{in}}_{o,v,(t-\tau)}\left(1 - \frac{2\mu_{o,v}}{c\rho R_{o,v}}\tau_{o,v,t}\right), \forall (o,v) \in \mathcal{P}, t, \tag{2.10}$$

which relates the outlet temperature $T^{\text{out}}_{o,v,t}$ at time t to past inlet temperature $T^{\text{in}}_{o,v,(t-\tau)}$ at previous time $t - \tau_{o,v,t}$ minus heat losses. These losses are given by thermal loss coefficient $\mu_{o,v}$, specific water capacity c, water density ρ and the radius of the pipe $R_{o,v}$. The time it takes for the fluid to travel along the pipeline is defined as varying time delay $\tau_{o,v,t}$ over pipeline length $PL_{o,v}$ by

$$\tau_{o,v,t} = \min\Big\{\eta \in \{0, ..., \overline{\tau}_{o,v}\}, \ \text{s.t.} \sum_{\delta=t-\eta}^{t} \frac{mf_{o,v,\delta}}{\pi R^2_{o,v}\rho}\Delta t \geq PL_{o,v}\Big\}, \forall (o,v) \in \mathcal{P}, t. \tag{2.11}$$

This transmission delay of heat networks can reach up to several hours ($\overline{\tau}_{o,v}$), allowing to temporally decouple heat production and consumption. Following the approach in [24], constraints (2.10)-(2.11) can be linearized using auxiliary binary variables and a Big-M formulation.

2.4 Coordination strategies

A major challenge for energy market design is to facilitate market access to flexible assets at the interface between systems to exploit this untapped source of flexibility. Currently, operation, planning, and the economics of different energy networks are managed in an uncoordinated manner as if completely decoupled. While the share of renewable energy sources is increasing, this lack of coordination among electricity, natural gas and heat sectors may cause market inefficiency, in the sense that the overall cost of operating the energy systems might be higher than theoretically necessary. Reasons for such an inefficiency are non-optimal dispatch decisions due to uncoordinated market clearing neglecting coupling effects. If flexible assets that operate at the interface of several energy systems are dispatched inefficiently, they impose stronger technical constraints in another system or are not available to mitigate imbalances. As a consequence, other actions, e.g., load or wind curtailment, might be required. The increasing coupling of energy carriers demands stronger coordination mechanisms. Stronger coordination of multiple energy systems requires adopting a more holistic market perspective acknowledging the growing interactions and interdependencies among energy carriers and considering the economic and physical aspects simultaneously. The coordination among power, natural gas and heat systems during the day-ahead dispatch has been a topic of research interest in recent years. Indeed, several works have highlighted the impact of natural gas supply and price uncertainty on scheduling in electricity systems [101, 102] and the effect of heat dispatch on available flexibility and electricity prices [28, 67]. Coordinated long-term planning is proposed in [103, 104] for coupled power and gas systems and in [105] for integrated electricity-heat systems, while the next sections describe coordination for short-term operational integration. The works in [17, 96, 106–108] and [35] investigate different levels of coordination for the short-term operation of power and natural gas systems as well as for power and heat systems, respectively. Coordination options range from re-design of integrated energy systems for full coordination to non-disruptive options improving the exchange and acknowledging the interactions and interdependencies among the systems via soft coordination, see Figure 2.5.

2.4.1 Full coordination

Full coordination of integrated energy systems requires re-designing the current market clearing and operations framework. This disruptive solution allows the interactions and interdependencies among the sectors to be explicitly anticipated and adequately reflected in the scheduling processes. Usually a central entity operates the whole integrated energy system such that information is shared among the specific sectors and the timing of decision making is aligned. Full coordination

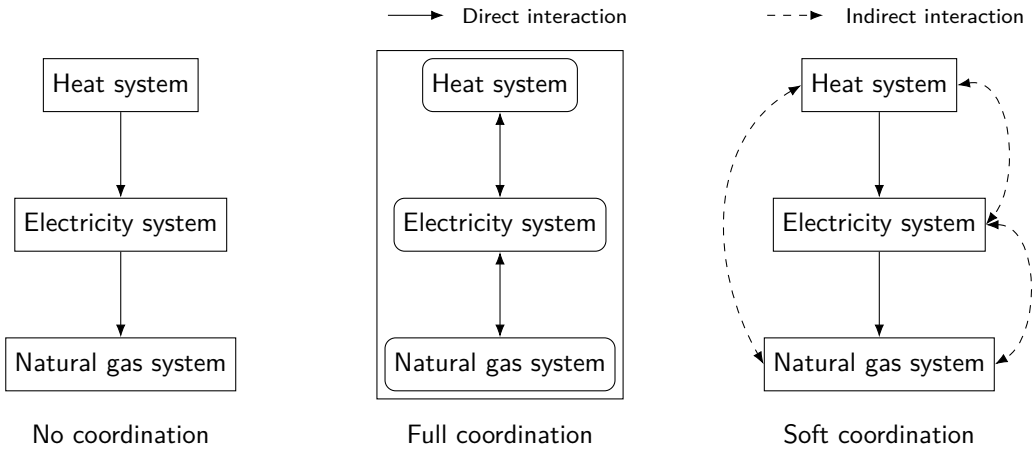

Figure 2.5: Different levels of energy systems coordination.

approaches with central control of gas-electric systems emphasize the importance of uncertainty [17, 109–116], detailed network modeling [17, 109, 117], and natural gas security constraints [19, 20, 118, 119] for decision-making and efficient dispatch. Full coordination models for power and heat systems in [24, 25, 28, 31, 98] focus on revealing operational flexibility from multi-carrier resources. Full coordination setups show the full potential of flexibility that can be harvested among energy carriers. Although these approaches are not directly implementable in practice, they are very useful as benchmark, providing the basis for evaluating other practical coordination schemes that align with current market regulations. Such market-based mechanisms are introduced in the following.

2.4.2 Soft coordination

As opposed to the disruptive re-design of perfectly coordinated energy systems, soft market-based mechanisms for enhancing the coordination of power, natural gas and heat markets preserve the current sequential and independent operations framework. Any mechanism or process that increases the overall system efficiency while respecting the current operational and economic setup and regulations provides what is referred to as soft coordination. These mechanisms aim at enhancing the information flow among the systems and creating incentives for each sector to dispatch resources in a way that benefits the overall system. These tools work as coordinator at the interface of different sectors and can enable flexibility provision from multi-carrier resources. Moreover, these proposed mechanisms should support decision-making in real-life markets. For a review on the literature dealing with design of market mechanisms, see [120–123].

Improved information exchange

Among others, less-disruptive, soft coordination of power, gas, and heat systems can be achieved by higher degrees of information exchange and awareness among energy markets. For example, [124] and [36] propose the exchange of physical and pricing data between electricity and natural gas markets in the intra-day stage for balancing purposes. The quality and accuracy of pricing data exchanged between power and gas systems in day-ahead are investigated in [37]. Natural gas price and fuel availability for gas-fired units are used as coordination parameters in [107] and [108] to generate proper flexibility signals for day-ahead electricity scheduling. More awareness

between power and gas and between heat and power systems are introduced in [34] and [18, 35], respectively, while adhering to sequential clearing of markets. This requires the exchange of proprietary information, which can be mitigated using privacy preserving mechanisms proposed in [125, 126].

New market products

Several market products and services for flexibility options like generators and storage units have been proposed and introduced in electricity markets to cope with uncertainty and variability. Extending these flexibility-oriented products and concepts allows to incorporate flexibility interfacing multiple energy carriers. For example, ramp products like "flexiramp" or "ramp capability" [40] as reserved and committed generation capacity, and affine reserve participation policies [39, 127] can be traded in day-ahead for reserve provision to meet deviations in real-time. These new trading mechanisms facilitate flexibility activation.

New bidding formats

Similarly to new flexibility products, new bidding formats can reveal the value of operational flexibility [41–44]. The existing bidding mechanisms in day-ahead markets, i.e., price-quantity and block bids, do not capture the specific techno-economic characteristics of flexibility resources at the interface with other energy markets. Bid formats can be extended to mimic the specific characteristics of flexible assets [34, 35, 42, 128]. In this direction, [129] generalizes bid formats to represent the complexity of cross-carrier load flexibility at the interface between heat and electricity systems.

New market players

Market players can act as coordinators at the interface of different energy markets and sectors. Self-scheduling market participants who decide their dispatch themselves instead of submitting bids to the day-ahead market [130], can enhance efficiency of electricity markets [51]. Especially the participation of CHP units, heat pumps, and gas fired-generators in power, gas and heat markets has potential to enhance the coordination among the systems through smarter coupling. While extending the toolbox of existing players with new products and bidding formats can help exploit existing synergies and flexibility more efficiently, introducing new market players can also bring more information and liquidity to the markets. For instance, virtual bidders, who are purely financial players, are supposed to enhance the efficiency of the two-settlement markets by arbitraging and bringing more competitiveness and transparency to energy markets [49, 131–133].

CHAPTER 3

Full Coordination: A Deterministic Benchmark

Since the need for operational flexibility to cope with variability and uncertainty increases with higher shares of renewables, growing interactions among energy systems pose the opportunity to reveal cross-carrier synergies. Flexible assets often operate at the interface of energy sectors and markets. Apart from that, the inherent ability of natural gas and district heating networks to store energy can provide additional flexibility. The goal of this chapter is to reveal the flexibility that natural gas and heat networks can potentially provide for power systems. For that purpose, combined multi-energy dispatch models are proposed, assuming either a single central system operator or perfect information exchange and timing among the systems. These full coordination models provide ideal benchmarks to quantify the added value of accounting for energy flow dynamics in terms of increased flexibility to the power system.

In general, it is quite complex to holistically model the multi-energy systems while incorporating flow dynamics of each specific energy network. The proposed fully coordinated benchmark aims at accounting for energy flow dynamics and network flexibility in an efficient manner. On top of the energy flow modeling described in Section 2.3, convexification strategies are described for improved tractability and computational efficiency towards market-compatibility.

First, Section 3.1 focuses on incorporating natural gas flow dynamics in the integrated energy dispatch model, while the heat system is added in Section 3.2. For notational simplicity general formulations of the proposed models are introduced, while the reader is referred to [**Paper A**] and [**Paper B**] for more detailed descriptions. Key results highlighting the added value in terms of reduced total system cost from coordination accounting for network flexibility and cross-carrier synergies are shown in Section 3.3.

3.1 Linepack flexibility

Strong links between electricity and natural gas systems play a major role in providing system flexibility. Natural gas-fired generators provide short-term flexibility and strengthen the interdependence between power and gas systems. When gas-fired power units are used to mitigate the uncertainty and intermittency of wind power production, the resulting variability and unpredictability of gas demand challenge natural gas system operations and fuel availability. At the same time, increasing injection of biogas into the natural gas network adds variability to gas network operations. On the gas side, there is potential of storing energy in pipelines since inflow into the pipeline is not necessarily equal to the respective outflow. This concept is called linepack. Linepack flexibility is accumulated by making use of available pressure differences which results in the storage of gas inside the pipeline. Linepack flexibility operates like a buffer that is filled first, and emptied at a later time. Thus, massive amounts of energy in form of natural gas can be stored

in pipelines. In order to harvest this source of short-term flexibility to be provided by the natural gas network to the power system, the direction of gas flows and the linepack, both controlled via pressure differences, need to be optimized as additional degrees of freedom.

3.1.1 Combined power and gas dispatch

The proposed co-optimization aims at minimizing the total cost of operating power and natural gas systems accounting for operational constraints of both power and gas sides as well as coupling constraints linking the two systems together. The power system is described by a simplified lossless DC power flow model, as outlined in Section 2.3.1, including operational limits on electricity generation, transmission, and nodal voltage angles. Nodal power balance ensures that power supply and demand are matched at all times. On the gas side, natural gas flow is represented by its steady-state gas flow equation, see Section 2.3.2. Natural gas flow and the amount of linepack are dependent on the pressure drop along a pipeline. In order to efficiently model gas flow and linepack, the flow dynamics are embedded by accounting for linepack through varying in- and outflows of pipelines. Compressor stations are represented in a simplified way, relating pressures at adjacent nodes linearly with constant compression factor. Natural gas supply capacity and nodal pressure bounds are limited by operational bounds. Coupling constraints describe the interdependencies among the energy carriers and how the units at the interface link the two systems together. Here, the dispatch of gas-fired units is translated into fuel consumption which constitutes a time varying nodal gas demand so that the nodal gas supply balance couples the systems. A general form of the combined power and natural gas dispatch problem is given as

$$\min_{\boldsymbol{x}^{\mathrm{E}},\boldsymbol{x}^{\mathrm{G}}} \quad f(\boldsymbol{x}^{\mathrm{E}}) + f(\boldsymbol{x}^{\mathrm{G}}) \tag{3.1a}$$

$$\text{subject to} \quad h^{\mathrm{E}}(\boldsymbol{x}^{\mathrm{E}}) = 0, \;\; g^{\mathrm{E}}(\boldsymbol{x}^{\mathrm{E}}) \leq 0, \tag{3.1b}$$

$$h^{\mathrm{G}}(\boldsymbol{x}^{\mathrm{G}}) = 0, \;\; g^{\mathrm{G}}(\boldsymbol{x}^{\mathrm{G}}) \leq 0, \tag{3.1c}$$

$$h^{\mathrm{E,G}}(\boldsymbol{x}^{\mathrm{E}}, \boldsymbol{x}^{\mathrm{G}}) = 0, \tag{3.1d}$$

where $\boldsymbol{x}^{\mathrm{E}}$ and $\boldsymbol{x}^{\mathrm{G}}$ are vectors of power and natural gas variables, respectively. The components of the linear objective function $f(\boldsymbol{x}^{\mathrm{E}})$ and $f(\boldsymbol{x}^{\mathrm{G}})$ pertain to power and natural-gas systems, respectively. Constraints $h^{\mathrm{E}}(\boldsymbol{x}^{\mathrm{E}}) = 0$ and $g^{\mathrm{E}}(\boldsymbol{x}^{\mathrm{E}}) \leq 0$ are the power system equality and inequality constraints, $h^{\mathrm{G}}(\boldsymbol{x}^{\mathrm{G}}) = 0$ and $g^{\mathrm{G}}(\boldsymbol{x}^{\mathrm{G}}) \leq 0$ are natural gas system constraints, and $h^{\mathrm{E,G}}(\boldsymbol{x}^{\mathrm{E}}, \boldsymbol{x}^{\mathrm{G}}) = 0$ represents coupling constraints linking both systems together. Linear DC power flow equations represent the power system constraints (3.1b), as described in Section 2.3. The natural-gas system constraints (3.1c) are modeled by non-linear and non-convex natural gas flow equations for which linearization or convexification is generally required to attain computational tractability and efficiency. Coupling constraints (3.1d) are linear.

Under the assumption that the direction of gas flow in all pipelines $\mathcal{Z}$ is known a priori, i.e., $q_{m,u} \geq 0, \forall (m,u) \in \mathcal{Z}$, Weymouth equation (2.3) becomes quadratic non-convex and non-linear and overall the proposed combined integrated energy dispatch results in a non-linear program (NLP). While known gas flow direction used to be a reasonable assumption in day-ahead operations of gas networks, the growing operational variability in natural gas networks due to increasingly intermittent fuel off-take by gas-fired power generators and injection of biogas into the grid challenges this assumption. Since the original steady-state equation (2.3) is piecewise quadratic and non-convex, binary decision variables $\boldsymbol{u}^{\mathrm{G}} \in \{0,1\}$ are introduced to account for the direction

of gas flow efficiently. Then the gas system inequality constraints $g^{\mathrm{E}}(\boldsymbol{x}^{\mathrm{E}}, \boldsymbol{u}^{\mathrm{G}}) \leq 0$ contain both continuous and binary variables. Including the additional degree of freedom from modeling bidirectional gas flow renders the co-optimization problem a mixed-integer non-linear program (MINLP). Note that non-convexities arise from non-convex constraints and discrete variables. Gas flow (not necessarily "optimal" gas flow) problems are typically solved using Newton-Raphson-based solvers. However, the main disadvantages of these approaches are that their convergence can be sensitive to the initialization and that they do not provide any guarantee on the quality of solution, whereas convexification provides bounds on the global optimum. Convex problems are also preferred towards market compatibility and deduction of meaningful prices. Convexification strategies are introduced in Section 3.1.2, while the reader is referred to **[Paper B]** for a detailed version of the MINLP, where the time horizon considered is one day divided into 24 hourly intervals.

3.1.2 Convexification strategies

Since non-convexities that arise from the energy flow dynamics lead to tractability and optimality issues, relaxation and approximation techniques are used to model energy flow dynamics efficiently. The steady-state gas flow equation (2.3) can be made convex using relaxation or approximation techniques. When these techniques do not provide exact solutions, at least bounds on the global optimum can be derived. The convexification techniques are described in the following.

Quadratic relaxation

Non-convex quadratic equality constraints $x^\top A^\top A x + b^\top x + d = 0$ can be made convex using second-order cone relaxation [134, 135]. Then these constraints can be reformulated to the second-order cone standard form

$$\|Ax + b\|_2 \leq c^\top x + d, \tag{3.2}$$

with variable x and parameters $A \in \mathbb{R}^{m \times n}$, $b \in \mathbb{R}^m$, $c \in \mathbb{R}^n$, $d \in \mathbb{R}$. Operator $\|\cdot\|_2$ indicates the Euclidean norm and $(\cdot)^\top$ the transpose operator.

When assuming the direction of gas flow in pipelines to be known, the steady-state equation (2.3) reduces to $q_{m,u} = K_{m,u}\sqrt{pr_m^2 - pr_u^2}, \ \forall (m,u) \in \mathcal{Z}$, which is a quadratic equality constraint. Hence, under the assumption of uni-directional gas flow along a pipeline, the steady-state equation (2.3) can be relaxed into the following second-order cone constraint,

$$\left\| \begin{matrix} q_{m,u} \\ K_{m,u}\, pr_u \end{matrix} \right\|_2 \leq K_{m,u}\, pr_m. \tag{3.3}$$

This concept is illustrated in Figs. 3.1 and 3.2. The original quadratic equality constraint is given by only the surface area in Figure 3.1 and, hence, is non-convex. The second-order cone relaxation extends the feasible space to include the interior of the cone, see Figure 3.2. If the optimal point over the second-order feasible set coincides with the surface area, the relaxation is exact. On the other hand, the relaxation is not exact if the optimal point is inside the cone and the optimal solution of the relaxation is infeasible for the original problem.

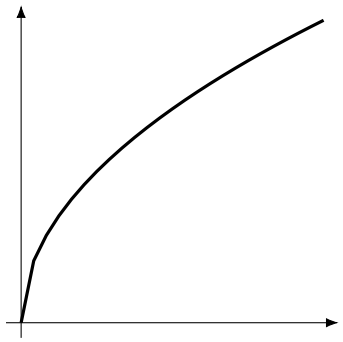

Figure 3.1: Quadratic equality.

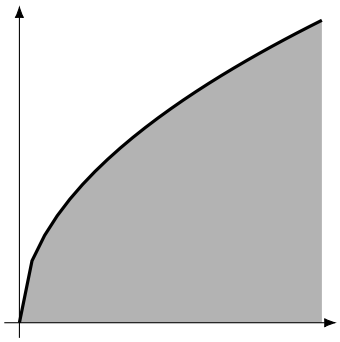

Figure 3.2: Relaxation.

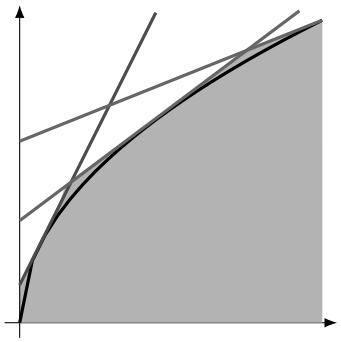

Figure 3.3: Approximation.

Outer linear approximation

For outer linear approximation, Taylor series expansion can be used [17, 136]. Instead of relaxing the original constraint, the approximation technique creates a number of planes tangent to the cone. Thus, the original equality constraint is replaced by a number of linear inequality constraints, see Figure 3.3.

The non-convex Weymouth equation can be replaced by a set of linear inequalities using an outer approximation based on Taylor series expansion around fixed pressured points $v \in \mathcal{V}$. The outer approximation is given by a number of tangent planes to the cone defined by the Weymouth equation, see Figure 3.3, using a set of fixed pressure points $PR_{m,v}, PR_{u,v}, \forall (m,u) \in \mathcal{Z}, v \in \mathcal{V}$ [17, 136, 137]. These linear constraints are calculated based on fixed pressure points generated by choosing multiple pressure values for adjacent nodes within pressure limits as

$$q_{m,u} \leq \frac{K_{m,u}\, PR_{m,v}}{\sqrt{PR_{m,v}^2 - PR_{u,v}^2}} pr_m - \frac{K_{m,u}\, PR_{u,v}}{\sqrt{PR_{m,v}^2 - PR_{u,v}^2}} pr_u, \forall (m,u) \in \mathcal{Z}, v. \tag{3.4}$$

The natural gas flow in each pipeline is approximated by the one linear inequality constraint that is binding out of set (3.4) [17, 136, 137].

For the next part, the assumption of known natural gas flow directions is dropped and both convex relaxation and linear approximation approaches are introduced for the bidirectional gas flow model.

Big-M method

Weymouth equation (2.3), which is piecewise quadratic due to the absolute value, can be rewritten as

$$q_{m,u} = K_{m,u}\sqrt{pr_m^2 - pr_u^2} \;\text{ for }\; q_{m,u} \geq 0; \text{ or} \tag{3.5a}$$

$$q_{m,u} = K_{m,u}\sqrt{pr_u^2 - pr_m^2} \;\text{ for }\; q_{m,u} \leq 0, \tag{3.5b}$$

functionally describing the sign of gas flow. The two cases can be differentiated using binary variable $u_{m,u}$, which determines the direction of gas flow. The following Big-M formulation

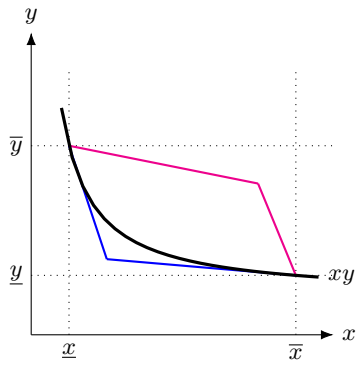

Figure 3.4: McCormick envelopes of bilinear term xy.

enforces auxiliary variables $q^+_{m,u}, q^-_{m,u} \in \mathbb{R}^+$ to describe bidirectional gas flow $q_{m,u} \in \mathbb{R}$:

$$q_{m,u} = q^+_{m,u} - q^-_{m,u}, \tag{3.6a}$$
$$0 \leq q^+_{m,u,t} \leq M\, u_{m,u}, \tag{3.6b}$$
$$0 \leq q^-_{m,u,t} \leq M(1 - u_{m,u}). \tag{3.6c}$$

Adding binary variables introduces non-convexities since discrete spaces are not convex. However, there are off-the-shelf solvers available to solve MILP and MISOCP to optimality. Therefore, the energy flow model is partly convexified by introducing discrete variables. Applying the outer linear approximation approach to the case of bidirectional gas flow is straightforward, while additional steps become necessary to achieve convex relaxation [55, 138].

Despite the relaxation reformulation, there are bilinear terms that make the aforementioned constraint non-convex. The McCormick relaxation [139], popular for approximating multi-linear terms by their linear convex envelopes, can be used to handle these bilinear terms as described in the next section.

Relaxation of bilinear terms

Pursuing convexity, bilinear terms $xy = z$ can be linearized using McCormick envelopes [139, 140]. This relaxation technique defines envelopes of a bilinear function based on variable bounds $\underline{x} \leq x \leq \overline{x}$, $\underline{y} \leq y \leq \overline{y}$. The following set of linear upper and lower bounding inequalities defines McCormick envelopes to replace the original bilinear term,

$$z \geq \underline{x}y + x\underline{y} - \underline{x}\underline{y} \tag{3.7a}$$
$$z \geq \overline{x}y + x\overline{y} - \overline{x}\overline{y} \tag{3.7b}$$
$$z \leq \underline{x}y + x\overline{y} - \underline{x}\overline{y} \tag{3.7c}$$
$$z \leq \overline{x}y + x\underline{y} - \overline{x}\underline{y}. \tag{3.7d}$$

This McCormick relaxation handles bilinear terms efficiently, see Figure 3.4. For further tightening McCormick envelopes, bounds can be tightened in an iterative manner, see [141].

To sum up, the original NLP (3.1) under the assumption of known gas flow direction can be relaxed into an SOCP or approximated by an LP. Including binary variables to account for variable flow directions renders model (3.1) an MINLP which can be relaxed into an MISOCP or approximated by an MILP.

3.2 Energy network flexibility

In this section, the heat sector in form of district heating networks is incorporated resulting in the combined power, gas and heat dispatch formulated as a co-optimization problem. The gas system is modeled based on the assumption of known flow directions and the steady-state equation is relaxed into a second-order cone constraint, as described in Section 3.1.2. The propagation of heat flow through parallel supply and return pipelines in the heating network was described in Section 2.3.3. The time delay of heat propagation allows to temporally decouple the heat production from the heat consumption. Since mass flow rates in the pipelines directly impact the time it takes for heat to propagate throughout the pipelines, there is potential to store a large amount of heat inside the pipelines. In particular, having both inlet temperatures and mass flow rates as control variables allows to optimize the energy stored in the pipelines. Thus, on top of linepack from the gas side, mass flow rates and inlet temperatures are modeled as control variables to account for the energy storage capacity in heat pipelines based on the model proposed in [24]. With these additional degrees of freedom the delay of heat propagation is optimized for energy storage purposes.

3.2.1 Combined power, natural gas and heat dispatch

In the following, the co-optimization from Section 3.1.1 is extended to include district heating networks. Heat demand and production are modeled as a combination of temperature difference between supply and return networks and mass flow at heat exchange stations, see equations (2.9). Limits on heat production capacity, mass flow rates, nodal pressures and nodal temperatures are enforced. Mass flows at network nodes are balanced. Heat propagation is defined by outlet temperatures depending on past inlet temperatures, heat losses, and varying time delays, see equations (2.10)-(2.11). Darcy-Weisbach equation (2.8) given in Section 2.3.3 describes the pressure loss along a pipeline due to friction. The minimum pressure drop is enforced between supply and return pipelines at heat exchange stations. Additional coupling constraints translate heat production by heat pumps into time varying nodal electricity load, and power and heat outputs of combined heat and power (CHP) units are linked through an output ratio describing the feasible operating region. A general form of the combined power, natural gas and heat dispatch problem is given as

$$\min_{\boldsymbol{x}^{\mathrm{E}},\boldsymbol{x}^{\mathrm{G}},\boldsymbol{x}^{\mathrm{H}},\boldsymbol{u}^{\mathrm{H}}} \quad f\boldsymbol{x}^{\mathrm{E}}) + f(\boldsymbol{x}^{\mathrm{G}}) + f(\boldsymbol{x}^{\mathrm{H}}) \tag{3.8a}$$

$$\text{subject to} \quad h^{\mathrm{E}}(\boldsymbol{x}^{\mathrm{E}}) = 0, \;\; g^{\mathrm{E}}(\boldsymbol{x}^{\mathrm{E}}) \leq 0, \tag{3.8b}$$

$$h^{\mathrm{G}}(\boldsymbol{x}^{\mathrm{G}}) = 0, \;\; g^{\mathrm{G}}(\boldsymbol{x}^{\mathrm{G}}) \leq 0, \tag{3.8c}$$

$$h^{\mathrm{H}}(\boldsymbol{x}^{\mathrm{H}}, \boldsymbol{u}^{\mathrm{H}}) = 0, \;\; g^{\mathrm{H}}(\boldsymbol{x}^{\mathrm{H}}, \boldsymbol{u}^{\mathrm{H}}) \leq 0, \tag{3.8d}$$

$$h^{\mathrm{E,G}}(\boldsymbol{x}^{\mathrm{E}}, \boldsymbol{x}^{\mathrm{G}}) = 0, \tag{3.8e}$$

$$h^{\mathrm{E,H}}(\boldsymbol{x}^{\mathrm{E}}, \boldsymbol{x}^{\mathrm{H}}) = 0, \;\; g^{\mathrm{E,H}}(\boldsymbol{x}^{\mathrm{E}}, \boldsymbol{x}^{\mathrm{H}}) \leq 0, \tag{3.8f}$$

where $\boldsymbol{x}^{\mathrm{H}}$ and $\boldsymbol{u}^{\mathrm{H}}$ are vectors of continuous and binary heat variables, respectively. Compared to the co-optimization problem (3.1), component $f(\boldsymbol{x}^{\mathrm{H}})$ pertaining to the heat system is added to the objective function. Constraints $h^{\mathrm{H}}(\boldsymbol{x}^{\mathrm{H}}, \boldsymbol{u}^{\mathrm{H}}) = 0$ and $g^{\mathrm{H}}(\boldsymbol{x}^{\mathrm{H}}, \boldsymbol{u}^{\mathrm{H}}) \leq 0$ are the heat system equality and inequality constraints, respectively. In these constraints, binary variables $\boldsymbol{u}^{\mathrm{H}} \in \{0, 1\}$ are required to model the time delays and temperature mixing. The additional coupling constraints $h^{\mathrm{E,H}}(\boldsymbol{x}^{\mathrm{E}}, \boldsymbol{x}^{\mathrm{H}}) = 0$ and $g^{\mathrm{E,H}}(\boldsymbol{x}^{\mathrm{E}}, \boldsymbol{x}^{\mathrm{H}}) \leq 0$ in (3.8f) link power and heat systems together. Linear inequality $g^{\mathrm{E,H}}(\boldsymbol{x}^{\mathrm{E}}, \boldsymbol{x}^{\mathrm{H}}) \leq 00$ describes the feasible operating regions of CHP units linking power

and heat outputs. Linear equality constraints $h^{\mathrm{E,H}}(\boldsymbol{x}^{\mathrm{E}}, \boldsymbol{x}^{\mathrm{H}}) =$ give heat production and power consumption of heat pumps as well as nodal power balance including electricity share of CHP generation and time-varying nodal electricity demand from heat pumps. Note that incorporating further coupling between heat and natural gas systems, e.g., via gas-fired boilers and gas-fired CHPs, is straightforward. The detailed version of MINLP (3.8) is given in [**Paper A**].

Heat system constraints (3.8f) are mixed-integer and non-convex. Discrete variables model the time delay of heat propagation in heat pipelines. Quadratic equality constraints (2.8) describe the pressure drop along pipelines. Bilinear terms are used to model heat demand and production as mass flow times nodal temperature difference between supply and return networks in (2.9). The relationship of heat propagation in heat pipelines, varying time delays and mass flow rates in equations (2.10)-(2.11) is non-convex.

3.2.2 Convexification

Apart from the discrete solution space, the non-convexities that arise from heat dynamics can be made convex using the techniques from Section 3.1.2. Quadratic relaxation is applied to the quadratic Darcy-Weisbach equation (2.8), see Figure 3.2. The equality is relaxed by allowing the pressure differences to be equal to or greater than the square of the mass flow rates resulting in second-order cone constraints. Additionally, McCormick envelopes are used to linearize bilinear terms. The products of temperature gradients and mass flow rates used to model heat production and consumption at heat exchange stations in (2.9) are relaxed into McCormick envelopes (3.7). Following the approach from [24], variable delay of heat propagation in (2.10)-(2.11) can be linearized using auxiliary binary variables and a Big-M formulation. Finally, the non-convex and non-linear relationship for mass flow of heat transfer in the pipelines is linearized in an exact way using auxiliary binary variables and Big-M formulation using the approach from [24]. Applying these convexification strategies to (3.8) results in a MISOCP which can be solved to optimality using off-the-shelf solvers.

3.3 Numerical examples: Value of multi-energy system coordination

This section analyzes the additional flexibility and synergies that can be harnessed among natural gas, heat and electricity systems. In this section, the proposed conic relaxation of the multi-energy dispatch models are compared to models neglecting energy flow dynamics and thus the energy storage capacity of gas and heat networks. The models are evaluated in terms of the total system cost and the share of power production covered by wind production.

Modified case studies are built upon the IEEE 24-bus Reliability Test System [142] and a 12-node natural gas system based on [17] and the 3-node district heating network in [24]. The scheduling horizon is 24 hours. Data and network topologies are provided in [**Paper A**] and [**Paper B**] and their online appendices, respectively.

3.3.1 Added value from cross-carrier synergies and network flexibility

The numerical results emphasize that gas-fired generators, CHP units and heat pumps offer cross-carrier flexibility. Gas-fired generators are used for covering peak load and reacting to variability of wind power production. Similarly, CHP units produce both electricity and heat during periods of high electricity demand or low wind production. When electricity demand is low and wind

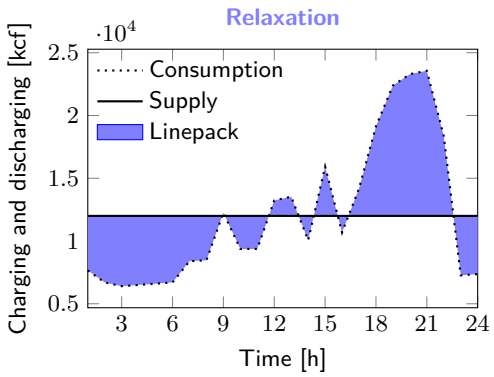

Figure 3.5: Hourly profiles of natural gas supply/consumption using a convex relaxation technique.

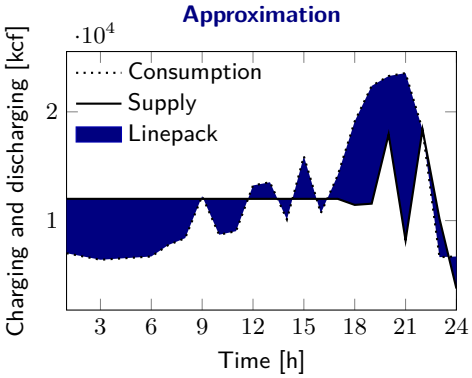

Figure 3.6: Hourly profiles of natural gas supply/consumption using a linear approximation technique.

production is high, heat pumps are used to produce heat from excess wind. This highlights the benefits of modeling and harnessing the cross-carrier flexibility of gas-fired units, CHPs and heat pumps. Furthermore, the flexibility from energy storage in gas and heat pipelines is unlocked. First, results are discussed for the combined natural gas and power dispatch model (3.1) including linepack and bidirectional gas flow from Section 3.1.1, comparing the relaxation technique with the outer linear approximation explained in Section 3.1.2. Afterwards, heat infrastructure is included and results for the convexified combined power, natural gas and heat dispatch model (3.8) from Section 3.2.1 are presented.

Linepack flexibility for power systems

Accounting for natural gas and heat flow dynamics using relaxation or approximation techniques unlocks the storage capacity of these energy networks. Figs. 3.5 and 3.6 show the total supply and consumption of natural gas over 24-hour time horizon. These graphs show that demand and supply of gas do not necessarily need to be matched in each time period. Supply and consumption are decoupled due to the amounts of energy stored in the pipelines as linepack, which is highlighted in shaded areas. Linepack is accumulated inside the pipelines, especially during periods of high wind power production and low levels of power and gas loads, e.g., during hours 1-9. This corresponds to "charging" the storage of natural gas network and the stored energy can be consumed later, i.e., "discharging". This storage function of the network directly impacts the profile of gas supply. Profiles of consumption, supply and linepack storage are slightly different for the relaxation technique compared to the approximation. While with the relaxation technique the gas supply profile completely flattens (see Figure 3.5), the linepack accumulated throughout the day under the approximation approach varies slightly such that the energy storage in pipelines is not sufficient to fuel all natural gas consumption in the last hours of the day in Figure 3.6.

Figure 3.7 shows the total cost of the integrated power and gas systems under varying levels of wind penetration which is defined as total wind power capacity divided by total power load. It is evident that the cost is decreasing with increasing levels of wind penetration. This plot shows the comparison of total system cost for four cases: i) neglecting linepack flexibility, ii) accounting for network flexibility using relaxation, or iii) approximation techniques, and iv) assuming ideal electricity storage. The ideal electricity storage allows shifting of power demand and supply over

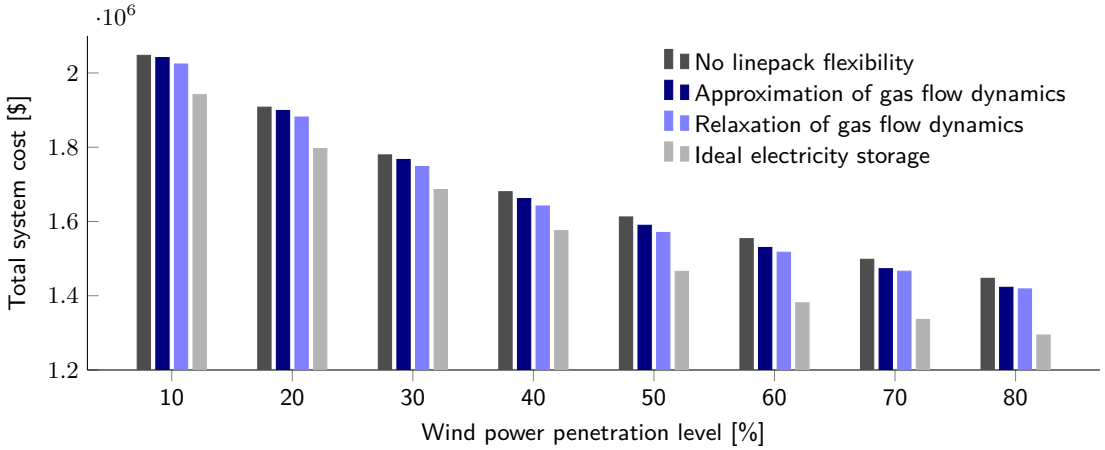

Figure 3.7: Total cost of the fully coordinated power and gas systems for different levels of wind power penetration, i.e., the share of total installed wind power capacity on maximum power demand.

the planning horizon, assuming unlimited storage as well as charging and discharging capacities. Upper and lower bounds for the total system cost are provided by the cases neglecting linepack and assuming ideal storage, respectively. Revealing linepack flexibility decreases the total system cost. Accounting for linepack by relaxing or approximating the gas flow dynamics results in a decreased total system cost by 2% and 1% on average, respectively. These two approaches yield mean cost savings equal to 25.5% and 13.1% of the ideal storage.

Network flexibility as virtual electricity storage

The supply and consumption of natural gas and heat over the simulated 24 hours are depicted in Figs. 3.8 and 3.10, respectively. These graphs show that demand and supply of gas and heat do not necessarily need to be matched in each time period. Supply and consumption are decoupled due to the amounts of energy stored in the pipelines, which are highlighted as shaded areas in Figs. 3.9 and 3.11. Accounting for the natural gas and heat flow dynamics unlocks the storage capacity of these energy networks. The storage function of the networks directly impacts the profiles of gas and heat supply. Energy is accumulated inside the pipelines, especially during periods of high wind power production and low levels of energy loads, e.g., in hours 1-8, 16-17 and 24. This corresponds to charging the virtual electricity storage, while the stored energy can be consumed later during discharging of the network storage. This leads to a cost-efficient shift of gas, heat and even power supply and demand. The flexibility revealed from the pipelines decreases the total system cost, see Figure 3.12. This plot shows the total cost of the integrated energy system with and without accounting for flow dynamics and network flexibility for different rates of wind power penetration. Results from the convexified version of model (3.8) are compared to a dispatch that does not account for network flexibility. By having network flexibility the total system cost decreases by around 2% on average.

Moreover, the revealed network flexibility allows to shift electricity production and consumption such that wind curtailment can be reduced. Figure 3.13 shows the effect of network flexibility on renewable penetration. Wind curtailment lowers by 1.2% on average, solely thanks to network flexibility from heat and gas sectors. This effect is mainly driven by power-to-heat units, i.e., heat

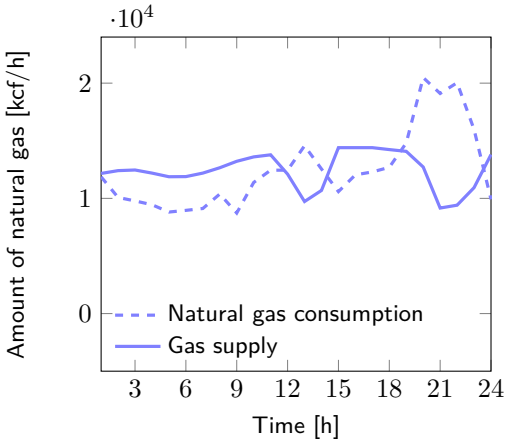

Figure 3.8: Hourly profile of natural gas supply/consumption.

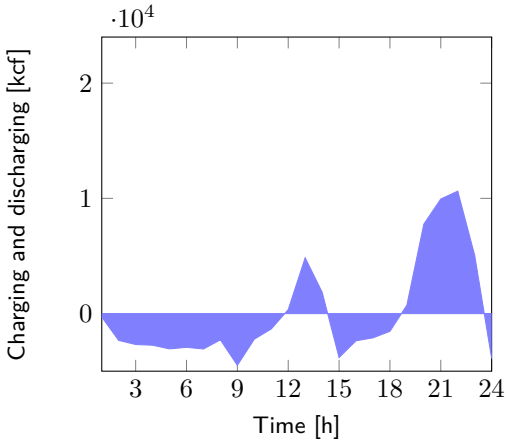

Figure 3.9: Hourly charging/discharging profile of linepack storage.

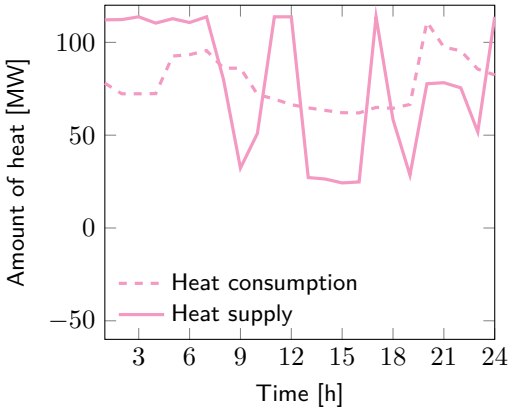

Figure 3.10: Hourly profile of heat production/consumption.

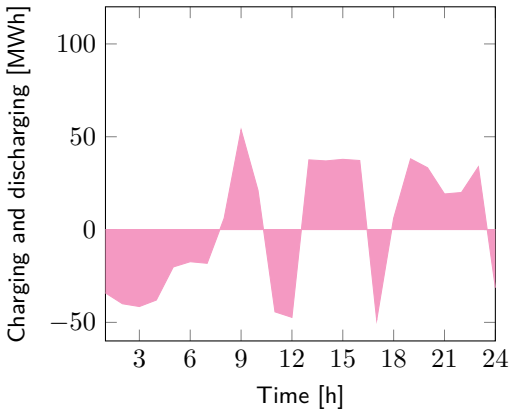

Figure 3.11: Hourly charging/discharging profile of heat network storage.

pumps, and can be expected to become even more important with power-to-gas units.

3.3.2 Feasibility evaluation

Since the presented solutions are based on relaxations and approximations of the original constraints, a check to see if the original constraints actually hold is performed a posteriori. This shows whether the relaxations and approximations are exact.

For the heat side, binary variables and mass flow rates are fixed to the results derived from the relaxation and then a linear program is solved for the original constraints. A feasible solution is obtained when adjusting the parametric temperature bounds. For the gas side, the left- and right-hand sides of the relaxed Weymouth equations for all time steps and all pipelines are compared. The relative error of the mismatch is computed as the inexactness gap and is below 2% for the unidirectional case as well as approximation and relaxation in the bidirectional case. The second-order cone relaxation of bidirectional gas flow without linepack dynamics is proven to provide a tight lower bound in [143] and proven exact for non-radial networks in [138]. Although

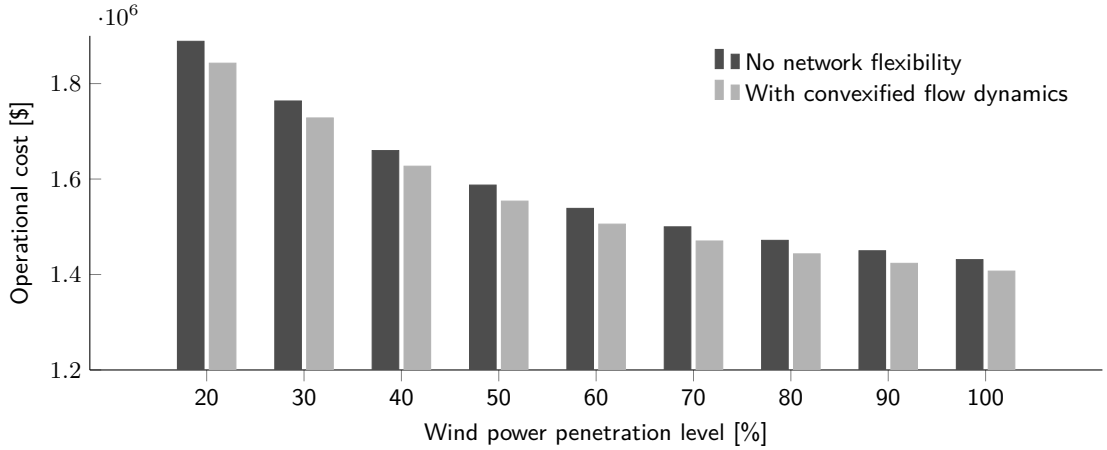

Figure 3.12: Total system cost of the integrated energy system with and without considering network flexibility for increasing levels of wind power penetration.

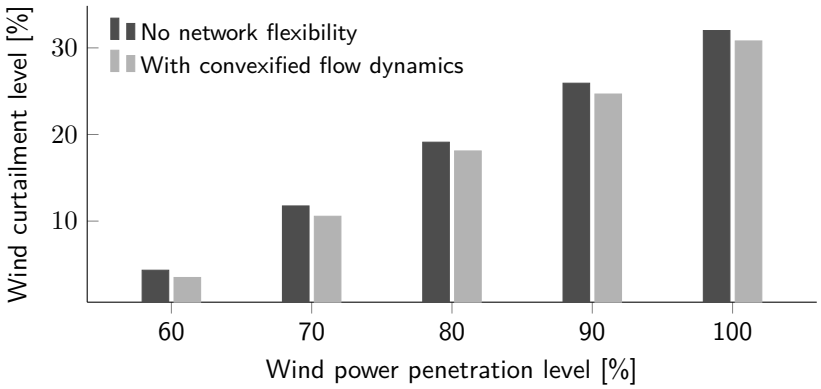

Figure 3.13: Comparison of wind curtailment level with and without accounting for network flexibility.

the relaxation is applied to a meshed network and linepack dynamics are included, the occurrence of mismatch is very low and mostly pipelines within the loop of the gas network are at risk of inexact relaxation. However, for the bidirectional case, the occurrence rate is higher since McCormick relaxation is also used, which is not exact. As potential ways to further tighten SOC and McCormick relaxations, see [141, 144]. Trade-offs need to be made between tightness, computational complexity and accuracy of the proposed solution methods.

The proposed co-optimization models provide an ideal benchmark of the optimal operation of integrated electricity, natural gas and heat systems at the day-ahead stage. Although this approach is not practical in the current market regulations, it provides the basis to quantify the value of increasing the coordination among energy systems. Coordination of energy carriers is an inexpensive solution to provide operational flexibility to the power system. Especially natural gas and heat networks provide flexibility to mitigate the variability of renewables in the power system. This motivates investigating the impact of uncertainty arising from wind power forecasts in Chapter 4 as well as new market-based coordination approaches, which will be presented in Chapter 5. While the next two chapters focus on power-gas coordination, the concepts can be deduced for the heat side given some modifications.

CHAPTER 4

Full Coordination: An Uncertainty-Aware Benchmark

The growing interdependence of power and natural gas systems causes short-term uncertainty to propagate from the power to the gas side[1]. Efficient procurement of flexibility for the power system from interfacing with the natural gas system requires not only the consideration of operational constraints of the natural gas system, but also awareness of existing uncertainty. In order to deal with uncertainty and correctly anticipate flexibility from natural gas systems, a unified power and gas coordination mechanism is developed that models the uncertainty propagation from the power to the gas side and enables the provision of short-term flexibility by the gas system. This chapter introduces *policy-based reserve products* enabling the coordinated response of agents in both sectors to deviations in power and gas systems due to uncertainty originated from the power side.

This chapter firstly discusses the concept of uncertainty awareness for coordination problems in Section 4.1. Then distributionally robust chance-constrained co-optimization of power and natural gas systems is introduced in Section 4.2. Since the resulting model is intractable, Section 4.3 describes the steps towards achieving tractability by defining affine policies for recourse actions of flexible assets, reformulating objective function and balance constraints, and eventually by conic approximation of probabilistic chance constraints. Finally, a case study in Section 4.4 numerically studies the mitigation of short-term uncertainty propagated from the power side to the gas system. The introduced reserve products reveal short-term operational flexibility that can be harnessed from flexible assets. Specifically, gas-side players including gas-fired units, gas suppliers, and the gas network are activated to provide response in real-time when facing spatio-temporal uncertainty.

4.1 Towards uncertainty awareness in coordination problems

The existing uncertainty-aware coordination problems in the literature for multi-energy systems are based on scenario-based stochastic programming [17, 18, 35, 145, 146], robust optimization [110, 147, 148], and chance-constrained optimization [111]. However, all these techniques have their own shortcomings. Since a large number of scenarios is in general necessary to adequately characterize the true probability distribution of the source of uncertainty, scenario-based approaches suffer from high computational expense [54, 149, 150]. Reducing the number of scenarios restores tractability, but may lead to weak out-of-sample performance [151]. Robust optimization, on the other hand, encapsulates the underlying distribution of uncertainty in a set, the so-called uncertainty set, assuming such a distribution is known [152]. Uncertainty sets are often ellipsoidal, polyhedral, or built in a data-driven way [86, 153]. A robust model optimizes against the worst-case realization over the support of the uncertainty set [154, 155], which may provide overly

[1] Uncertainty propagation could be in both directions in the future by integrating renewable biogas sources.

conservative decisions [156]. Chance-constrained optimization is used to obtain the optimal solution that satisfies constraints at certain probabilities, i.e., the user-defined constraint violation probabilities [52, 53, 111]. Chance-constrained programming allows for tuning the probability of violating operational limits under extreme realizations of uncertainty. Analytical reformulation and convexification strategies for chance constraints allow adjustable conservativeness at low computational cost providing a satisfactory out-of-sample performance [157, 158].

While the aforementioned approaches usually assume some knowledge of the underlying distribution of the uncertain parameter, distributionally robust optimization as a data-driven approach assumes partial distributional information only. This approach, firstly introduced in [52], has conceptual and computational advantages for coping with uncertainty [159]. The distribution of uncertain parameters can be unknown while available information regarding uncertainty is taken into account without relying on a single probabilistic model. Distributionally robust programming optimizes in *expectation* against the *worst-case* distribution among a family of distributions collected in a set, the so-called ambiguity set. Outcomes of distributionally robust optimization offer a strong performance guarantee for all distributions in the ambiguity set. Moreover, distributionally robust optimization problems can often be solved exactly while maintaining computational efficiency [53, 159]. In summary, in contrast to other uncertainty modeling techniques, the distributionally robust approach bridges the gap between robustness and assumptions on distributional information while allowing tractability and computational efficiency [159].

A comprehensive review for distributionally robust optimization is available in [159], a tutorial is found in [160], while [161] provides a technical survey. Distributionally robust optimal power flow problems are explored in [162–166], a distributionally robust electricity market clearing is proposed in [167], while a distributionally robust power and gas coordination problem is proposed in [168, 169].

4.2 Distributionally robust chance-constrained power and gas coordination

The concept of distributionally robust power and gas coordination is illustrated in Figure 4.1. Out-of-sample simulations are necessary to assess the performance of the optimal solution based on the "training" dataset with respect to "test datasets" during real-time operations. However, in this chapter out-of-sample simulations are conducted without re-optimization. Thus, the out-of-sample analysis is carried out based on projected instead of realistic operations [169]. These projected out-of-sample simulations without re-optimization are referred to as "ex-ante" out-of-sample simulations in the following and are used to evaluate the quality of optimal day-ahead schedules and affine policies.

4.2.1 Definition of moment-based ambiguity sets

The key feature of distributionally robust optimization is the representation of uncertainty through an ambiguity set, which describes a family of probability distributions consistent with available data. In order to reduce conservativeness while keeping the problem robust against the unknown true distribution, the ambiguity set should be chosen to be as small as possible, while containing the unknown true distribution with certainty or at least with a high confidence [159]. Using data-driven approaches to build ambiguity sets facilitates them to comprise probability distributions consistent with available information. Based on the construction method, ambiguity sets can be separated into two categories: *Metric-based* ambiguity sets are determined by the distributions that are close

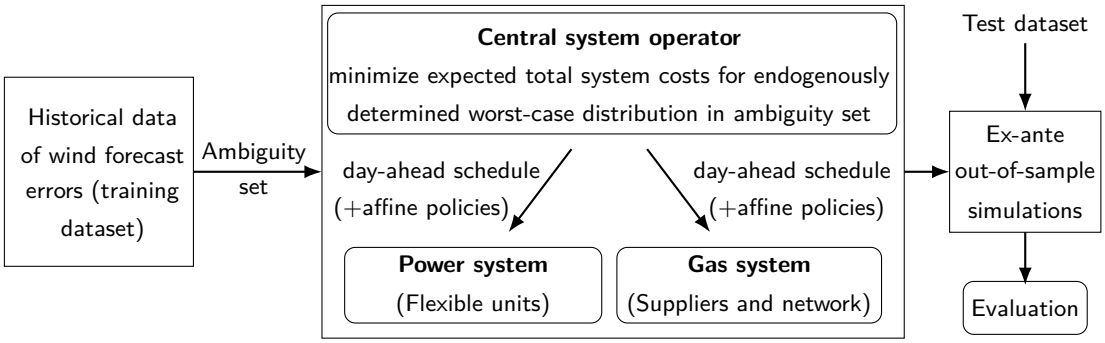

Figure 4.1: Uncertainty-aware coordinated power and natural gas day-ahead dispatch: A distributionally robust approach.

to an empirical one with respect to a discrepancy measure [53], while *moment-based* ambiguity sets are defined by imposing constraints on moments of the distribution [52, 170]. For metric-based ambiguity sets showing the notion of distance from a reference distribution, the interested reader is referred to [53, 171], whereas the focus is on moment-based ambiguity sets in the following.

Typically, a family of probability distributions with identical first- and second-order moments, i.e., mean vector and its covariance matrix, is selected, since second-order moment information helps to properly model existing spatial and temporal correlations of uncertainties.

An ambiguity set Π is defined as a collection of all multivariate probability distributions $\mathbb{P} \in \Pi$ with the same first and second-order moments $\boldsymbol{\mu}^{\Pi}$ and $\boldsymbol{\Sigma}^{\Pi}$, respectively. When the value for these two moments is derived from historical data, this approach can be treated as a "data-driven" method. The moment-based ambiguity set is given as

$$\Pi = \{\mathbb{P} \in \Pi : \mathbb{E}_{\mathbb{P}}[\Omega] = \boldsymbol{\mu}^{\Pi}, \mathbb{E}_{\mathbb{P}}\left[\Omega\Omega^{\top}\right] = \boldsymbol{\Sigma}^{\Pi}\}, \tag{4.1}$$

with $\mathbb{E}$ as the expectation operator and Ω denoting the vector of uncertainties. Each probability distribution $\mathbb{P}$ in the ambiguity set represents a potential distribution of uncertainty faced by the problem and the true probability distribution is assumed to come from within this moment-based ambiguity set Π. Thus, the true values of moments are assumed to be estimated from historical data, while for inexact moments see [163]. The moment-based ambiguity set can be shrunk further by adding higher-order moments [151] or additional features, e.g., uni-modality [172].

4.2.2 Distributionally robust chance-constrained modeling framework

The full coordination models (3.1) and (3.8) in Chapter 3 dealt with uncertainty in an agnostic manner using deterministic forecasts of uncertain renewable power production. However, the combined energy dispatch is affected by substantial short-term uncertainty because wind power forecast parameters $\boldsymbol{W}$ are subject to errors at the day-ahead scheduling stage. The full coordination model is extended to embed the characterization of short-term uncertainty following an unknown distribution, see Figure 4.1. Here, Ω denotes the vector of forecast errors, which is assumed to follow a distribution whose first- and second-order moments can be estimated from historical data.

The proposed uncertainty-aware combined power and natural gas dispatch model determines the optimal power generation and gas supply schedules, resulting in the minimum expected total system cost under the worst-case distribution in the ambiguity set. This distribution is

endogenously determined by the proposed model. Operational limits are enforced in the form of distributionally robust chance constraints which enable adjusting the conservativeness of operational decisions against the worst distribution of short-term uncertainties, i.e., wind power forecast errors. Assuming that uncertainty distributions are not perfectly known, distributionally robust chance-constraints ensure that operational limits are satisfied with a certain probability for any distribution in an ambiguity set. In a generic form the coordinated optimal dispatch problem is written as

$$\min_{\tilde{\boldsymbol{x}}^{\mathrm{E}}(\Omega),\tilde{\boldsymbol{x}}^{\mathrm{G}}(\Omega)} \quad \max_{\mathbb{P}\in\Pi} \ \mathbb{E}_{\mathbb{P}}\left[{c^{\mathrm{E}}}^{\top}\tilde{\boldsymbol{x}}^{\mathrm{E}}(\Omega) + {c^{\mathrm{G}}}^{\top}\tilde{\boldsymbol{x}}^{\mathrm{G}}(\Omega)\right] \tag{4.2a}$$

$$\text{subject to} \ \min_{\mathbb{P}\in\Pi} \ \mathbb{P}\left[\tilde{x}_i^{\mathrm{E}}(\Omega) \le \overline{x}_i^{\mathrm{E}}\right] \ge (1-\epsilon_i), \ \ \forall i, \tag{4.2b}$$

$$\min_{\mathbb{P}\in\Pi} \ \mathbb{P}\left[\tilde{x}_k^{\mathrm{G}}(\Omega) \le \overline{x}_k^{\mathrm{G}}\right] \ge (1-\epsilon_k), \ \ \forall k, \tag{4.2c}$$

$$\boldsymbol{e}^{\top}\tilde{\boldsymbol{x}}^{\mathrm{E}}(\Omega) - \boldsymbol{e}^{\top}\left(\boldsymbol{W}-\Omega\right) - \boldsymbol{e}^{\top}\boldsymbol{D}^{\mathrm{E}} = 0, \tag{4.2d}$$

$$\boldsymbol{e}^{\top}\tilde{\boldsymbol{x}}^{\mathrm{G}}(\Omega) - \phi^{\top}\tilde{\boldsymbol{x}}^{\mathrm{E}}(\Omega) - \boldsymbol{e}^{\top}\boldsymbol{D}^{\mathrm{G}} = 0, \tag{4.2e}$$

$$h^{\mathrm{E}}\left(\tilde{\boldsymbol{x}}^{\mathrm{E}}(\Omega)\right) = 0, \ \ h^{\mathrm{G}}\left(\tilde{\boldsymbol{x}}^{\mathrm{G}}(\Omega)\right) = 0, \tag{4.2f}$$

where the vector of stochastic decision variables $\tilde{\boldsymbol{x}}^{\mathrm{E}}(\Omega) = \left[\tilde{x}_1^{\mathrm{E}}(\Omega) \ ... \ \tilde{x}_i^{\mathrm{E}}(\Omega) \ ... \ \tilde{x}_I^{\mathrm{E}}(\Omega)\right]^{\top}$ contains variables pertaining to the power side including generator power production and nodal power injections. Similarly, for the gas side the vector of stochastic variables $\tilde{\boldsymbol{x}}^{\mathrm{G}}(\Omega) = \left[\tilde{x}_1^{\mathrm{G}}(\Omega) \ ... \ \tilde{x}_k^{\mathrm{G}}(\Omega) \ ... \ \tilde{x}_K^{\mathrm{G}}(\Omega)\right]^{\top}$ comprises gas supplier injections, pressure at gas nodes, gas flow rates, and linepack. Note that $\boldsymbol{e}$ is an appropriately sized vector of ones and that there are different sets of individual chance constraints indexed by $i \in I$ and $k \in K$ for power and gas systems, respectively.

The objective function (4.2a) with a two-stage min-max structure seeks to minimize the expected total system cost under the worst probability distribution $\mathbb{P}$ within the ambiguity set Π. The first term describes power production cost and the second term gas supply cost with parameters c^{E} and c^{G} as marginal costs.

Note that $\tilde{x}_i^{\mathrm{E}}(\Omega) \le \overline{x}_i^{\mathrm{E}}$ and $\tilde{x}_k^{\mathrm{G}}(\Omega) \le \overline{x}_k^{\mathrm{G}}$ in (4.2b) and (4.2c) are infinite-dimensional constraints, i.e., they are valid for the entire distribution representing Ω. In order to make these constraints single-dimensional and therefore tractable, an operator is needed, in this case chance-constraints. Alternatively, Conditional Value-at-Risk (CVaR) [173] operator could be used, but at the expense of additional modeling complexity and potentially conservativeness [174]. By using CVaR constraints, not only the violation probability but also the violation magnitude can be limited, but it is outside the scope of this thesis. Here, operational bounds and limits (4.2b) and (4.2c) are formulated as distributionally robust individual chance constraints defined over ambiguity set Π. These chance constraints need to be satisfied for all distributions within the moment-based ambiguity set (4.1) with predefined violation probabilities ϵ_i and ϵ_k, respectively. Parameters $\epsilon_i, \epsilon_k \in [0,1]$ reflect the safety factor for the ambiguous chance constraints to hold or the risk attitude of the decision maker, such that under the worst distribution in ambiguity set Π, the probability that each constraint is met is greater than or equal to $1-\epsilon_i$ or $1-\epsilon_k$, respectively. In this manner, the conservativeness of the model can be adjusted. Inequalities (4.2b) include parameters $\overline{x}_i$ for generator limits and power line flow limits. The bounds (4.2c) denote gas supply limits, pressure limits and direction of gas flow with parameters $\overline{x}_k$. Note that the worst distribution is not necessarily identical for each individual chance constraint (4.2b) and (4.2c) or identical to that of objective function (4.2a). For distributionally robust joint chance constraints see [170, 175].

Nodal power balance (4.2d) ensures that the total deterministic fixed power load $\boldsymbol{D}^{\mathrm{E}}$ is met by power production from conventional and wind units with parameter $\boldsymbol{W}$ as the mean forecast, and $\boldsymbol{W} - \Omega$ as the uncertain wind production containing the mean wind forecast and the forecast error.

Nodal gas balance (4.2e) couples the gas and power systems together, by ensuring that gas supply meets total gas demand including fuel consumption of gas-fired units via fuel conversion factor ϕ and deterministic fixed gas demand $\boldsymbol{D}^{\mathrm{G}}$. Linear functions $h^{\mathrm{E}}\left(\tilde{\boldsymbol{x}}^{\mathrm{E}}(\Omega)\right)$ and $h^{\mathrm{G}}\left(\tilde{\boldsymbol{x}}^{\mathrm{G}}(\Omega)\right)$ represent other equality constraints pertaining to power and gas systems, respectively. For instance, the power flow through the transmission lines is determined using the power transfer distribution factor matrix, which defines the power flow as a linear function of nodal injections and withdrawals, as described in equation (2.2) in Section 2.3. Intertemporal dynamics of operating linepack in pipelines as well as quadratic unidirectional Weymouth equation governing the physics of steady-state gas flow are captured in $h^{\mathrm{G}}\left(\tilde{\boldsymbol{x}}^{\mathrm{G}}(\Omega)\right)$. All equality constraints are enforced surely and are supposed to be respected for any potential realization of uncertainty, though they also depend on short-term uncertainty Ω. The reason is twofold: On the one hand, balance constraints are considered crucial for the physical operation meaning that they should be satisfied for entire Ω. On the other hand, the probabilistic nature of equalities can be handled mathematically (unlike inequalities (4.2b) and (4.2c)), as it will be described later in Sections 4.3.3 and 4.3.2.

The distributionally robust chance-constrained power and natural gas co-optimization model (4.2) is intractable due to the infinite-dimensional nature of the problem. To achieve computational tractability, linear decision rules [176] are applied to analytically reformulate the probabilistic constraints (4.2b) and (4.2c), as well as the objective function and equality constraints. Furthermore, quadratic and McCormick relaxations are used to convexify gas flow equations as described in Section 3.1.2.

4.3 Towards tractability

The issue with the current formulation of model (4.2) is that the stochastic nature of decision variables makes the constraints infinite-dimensional and the problem becomes unsolvable. To ensure solvability a moment-based ambiguity set Π of uncertainty is defined that contains all probability distributions with zero mean, i.e., $\boldsymbol{\mu}^{\Pi} = 0$, and covariance $\boldsymbol{\Sigma}^{\Pi}$ available through analysis of historical forecast errors. Note that the wind power forecast $\boldsymbol{W}$ can be adjusted so that the mean of forecast errors $\boldsymbol{\mu}^{\Pi}$ becomes 0 without loss of generality. In the following, affine policies are introduced and reformulation of the objective function, equality constraints and chance constraints are explained. These steps allow recasting the proposed model as a second-order cone program with reasonable computational performance such that a tractable reformulation of the distributionally robust chance-constrained problem (4.2) is achieved.

Alternatively, a solution for (4.2) can be obtained via a sample average approximation (SAA) based on randomization of uncertainty bounds and computation by scenario-based approach, see [177].

4.3.1 Affine policies

To mitigate the intractability of the proposed model, recourse actions for real-time adjustments are defined as affine policies based on linear decision rules [176]. Restricting the adjustable variables to be affine functions of the uncertain data was initially proposed in [178] and referred to as the linear decision rule approach in [176]. These affine policies are developed to control the flexibility

procurement from conventional power generators, gas suppliers, and gas network operator to react to deviations in real-time operations. Moreover, the affine policies help to analytically reformulate the distributionally robust chance constraints. Affine policies are useful tools for approximation of adjustable robust optimization problems since linear decision rules have been proven to be effective for decision making under uncertainty [179] and even optimal under some conditions [180]. Reference [179] empirically shows the appropriate performance of affine policies in two-stage robust optimization problems. In [180] necessary and sufficient conditions are provided for affine policies to be optimal in multi-stage robust optimization problems. Generalized (e.g., non-linear) decision rules are discussed in [181].

Following the approach in [127], affine policies are selected such that the activation of flexibility during the real-time operation stage is a linear function of the total balancing need due to wind power deviation system-wide. Assets from both power and gas systems can contribute to these recourse actions. Affine policies for flexible agents to perform recourse actions that can be activated in real-time are defined as a function of uncertainty Ω. The eventual schedules $\tilde{\boldsymbol{x}}^E(\Omega)$ and $\tilde{\boldsymbol{x}}^G(\Omega)$ are given by the tentative day-ahead schedules $\boldsymbol{x}^{\mathrm{E}}$ and $\boldsymbol{x}^{\mathrm{G}}$ and the recourse actions with respect to the forecast deviation of uncertainty Ω and participation factors $\boldsymbol{\alpha} \in [-1, 1]$ and $\boldsymbol{\beta}$ according to

$$\tilde{\boldsymbol{x}}^E(\Omega) = \boldsymbol{x}^{\mathrm{E}} + (\boldsymbol{e}^\top \Omega)\boldsymbol{\alpha}, \tag{4.3a}$$

$$\tilde{\boldsymbol{x}}^G(\Omega) = \boldsymbol{x}^{\mathrm{G}} + (\boldsymbol{e}^\top \Omega)\boldsymbol{\beta}, \tag{4.3b}$$

such that schedules are defined as the sum of a *deterministic* and a *stochastic* component. Tentative schedules and affine policies are decided endogenously through the day-ahead dispatch. The participation factor determines the share each flexible unit provides towards the mitigation of uncertainty. In other words, depending on whether there is a surplus or deficit in the system due to forecast errors, flexible assets adjust by increasing or decreasing their supply to balance the deviation in the system. Affine policies are optimized so that the cost of redispatch, which needs to be done closer to real-time, can be reduced.

Using these affine control policies with $\boldsymbol{\mu}^{\Pi} = 0$, objective function (4.2a), and equality constraints (4.2d), (4.2e) and (4.2f) can be analytically reformulated as explained below.

4.3.2 Reformulation of objective function

Following the argumentation of [182], objective function (4.2a), which is a two-stage min-max problem, can be recast as a single-stage minimization problem. Stochastic variables $\tilde{\boldsymbol{x}}^{\mathrm{E}}(\Omega)$ and $\tilde{\boldsymbol{x}}^{\mathrm{E}}(\Omega)$ are substituted with linear decision rules (4.3), so that (4.2a) rewrites as

$$\min_{\boldsymbol{x}^{\mathrm{E}}, \boldsymbol{\alpha}, \boldsymbol{x}^{\mathrm{G}}, \boldsymbol{\beta}} \max_{\mathbb{P} \in \Pi} \mathbb{E}_{\mathbb{P}} \left[{c^{\mathrm{E}}}^\top \left(\boldsymbol{x}^{\mathrm{E}} + (\boldsymbol{e}^\top \Omega)\boldsymbol{\alpha} \right) + {c^{\mathrm{G}}}^\top \left(\boldsymbol{x}^{\mathrm{G}} + (\boldsymbol{e}^\top \Omega)\boldsymbol{\beta} \right) \right]. \tag{4.4}$$

As the ambiguity set Π is chosen with zero-mean forecast error distribution, i.e., $\mathbb{E}_{\mathbb{P}}(\Omega) = \mu^{\Pi} = 0$, in expectation the cost of recourse actions $\mathbb{E}_{\mathbb{P}} \left[{c^{\mathrm{E}}}^\top (\boldsymbol{e}^\top \Omega)\boldsymbol{\alpha} + {c^{\mathrm{G}}}^\top (\boldsymbol{e}^\top \Omega)\boldsymbol{\beta} \right]$ is zero and (4.4) reduces to

$$\min_{\boldsymbol{x}^{\mathrm{E}}, \boldsymbol{x}^{\mathrm{G}}, \boldsymbol{\alpha}, \boldsymbol{\beta}} \left[{c^{\mathrm{E}}}^\top \boldsymbol{x}^{\mathrm{E}} + {c^{\mathrm{G}}}^\top \boldsymbol{x}^{\mathrm{G}} \right]. \tag{4.5}$$

Since forecast error Ω is no longer in the objective function, $\max_{\mathbb{P} \in \Pi}$ can be removed [164] and the objective function reduces to an uncertainty-independent linear minimization. Note that the set of decision variables is updated to incorporate nominal dispatch and recourse decisions substituting the stochastic variables as described in decision rules (4.3).

4.3.3 Reformulation of equality constraints

Given the recourse actions based on linear decision rules (4.3), equality constraints (4.2d) can be reformulated to

$$\boldsymbol{e}^\top \left(\boldsymbol{x}^{\mathrm{E}} + (\boldsymbol{e}^\top \Omega)\boldsymbol{\alpha}\right) - \boldsymbol{e}^\top (\boldsymbol{W} - \Omega) - \boldsymbol{e}^\top \boldsymbol{D}^{\mathrm{E}} = 0. \tag{4.6}$$

When separating the terms based on their independence and dependence of Ω, balance of supply and demand as well as activation of flexibility during real time to counter the random forecast errors are ensured in the power system by

$$\boldsymbol{e}^\top \boldsymbol{x}^{\mathrm{E}} + \boldsymbol{e}^\top \boldsymbol{W} - \boldsymbol{e}^\top \boldsymbol{D}^{\mathrm{E}} = 0, \tag{4.7a}$$

$$\boldsymbol{e}^\top \boldsymbol{\alpha} = 1, \tag{4.7b}$$

which hold true for any realization of uncertainty Ω. Constraints (4.7) are uncertainty-independent equality constraints, as Ω was canceled out on both sides of (4.7b).

Recourse actions for gas-fired generators require response to uncertainty by flexible assets from the gas system. Therefore, deviations from wind power forecast and resulting mitigation actions of flexible power units translate into uncertainty in the natural gas system. Nodal gas balance (4.2e) coupling power and gas systems together can also be reformulated such that Ω is no longer included. Consequently, the gas system is balanced by

$$\boldsymbol{e}^\top \boldsymbol{x}^{\mathrm{G}} - \phi^\top \boldsymbol{x}^{\mathrm{E}} - \boldsymbol{e}^\top \boldsymbol{D}^{\mathrm{G}} = 0, \tag{4.8a}$$

$$\boldsymbol{e}^\top \boldsymbol{\beta} = \phi^\top \boldsymbol{\alpha}, \tag{4.8b}$$

so that responses $\boldsymbol{\beta}$ by gas suppliers and network assets depend on response actions by gas-fired units reflected in $\boldsymbol{\alpha}$. These balance constraints (4.7) and (4.8) are derived from (4.2d) and (4.2e) by separating the nominal and uncertainty-dependent terms, respectively.

During the real-time operation power flows change depending on the realization of uncertainty, affine responses and spatial configuration of wind farms and generators. Moreover, the recourse actions from the gas system depend on the allocation of affine policies subject to the gas network topology and physical gas flow constraints. Despite the non-linearity inherent in the network flow dynamics, changes in power and gas flows can be approximated through affine functions. In order to properly model the effect of adjustments throughout the gas system, auxiliary variables describing the sensitivities of gas flows and nodal pressures to uncertainty are introduced, which depend on $\boldsymbol{\beta}$ and thus, $\boldsymbol{\alpha}$. It is worth noting that linepack dynamics impose intertemporal coupling between dispatch decisions requiring proper modeling of spatial and temporal correlation of the uncertain parameter. Note that the non-convex Weymouth equation in (4.2f) under uncertainty can be split into three separate equality constraints when differentiating terms which are independent, quadratically-, and linearly-dependent on uncertainty. While the former two can be relaxed into second-order cone constraints following the approach in Section 3.1.2, bilinear terms in the latter need to be replaced with their McCormick envelopes (3.7). See [**Paper C**] for detailed reformulation.

Lastly, the distributionally robust chance constraints (4.2b) and (4.2c) need to be reformulated in order to make the original problem tractable, which is described in the following.

4.3.4 Conic approximation of probabilistic constraints

Probabilistic chance constraints can be analytically reformulated under certain assumptions. Most chance-constrained approaches assume that wind power forecast errors are Gaussian to analytically reformulate chance constraints [157, 158, 183]. In fact, each chance constraint with a Gaussian distribution can be analytically reformulated as a second-order cone constraint [157]. However, since the accurate distribution of wind power forecast errors is unknown, distributionally robust chance constraints (4.2b) and (4.2c) can be approximated by applying Chebyshev's inequality, see [163, 182, 184]. Using linear decision rules (4.3) the distribitionally robust chance constraints (4.2b) and (4.2c) are rewritten as

$$\min_{\mathbb{P}\in\Pi} \ \mathbb{P}\left[\left(x_i^{\mathrm{E}} + (\boldsymbol{e}^\top\Omega)\alpha_i\right) \leq \overline{x}_i^{\mathrm{E}}\right] \geq (1-\epsilon_i), \ \ \forall i, \tag{4.9a}$$

$$\min_{\mathbb{P}\in\Pi} \ \mathbb{P}\left[\left(x_k^{\mathrm{G}} + (\boldsymbol{e}^\top\Omega)\beta_k\right) \leq \overline{x}_k^{\mathrm{G}}\right] \geq (1-\epsilon_k), \ \ \forall k, \tag{4.9b}$$

with the vectors of participation factors $\boldsymbol{\alpha} = [\alpha_1 \ldots \alpha_i \ldots \alpha_I]^\top$ and $\boldsymbol{\beta} = [\beta \ldots \beta_k \ldots \beta_K]^\top$. Following the approach in [163, 182, 184] to apply Chebyshev's inequality with $\boldsymbol{\mu}^\Pi = 0$ the distribitionally robust chance-constraints are approximated by

$$x_i^{\mathrm{E}} \leq \overline{x}_i^{\mathrm{E}} - \sqrt{\frac{1-\epsilon_i}{\epsilon_i}}\sqrt{\alpha_i \boldsymbol{e}^\top \boldsymbol{\Sigma}^\Pi \boldsymbol{e}\alpha_i}, \ \ \forall i, \tag{4.10a}$$

$$x_k^{\mathrm{G}} \leq \overline{x}_k^{\mathrm{G}} - \sqrt{\frac{1-\epsilon_k}{\epsilon_k}}\sqrt{\beta_k \boldsymbol{e}^\top \boldsymbol{\Sigma}^\Pi \boldsymbol{e}\beta_k}, \ \ \forall k, \tag{4.10b}$$

which can be finally be rewritten as the following convex second-order cone constraints

$$\sqrt{\frac{1-\epsilon_i}{\epsilon_i}}||\alpha_i \boldsymbol{e}^\top (\boldsymbol{\Sigma}^\Pi)^{1/2}||_2 \leq -x_i^{\mathrm{E}} + \overline{x}_i^{\mathrm{E}}, \ \ \forall i, \tag{4.11a}$$

$$\sqrt{\frac{1-\epsilon_k}{\epsilon_k}}||\beta_k \boldsymbol{e}^\top (\boldsymbol{\Sigma}^\Pi)^{1/2}||_2 \leq -x_k^{\mathrm{G}} + \overline{x}_k^{\mathrm{G}}, \ \ \forall k. \tag{4.11b}$$

However, this reformulation approach is not exact and the accuracy of the provided approximation depends on the confidence levels $1-\epsilon_i$ and $1-\epsilon_k$. The accuracy of the approximation reduces when ϵ_i and ϵ_k are close to zero, i.e., when confidence levels are close to 1, resulting in overly conservative solutions and ultimately infeasibility. Thus, this reformulation requires that large enough violation probabilities ϵ_i and ϵ_k are considered to avoid infeasibility [164, 167]. For exact reformulation of chance constraints, which increases the modeling complexity, see [164].

In summary, the original problem (4.2) can be recast as a second-order cone program (SOCP), whose detailed formulation is given in [**Paper C**]. This proposed framework is efficiently solvable allowing to harvest flexibility from agents in power and gas systems, i.e., flexible power generators, natural gas suppliers and gas grid assets, based on affine policies deriving tentative dispatch schedules and recourse actions for mitigation of uncertainty. The features of uncertainty are drawn from historical measurement without specific distributional restrictions or assumptions on random variables.

4.4 Numerical results: Uncertainty propagation and mitigation

The proposed methodology is tested on a modified case study based on the 24-bus IEEE reliability test system [142] and a 12-node gas system [17] over one day with hourly time granularity. Mean and covariance of wind power production forecast errors are extracted from historical data. A set of

1,000 wind forecast scenarios of wind farms located in Denmark [185] is used to compute the mean and the covariance for the central system operator to assign not only the optimal dispatch but also the optimal flexibility procurement in the form of affine policies. The tractable SOCP form of the distributionally robust chance-constrained energy dispatch provides optimal day-ahead dispatch schedules for power and gas systems and affine participation policies for power generators, gas suppliers and network operators for the flexibility provision in real-time. Parameters ϵ_i and ϵ_k are chosen such that they represent the risk tolerance and preference of the system operator. For simplicity, identical values ϵ for all chance constraints are selected, consequently $1-\epsilon$ becomes the confidence level that chance constraints hold.

4.4.1 Optimal affine policies

The optimal affine policies obtained from solving the uncertainty-aware power and gas dispatch model can be interpreted as flexibility-oriented products that represent the operational reserve of market participants across temporal and spatial dimensions as well as across multiple energy carriers. The framework of policy-based reserve products allows the coordinated reaction of market participants to deviations in electricity and subsequently natural gas systems as linear decision rules. Figure 4.2 shows the optimal dispatch and affine policies for power generators, grouped into gas-fired and non gas-fired units for $\epsilon = 0.05$. Only units that are dispatched below full capacity are assigned affine policies to participate in the provision of flexibility. For economic reasons, low-cost options are preferred as flexibility sources. Not only the cost but also the spatial correlation of uncertainty sources and locations of flexible agents decide the allocation of affine policies. As natural gas-fired units are the main flexibility providers during hours 8-24, the gas system needs to react to the uncertainty resulting from variable gas-off take. Gas injections into the grid in the early hours of the day ensure fuel availability via linepack towards later hours of the day, effectively decoupling supply and demand in the gas system, see Figure 4.3. With gas-fired power plants providing real-time recourse actions, gas suppliers are also assigned affine policies to mitigate the uncertain fuel consumption. Scheduling decisions and the allocation of affine policies in the gas system depend on both cost and network effects, such that the most expensive gas supplier is only dispatched and assigned affine policies in few hours late in the day, to compensate for the depletion of linepack in pipelines.

4.4.2 A trade off between system cost and violation probabilities

Choosing appropriate confidence levels for chance constraints to hold is not straightforward. Figure 4.4 shows that with increasing confidence level the cost of dispatch increases. This represents the trade-off between risk and cost for the system operator.

Ex-ante out-of-sample simulations help to choose appropriate confidence level $1-\epsilon$ and also to evaluate the quality of the solution. The day-ahead decision, i.e., tentative schedules and affine policies, are fixed to their optimal values in the solution. Then another set of wind forecast scenarios (test dataset), different from the set used to obtain the covariance matrix (training dataset), is simulated and the violation probability of the distributionally robust chance constraints under these new scenarios is computed. For given optimal in-sample values obtained for the tentative day-ahead schedule and participation factor of generating units, the linear decision rule is applied to calculate the recourse action of each unit under each test sample. In this way, the feasibility of

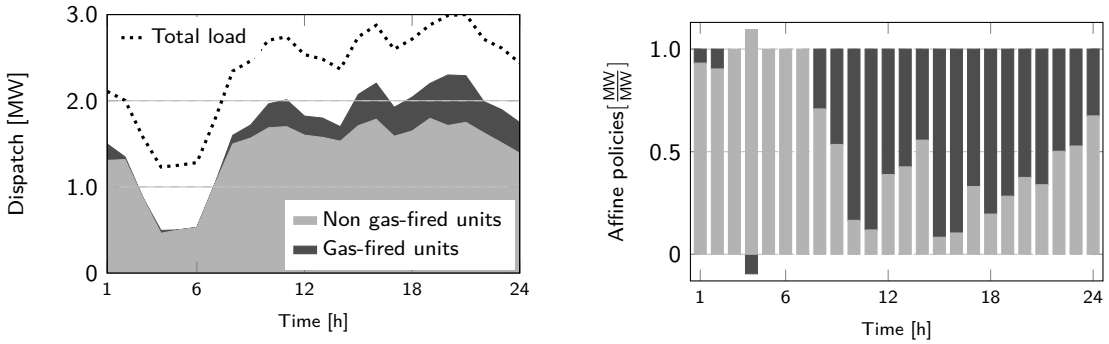

Figure 4.2: Optimal dispatch and affine policies for power generators with $\epsilon = 0.05$.

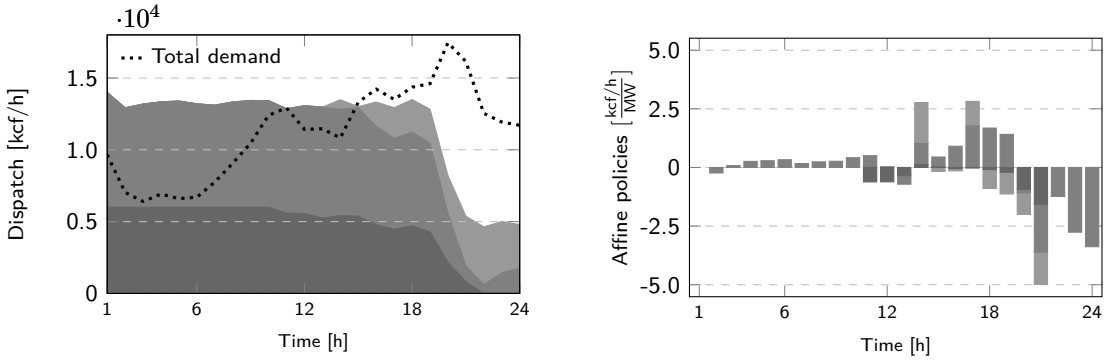

Figure 4.3: Optimal dispatch and affine policies for gas suppliers with $\epsilon = 0.05$.

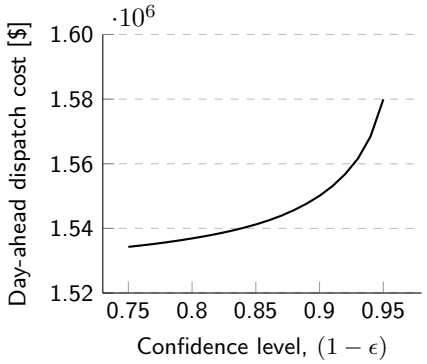

Figure 4.4: Day-ahead dispatch cost as function of confidence levels for distributionally robust chance constraints.

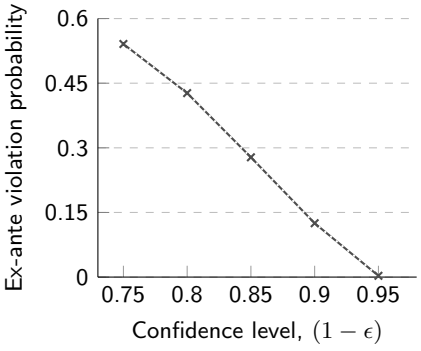

Figure 4.5: Ex-ante violation probability of distributionally robust chance constraints, evaluated for 1,000 new test samples.

chance-constraints in real-time is tested. Figure 4.5 shows that by increasing the confidence level the ex-ante violation probability over all constraints decreases.

The individual violation probability of each group of distributionally robust chance constraints are shown in Figure 4.6 for different values of ϵ. The plot illustrates the susceptibility of the individual groups of constraints showing that while the violation probability decreases for increasing confidence levels, generation production limits, gas flow unidirectionality and pressure bounds stay the constraints most prone to violations. Line flow limits and maintaining linepack

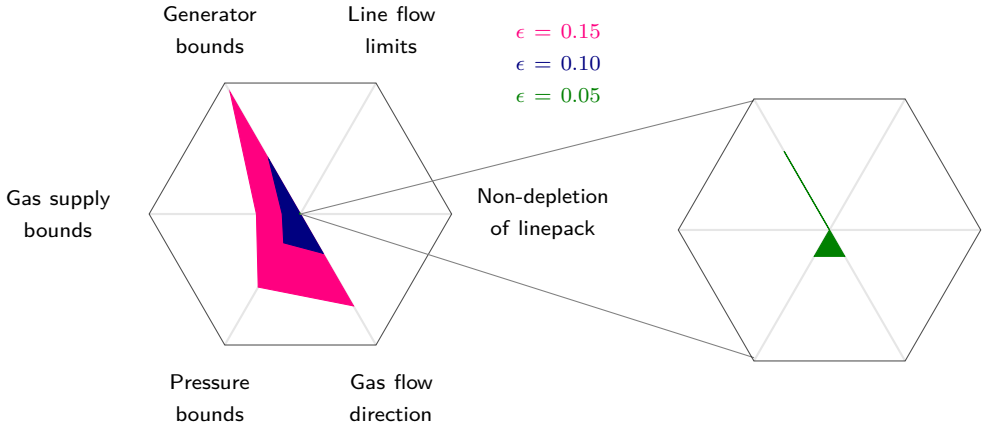

Figure 4.6: Ex-ante violation probabilities by constraint type. Corners of the hexagons represent a violation probability of 0.3 and 0.005 for the plot on the left- and right-hand side, respectively.

are not susceptible to violation in this specific case study.

CHAPTER 5

Soft Coordination Via Financial Instruments

The goal of coordination among energy markets is to dispatch flexible assets in a way that enables them to serve all sectors. The lack of coordination among energy markets and trading floors may result in day-ahead dispatch decisions that are suboptimal for the overall energy system. Among all potential coordination schemes, recall from Chapter 2 that soft coordination approaches respect the current market frameworks and regulations. Non-disruptive, market-based coordination mechanisms enhance the information flow among sectors and create incentives for each sector to dispatch flexible resources in a way that benefits the overall energy system.

The main goal of this chapter is to explore how financial instruments can help as a coordination tool in interdependent but independently operated power and natural gas markets. This chapter first discusses different levels of sectoral and temporal coordination in coupled two-settlement power and natural gas markets in Section 5.1. Fully coordinated and uncoordinated market-clearing frameworks are formulated as optimization and equivalent equilibrium models in Section 5.2. The concept of virtual bidding for agents with and without physical assets is introduced in Section 5.3. Virtual bidders are included in the market clearing-formulation in Section 5.4. The solution methodologies for the respective Nash and generalized Nash equilibrium problems are explained. Finally, a case study in Section 5.5 shows that virtual bidding is able to bring additional efficiency to coupled electricity and natural gas markets in comparison to the current sequential setup. A stochastic integrated market clearing is used as an ideal benchmark.

5.1 Sectoral and temporal coordination

The current design of energy markets requires separate and sequential clearing of power and natural gas markets. Two dimensions for improved coordination in separate and sequential two-settlement electricity and natural gas markets are identified: *Sectoral* and *temporal* coordination. These two dimensions are described in the following and then different degrees of sectoral and temporal coordination are summarized.

5.1.1 Sectoral coordination

As detailed in Section 2.4, there are different degrees of coordination among energy sectors. In the sectorally uncoordinated setup with sequential timing, the electricity market is cleared based on estimated natural gas prices. Since gas prices affect power generation costs, realized or expected prices in one market affect offers in the other. Therefore, the merit order in the electricity market is affected by potentially inaccurate gas price estimation. The gas market is cleared afterwards for given fuel demand from gas-fired units, which is determined by their dispatch in the electricity market, and actual gas prices are derived. Due to growing interactions and flexibility requirements,

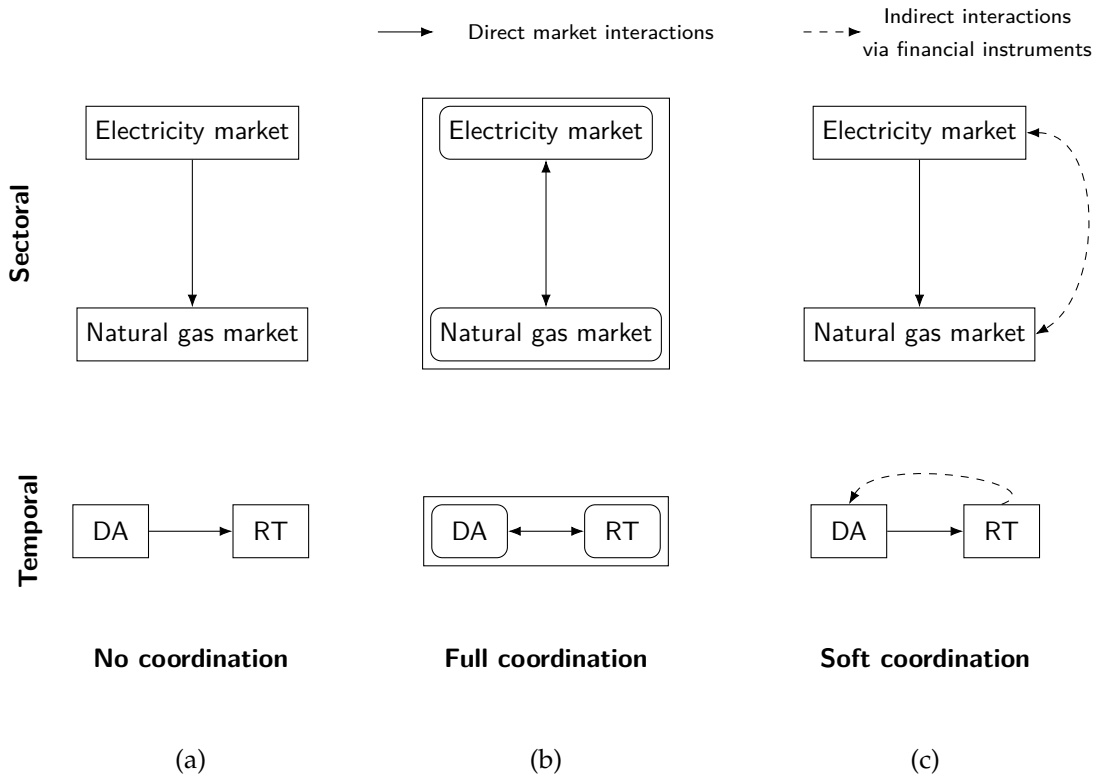

Figure 5.1: Different degrees of sectoral and temporal coordination between electricity and natural gas markets in day-ahead (DA) and real-time (RT) stages.

sectoral coordination becomes crucial. Full coordination approaches require major updates of the current practice. Necessary updates include aligning market timings, enabling information exchange between system operators or centralizing decision making. Alternatively, the interactions between sectors can be improved via soft coordination. These coordination mechanisms are based on widening the scope of operational information exchanged by the two sectors. With such mechanisms, the electricity market becomes "gas-aware", while respecting the sequential order of markets.

5.1.2 Temporal coordination

Market operators clear day-ahead and real-time markets separately and sequentially for power and gas sectors. Without coordination, the day-ahead market is cleared with deterministic description of forecast uncertainties. Deviations from fixed day-ahead schedules are then balanced in the real-time stage once uncertainty is realized. In the real-time market, adjustments are made to the day-ahead schedules in order to offset imbalances. With significant shares of uncertain renewable energy sources, lacking foresight into potential deviations in real-time results in high balancing cost to mitigate erroneous forecasts. While full temporal coordination implies explicit probabilistic representation of uncertainties in day-ahead scheduling, soft temporal coordination includes any mechanisms that maintain deterministic day-ahead market clearing while improving "real-time awareness" in the day-ahead stage.

5.1.3 Degrees of sectoral and temporal coordination

The three different degrees of sectoral and temporal coordination between electricity and natural gas systems and trading floors, i.e., no coordination, full coordination and soft coordination, are illustrated in Figure 5.1. No coordination in Figure 5.1 (a) resembles the current sequential setup of markets with only limited coordination between sectors and trading floors. Full coordination in Figure 5.1 (b) is uncertainty-aware and treats the overall energy system holistically anticipating future uncertainties in day-ahead. Full coordination requires complete redesign of markets but serves as an ideal benchmark. Soft coordination illustrated in Figure 5.1 (c) gradually strengthens the coordination between sectors and trading floors via mechanisms that create implicit exchange of information and market interactions. Virtual bidders as financial instruments can act as soft coordinators among trading floors and sectors. Market clearing models for different levels of sectoral and temporal coordination are provided in the following.

5.2 Market clearing: Optimization and equilibrium frameworks

Market operators clear power and natural gas markets in day-ahead and real-time stages aiming at maximizing the social welfare. When demand is inelastic to price, maximum social welfare is achieved by minimizing operational cost. Under the assumption of perfect competition, all market players act competitively, non-strategically and in a risk-neutral manner when participating in the markets so that they offer at prices identical to their marginal cost.

The optimization problem for clearing markets is equivalent to an equilibrium model. This equilibrium model comprises a set of optimization problems of profit-maximizing agents along with a price-setting agent determining the market-clearing prices. This means that any solution for the optimization problem is a solution for the corresponding equilibrium problem, and vice versa. This is proven by the fact that the Karush-Kuhn-Tucker (KKT) optimality conditions of the optimization problem and those of the corresponding equilibrium problem are identical. Optimization and equilibrium problems modeling different levels of coordination will be provided in the rest of this chapter and their equivalence will be discussed.

The probability distribution of uncertainty is represented by a set of scenarios indexed by ω. Wind power forecast in day-ahead is the only source of uncertainty and actual wind power production is realized in real-time. The wind power forecast in day-ahead is a single-point (deterministic) value, while different scenarios may occur in real-time. Functions $f(\cdot)$, $g(\cdot)$, $h(\cdot)$, and $p(\cdot)$ denote linear functions. Note that these functions are not necessarily identical for different optimization problems. In the next section, full coordination of electricity and natural gas systems in day-ahead and real-time is described.

5.2.1 Full coordination: Ideal benchmark

Full sectoral and temporal coordination based on Figure 5.1 (a) is achieved by designing a stochastic integrated energy market in a disruptive way disregarding the current sequence of market clearings. The co-optimization of power and natural gas markets anticipates potential recourse actions in real-time already in the day-ahead decision-making, and thus allocates flexible assets, especially those at the interface of the sectors, with all available information and foresight.

Stochastic co-optimized power and natural gas market clearing

Stochastic integrated power and natural gas market clearing aims at minimizing the total expected operational cost of both sectors with respect to operational constraints as well as supply and demand balances in day-ahead and real-time stages. The central market operator solves a two-stage stochastic linear program to optimize day-ahead schedules (here-and-now decisions) in the first-stage and adjust energy imbalances due to wind power deviations (wait-and see decisions) in the second stage, thus minimizing the total expected cost of the whole energy system, according to

$$\min_{\boldsymbol{x}^{\mathrm{E}},\boldsymbol{x}^{\mathrm{G}},\hat{\boldsymbol{x}}^{\mathrm{E}}_{\omega},\hat{\boldsymbol{x}}^{\mathrm{G}}_{\omega}} \quad f(\boldsymbol{x}^{\mathrm{E}},\boldsymbol{x}^{\mathrm{G}}) + \mathbb{E}\left[f(\hat{\boldsymbol{x}}^{\mathrm{E}}_{\omega},\hat{\boldsymbol{x}}^{\mathrm{G}}_{\omega})\right] \tag{5.1a}$$

$$\text{subject to} \quad g^{\mathrm{E}}(\boldsymbol{x}^{\mathrm{E}}) \leq 0,\ \ h^{\mathrm{E}}(\boldsymbol{x}^{\mathrm{E}}) = 0 \ \ : \ \ \boldsymbol{\lambda}^{\mathrm{E}}, \tag{5.1b}$$

$$g^{\mathrm{G}}(\boldsymbol{x}^{\mathrm{G}}) \leq 0,\ \ h^{\mathrm{G}}(\boldsymbol{x}^{\mathrm{G}},\boldsymbol{x}^{\mathrm{E}}) = 0 \ \ : \ \ \boldsymbol{\lambda}^{\mathrm{G}}, \tag{5.1c}$$

$$g^{\mathrm{E}}(\hat{\boldsymbol{x}}^{\mathrm{E}}_{\omega},\boldsymbol{x}^{\mathrm{E}}) \leq 0,\ \ h^{\mathrm{E}}(\hat{\boldsymbol{x}}^{\mathrm{E}}_{\omega}) = 0 \ \ : \ \ \hat{\boldsymbol{\lambda}}^{\mathrm{E}}_{\omega},\ \ \forall\omega, \tag{5.1d}$$

$$g^{\mathrm{G}}(\hat{\boldsymbol{x}}^{\mathrm{G}}_{\omega},\boldsymbol{x}^{\mathrm{G}}) \leq 0,\ \ h^{\mathrm{G}}(\hat{\boldsymbol{x}}^{\mathrm{G}}_{\omega},\hat{\boldsymbol{x}}^{\mathrm{E}}_{\omega}) = 0 \ \ : \ \ \hat{\boldsymbol{\lambda}}^{\mathrm{G}}_{\omega},\ \ \forall\omega, \tag{5.1e}$$

where $\boldsymbol{x}^{\mathrm{E}}$ and $\boldsymbol{x}^{\mathrm{G}}$ denote the vectors of day-ahead scheduling decisions in power and gas systems, respectively. In addition, $\hat{\boldsymbol{x}}^{\mathrm{E}}_{\omega}$ and $\hat{\boldsymbol{x}}^{\mathrm{G}}_{\omega}$ are the adjustments in real-time for power and gas markets under scenario ω. Objective function (5.1a) minimizes the total expected system cost including cost of day-ahead power production and gas supply schedules in the first term $f(\boldsymbol{x}^{\mathrm{E}},\boldsymbol{x}^{\mathrm{G}})$ and the expected real-time balancing cost in both sectors to cover excess or deficit of wind power production in the second term $\mathbb{E}\left[f(\hat{\boldsymbol{x}}^{\mathrm{E}}_{\omega},\hat{\boldsymbol{x}}^{\mathrm{G}}_{\omega})\right]$. Day-ahead operational constraints (5.1b) and (5.1c) include operational limits of the power system as linear inequalities $g^{\mathrm{E}}(\boldsymbol{x}^{\mathrm{E}}) \leq 0$ and linear power balance equality $h^{\mathrm{E}}(\boldsymbol{x}^{\mathrm{E}}) = 0$, as well as operational limits of the gas system (linear inequalities $g^{\mathrm{G}}(\boldsymbol{x}^{\mathrm{G}}) \leq 0$) and balance of gas supply and demand (linear equality constraint $h^{\mathrm{G}}(\boldsymbol{x}^{\mathrm{G}},\boldsymbol{x}^{\mathrm{E}}) = 0$). Note that the dispatch of gas-fired units is translated into fuel consumption, which represents gas load in the gas balance. The dispatch of gas-fired units is endogenously optimized taking true marginal cost and its effect on the gas system into account. The real-time constraints are enforced by (5.1d) and (5.1e) for every scenario ω which ensure that adjustments lie within operational limits in power and gas sectors in $g^{\mathrm{E}}(\hat{\boldsymbol{x}}^{\mathrm{E}}_{\omega},\boldsymbol{x}^{\mathrm{E}}) \leq 0$ and $g^{\mathrm{G}}(\hat{\boldsymbol{x}}^{\mathrm{G}}_{\omega},\boldsymbol{x}^{\mathrm{G}}) \leq 0$, respectively. Deficit or excess of wind power production due to day-ahead forecast error is balanced out in $h^{\mathrm{E}}(\hat{\boldsymbol{x}}^{\mathrm{E}}_{\omega}) = 0$ and changes in gas demand due to variable fuel consumption of gas-fired units mitigating wind forecast error are offset in $h^{\mathrm{G}}(\hat{\boldsymbol{x}}^{\mathrm{G}}_{\omega},\hat{\boldsymbol{x}}^{\mathrm{E}}_{\omega}) = 0$. Dual variables associated with equality constraints, which enforce balance of production and consumption in day-ahead and real-time, present day-ahead power and natural gas prices ($\boldsymbol{\lambda}^{\mathrm{E}}$ and $\boldsymbol{\lambda}^{\mathrm{G}}$) as well as probability-weighted real-time prices ($\hat{\boldsymbol{\lambda}}^{\mathrm{E}}_{\omega}$ and $\hat{\boldsymbol{\lambda}}^{\mathrm{G}}_{\omega}$).

The linear program (5.1) can be equivalently reformulated as an equilibrium problem in which each market player is a stochastic decision-maker with perfect and symmetric information regarding uncertainty and prices in both sectors, see Figure 5.2. This equivalent equilibrium problem is given in the following.

Stochastic Nash equilibrium model

In the context of a market game with price-taking agents, each player chooses quantities to maximize her expected profit, subject to day-ahead and real-time operational constraints. Within the equilibrium model (5.2)-(5.8), optimization problem (5.2) represents the expected profit

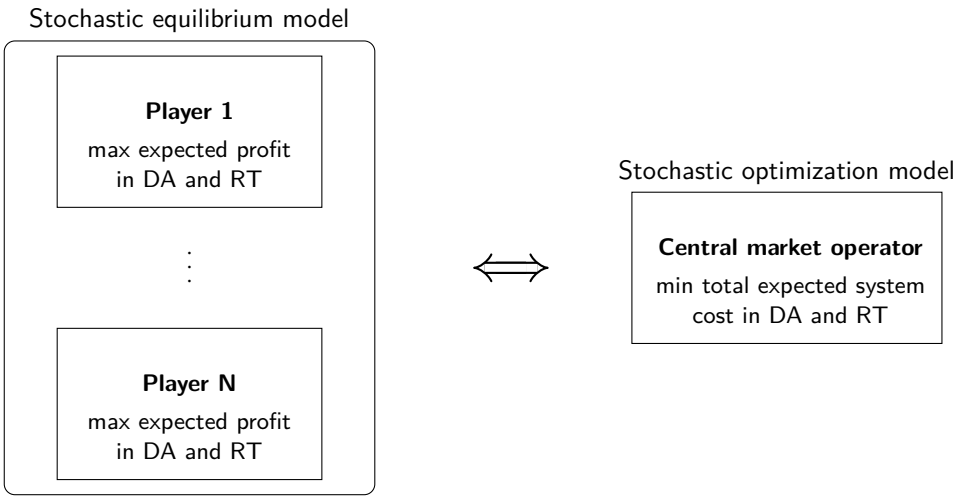

Figure 5.2: Full coordination: Stochastic equilibrium model (5.2)-(5.8) equivalent to stochastic optimization model (5.1). Player 1 to Player N represent all agents participating in either power or gas market as well as agents at the interface of the markets, i.e., gas-fired units. DA: day-ahead; RT: real-time.

maximization problem for each power market participant $\mathcal{I}$ as given below:

$$\max_{\boldsymbol{x}^{\mathrm{E}},\hat{\boldsymbol{x}}^{\mathrm{E}}_{\omega}} \; p(\boldsymbol{x}^{\mathrm{E}},\boldsymbol{\lambda}^{\mathrm{E}}) + \mathbb{E}\left[p(\hat{\boldsymbol{x}}^{\mathrm{E}}_{\omega},\hat{\boldsymbol{\lambda}}^{\mathrm{E}}_{\omega})\right] \tag{5.2a}$$

$$\text{subject to } \; g^{\mathrm{E}}(\boldsymbol{x}^{\mathrm{E}}) \leq 0, \;\; g^{\mathrm{E}}(\hat{\boldsymbol{x}}^{\mathrm{E}}_{\omega},\boldsymbol{x}^{\mathrm{E}}) \leq 0, \;\; \forall\omega. \tag{5.2b}$$

Note that day-ahead and expected real-time prices $\boldsymbol{\lambda}^{\mathrm{E}}$ and $\hat{\boldsymbol{\lambda}}^{\mathrm{E}}_{\omega}$ are variables within the equilibrium model but treated as exogenous parameters within the agents' optimization problems. Each agent's feasible space is determined by her operational limits in day-ahead and real-time in (5.2b).

Similarly, each agent $\mathcal{G}$ at the interface of power and gas markets, e.g., gas-fired units, maximizes her expected profit depending on day-ahead and expected real-time prices for power ($\boldsymbol{\lambda}^{\mathrm{E}}$, $\hat{\boldsymbol{\lambda}}^{\mathrm{E}}_{\omega}$) and natural gas ($\boldsymbol{\lambda}^{\mathrm{G}}$, $\hat{\boldsymbol{\lambda}}^{\mathrm{G}}_{\omega}$) according to

$$\max_{\boldsymbol{x}^{\mathrm{E}},\hat{\boldsymbol{x}}^{\mathrm{E}}_{\omega}} \; p(\boldsymbol{x}^{\mathrm{E}},\boldsymbol{\lambda}^{\mathrm{E}},\boldsymbol{\lambda}^{\mathrm{G}}) + \mathbb{E}\left[p(\hat{\boldsymbol{x}}^{\mathrm{E}}_{\omega},\hat{\boldsymbol{\lambda}}^{\mathrm{E}}_{\omega},\hat{\boldsymbol{\lambda}}^{\mathrm{G}}_{\omega})\right] \tag{5.3a}$$

$$\text{subject to } \; g^{\mathrm{E}}(\boldsymbol{x}^{\mathrm{E}}) \leq 0, \;\; g^{\mathrm{E}}(\hat{\boldsymbol{x}}^{\mathrm{E}}_{\omega},\boldsymbol{x}^{\mathrm{E}}) \leq 0, \;\; \forall\omega. \tag{5.3b}$$

Furthermore, each natural gas market participant $\mathcal{K}$ maximizes her expected profit as

$$\max_{\boldsymbol{x}^{\mathrm{G}},\hat{\boldsymbol{x}}^{\mathrm{G}}_{\omega}} \; p(\boldsymbol{x}^{\mathrm{G}},\boldsymbol{\lambda}^{\mathrm{G}}) + \mathbb{E}\left[p(\hat{\boldsymbol{x}}^{\mathrm{G}}_{\omega},\hat{\boldsymbol{\lambda}}^{\mathrm{G}}_{\omega})\right] \tag{5.4a}$$

$$\text{subject to } \; g^{\mathrm{G}}(\boldsymbol{x}^{\mathrm{G}}) \leq 0, \;\; g^{\mathrm{G}}(\hat{\boldsymbol{x}}^{\mathrm{G}}_{\omega},\boldsymbol{x}^{\mathrm{G}}) \leq 0, \;\; \forall\omega. \tag{5.4b}$$

These agents $\mathcal{I}$, $\mathcal{G}$ and $\mathcal{K}$ choose vectors $\boldsymbol{x}^{\mathrm{E}}$ and $\hat{\boldsymbol{x}}^{\mathrm{E}}_{\omega}$ as well as $\boldsymbol{x}^{\mathrm{G}}$ and $\hat{\boldsymbol{x}}^{\mathrm{G}}_{\omega}$, respectively, subject to operational restrictions, which are independent of others' actions, and receive profits according to their individual linear payoff functions $p(\cdot)$. A Nash equilibrium is a set of strategies, one for each player, such that each player's strategy is her best response to others' strategies. In combination with market-clearing constraints, this results in a market equilibrium. As proposed in [186], market constraints for power and gas balances in day-ahead and real-time are included

by a fictitious market participant who chooses prices. This price-setting agent determines the day-ahead electricity price $\boldsymbol{\lambda}^{\mathrm{E}}$ for given dispatch decisions as

$$\min_{\boldsymbol{\lambda}^{\mathrm{E}}} \ \boldsymbol{\lambda}^{\mathrm{E}^\top} h^{\mathrm{E}}(\boldsymbol{x}^{\mathrm{E}}). \tag{5.5}$$

Note that KKT condition of unconstrained optimization (5.5) simply enforces power balance equality, i.e., $h^{\mathrm{E}}(\boldsymbol{x}^{\mathrm{E}}) = 0$. Similarly, the day-ahead natural gas price $\boldsymbol{\lambda}^{\mathrm{G}}$ is chosen as

$$\min_{\boldsymbol{\lambda}^{\mathrm{G}}} \ \boldsymbol{\lambda}^{\mathrm{G}^\top} h^{\mathrm{G}}(\boldsymbol{x}^{\mathrm{G}}, \boldsymbol{x}^{\mathrm{E}}). \tag{5.6}$$

Finally, the real-time electricity and gas prices are determined for each scenario ω according to

$$\left\{\min_{\hat{\boldsymbol{\lambda}}^{\mathrm{E}}_\omega} \ \hat{\boldsymbol{\lambda}}^{\mathrm{E}^\top}_\omega h^{\mathrm{E}}(\hat{\boldsymbol{x}}^{\mathrm{E}}_\omega) = 0\right\} \ \forall\omega, \tag{5.7}$$

and

$$\left\{\min_{\hat{\boldsymbol{\lambda}}^{\mathrm{G}}_\omega} \ \hat{\boldsymbol{\lambda}}^{\mathrm{G}^\top}_\omega h^{\mathrm{G}}(\hat{\boldsymbol{x}}^{\mathrm{G}}_\omega, \hat{\boldsymbol{x}}^{\mathrm{E}}_\omega) = 0\right\} \ \forall\omega, \tag{5.8}$$

respectively. In equilibrium, (5.5)-(5.8) precisely balance supply and demand.

Following the argumentation in [85], the equilibrium model given by (5.2)-(5.8) is mathematically proven to be equivalent to optimization model (5.1). As illustrated in Figure 5.2, the KKT conditions of (5.1) are identical to those of the equilibrium model (5.2)-(5.8).

5.2.2 No coordination: Separate and sequential setup

Without coordination as illustrated in Figure 5.1 (b), the coupled electricity and natural gas markets are cleared separately and sequentially, first in the day-ahead stage with deterministic forecast of uncertain wind power production and then in real-time to adjust imbalances once uncertainty is realized. In this setup, the exchange of information between sectors and trading floors is limited. The day-ahead electricity market clears based on estimated natural gas prices and deterministic forecast of uncertain wind power production. Then, the natural gas market clears in day-ahead based on fixed fuel demand derived from the day-ahead schedule of natural gas-fired units from the power side. These day-ahead decisions are adjusted in real-time markets once uncertainty is realized. After the real-time electricity market is cleared to resolve imbalances caused by wind power forecast errors, deviations due to updated real-time production schedules of gas-fired power plants are balanced in the real-time gas market.

Day-ahead electricity market

For given estimation of natural gas prices $\tilde{\boldsymbol{\lambda}}^{\mathrm{G}}$ in order to forecast the production cost of gas-fired power producers, the electricity day-ahead market clears as

$$\min_{\boldsymbol{x}^{\mathrm{E}}} \ f(\boldsymbol{x}^{\mathrm{E}}, \tilde{\boldsymbol{\lambda}}^{\mathrm{G}}) \tag{5.9a}$$

$$\text{subject to } \ g^{\mathrm{E}}(\boldsymbol{x}^{\mathrm{E}}) \leq 0, \ \ h^{\mathrm{E}}(\boldsymbol{x}^{\mathrm{E}}) = 0, \tag{5.9b}$$

aiming at minimizing the total day-ahead power generation cost in objective function (5.9a), which stems from operational cost of non gas-fired and gas-fired power plants. Constraints (5.9b) describe the operational constraints and power balance in the power system given deterministic forecast of wind power production.

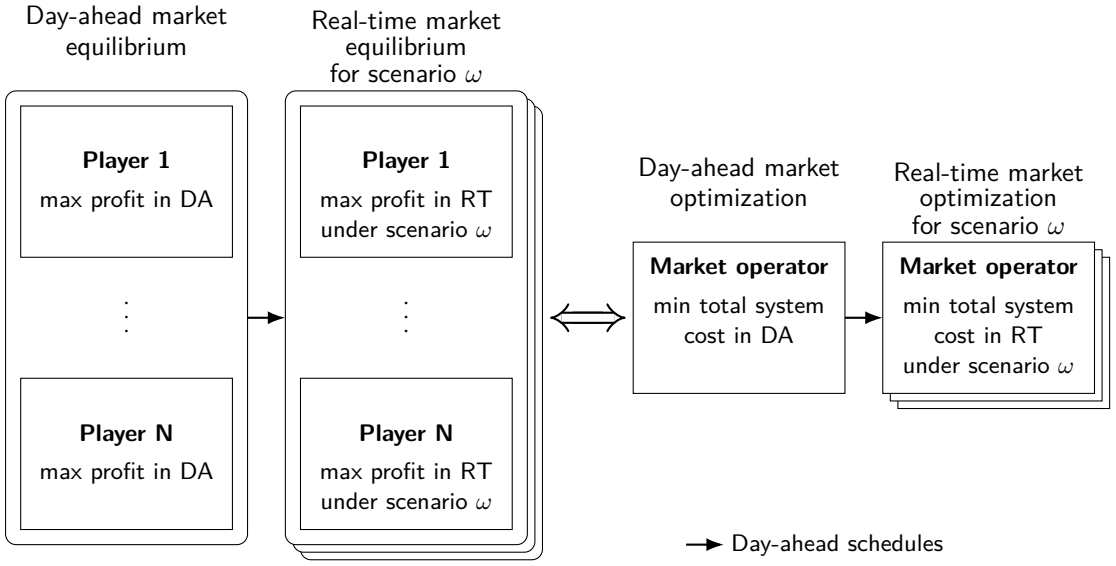

Figure 5.3: No coordination: Each optimization problem for day-ahead (DA) and real-time (RT) stage is equivalent to an equilibrium problem for DA and for RT market clearing for both sequential power and gas markets.

Note that (5.9) is a deterministic linear program. The optimization problem for day-ahead electricity market clearing can be equivalently formulated as the following equilibrium model with each unit maximizing her profit and a price-setting agent. Each non gas-fired generator $\mathcal{I}$ maximizes her day-ahead profit with respect to her operational constraints according to

$$\max_{\boldsymbol{x}^{\mathrm{E}}} \; p(\boldsymbol{x}^{\mathrm{E}}, \boldsymbol{\lambda}^{\mathrm{E}}) \tag{5.10a}$$

$$\text{subject to } \; g^{\mathrm{E}}(\boldsymbol{x}^{\mathrm{E}}) \leq 0. \tag{5.10b}$$

Similarly, each gas-fired unit $\mathcal{G}$ determines her day-ahead production based on the forecasted marginal cost given natural gas price estimation $\tilde{\boldsymbol{\lambda}}^{\mathrm{G}}$:

$$\max_{\boldsymbol{x}^{\mathrm{E}}} \; p(\boldsymbol{x}^{\mathrm{E}}, \boldsymbol{\lambda}^{\mathrm{E}}, \tilde{\boldsymbol{\lambda}}^{\mathrm{G}}) \tag{5.11a}$$

$$\text{subject to } \; g^{\mathrm{E}}(\boldsymbol{x}^{\mathrm{E}}) \leq 0. \tag{5.11b}$$

A price-setting agent reveals the day-ahead electricity price $\boldsymbol{\lambda}^{\mathrm{E}}$ according to

$$\min_{\boldsymbol{\lambda}^{\mathrm{E}}} \; \boldsymbol{\lambda}^{\mathrm{E}^{\top}} h^{\mathrm{E}}(\boldsymbol{x}^{\mathrm{E}}). \tag{5.12}$$

The equilibrium problem (5.10)-(5.12) is equivalent to the day-ahead market optimization problem (5.9), see Figure 5.3.

Day-ahead natural gas market

The optimal day-ahead dispatch of gas-fired units $\boldsymbol{x}^{\mathrm{E}^{\star}}$ derived from (5.9) is taken as input into the day-ahead natural gas market clearing (5.13). The aim is to minimize the operating cost $f(\boldsymbol{x}^{\mathrm{G}})$ of the natural gas system according to

$$\min_{\boldsymbol{x}^{\mathrm{G}}} \; f(\boldsymbol{x}^{\mathrm{G}}) \tag{5.13a}$$

$$\text{subject to } \; g^{\mathrm{G}}(\boldsymbol{x}^{\mathrm{G}}) \leq 0, \;\; h^{\mathrm{G}}(\boldsymbol{x}^{\mathrm{G}}, \boldsymbol{x}^{\mathrm{E}^{\star}}) = 0, \tag{5.13b}$$

where operational constraints and system-wide natural gas balance are given in (5.13b).

Optimization problem (5.13) for day-ahead gas market clearing can be equivalently formulated as the following equilibrium model with each supplier maximizing her profit and a price-setting agent.

Each natural gas agent $\mathcal{K}$ maximizes her day-ahead profit with respect to her operational constraints according to

$$\max_{\boldsymbol{x}^{\mathrm{G}}} \ p(\boldsymbol{x}^{\mathrm{G}}, \boldsymbol{\lambda}^{\mathrm{G}}) \tag{5.14a}$$

$$\text{subject to } \ g^{\mathrm{G}}(\boldsymbol{x}^{\mathrm{G}}) \leq 0, \tag{5.14b}$$

and the true natural gas price $\boldsymbol{\lambda}^{\mathrm{G}}$ in day-ahead is determined by

$$\min_{\boldsymbol{\lambda}^{\mathrm{G}}} \ \boldsymbol{\lambda}^{\mathrm{G}^\top} h^{\mathrm{G}}(\boldsymbol{x}^{\mathrm{G}}, \boldsymbol{x}^{\mathrm{E}^\star}). \tag{5.15}$$

In real-time operations, wind power production scenario ω is realized, which may not be identical to the deterministic forecast, and real-time markets are cleared to adjust for imbalances. Optimal day-ahead schedules $\boldsymbol{x}^{\mathrm{E}^\star}$ and $\boldsymbol{x}^{\mathrm{G}^\star}$ are treated as fixed inputs in the following formulations and real-time markets are cleared for the realization of uncertainty ω.

Real-time electricity market

In the real-time market, the cost of power adjustments is minimized under scenario ω as

$$\Big\{\min_{\hat{\boldsymbol{x}}^{\mathrm{E}}_\omega} \ f(\hat{\boldsymbol{x}}^{\mathrm{E}}_\omega, \tilde{\boldsymbol{\lambda}}^{\mathrm{G}}_\omega) \tag{5.16a}$$

$$\text{subject to } \ g^{\mathrm{E}}(\hat{\boldsymbol{x}}^{\mathrm{E}}_\omega, \boldsymbol{x}^{\mathrm{E}^\star}) \leq 0, \ \ h^{\mathrm{E}}(\hat{\boldsymbol{x}}^{\mathrm{E}}_\omega) = 0\Big\} \ \forall\omega, \tag{5.16b}$$

where objective function (5.16a) describes the real-time cost of power adjustments to cover excess or deficit of wind power production based on real-time natural gas price estimation $\tilde{\boldsymbol{\lambda}}^{\mathrm{G}}_\omega$. Operational constraints in the real-time stage (5.16b) depend on given day-ahead schedules $\boldsymbol{x}^{\mathrm{E}^\star}$ and any imbalance due to deviation from the day-ahead forecast is mitigated in real-time power balance.

The following equilibrium problem (5.17)-(5.19) is equivalent to the real-time market optimization problem (5.16) for each scenario ω, as illustrated in Figure 5.3.

Each non gas-fired generator $\mathcal{I}$ maximizes her profit in scenario ω with respect to her fixed day-ahead schedule $\boldsymbol{x}^{\mathrm{E}^\star}$ as

$$\Big\{\max_{\hat{\boldsymbol{x}}^{\mathrm{E}}_\omega} \ p(\hat{\boldsymbol{x}}^{\mathrm{E}}_\omega, \hat{\boldsymbol{\lambda}}^{\mathrm{E}}_\omega) \tag{5.17a}$$

$$\text{subject to } \ g^{\mathrm{E}}(\hat{\boldsymbol{x}}^{\mathrm{E}}_\omega, \boldsymbol{x}^{\mathrm{E}^\star}) \leq 0\Big\} \ \forall\omega. \tag{5.17b}$$

Similarly, gas-fired generator $\mathcal{G}$ optimizes her production in real-time based on real-time natural gas price estimation $\tilde{\boldsymbol{\lambda}}^{\mathrm{G}}_\omega$ as

$$\Big\{\max_{\hat{\boldsymbol{x}}^{\mathrm{E}}_\omega} \ p(\hat{\boldsymbol{x}}^{\mathrm{E}}_\omega, \hat{\boldsymbol{\lambda}}^{\mathrm{E}}_\omega, \tilde{\boldsymbol{\lambda}}^{\mathrm{G}}_\omega) \tag{5.18a}$$

$$\text{subject to } \ g^{\mathrm{E}}(\hat{\boldsymbol{x}}^{\mathrm{E}}_\omega, \boldsymbol{x}^{\mathrm{E}^\star}) \leq 0\Big\} \ \forall\omega. \tag{5.18b}$$

For each scenario, the real-time electricity price is set according to

$$\Big\{\min_{\hat{\boldsymbol{\lambda}}^{\mathrm{E}}_\omega} \ \hat{\boldsymbol{\lambda}}^{\mathrm{E}^\top}_\omega h^{\mathrm{E}}(\hat{\boldsymbol{x}}^{\mathrm{E}}_\omega)\Big\} \ \forall\omega. \tag{5.19}$$

Table 5.1: Equivalence of optimization and equilibrium models for full coordination and no coordination.

		Optimization	Equilibirum
Full coordination (*Ideal*)	Stochastic integrated energy market	(5.1)	(5.2)-(5.8)
No coordination (*Seq*)	Day-ahead electricity market	(5.9)	(5.10)-(5.12)
	Day-ahead natural gas market	(5.13)	(5.14),(5.15)
	Real-time electricity market	(5.16),$\forall\omega$	(5.17)-(5.19),$\forall\omega$
	Real-time natural gas market	(5.20),$\forall\omega$	(5.21)-(5.22),$\forall\omega$

Real-time natural gas market

Lastly, the real-time natural gas market is cleared for adjusted fuel consumption by gas-fired units based on the real-time adjustment of their dispatch $\hat{\boldsymbol{x}}_{\omega}^{\mathrm{E}^\star}$. The day-ahead schedule of electricity and natural gas systems as well as the real-time adjustments of gas-fired units are treated as fixed parameters in the following formulation:

$$\Big\{\min_{\hat{\boldsymbol{x}}_{\omega}^{\mathrm{G}}} \;\; f(\hat{\boldsymbol{x}}_{\omega}^{\mathrm{G}}) \tag{5.20a}$$

$$\text{subject to} \;\; g^{\mathrm{G}}(\hat{\boldsymbol{x}}_{\omega}^{\mathrm{G}}, \boldsymbol{x}^{\mathrm{G}^\star}) \leq 0, \;\; h^{\mathrm{G}}(\hat{\boldsymbol{x}}_{\omega}^{\mathrm{G}}, \hat{\boldsymbol{x}}_{\omega}^{\mathrm{E}^\star}) = 0\Big\} \;\; \forall\omega. \tag{5.20b}$$

Real-time natural gas market-clearing problem (5.20) is equivalent to the following equilibrium problem (5.21)-(5.22). Each gas supplier maximizes her profit in real-time as

$$\Big\{\max_{\hat{\boldsymbol{x}}_{\omega}^{\mathrm{G}}} \;\; p(\hat{\boldsymbol{x}}_{\omega}^{\mathrm{G}}, \hat{\boldsymbol{\lambda}}_{\omega}^{\mathrm{G}}) \tag{5.21a}$$

$$\text{subject to} \;\; g_k^{\mathrm{G}}(\hat{\boldsymbol{x}}_{\omega}^{\mathrm{G}}, \boldsymbol{x}^{\mathrm{G}^\star}) \leq 0\Big\} \;\; \forall\omega, \tag{5.21b}$$

and real-time natural gas price vector $\hat{\boldsymbol{\lambda}}_{\omega}^{\mathrm{G}}$ is decided for each scenario ω as

$$\Big\{\min_{\hat{\boldsymbol{\lambda}}_{\omega}^{\mathrm{G}}} \;\; \hat{\boldsymbol{\lambda}}_{\omega}^{\mathrm{G}^\top} h^{\mathrm{G}}(\hat{\boldsymbol{x}}_{\omega}^{\mathrm{G}}, \hat{\boldsymbol{x}}_{\omega}^{\mathrm{E}})\Big\} \;\; \forall\omega. \tag{5.22}$$

Table 5.1 summarizes all proposed optimization problems and corresponding equilibrium models for the two extreme forms of coordination, no and full coordination. In the following soft coordination via financial instruments is introduced.

5.3 The concept of virtual bidding

Virtual bidding is a purely financial instrument, which allows market players including suppliers, consumers and financial traders, to do arbitrage based on price differences between two trading floors in energy markets, e.g., day-ahead and real-time, without physically consuming or producing energy [49, 50, 131, 133]. Market players who anticipate price differences between day-ahead and real-time markets can earn profit from this price spread by performing arbitrage. Virtual bidding is also called "convergence bidding" [131], because this form of arbitraging leads to price convergence, which will be shown in the following. Virtual bidders have the potential to improve coordination between trading floors by fostering competition and improving market efficiency [49, 51]. Due to price convergence in expectation, the coordination between day-ahead and real-time markets is improved so that day-ahead prices already reflect anticipated real-time

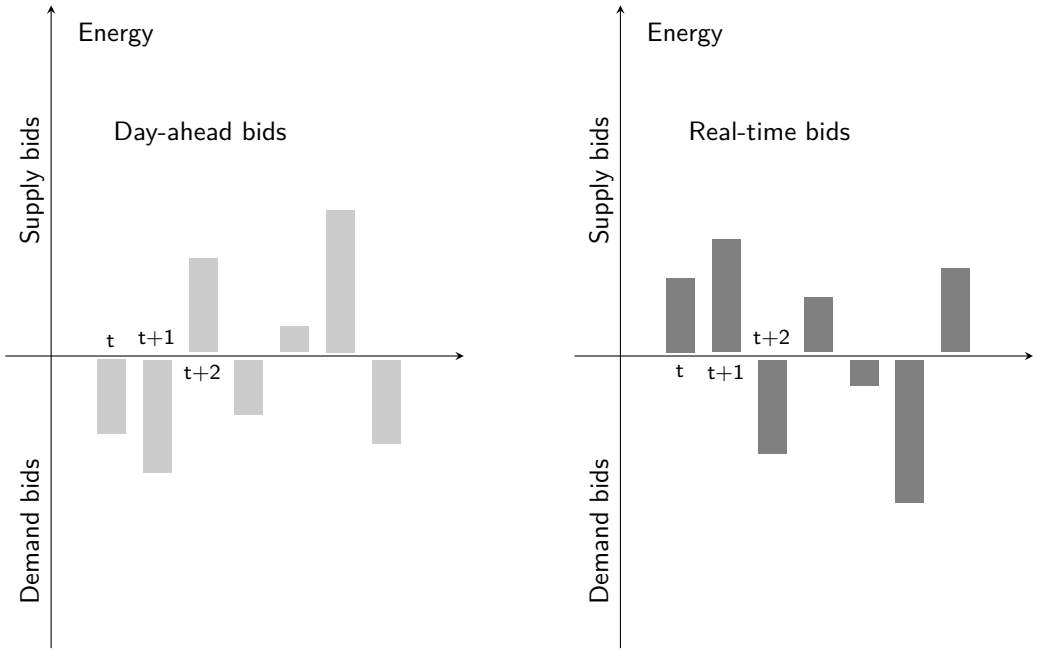

Figure 5.4: An example of day-ahead and real-time trades by an explicit virtual bidder.

uncertainty, making the day-ahead stage more "real-time aware". This is supposed to update schedules in the day-ahead market towards allocating available flexibility more efficiently. Virtual bidders are supposed to bring more information, competitiveness, liquidity and transparency to two-settlement energy markets [51, 133]. However, transaction cost associated with financial transactions, risk awareness of financial players, and potential strategic behaviour reduce the effectiveness of virtual bidding [50, 132]. Undesirable effects from cross-product manipulations with other financial products are discussed in [187]. Two categories of virtual bidding, i.e., explicit and implicit, are described in the following.

5.3.1 Explicit virtual bidding for temporal coordination

An explicit virtual bidder does not own any physical assets. Thus, her positions in day-ahead and real-time markets need to cancel each other out. In other words, if the explicit virtual bidder buys or sells a certain amount of energy for a specific hour in the day-ahead market, she needs to sell or buy back the exact same amount at the same hour in the real-time market, see Figure 5.4. Payoffs from virtual transactions amount to the difference between day-ahead and real-time prices times the amount of virtually traded energy.

Under the assumptions that explicit virtual bidders are price-taker with perfect knowledge of the distribution of real-time prices, the expected profit maximization problem of each explicit virtual bidder $\mathcal{R}$ participating in the electricity market is given as a two-stage stochastic linear program below:

$$\max_{\boldsymbol{v}^{\mathrm{E}}, \hat{\boldsymbol{v}}^{\mathrm{E}}} \ \boldsymbol{\lambda}^{\mathrm{E}^\top} \boldsymbol{v}^{\mathrm{E}} + \mathbb{E}\left[\hat{\boldsymbol{\lambda}}_{\omega}^{\mathrm{E}^\top} \hat{\boldsymbol{v}}^{\mathrm{E}}\right] \tag{5.23a}$$

$$\text{subject to} \ \ \boldsymbol{v}^{\mathrm{E}} + \hat{\boldsymbol{v}}^{\mathrm{E}} = 0, \tag{5.23b}$$

where $\boldsymbol{v}^{\mathrm{E}}$ and $\hat{\boldsymbol{v}}^{\mathrm{E}}$ denote the vectors of virtual trades in day-ahead and real-time markets, respectively. Objective function (5.23a) maximizes the expected profit of arbitraging in the day-ahead and

real-time electricity markets. Equation (5.23b) ensures that the explicit virtual bidder sells (buys) the same amount back in the real-time market that was bought (sold) in the day-ahead market. Note that the amount of virtual trade in real-time $\hat{\boldsymbol{v}}^{\mathrm{E}}$ is not indexed by scenario ω, since all virtual bids need to be cleared in real-time irrespective of uncertainty realization. Market clearing prices $\boldsymbol{\lambda}^{\mathrm{E}}$ and $\hat{\boldsymbol{\lambda}}^{\mathrm{E}}_{\omega}$ are exogenous variables in the explicit virtual bidder's optimization problem.

The KKT optimality conditions of the linear program (5.23) enforce day-ahead and real-time prices to converge in expectation [51], i.e., $\boldsymbol{\lambda}^{\mathrm{E}} = \mathbb{E}[\hat{\boldsymbol{\lambda}}^{\mathrm{E}}_{\omega}]$. The day-ahead stage implicitly becomes more aware of real-time uncertainty through prices. In this way, explicit virtual bidders improve coordination between day-ahead and real-time trading floors.

Explicit virtual bidding is also introduced in the natural gas markets. Similarly to explicit virtual bidding in electricity markets, the profit maximization problem of each explicit virtual bidder $\mathcal{Q}$ participating in natural gas markets is given below for day-ahead and real-time distribution of natural gas prices ($\boldsymbol{\lambda}^{\mathrm{G}}$ and $\hat{\boldsymbol{\lambda}}^{\mathrm{G}}_{\omega}$):

$$\max_{\boldsymbol{v}^{\mathrm{G}}, \hat{\boldsymbol{v}}^{\mathrm{G}}} \ \boldsymbol{\lambda}^{\mathrm{G}^{\top}} \boldsymbol{v}^{\mathrm{G}} + \mathbb{E}\left[\hat{\boldsymbol{\lambda}}^{\mathrm{G}^{\top}}_{\omega} \hat{\boldsymbol{v}}^{\mathrm{G}}\right] \tag{5.24a}$$

$$\text{subject to} \ \ \boldsymbol{v}^{\mathrm{G}} + \hat{\boldsymbol{v}}^{\mathrm{G}} = 0, \tag{5.24b}$$

where $\boldsymbol{v}^{\mathrm{G}}$ and $\hat{\boldsymbol{v}}^{\mathrm{G}}$ denote the vectors of virtual trades in natural gas day-ahead and real-time markets, respectively. Objective function (5.24a) maximizes the expected profit of the explicit virtual bidder participating in the day-ahead and real-time natural gas markets and equation (5.24b) balances the explicit virtual bidder's day-ahead and real-time trade. In the same way (5.23) enforces electricity prices to converge in expectation, the optimality conditions of (5.24) enforce day-ahead and expected real-time prices of natural gas to be equal, i.e., $\boldsymbol{\lambda}^{\mathrm{G}} = \mathbb{E}[\hat{\boldsymbol{\lambda}}^{\mathrm{G}}_{\omega}]$.

5.3.2 Implicit virtual bidding for sectoral and temporal coordination

Implicit virtual bidding blends virtual bids with physical bids [133, 188]. This method of arbitrage is limited to market participants with physical assets or load. Market participants who own physical assets can benefit from *self-scheduling* by solving a more detailed optimization with better representation of uncertainty and technical constraints for a longer time horizon [51, 130, 189]. These self-scheduling units, who determine their actual production level outside the market, can use existing physical assets to arbitrage prices and also perform (purely) financial transactions. The terms "implicit virtual bidding" and "self-scheduling" are used interchangeably in the following.

Gas-fired generators who operate at the interface of power and natural gas markets may find it profitable to forgo the market and dispatch their production themselves outside the market [190]. Since these units link the systems economically and physically, they have additional incentives to self-schedule if they can better anticipate real-time cost and availability of fuel. Each gas-fired unit decides her power dispatch and fuel consumption schedule to maximize her expected profit for given day-ahead and expected real-time prices in power and gas markets. The profit maximization problem of implicit virtual bidder $\mathcal{G}$ participating in electricity and natural gas markets is given below:

$$\max_{\boldsymbol{x}^{\mathrm{E}}, \hat{\boldsymbol{x}}^{\mathrm{E}}_{\omega}} \ p(\boldsymbol{x}^{\mathrm{E}}, \boldsymbol{\lambda}^{\mathrm{E}}, \boldsymbol{\lambda}^{\mathrm{G}}) + \mathbb{E}\left[p(\hat{\boldsymbol{x}}^{\mathrm{E}}_{\omega}, \hat{\boldsymbol{\lambda}}^{\mathrm{E}}_{\omega}, \hat{\boldsymbol{\lambda}}^{\mathrm{G}}_{\omega})\right] \tag{5.25a}$$

$$\text{subject to} \ \ g^{\mathrm{E}}(\hat{\boldsymbol{x}}^{\mathrm{E}}_{\omega}, \boldsymbol{x}^{\mathrm{E}}) \leq 0, \ \ \forall \omega, \tag{5.25b}$$

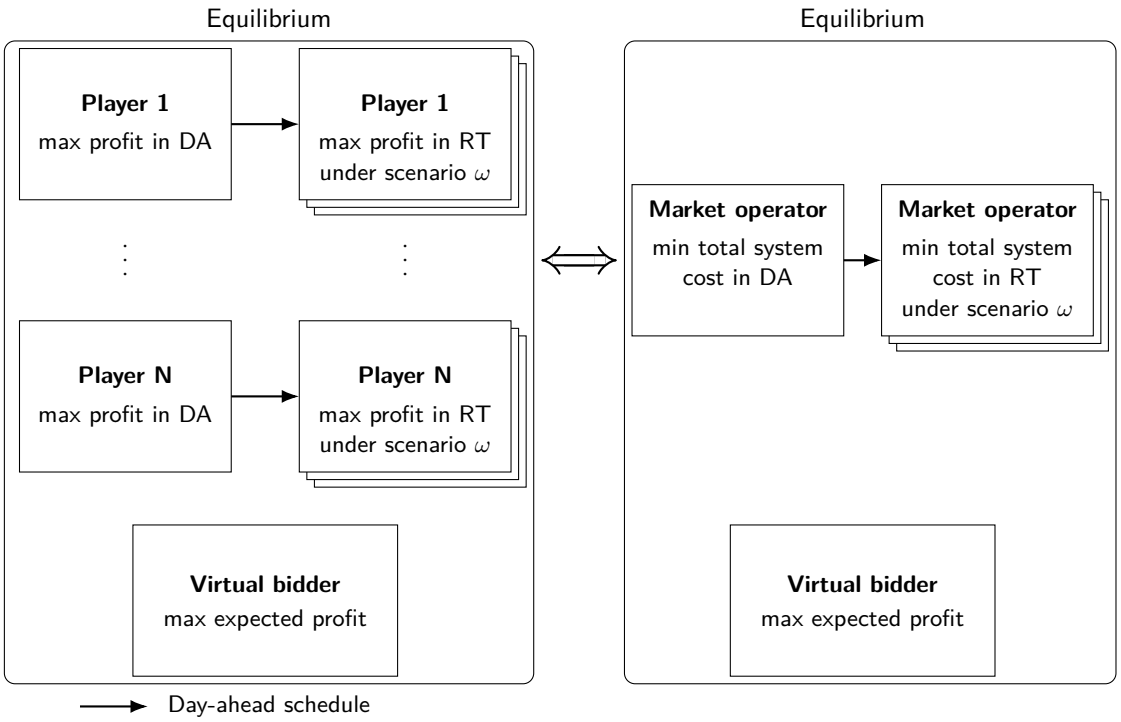

Figure 5.5: Soft-coordination: Equilibrium problem with virtual bidding integrated in market clearing.

where objective function (5.25a) maximizes the expected profit of self-scheduling gas-fired generators and simultaneously considering only real-time operation constraints (5.25b), so that gas-fired units can participate in virtual trading as long as final real-time positions lie within their actual operational limits.

5.4 Augmented market clearing with virtual bidders: An equilibrium model

5.4.1 Soft coordination

Figure 5.5 illustrates how virtual bidders, either explicit or implicit, are integrated into the separate and sequential market setup. In the following, virtual bidders are assumed to perfectly anticipate the distribution of real-time prices across scenarios in both sectors. Prices are treated as exogenous values in the problems of virtual bidders, while market operators treat the dispatch decisions of virtual bidders as fixed inputs into the market-clearing problems. Therefore, balance constraints in power and gas day-ahead and real-time markets need to be updated to account for the amount of virtual trade by explicit and implicit virtual traders as exogenous variables. In the electricity markets, balance constraints in day-ahead and real-time are extended to include virtual trades as $h^{\mathrm{E}}(\boldsymbol{x}^{\mathrm{E}}, \boldsymbol{v}^{\mathrm{E}}) = 0$ and $h^{\mathrm{E}}(\hat{\boldsymbol{x}}^{\mathrm{E}}_{\omega}, \hat{\boldsymbol{v}}^{\mathrm{E}}) = 0, \ \ \forall\omega$. Gas markets account for virtual trades in day-ahead and real-time with $h^{\mathrm{G}}(\boldsymbol{x}^{\mathrm{G}}, \boldsymbol{x}^{\mathrm{E}}, \boldsymbol{v}^{\mathrm{G}}) = 0$ and $h^{\mathrm{G}}(\hat{\boldsymbol{x}}^{\mathrm{G}}_{\omega}, \hat{\boldsymbol{x}}^{\mathrm{E}}_{\omega}, \hat{\boldsymbol{v}}^{\mathrm{G}}) = 0, \ \ \forall\omega$. Note that the dispatch decisions of self-scheduling gas-fired generators are also treated as fixed parameters in all four equality constraints. Thus, optimization problems (5.23)-(5.25) become interrelated with the models from the no coordination approach *Seq*, resulting in stochastic equilibrium problems. These equilibrium problems are summarized in Table 5.2 and provide simulation tools for exploring how much virtual bidding can improve sectoral and temporal coordination. Due to virtual bidders solving stochastic

Table 5.2: Equilibrium models for soft coordination.

Soft coordination		Equilibrium
Temporal via explicit virtual bidders	*Seq+eVB*	(5.9), (5.16)$\forall\omega$, (5.23) (5.13), (5.20)$\forall\omega$, (5.24)
Sectoral and temporal via implicit virtual bidders	*Seq+iVB*	(5.9), (5.13), (5.16)$\forall\omega$, (5.20)$\forall\omega$, (5.25)
Sectoral and temporal via all virtual bidders	*Seq+VB*	(5.9), (5.13), (5.16)$\forall\omega$, (5.20)$\forall\omega$, (5.23)-(5.25)

optimization problems, market clearing problems are solved simultaneously in the equilibrium problem, but the sequentiality and independence of sectors and trading floors are maintained in the models.

Soft temporal coordination via explicit virtual bidders

In order to improve temporal coordination explicit virtual bidding is included in both electricity and natural gas markets such that two stochastic equilibrium problems are solved sequentially, one per energy sector. First the equilibrium problem related to the electricity sector is solved based on estimated natural gas prices and then the natural gas equilibrium is solved for given day-ahead and real-time schedules of gas-fired power plants. Explicit virtual bidders increase "real-time awareness" of the day-ahead stage in both electricity and natural gas markets by enforcing day-ahead and real-time prices to be equal in expectation, but do not specifically create links between the sectors.

Soft sectoral and temporal coordination via implicit virtual bidders

For improving sectoral coordination, natural gas-fired units are allowed to self-schedule outside the markets as implicit virtual bidders for optimally allocating their flexibility in power and natural gas markets. Allowing units at the interface of power and gas sectors, e.g., gas-fired units, to submit virtual bids and maximize their expected profit participating in both sectors, links energy sectors and trading floors. Including these gas-fired generators as self-schedulers in the model links power and natural gas markets requiring a single stochastic equilibrium problem to be solved.

Soft sectoral and temporal coordination via explicit and implicit virtual bidders

Soft coordination with explicit and implicit virtual bidders is proven to provide the same solution as full coordination in some cases. Under the conditions that inequality constraints in day-ahead ($g^{\mathrm{E}}(\boldsymbol{x}^{\mathrm{E}}) \leq 0$ and $g^{\mathrm{G}}(\boldsymbol{x}^{\mathrm{G}}) \leq 0$) are non-binding, day-ahead and real-time prices converge in expectation in the full coordination model (5.1). All gas-fired units acting as self-schedulers with perfect price anticipation at the interface of power and gas markets lead to sector integration. Under these conditions, the KKT optimality conditions of the stochastic two-stage optimization problem *Ideal* and equilibrium problem *Seq+VB* are identical, see [**Paper D**]. Thus, the equilibrium solution for *Seq+VB* may be identical to the outcomes of the fully integrated, stochastic energy market.

5.4.2 Equilibrium analysis

Equilibrium problems *Seq+eVB*, *Seq+iVB*, and *Seq+VB* describe non-cooperative games with dependent or joint strategy sets because some agents' strategies affect not only the payoff functions

but also the feasible set of others. The feasibility interactions arise from virtual bidders as stochastic decision-makers participating simultaneously in the deterministic day-ahead and real-time setups, such that one player's decision variables appear in the constraint set of others. In the equilibrium model depicted on the left-hand side of Figure 5.5, each player's day-ahead schedule decisions impact the same player's real-time constraints. In the equivalent equilibrium on the right-hand side of Figure 5.5, each virtual bidder's decisions (i.e., virtual trades) appear in market operators' balance constraints. Since the feasible sets of some players (players in real-time or market operators) depend on other players' decisions (players in day-ahead or virtual bidders), generalized Nash equilibrium (GNE) problems emerge [191]. Mathematically, such a GNE problem is formulated as a quasi-variational inequality (QVI) [46], which may admit multiple solutions that arise from coupling constraints. Note that the coupling constraints are not shared among players, so that a normalized Nash equilibrium [192] cannot be derived as a subset of the GNE and the QVI cannot be reduced to a variational inequality [14]. All equilibrium models are recast as mixed-complementarity problems (MCP) by concatenating the KKT optimality conditions of all players [193]. No equivalent optimization problem can be derived [45, 46]. Following the argumentation in [47], existence of solutions for GNE can be proven under mild assumption. Provided that each agent's feasible set is non-empty, convex and compact by assuming caps on market prices and budget constraints for virtual bidders, there exists at least one solution to each equilibrium problem *Seq+eVB*, *Seq+iVB*, and *Seq+VB*. However, there are potentially multiple solutions, since proving uniqueness of solution for GNE is not straightforward [47, 56].

5.5 Numerical results: Virtual bidding as an effective tool for improving coordination

The proposed levels of coordination are tested on a case study given in [**Paper D**] based on a power system with six non gas-fired generators and four gas-fired generators connected to a natural gas system with four gas suppliers over a 24-hour time horizon. The electricity market operator uses the average gas supply cost as a deterministic and static estimation of natural gas prices $\tilde{\boldsymbol{\lambda}}^{\mathrm{G}}$ and $\tilde{\boldsymbol{\lambda}}^{\mathrm{G}}_{\omega}$. The wind power penetration, i.e., total wind power capacity installed divided by the total electricity demand, is 34%. The profiles of deterministic wind power day-ahead forecast and expected real-time realization based on five equiprobable wind scenarios ω are illustrated in Fig. 5.6. Due to potential forecast errors in day-ahead, the deterministic point forecast is not necessarily identical to the expected wind power realization in real-time so that available wind power production is underestimated during hours 1 to 6 and 19 to 23 and overestimated in hours 7 to 18.

5.5.1 Total system cost

Table 5.3 compares the total expected cost of electricity and natural gas systems for different levels of coordination. As expected, the lack of coordination incurs the highest system cost. Full coordination in model *Ideal* yields the lowest cost as the ideal benchmark with 7.06% cost reduction compared to no coordination in *Seq*. System costs achieved in soft coordination setups *Seq+eVB*, *Seq+iVB* and *Seq+VB* lie between the two extremes. Soft sectoral and temporal coordination via virtual bidding provides partial coordination. Among these soft coordination approaches, *Seq+VB* with both implicit and explicit virtual bidders yields the highest cost saving, which is 6.94%. Opening the market to more players and bidding activity creates soft temporal and sectoral market coordination.

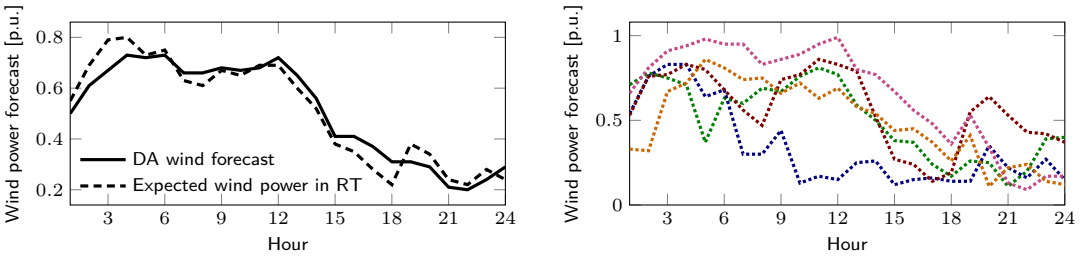

Figure 5.6: Wind power forecast in day-ahead (DA) and potential scenarios in real-time (RT): The left-hand side plot shows the deterministic wind power forecast in DA and the expected value of five wind power scenarios in RT. These five equiprobable scenarios in RT are depicted in the right-hand side plot.

	No coordination (*Seq*)	Soft temporal coordination via explicit virtual bidders (*Seq+eVB*)	Soft sectoral and temporal coordination via implicit virtual bidders (*Seq+iVB*)	Soft sectoral and temporal coordination via explicit and implicit virtual bidders (*Seq+VB*)	Full coordination (*Ideal*)
In-sample	\$1,464,369	-6.83%	-6.37%	-6.94%	-7.06%
Out-of-sample	\$1,360,886	-4.49%	-3.36%	-4.29%	-5.33%

Table 5.3: Total expected cost of the electricity and natural gas systems under different levels of coordination. The percentages show the differences in the total expected system cost compared to that cost in the fully uncoordinated sequential setup (first column).

5.5.2 Market-clearing prices

The increased cost efficiency indicates that soft coordination reveals available flexibility and better allocates flexible resources. Better price signals are supposed to improve day-ahead schedules. Improved day-ahead scheduling makes relatively more flexibility available. Since with no coordination in *Seq*, day-ahead schedules are unaware of uncertainty in real-time operations and sectoral interactions between power and gas systems, day-ahead and expected real-time market prices can significantly differ, see Figure 5.7 (a). In Figure 5.7 (b) with full coordination, day-ahead and expected real-time prices converge in both electricity and natural gas markets. Explicit virtual bidders in *Seq+eVB* improve coordination between trading floors so that day-ahead price signals better reflect the uncertainty inherent in real-time operations. This is shown in price convergence in both power and gas markets in Figure 5.7 (c) illustrating stronger coordination between trading floors via real-time awareness in the day-ahead stage through improved price signals. Implicit virtual bidders improve sectoral and temporal coordination in *Seq+iVB*. Unlike explicit virtual bidders, they do not enforce price convergence in expectation. However, as Figure 5.7 (d) shows, price differences between day-ahead and expected real-time prices decrease compared to *Seq* because of soft coordination via gas-fired self-scheduler with better foresight of natural gas and real-time prices. Finally, soft coordination with both explicit and implicit virtual bidders in *Seq+VB* leads to price convergence in Figure 5.7 (e).

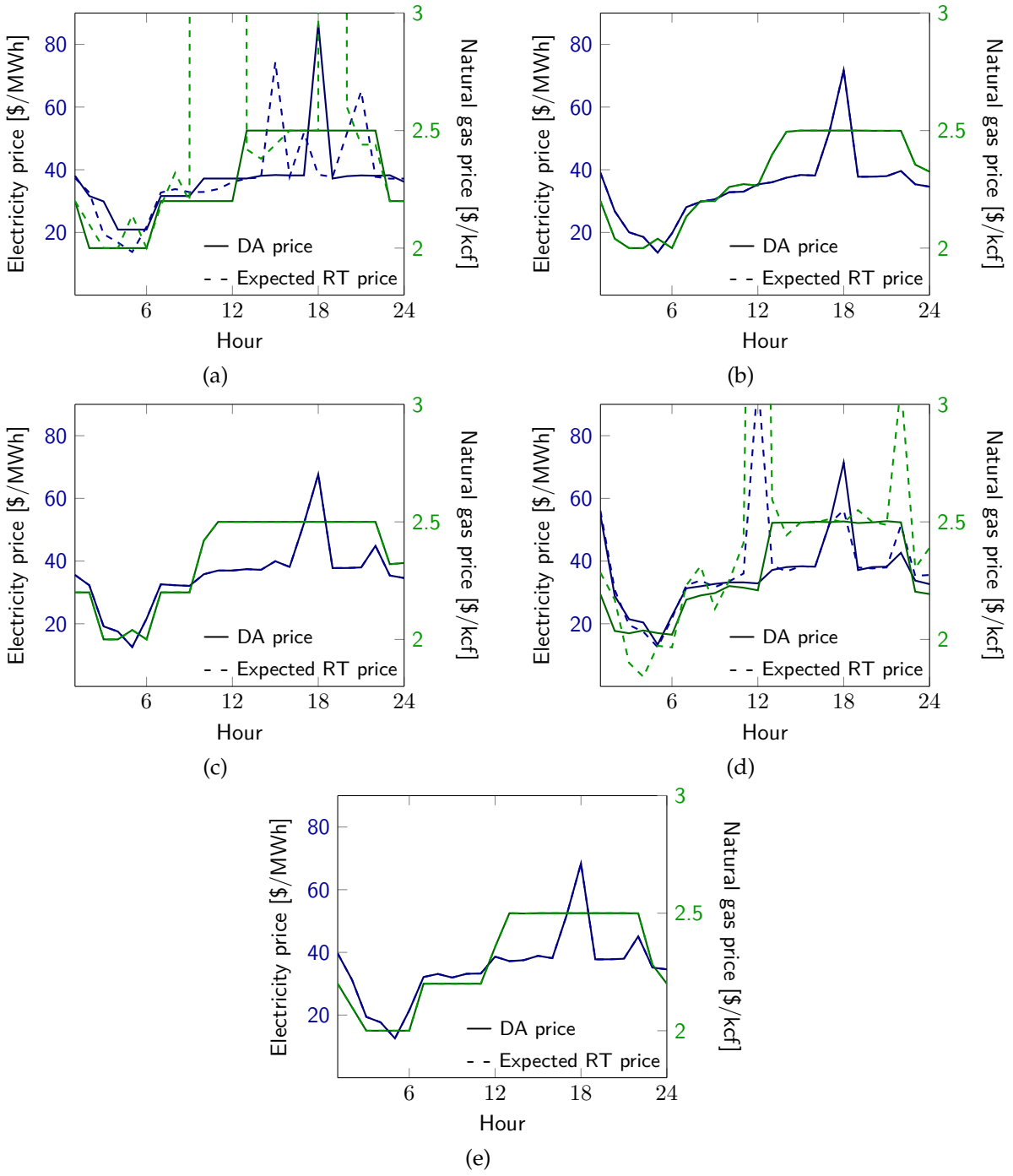

Figure 5.7: Hourly day-ahead (DA) and expected real-time (RT) market clearing prices obtained for different levels of coordination: (a) No coordination, (b) full coordination, and (c)-(e) soft coordination. Soft coordination approaches include (c) improved temporal coordination via explicit virtual bidders and improved sectoral and temporal coordination via (d) implicit virtual bidders and (e) explicit and implicit virtual bidders.

5.5.3 Imperfect knowledge of virtual bidders

An ex-post out-of-sample analysis is conducted in order to evaluate the performance of the proposed coordination approaches against the assumption of perfect knowledge of virtual bidders. For this purpose, the impact of unseen scenarios is tested for different degrees of coordination. A

set of 100 new scenarios is generated from the same distribution as the original scenarios in Figure 5.6. After fixing the day-ahead schedules to those obtained for the in-sample simulations, real-time electricity market model (5.16) and real-time gas market (5.20) are solved for each out-of-sample scenario. Since out-of-sample cost decrease with financial instruments, the effectiveness of virtual bidding to increase sectoral and temporal coordination and make day-ahead schedules more efficient depends on the quality of information available to virtual bidders, but not necessarily on perfect knowledge.

CHAPTER 6

Conclusion and Perspectives

In this thesis, the main challenge of improving the coordination in multi-energy systems in response to the ongoing shift towards renewable-based integrated energy systems was addressed. The focus was directed at two main research questions regarding the coordination of electricity, natural gas and heat systems. The first research question focused on quantifying the value of improving coordination among energy sectors. Full coordination approaches, that centrally operate all energy carriers, were proposed to reveal and exploit existing cross-carrier synergies in deterministic and uncertainty-aware manners. The potential value of flexibility available from multi-energy networks was shown, providing the basis to investigate new market-based tools to enhance the utilization of the revealed synergies while respecting existing market structure. In this direction, the second question aimed at strengthening the coordination of multi-energy systems from a pure market perspective. A non-disruptive option adhering to the current market regulations was introduced in the form of virtual bidders at the interface of sectors and trading floors. As financial instruments, virtual bidders without physical assets perform arbitrage by anticipating price differences between trading floors. Market players at the interface of sectors submit virtual bids by self-scheduling their dispatch. Through comparison of different degrees of sectoral and temporal coordination including no coordination, soft coordination, and full coordination, the value and the effectiveness of financial instruments to contribute to coordination efforts was shown. This chapter concludes with an overview of the contributions to coordinate electricity, natural gas and heat systems and identifies challenges that should be addressed as future research.

6.1 Overview of contributions

The new concepts introduced in this thesis included both full and soft coordination of power, natural gas and heat systems. In order to apply these new concepts, various optimization and equilibrium models were proposed to investigate the coordination of energy infrastructures and markets. The proposed full coordination approaches focused on accounting for energy storage in gas and heat networks to mitigate variability and uncertainty in the power system. In order to account for all potential flexibility, detailed information about natural gas and heat flow dynamics and networks were incorporated in economic dispatch and scheduling tools. For that purpose, co-optimization problems were developed using advanced optimization models and probabilistic methods. These models accounted for energy flow dynamics and virtual electricity storage of multi-energy networks. A holistic model of fully coordinated power, gas, and heat systems accounting for gas and district heating grids was proposed and efficiently solved. The impact of linepack and flow directions as additional degrees of freedom to provide flexibility from gas networks to power systems was investigated. Furthermore, the characterization of uncertainty was embedded to investigate the ability of natural gas systems to provide short-term flexibility to power systems, highlighting the propagation of uncertainty between energy sectors.

Policy-based recourse actions were extended to include flexible assets from the gas system for mitigation of uncertainty. As new reserve products they were shown to bring linepack flexibility from the gas side to the day-ahead power scheduling stage. These perfectly coordinated setups enabled to properly account for potential synergies and available flexibility among the energy systems.

Combined dispatch models were proposed for coordinated scheduling of power, gas and heat systems. Based on a centrally operated energy system, these models accounted for cross-carrier interactions and synergies as well as potential network flexibility from gas and heat storage in pipelines. Full coordination of electricity, heat and natural gas systems was represented in a combined energy dispatch model that served as a deterministic benchmark. Energy flow dynamics were incorporated based on convexification techniques accounting for delay of heat propagation and linepack in pipelines. Second-order cone relaxation, McCormick envelopes and linearization methods were applied to efficiently account for gas and heat network storage effects. Thus, the combined multi-energy dispatch could be formulated as a mixed-integer second-order cone program (MISOCP). The value of energy flow dynamics was quantified when accounting for inlet temperatures, mass flow rates and linepack as controllable variables. This facilitated shifting demand and supply in all energy systems in a cost efficient manner. Focusing on linepack flexibility from the natural gas network for the power system, a deterministic combined power and gas dispatch model was proposed that accounted for bi-directional gas flow and linepack. A novel convexification method using quadratic relaxation, McCormick relaxation and the Big-M method was compared to an outer linear approximation technique from the literature. The resulting combined power and gas dispatch models formulated as MISOCP and mixed-integer linear program showed a trade-off between computational efficiency and accuracy of the two approaches.

In order to investigate the impact of uncertainty in coordinated energy systems, probabilistic modeling was included in the combined energy dispatch. In particular, the propagation of wind power forecast uncertainty from the power system to the gas sector was investigated. For that purpose, a tractable reformulation of the distributionally robust chance-constrained power and gas co-optimization was developed that accounted for flexibility procurement from flexible assets in power and gas systems as well as at the interface of the sectors. The chance-constrained power flow model was extended to include the natural gas system controlling gas supply, flow, and linepack. Moment-based ambiguity sets were defined to represent short-term uncertainty arising from wind power forecast errors without perfect knowledge of its probability distribution. This uncertainty in real-time operations was anticipated in day-ahead scheduling by defining affine policies for flexibility providers. These affine policies, which were based on linear decision rules act as reserve products modeling the coordinated response of market participants to deviations in energy systems. Day-ahead scheduling and dispatch decisions were adjusted via participation factors that define each agent's reaction to deviations in real-time. A tractable reformulation of the distributionally robust chance-constrained power and gas co-optimization was given as a second-order cone program. Numerical results showed propagation of wind power forecast uncertainty to the gas system and the effectiveness of affine policies to activate flexible assets in the gas system to help mitigate this effect. Total system cost and violation probabilities of operational limits depended on confidence levels chosen by the central system operator. Therefore, a trade-off between economic objectives and risk aversion was explored.

Since the full coordination approaches do not align with current regulations and practices of operating energy systems separately and sequentially, a novel market-based coordination

mechanism was developed and investigated. Specifically, virtual bidders as financial instruments and market agents were introduced in both electricity and natural gas markets to enhance the coordination between sectors and trading floors. This soft coordination approach was designed to harness the value of flexible multi-energy resources and synergies between energy carriers while respecting the sequential order of energy markets. The efficiency of this soft coordination mechanism was evaluated against the ideal benchmark of full coordination. Virtual bidders, who take advantage of price differences between trading floors by performing arbitrage in two-settlement markets, were shown to improve the efficiency of markets and bring value to the overall energy system by facilitating smart scheduling decisions for flexible assets in the day-ahead stage.

Equilibrium models were proposed as market simulation tools. These multi-period mixed-complementarity programs were based on deterministic and scenario-based stochastic programming. A full coordination model as stochastic market clearing was used as an ideal benchmark to evaluate the proposed coordination mechanisms against the uncoordinated setup with separate and sequential clearing of markets. While electricity and gas market operators optimized total system cost based on deterministic information, virtual bidders solved two-stage stochastic programs to maximize their expected profit by optimizing their bidding in day-ahead and real-time markets simultaneously. Similarly, self-scheduling gas-fired units optimized their expected profit when participating in electricity and natural gas day-ahead markets anticipating real-time adjustments. This non-cooperative game with coupled strategy sets resulted in a generalized Nash equilibrium with potentially multiple solutions. Explicit and implicit virtual bidders at the interface of power and gas sectors and trading floors were shown both analytically and numerically to help approximate the ideal stochastic integrated energy market while preserving the current sequential and separated market setup. It was shown that virtual bidding in interdependent energy markets helped unlock and exploit the existing sources of cross-carrier flexibility within the current regulatory framework.

6.2 Perspectives for future research

Overall, the work in this thesis motivates more coordination among energy systems either through disruptive restructuring and alignment of energy markets or in a less-disruptive way via financial instruments. This thesis has addressed a number of challenges related to integrated energy systems. While the proposed coordination approaches for power, gas and heat systems are not comprehensive, this work has opened up several directions for future research. Future research directions should also account for interactions and synergies with other energy vectors, e.g., cooling, hydrogen, transportation and water. The proposed frameworks can be adapted to improve coordination of coupled network infrastructures beyond power, gas and heat systems. Different aspects to be addressed in the future range from the technical level to systems, markets, and regulatory implications in the context of accommodating even larger shares of renewable energy sources system-wide. Hereby, some other interesting and challenging ideas are outlined from technical, computational and economic perspectives.

The tightness of relaxation techniques used in the mathematical models introduced in this thesis needs to be further investigated. In particular, quadratic relaxations can be tightened by adding planes approximating the dropped non-convex constraints. Since the quality of McCormick envelopes depends on the choice of upper and lower bounds of each variable, iteratively deriving tighter bounds for each variable could further improve the tightness of the relaxation. Incorporating multi-energy technologies, e.g., power-to-gas units, gas-fueled combined heat and power plants,

and power-fueled compressors or water pumps, is expected to strengthen the coupling between energy sectors and bidirectional interactions. The proposed combined energy dispatch models highlighted the need for more accurate representation of energy networks in a market environment. Advanced non-convex mathematical models accurately representing the (alternating current) AC power flow as well as the underlying physics of energy networks including partial differential equations and non-convex constraints may become critical for real-time operations.

With increasing complexity of mathematical models, full coordination approaches can be solved in a distributed manner. Distributed optimization techniques provide not only computational benefits but also opportunities for the design of market schemes. In order to integrate comprehensive energy flow models in a market environment while preserving the current setup, decentralized optimization tools based on Lagrangian relaxation and consensus-based alternating direction method of multipliers (ADMM) can simulate appropriate market-clearing procedures limiting the information exchange among the systems. Similarly, equilibrium problems can be solved as iterative Walrasian auction using distributed optimization, e.g., ADMM-based algorithms. Such approaches may lead to finding potentially multiple solutions for generalized Nash equilibrium problems.

The accurate representation of energy flows in a market context, particularly spatial and temporal dimensions of network storage, requires extending products, bidding and pricing methods to deal with added complexity and non-convexities. Given different maturity levels of energy markets with limited efficiency, mechanisms similar to financial transmission and storage rights in the power system could be defined for heat and gas markets to hedge prices in space and time, creating financial incentives to fully exploit temporal and spatial dimension of flexibility from multi-energy assets and energy storage in networks. Generalized policies can be introduced to reflect the non-linearity and complexity of reserves provided by multi-energy assets to fully capture flexibility of diverse assets.

It will be interesting to consider energy arbitragers with different information and risk attitudes and how strategic behaviour in multi-commodity trading affects market outcomes. In particular, financial implications of risk attitudes and risk-aware coordination mechanisms should be studied with a focus on incentivizing risk-aware solution in interconnected energy systems.

The study of uncertainty propagation among energy systems and markets can be extended to account for additional sources of uncertainty and bidirectional migration of uncertainty between systems. Metric-based ambiguity sets could be used without any assumptions regarding parametric family of the true distribution. Joint chance constraints that can handle multiple constraints simultaneously, would allow to define a joint violation probability achieving integrated scheduling with probabilistic and robust safety guarantees. This is important for system operators, since system-wide risk parameters for the overall system security can be established leading to a rigorous study of systemic risk due to interactions and coupling of energy systems. To strengthen resilience and reliability of integrated energy systems, uncertainty and risk should be revealed, accounted for and properly controlled. Market-based control mechanisms to manage the propagation of uncertainty in interdependent energy systems are needed and the value of assets not only for providing flexibility but also resilience to the overall energy system should be quantified. While energy sector coordination provides flexibility and supports the accommodation of renewable energy, it becomes crucial to ensure awareness and management of uncertainty propagation due to sector coupling so that the security of supply is guaranteed in integrated energy systems.

Bibliography

[1] Jacob Gronholt-Pedersen. Denmark sources record 47% of power from wind in 2019, 2020. https://www.reuters.com/article/us-climate-change-denmark-windpower/denmark-sources-record-47-of-power-from-wind-in-2019-idUSKBN1Z10KE. Online; Accessed June 24, 2020.

[2] Danish Energy Agency. Biogas in Denmark, 2020. https://ens.dk/en/our-responsibilities/bioenergy/biogas-denmark. Online; Accessed July 10, 2020.

[3] Ministry of Climate Energy and Building. The Danish energy model, Technical report, 2012. https://ens.dk/sites/ens.dk/files/Globalcooperation/the_danish_energy_model.pdf. Online; Accessed July 10, 2020.

[4] Stefanos Delikaraoglou, Juan M. Morales, and Pierre Pinson. Impact of inter-and intra-regional coordination in markets with a large renewable component. *IEEE Transactions on Power Systems*, 31(6):5061–5070, 2016.

[5] Mark J. O'Malley, Muhammad Bashar Anwar, Steve Heinen, Tom Kober, James McCalley, Madeleine McPherson, Matteo Muratori, Antje Orths, Mark Ruth, Thomas J. Schmidt, and Aidan Tuohy. Multicarrier energy systems: Shaping our energy future. *Proceedings of the IEEE*, 108(9):1437–1456, 2020.

[6] Pierluigi Mancarella. MES (multi-energy systems): An overview of concepts and evaluation models. *Energy*, 65:1–17, 2014.

[7] Emiliano Dall'Anese, Pierluigi Mancarella, and Antonello Monti. Unlocking flexibility: Integrated optimization and control of multienergy systems. *IEEE Power and Energy Magazine*, 15(1):43–52, 2017.

[8] Paul J. Hibbard and Todd Schatzki. The interdependence of electricity and natural gas: current factors and future prospects. *The Electricity Journal*, 25(4):6–17, 2012.

[9] Joshua A. Taylor. *Convex optimization of power systems*. Cambridge University Press, 2015.

[10] Stephen Boyd and Lieven Vandenberghe. *Convex optimization*. Cambridge University Press, 2004.

[11] Juan M. Morales, Antonio J. Conejo, Henrik Madsen, Pierre Pinson, and Marco Zugno. *Integrating renewables in electricity markets: Operational problems*, volume 205. Springer Science & Business Media, 2013.

[12] Frederick S. Hillier and Gerald J. Lieberman. *Introduction to Operations Research*. McGraw-Hill Science, Engineering & Mathematics, 1995.

[13] Martin J. Osborne and Ariel Rubinstein. *A course in game theory*. MIT press, 1994.

[14] Ankur A. Kulkarni and Uday V. Shanbhag. Revisiting generalized Nash games and variational inequalities. *Journal of Optimization Theory and Applications*, 154(1):175–186, 2012.

[15] Jinye Zhao, Tongxin Zheng, and Eugene Litvinov. A unified framework for defining and measuring flexibility in power system. *IEEE Transactions on Power Systems*, 31(1):339–347, 2016.

[16] Anatoly Zlotnik, Line Roald, Scott Backhaus, Michael Chertkov, and Göran Andersson. Coordinated scheduling for interdependent electric power and natural gas infrastructures. *IEEE Transactions on Power Systems*, 32(1):600–610, 2016.

[17] Christos Ordoudis, Pierre Pinson, and Juan M. Morales. An integrated market for electricity and natural gas systems with stochastic power producers. *European Journal of Operational Research*, 272(2):642–654, 2019.

[18] Lesia Mitridati, Pascal Van Hentenryck, and Jalal Kazempour. Electricity-aware heat unit commitment: A bid-validity approach. *arXiv preprint arXiv:2005.03120*, 2020.

[19] Tao Li, Mircea Eremia, and Mohammad Shahidehpour. Interdependency of natural gas network and power system security. *IEEE Transactions on Power Systems*, 23(4):1817–1824, 2008.

[20] Cong Liu, Mohammad Shahidehpour, Yong Fu, and Zuyi Li. Security-constrained unit commitment with natural gas transmission constraints. *IEEE Transactions on Power Systems*, 24(3):1523–1536, 2009.

[21] Lajos Maurovich-Horvat, Paula Rocha, and Afzal S. Siddiqui. Optimal operation of combined heat and power under uncertainty and risk aversion. *Energy and Buildings*, 110:415–425, 2016.

[22] Carlos M. Correa-Posada and Pedro Sanchez-Martin. Integrated power and natural gas model for energy adequacy in short-term operation. *IEEE Transactions on Power Systems*, 30(6):3347–3355, 2014.

[23] Sheng Chen, Antonio J. Conejo, Ramteen Sioshansi, and Zhinong Wei. Unit commitment with an enhanced natural gas-flow model. *IEEE Transactions on Power Systems*, 34(5):3729–3738, 2019.

[24] Lesia Mitridati and Josh A. Taylor. Power systems flexibility from district heating networks. In *2018 Power Systems Computation Conference (PSCC)*. IEEE, 2018.

[25] Zhigang Li, Wenchuan Wu, Mohammad Shahidehpour, Jianhui Wang, and Boming Zhang. Combined heat and power dispatch considering pipeline energy storage of district heating network. *IEEE Transactions on Sustainable Energy*, 7(1):12–22, 2015.

[26] Martin Geidl, Gaudenz Koeppel, Patrick Favre-Perrod, Bernd Klöckl, Göran Andersson, and Klaus Fröhlich. The energy hub–A powerful concept for future energy systems. In *Third annual Carnegie Mellon conference on the electricity industry*, volume 13, 2007.

[27] Pierre Pinson, Lesia Mitridati, Christos Ordoudis, and Jacob Ostergaard. Towards fully renewable energy systems: Experience and trends in Denmark. *CSEE Journal of Power and Energy Systems*, 3(1):26–35, 2017.

[28] Xinyu Chen, Chongqing Kang, Mark O'Malley, Qing Xia, Jianhua Bai, Chun Liu, Rongfu Sun, Weizhou Wang, and Hui Li. Increasing the flexibility of combined heat and power for wind power integration in China: Modeling and implications. *IEEE Transactions on Power Systems*, 30(4):1848–1857, 2014.

[29] Richard D. Tabors, Scott Englander, and Robert Stoddard. Who's on first? The coordination of gas and power scheduling. *The Electricity Journal*, 25(5):8–15, 2012.

[30] Pierluigi Mancarella, Göran Andersson, J. A. Peças-Lopes, and Keith R. W. Bell. Modelling of integrated multi-energy systems: Drivers, requirements, and opportunities. In *2016 Power Systems Computation Conference (PSCC)*. IEEE, 2016.

[31] Eduardo Alejandro Martínez Ceseña and Pierluigi Mancarella. Energy systems integration in smart districts: Robust optimisation of multi-energy flows in integrated electricity, heat and gas networks. *IEEE Transactions on Smart Grid*, 10(1):1122–1131, 2018.

[32] Antonio J. Conejo, Miguel Carrión, Juan M. Morales, et al. *Decision making under uncertainty in electricity markets*, volume 1. Springer, 2010.

[33] Alvin E. Roth. Game theory as a tool for market design. In *Game practice: Contributions from applied game theory*, pages 7–18. Springer, 2000.

[34] Geunyeong Byeon and Pascal Van Hentenryck. Unit commitment with gas network awareness. *IEEE Transactions on Power Systems*, 35(2):1327–1339, 2020.

[35] Lesia Mitridati, Jalal Kazempour, and Pierre Pinson. Heat and electricity market coordination: A scalable complementarity approach. *European Journal of Operational Research*, 283(3):1107–1123, 2020.

[36] Bining Zhao, Anatoly Zlotnik, Antonio J. Conejo, Ramteen Sioshansi, and Aleksandr M. Rudkevich. Shadow price-based co-ordination of natural gas and electric power systems. *IEEE Transactions on Power Systems*, 34(3):1942–1954, 2018.

[37] Sheng Chen, Antonio J. Conejo, Ramteen Sioshansi, and Zhinong Wei. Operational equilibria of electric and natural gas systems with limited information interchange. *IEEE Transactions on Power Systems*, 35(1):662–671, 2019.

[38] Runze Chen, Jianhui Wang, and Hongbin Sun. Clearing and pricing for coordinated gas and electricity day-ahead markets considering wind power uncertainty. *IEEE Transactions on Power Systems*, 33(3):2496–2508, 2018.

[39] Joseph Warrington, Paul Goulart, Sébastien Mariéthoz, and Manfred Morari. Policy-based reserves for power systems. *IEEE Transactions on Power Systems*, 28(4):4427–4437, 2013.

[40] Beibei Wang and Benjamin F. Hobbs. Real-time markets for flexiramp: A stochastic unit commitment-based analysis. *IEEE Transactions on Power Systems*, 31(2):846–860, 2016.

[41] Trine Krogh Boomsma, Nina Juul, and Stein-Erik Fleten. Bidding in sequential electricity markets: The Nordic case. *European Journal of Operational Research*, 238(3):797–809, 2014.

[42] Yanchao Liu, Jesse T. Holzer, and Michael C. Ferris. Extending the bidding format to promote demand response. *Energy Policy*, 86:82–92, 2015.

[43] Niamh O'Connell, Pierre Pinson, Henrik Madsen, and Mark O'Malley. Economic dispatch of demand response balancing through asymmetric block offers. *IEEE Transactions on Power Systems*, 31(4):2999–3007, 2016.

[44] Iacopo Savelli, Bertrand Cornélusse, Antonio Giannitrapani, Simone Paoletti, and Antonio Vicino. A new approach to electricity market clearing with uniform purchase price and curtailable block orders. *Applied Energy*, 226:618–630, 2018.

[45] Steven A. Gabriel, Antonio J. Conejo, J. David Fuller, Benjamin F. Hobbs, and Carlos Ruiz. *Complementarity modeling in energy markets*, volume 180. Springer Science & Business Media, 2012.

[46] Francisco Facchinei and Jong-Shi Pang. *Finite-dimensional variational inequalities and complementarity problems*. Springer Science & Business Media, 2007.

[47] Patrick T. Harker and Jong-Shi Pang. Finite-dimensional variational inequality and nonlinear complementarity problems: a survey of theory, algorithms and applications. *Mathematical Programming*, 48(1-3):161–220, 1990.

[48] Gui Wang, Matias Negrete-Pincetic, Anupama Kowli, Ehsan Shafieepoorfard, Sean Meyn, and Uday V. Shanbhag. Dynamic competitive equilibria in electricity markets. In *Control and Optimization Methods for Electric Smart Grids*, pages 35–62. Springer, 2012.

[49] William W. Hogan. Virtual bidding and electricity market design. *The Electricity Journal*, 29(5):33–47, 2016.

[50] Koichiro Ito and Mar Reguant. Sequential markets, market power, and arbitrage. *American Economic Review*, 106(7):1921–57, 2016.

[51] Jalal Kazempour and Benjamin F. Hobbs. Value of flexible resources, virtual bidding, and self–scheduling in two–settlement electricity markets with wind generation– Part I: Principles and competitive model. *IEEE Transactions on Power Systems*, 33(1):749–759, 2018.

[52] Erick Delage and Yinyu Ye. Distributionally robust optimization under moment uncertainty with application to data-driven problems. *Operations Research*, 58(3):595–612, 2010.

[53] Peyman Mohajerin Esfahani and Daniel Kuhn. Data-driven distributionally robust optimization using the Wasserstein metric: Performance guarantees and tractable reformulations. *Mathematical Programming*, 171(1-2):115–166, 2018.

[54] Alexander Shapiro, Darinka Dentcheva, and Andrzej Ruszczyński. *Lectures on stochastic programming: Modeling and theory*. SIAM, 2014.

[55] Manish K. Singh and Vassilis Kekatos. Natural gas flow solvers using convex relaxation. *IEEE Transactions on Control of Network Systems*, 2020, doi: 10.1109/TCNS.2020.2972593.

[56] Uma Ravat and Uday V. Shanbhag. On the existence of solutions to stochastic quasi-variational inequality and complementarity problems. *Mathematical Programming*, 165(1):291–330, 2017.

[57] European Commission. EU energy in figures, 2019. https://op.europa.eu/en/publication-detail/-/publication/e0544b72-db53-11e9-9c4e-01aa75ed71a1. Online; Accessed August 20, 2020.

[58] Baraa Mohandes, Mohamed Shawky El Moursi, Nikos Hatziargyriou, and Sameh El Khatib. A review of power system flexibility with high penetration of renewables. *IEEE Transactions on Power Systems*, 34(4):3140–3155, 2019.

[59] Gianfranco Chicco, Shariq Riaz, Andrea Mazza, and Pierluigi Mancarella. Flexibility from distributed multienergy systems. *Proceedings of the IEEE*, 108(9):1496–1517, 2020.

[60] Communication from the Commission to the European Parliament, the Council, the European Economic and Social Committee and the Committee of the Regions. Powering a climate-neutral economy: An EU strategy for energy system integration, 2020. https://ec.europa.eu/energy/sites/ener/files/energy_system_integration_strategy_.pdf. Online; Accessed July 17, 2020.

[61] Peter Meibom, Klaus Baggesen Hilger, Henrik Madsen, and Dorthe Vinther. Energy comes together in Denmark: The key to a future fossil-free danish power system. *IEEE Power and Energy Magazine*, 11(5):46–55, 2013.

[62] Stein-Erik Fleten and Erkka Näsäkkälä. Gas-fired power plants: Investment timing, operating flexibility and CO2 capture. *Energy Economics*, 32(4):805–816, 2010.

[63] José Gil, Ángel Caballero, and Antonio J. Conejo. Power cycling: CCGTs: The critical link between the electricity and natural gas markets. *IEEE Power and Energy Magazine*, 12(6):40–48, 2014.

[64] International Energy Agency. Status of power system transformation 2019, 2019. https://www.iea.org/reports/status-of-power-system-transformation-2019. Online; Accessed June 5, 2020.

[65] Mark Babula and Kevin Petak. The cold truth: Managing gas-electric integration: The ISO New England experience. *IEEE Power and Energy Magazine*, 12(6):20–28, 2014.

[66] Bart C. Ummels, Madeleine Gibescu, Engbert Pelgrum, Wil L. Kling, and Arno J Brand. Impacts of wind power on thermal generation unit commitment and dispatch. *IEEE Transactions on Energy Conversion*, 22(1):44–51, 2007.

[67] Vilma Virasjoki, Afzal S. Siddiqui, Behnam Zakeri, and Ahti Salo. Market power with combined heat and power production in the Nordic energy system. *IEEE Transactions on Power Systems*, 33(5):5263–5275, 2018.

[68] Daniel S. Kirschen and Goran Strbac. *Fundamentals of power system economics*. John Wiley & Sons, 2018.

[69] Darryl R. Biggar and Mohammad Reza Hesamzadeh. *The economics of electricity markets*. John Wiley & Sons, 2014.

[70] Henrik Lund, Bernd Möller, Brian Vad Mathiesen, and A. Dyrelund. The role of district heating in future renewable energy systems. *Energy*, 35(3):1381–1390, 2010.

[71] Marie Münster, Poul Erik Morthorst, Helge V. Larsen, Lars Bregnbæk, Jesper Werling, Hans Henrik Lindboe, and Hans Ravn. The role of district heating in the future Danish energy system. *Energy*, 48(1):47–55, 2012.

[72] Jean-Michel Glachant, Michelle Hallack, and Miguel Vazquez. *Building competitive gas markets in the EU*. Edward Elgar Publishing, 2013.

[73] Thorsten Koch, Benjamin Hiller, Marc E. Pfetsch, and Lars Schewe. *Evaluating gas network capacities*. SIAM, 2015.

[74] Ruth Domínguez, Giorgia Oggioni, and Yves Smeers. Reserve procurement and flexibility services in power systems with high renewable capacity: Effects of integration on different market designs. *International Journal of Electrical Power & Energy Systems*, 113:1014–1034, 2019.

[75] Lesia Marie-Jeanne Mariane Mitridati. *Market-Based Coordination of Heat and Electricity Systems*. PhD thesis, Technical University of Denmark, 2019 [Online]. Available: https://drive.google.com/file/d/1h11bCp8ETHHRHf7shDw1z32kzknZi0r3/view.

[76] Christos Ordoudis. *Market-based Approaches for the Coordinated Operation of Electricity and Natural Gas Systems*. PhD thesis, Technical University of Denmark, 2018 [Online]. Available: https://drive.google.com/file/d/16w2KupRfAkQ56hmtgnYGF0mnaHss6TOp/view.

[77] Lejla Halilbašić, Florian Thams, Andreas Venzke, Spyros Chatzivasileiadis, and Pierre Pinson. Data-driven security-constrained ac-opf for operations and markets. In *2018 Power Systems Computation Conference (PSCC)*. IEEE, 2018.

[78] Jian Yao, Shmuel S. Oren, and Ilan Adler. Two-settlement electricity markets with price caps and Cournot generation firms. *European Journal of Operational Research*, 181(3):1279–1296, 2007.

[79] Trading platforms, 2020. https://en.energinet.dk/Gas/Shippers/Trading-Platforms. Online; Accessed August 23, 2020.

[80] Miguel Vazquez and Michelle Hallack. Interaction between gas and power market designs. *Utilities Policy*, 33:23–33, 2015.

[81] Miguel Vazquez, Michelle Hallack, and Jean-Michel Glachant. Designing the European gas market: More liquid & less natural? *Economics of Energy & Environmental Policy*, 1(3):25–38, 2012.

[82] Ali Daraeepour, Dalia Patino-Echeverri, and Antonio J. Conejo. Economic and environmental implications of different approaches to hedge against wind production uncertainty in two-settlement electricity markets: A PJM case study. *Energy Economics*, 80:336–354, 2019.

[83] Tryggvi Jónsson, Pierre Pinson, and Henrik Madsen. On the market impact of wind energy forecasts. *Energy Economics*, 32(2):313–320, 2010.

[84] Juan M. Morales and Salvador Pineda. On the inefficiency of the merit order in forward electricity markets with uncertain supply. *European Journal of Operational Research*, 261:789–799, 2017.

[85] Jalal Kazempour, Pierre Pinson, and Benjamin F. Hobbs. A stochastic market design with revenue adequacy and cost recovery by scenario: Benefits and costs. *IEEE Transactions on Power Systems*, 33(4):3531–3545, 2018.

[86] Alexandre Velloso, Alexandre Street, David Pozo, José M Arroyo, and Noemi G. Cobos. Two-stage robust unit commitment for co-optimized electricity markets: An adaptive data-driven approach for scenario-based uncertainty sets. *IEEE Transactions on Sustainable Energy*, 11(2):958–969, 2019.

[87] Richard P. O'Neill, Paul M. Sotkiewicz, Benjamin F. Hobbs, Michael H. Rothkopf, and William R. Stewart Jr. Efficient market-clearing prices in markets with nonconvexities. *European Journal of Operational Research*, 164(1):269–285, 2005.

[88] Andreas Venzke, Lejla Halilbasic, Uros Markovic, Gabriela Hug, and Spyros Chatzivasileiadis. Convex relaxations of chance constrained AC optimal power flow. *IEEE Transactions on Power Systems*, 33(3):2829–2841, 2017.

[89] Lejla Halilbašić, Pierre Pinson, and Spyros Chatzivasileiadis. Convex relaxations and approximations of chance-constrained AC-OPF problems. *IEEE Transactions on Power Systems*, 34(2):1459–1470, 2018.

[90] Richard D. Christie, Bruce F. Wollenberg, and Ivar Wangensteen. Transmission management in the deregulated environment. *Proceedings of the IEEE*, 88(2):170–195, 2000.

[91] Jan Fredrik Helgaker, Bernhard Müller, and Tor Ytrehus. Transient flow in natural gas pipelines using implicit finite difference schemes. *Journal of Offshore Mechanics and Arctic Engineering*, 136(3), 2014.

[92] Anatoly Zlotnik, Michael Chertkov, and Scott Backhaus. Optimal control of transient flow in natural gas networks. In *2015 54th IEEE Conference on Decision and Control (CDC)*, pages 4563–4570. IEEE, 2015.

[93] Terrence W. K. Mak, Pascal Van Hentenryck, Anatoly Zlotnik, and Russell Bent. Dynamic compressor optimization in natural gas pipeline systems. *INFORMS Journal on Computing*, 31(1):40–65, 2019.

[94] Conor O Malley, Drosos Kourounis, Gabriela Hug, and Olaf Schenk. Finite volume methods for transient modeling of gas pipelines. In *2018 IEEE International Energy Conference (ENERGYCON)*. IEEE, 2018.

[95] Andreas Belderbos, Thomas Valkaert, Kenneth Bruninx, Erik Delarue, and William D'haeseleer. Facilitating renewables and power-to-gas via integrated electrical power-gas system scheduling. *Applied Energy*, 275:115082, 2020.

[96] Carlos M. Correa-Posada and Pedro Sánchez-Martín. Integrated power and natural gas model for energy adequacy in short-term operation. *IEEE Transactions on Power Systems*, 30(6):3347–3355, 2015.

[97] Line A. Roald, Kaarthik Sundar, Anatoly Zlotnik, Sidhant Misra, and Göran Andersson. An uncertainty management framework for integrated gas-electric energy systems. *Proceedings of the IEEE*, 108(9):1518–1540, 2020.

[98] Zhigang Li, Wenchuan Wu, Jianhui Wang, Boming Zhang, and Taiyi Zheng. Transmission-constrained unit commitment considering combined electricity and district heating networks. *IEEE Transactions on Sustainable Energy*, 7(2):480–492, 2016.

[99] Menglin Zhang, Qiuwei Wu, Jinyu Wen, Zhongwei Lin, Fang Fang, and Qun Chen. Optimal operation of integrated electricity and heat system: A review of modeling and solution methods. *Renewable and Sustainable Energy Reviews*, 135:110098, 2020.

[100] Guillaume Sandou, S. Font, Sihem Tebbani, A. Hiret, and C. Mondon. Predictive control of a complex district heating network. In *Proceedings of the 44th IEEE Conference on Decision and Control*, pages 7372–7377, 2005.

[101] Bining Zhao, Antonio J. Conejo, and Ramteen Sioshansi. Unit commitment under gas-supply uncertainty and gas-price variability. *IEEE Transactions on Power Systems*, 32(3):2394–2405, 2017.

[102] Ahmed Alabdulwahab, Abdullah Abusorrah, Xiaping Zhang, and Mohammad Shahidehpour. Stochastic security-constrained scheduling of coordinated electricity and natural gas infrastructures. *IEEE Systems Journal*, 11(3):1674–1683, 2015.

[103] Russell Bent, Seth Blumsack, Pascal Van Hentenryck, Conrado Borraz Sánchez, and Scott Backhaus. Joint expansion planning for natural gas and electric transmission with endogenous market feedbacks. In *Proceedings of the 51st Hawaii International Conference on System Sciences (HICSS)*, 2018.

[104] Conrado Borraz Sánchez, Russell Bent, Scott Backhaus, Seth Blumsack, Hassan Hijazi, and Pascal Van Hentenryck. Convex optimization for joint expansion planning of natural gas and power systems. In *Proceedings of the 49th Hawaii International Conference on System Sciences (HICSS)*, 2016.

[105] Steve Heinen and Mark J. O'Malley. Complementarities of supply and demand sides in integrated energy systems. *IEEE Transactions on Smart Grid*, 10(1):1156–1165, 2018.

[106] Anatoly Zlotnik, Line Roald, Scott Backhaus, Michael Chertkov, and Göran Andersson. Coordinated scheduling for interdependent electric power and natural gas infrastructures. *IEEE Transactions on Power Systems*, 32(1):600–610, 2017.

[107] Christos Ordoudis, Stefanos Delikaraoglou, Pierre Pinson, and Jalal Kazempour. Exploiting flexibility in coupled electricity and natural gas markets: A price-based approach. In *2017 IEEE Manchester PowerTech*. IEEE, 2017.

[108] Christos Ordoudis, Stefanos Delikaraoglou, Jalal Kazempour, and Pierre Pinson. Market-based coordination of integrated electricity and natural gas systems under uncertain supply. *European Journal of Operational Research*, 287(3):1105–1119, 2020.

[109] Hossein Ameli, Meysam Qadrdan, and Goran Strbac. Coordinated operation strategies for natural gas and power systems in presence of gas-related flexibilities. *Energy Systems Integration*, 1(1):3–13, 2019.

[110] Cheng Wang, Wei Wei, Jianhui Wang, and Tianshu Bi. Convex optimization based adjustable robust dispatch for integrated electric-gas systems considering gas delivery priority. *Applied Energy*, 239:70–82, 2019.

[111] Babatunde Odetayo, John MacCormack, WD Rosehart, and Hamidreza Zareipour. A chance constrained programming approach to integrated planning of distributed power generation and natural gas network. *Electric Power Systems Research*, 151:197–207, 2017.

[112] Cong Liu, Changhyeok Lee, and Mohammad Shahidehpour. Look ahead robust scheduling of wind-thermal system with considering natural gas congestion. *IEEE Transactions on Power Systems*, 30(1):544–545, 2015.

[113] Linquan Bai, Fangxing Li, Tao Jiang, and Hongjie Jia. Robust scheduling for wind integrated energy systems considering gas pipeline and power transmission N–1 contingencies. *IEEE Transactions on Power Systems*, 32(2):1582–1584, 2017.

[114] Jingwei Yang, Ning Zhang, Chongqing Kang, and Qing Xia. Effect of natural gas flow dynamics in robust generation scheduling under wind uncertainty. *IEEE Transactions on Power Systems*, 33(2):2087–2097, 2018.

[115] Stephen Clegg and Pierluigi Mancarella. Integrated electrical and gas network flexibility assessment in low-carbon multi-energy systems. *IEEE Transactions on Sustainable Energy*, 7(2):718–731, 2016.

[116] Andrea Antenucci and Giovanni Sansavini. Gas-constrained secure reserve allocation with large renewable penetration. *IEEE Transactions on Sustainable Energy*, 9(2):685–694, 2017.

[117] Yubin He, Mingyu Yan, Mohammad Shahidehpour, Zhiyi Li, Chuangxin Guo, Lei Wu, and Yi Ding. Decentralized optimization of multi-area electricity-natural gas flows based on cone reformulation. *IEEE Transactions on Power Systems*, 33(4):4531–4542, 2017.

[118] Sobhan Badakhshan, Mostafa Kazemi, and Mahdi Ehsan. Security constrained unit commitment with flexibility in natural gas transmission delivery. *Journal of Natural Gas Science and Engineering*, 27:632–640, 2015.

[119] Carlos M. Correa-Posada, Pedro Sanchez-Martin, and Sara Lumbreras. Security-constrained model for integrated power and natural-gas system. *Journal of Modern Power Systems and Clean Energy*, 5(3):326–336, 2017.

[120] Leonid Hurwicz. The design of mechanisms for resource allocation. *The American Economic Review*, 63(2):1–30, 1973.

[121] Carlos Silva, Bruce F. Wollenberg, and Charles Z. Zheng. Application of mechanism design to electric power markets (republished). *IEEE Transactions on Power Systems*, 16(4):862–869, 2001.

[122] Nir Vulkan, Alvin E. Roth, and Zvika Neeman. *The handbook of market design*. OUP Oxford, 2013.

[123] Leonid Hurwicz and Stanley Reiter. *Designing economic mechanisms*. Cambridge University Press, 2006.

[124] Aleksandr Rudkevich, Anatoly Zlotnik, Pablo Ruiz, Evgeniy Goldis, Aleksandr Beylin, Richard Hornby, Richard Tabors, Scott Backhaus, Michael Caramanis, and Russ Philbrick. Market based intraday coordination of electric and natural gas system operation. In *Proceedings of the 51st Hawaii International Conference on System Sciences (HICSS)*, 2018.

[125] Ferdinando Fioretto, Lesia Mitridati, and Pascal Van Hentenryck. PPSM: A privacy-preserving Stackelberg mechanism: Privacy guarantees for the coordination of sequential electricity and gas markets. *arXiv preprint arXiv:1911.10178*, 2019.

[126] Ferdinando Fioretto, Lesia Mitridati, and Pascal Van Hentenryck. Differential privacy for Stackelberg games. *arXiv preprint arXiv:2002.00944*, 2020.

[127] Anubhav Ratha, Jalal Kazempour, Ana Virag, and Pierre Pinson. Exploring market properties of policy-based reserve procurement for power systems. In *2019 IEEE 58th Conference on Decision and Control (CDC)*, pages 7498–7505. IEEE, 2019.

[128] Lucien Bobo, Stefanos Delikaraoglou, Niklas Vespermann, Jalal Kazempour, and Pierre Pinson. Offering strategy of a flexibility aggregator in a balancing market using asymmetric block offers. In *2018 Power Systems Computation Conference (PSCC)*. IEEE, 2018.

[129] Lesia Mitridati, Jalal Kazempour, and Pierre Pinson. Design and game-theoretic analysis of community-based market mechanisms in heat and electricity systems. *Omega*, 102177, 2019, doi: 10.1016/j.omega.2019.102177.

[130] Ramteen Sioshansi, Shmuel Oren, and Richard O'Neill. Three-part auctions versus self-commitment in day-ahead electricity markets. *Utilities Policy*, 18(4):165–173, 2010.

[131] Ruoyang Li, Alva J. Svoboda, and Shmuel S. Oren. Efficiency impact of convergence bidding in the California electricity market. *Journal of Regulatory Economics*, 48(3):245–284, 2015.

[132] John Birge, Ali Hortaçsu, Ignacia Mercadal, and Michael Pavlin. Limits to arbitrage in electricity markets: A case study of MISO. *Energy Economics*, 75:518–533, 2018.

[133] Alan G. Isemonger. The benefits and risks of virtual bidding in multi-settlement markets. *The Electricity Journal*, 19(9):26–36, 2006.

[134] Miguel Sousa Lobo, Lieven Vandenberghe, Stephen Boyd, and Hervé Lebret. Applications of second-order cone programming. *Linear Algebra and its Applications*, 284(1-3):193–228, 1998.

[135] Farid Alizadeh and Donald Goldfarb. Second-order cone programming. *Mathematical Programming*, 95(1):3–51, 2003.

[136] Asgeir Tomasgard, Frode Rømo, Marte Fodstad, and Kjetil Midthun. Optimization models for the natural gas value chain. In *Geometric Modelling, Numerical Simulation, and Optimization*, pages 521–558. Springer, 2007.

[137] Marte Fodstad, Kjetil T. Midthun, and Asgeir Tomasgard. Adding flexibility in a natural gas transportation network using interruptible transportation services. *European Journal of Operational Research*, 243(2):647–657, 2015.

[138] Manish K. Singh and Vassilis Kekatos. Natural gas flow equations: Uniqueness and an mi-socp solver. In *2019 American Control Conference (ACC)*, pages 2114–2120. IEEE, 2019.

[139] Garth P. McCormick. Computability of global solutions to factorable nonconvex programs: Part I Convex underestimating problems. *Mathematical Programming*, 10(1):147–175, 1976.

[140] James Luedtke, Mahdi Namazifar, and Jeff Linderoth. Some results on the strength of relaxations of multilinear functions. *Mathematical Programming*, 136(2):325–351, 2012.

[141] John E. Mitchell, Jong-Shi Pang, and Bin Yu. Convex quadratic relaxations of nonconvex quadratically constrained quadratic programs. *Optimization Methods and Software*, 29(1):120–136, 2014.

[142] Christos Ordoudis, Pierre Pinson, Juan Miguel Morales González, and Marco Zugno. An updated version of the IEEE RTS 24-bus system for electricity market and power system operation studies. Technical University of Denmark, 2016. https://core.ac.uk/download/pdf/43255921.pdf.

[143] Conrado Borraz-Sánchez, Russell Bent, Scott Backhaus, Hassan Hijazi, and Pascal Van Hentenryck. Convex relaxations for gas expansion planning. *INFORMS Journal on Computing*, 28(4):645–656, 2016.

[144] Carleton Coffrin, Hassan L. Hijazi, and Pascal Van Hentenryck. Strengthening the SDP relaxation of AC power flows with convex envelopes, bound tightening, and valid inequalities. *IEEE Transactions on Power Systems*, 32(5):3549–3558, 2017.

[145] Ahmed Alabdulwahab, Abdullah Abusorrah, Xiaping Zhang, and Mohammad Shahidehpour. Coordination of interdependent natural gas and electricity infrastructures for firming the variability of wind energy in stochastic day-ahead scheduling. *IEEE Transactions on Sustainable Energy*, 6(2):606–615, 2015.

[146] Yong Li, Yao Zou, Yi Tan, Yijia Cao, Xindong Liu, Mohammad Shahidehpour, Shiming Tian, and Fanpeng Bu. Optimal stochastic operation of integrated low-carbon electric power, natural gas, and heat delivery system. *IEEE Transactions on Sustainable Energy*, 9(1):273–283, 2017.

[147] Chuan He, Tianqi Liu, Lei Wu, and Mohammad Shahidehpour. Robust coordination of interdependent electricity and natural gas systems in day-ahead scheduling for facilitating volatile renewable generations via power-to-gas technology. *Journal of Modern Power Systems and Clean Energy*, 5(3):375–388, 2017.

[148] Yubin He, Mohammad Shahidehpour, Zhiyi Li, Chuangxin Guo, and Bingquan Zhu. Robust constrained operation of integrated electricity-natural gas system considering distributed natural gas storage. *IEEE Transactions on Sustainable Energy*, 9(3):1061–1071, 2017.

[149] Francesca Maggioni, Matteo Cagnolari, and Luca Bertazzi. The value of the right distribution in stochastic programming with application to a newsvendor problem. *Computational Management Science*, 16(4):739–758, 2019.

[150] John R. Birge and Francois Louveaux. *Introduction to stochastic programming*. Springer Science & Business Media, 2011.

[151] Wolfram Wiesemann, Daniel Kuhn, and Melvyn Sim. Distributionally robust convex optimization. *Operations Research*, 62(6):1358–1376, 2014.

[152] Aharon Ben-Tal and Arkadi Nemirovski. Robust convex optimization. *Mathematics of Operations Research*, 23(4):769–805, 1998.

[153] Dimitris Bertsimas, Vishal Gupta, and Nathan Kallus. Data-driven robust optimization. *Mathematical Programming*, 167(2):235–292, 2018.

[154] Dimitris Bertsimas and Melvyn Sim. Tractable approximations to robust conic optimization problems. *Mathematical Programming*, 107(1-2):5–36, 2006.

[155] Aharon Ben-Tal, Laurent El Ghaoui, and Arkadi Nemirovski. *Robust optimization*, volume 28. Princeton University Press, 2009.

[156] Dimitris Bertsimas and Melvyn Sim. The price of robustness. *Operations Research*, 52(1):35–53, 2004.

[157] Daniel Bienstock, Michael Chertkov, and Sean Harnett. Chance-constrained optimal power flow: Risk-aware network control under uncertainty. *SIAM Review*, 56(3):461–495, 2014.

[158] Bowen Li and Johanna L. Mathieu. Analytical reformulation of chance-constrained optimal power flow with uncertain load control. In *2015 IEEE Eindhoven PowerTech*. IEEE, 2015.

[159] Hamed Rahimian and Sanjay Mehrotra. Distributionally robust optimization: A review. *arXiv preprint arXiv:1908.05659*, 2019.

[160] Alexander Shapiro. Tutorial on risk neutral, distributionally robust and risk averse multistage stochastic programming. *European Journal of Operational Research*, 288(1):1–13, 2021.

[161] Krzysztof Postek, Dick den Hertog, and Bertrand Melenberg. Computationally tractable counterparts of distributionally robust constraints on risk measures. *SIAM Review*, 58(4):603–650, 2016.

[162] Line Roald, Frauke Oldewurtel, Bart Van Parys, and Göran Andersson. Security constrained optimal power flow with distributionally robust chance constraints. *arXiv preprint arXiv:1508.06061*, 2015.

[163] Yiling Zhang, Siqian Shen, and Johanna L. Mathieu. Distributionally robust chance-constrained optimal power flow with uncertain renewables and uncertain reserves provided by loads. *IEEE Transactions on Power Systems*, 32(2):1378–1388, 2016.

[164] Weijun Xie and Shabbir Ahmed. Distributionally robust chance constrained optimal power flow with renewables: A conic reformulation. *IEEE Transactions on Power Systems*, 33(2):1860–1867, 2017.

[165] Yi Guo, Kyri Baker, Emiliano Dall'Anese, Zechun Hu, and Tyler Holt Summers. Data-based distributionally robust stochastic optimal power flow - Part I: Methodologies. *IEEE Transactions on Power Systems*, 34(2):1483–1492, 2018.

[166] Tyler Summers, Joseph Warrington, Manfred Morari, and John Lygeros. Stochastic optimal power flow based on conditional value at risk and distributional robustness. *International Journal of Electrical Power & Energy Systems*, 72:116–125, 2015.

[167] Yury Dvorkin. A chance-constrained stochastic electricity market. *IEEE Transactions on Power Systems*, 35(4):2993–3003, 2020.

[168] Chuan He, Xiaping Zhang, Tianqi Liu, and Lei Wu. Distributionally robust scheduling of integrated gas-electricity systems with demand response. *IEEE Transactions on Power Systems*, 34(5):3791–3803, 2019.

[169] Christos Ordoudis, Viet Anh Nguyen, Daniel Kuhn, and Pierre Pinson. Energy and reserve dispatch with distributionally robust joint chance constraints. Technical report, Tech. Rep., 2018.[Online]. Available: http://www.optimization-online.org/DB FILE/2018/12/6962.pdf, 2018.

[170] Steve Zymler, Daniel Kuhn, and Berç Rustem. Distributionally robust joint chance constraints with second-order moment information. *Mathematical Programming*, 137(1-2):167–198, 2013.

[171] Grani A. Hanasusanto and Daniel Kuhn. Conic programming reformulations of two-stage distributionally robust linear programs over Wasserstein balls. *Operations Research*, 66(3):849–869, 2018.

[172] Bowen Li, Ruiwei Jiang, and Johanna L. Mathieu. Distributionally robust chance-constrained optimal power flow assuming unimodal distributions with misspecified modes. *IEEE Transactions on Control of Network Systems*, 6(3):1223–1234, 2019.

[173] R. Tyrrell Rockafellar and Stanislav Uryasev. Optimization of conditional value-at-risk. *Journal of Risk*, 2:21–42, 2000.

[174] Bart P. G. Van Parys, Daniel Kuhn, Paul J. Goulart, and Manfred Morari. Distributionally robust control of constrained stochastic systems. *IEEE Transactions on Automatic Control*, 61(2):430–442, 2015.

[175] Grani A. Hanasusanto, Vladimir Roitch, Daniel Kuhn, and Wolfram Wiesemann. Ambiguous joint chance constraints under mean and dispersion information. *Operations Research*, 65(3):751–767, 2017.

[176] Daniel Kuhn, Wolfram Wiesemann, and Angelos Georghiou. Primal and dual linear decision rules in stochastic and robust optimization. *Mathematical Programming*, 130(1):177–209, 2011.

[177] Kostas Margellos, Paul Goulart, and John Lygeros. On the road between robust optimization and the scenario approach for chance constrained optimization problems. *IEEE Transactions on Automatic Control*, 59(8):2258–2263, 2014.

[178] Aharon Ben-Tal, Alexander Goryashko, Elana Guslitzer, and Arkadi Nemirovski. Adjustable robust solutions of uncertain linear programs. *Mathematical Programming*, 99(2):351–376, 2004.

[179] Omar El Housni and Vineet Goyal. On the optimality of affine policies for budgeted uncertainty sets. *arXiv preprint arXiv:1807.00163*, 2018.

[180] Dimitris Bertsimas, Dan A. Iancu, and Pablo A. Parrilo. Optimality of affine policies in multistage robust optimization. *Mathematics of Operations Research*, 35(2):363–394, 2010.

[181] Angelos Georghiou, Wolfram Wiesemann, and Daniel Kuhn. Generalized decision rule approximations for stochastic programming via liftings. *Mathematical Programming*, 152(1-2):301–338, 2015.

[182] Farzaneh Pourahmadi, Jalal Kazempour, Christos Ordoudis, Pierre Pinson, and Seyed Hamid Hosseini. Distributionally robust chance-constrained generation expansion planning. *IEEE Transactions on Power Systems*, 35(4):2888–2903, 2020.

[183] Line Roald, Frauke Oldewurtel, Thilo Krause, and Göran Andersson. Analytical reformulation of security constrained optimal power flow with probabilistic constraints. In *2013 IEEE Grenoble Conference*. IEEE, 2013.

[184] Michael R. Wagner. Stochastic 0–1 linear programming under limited distributional information. *Operations Research Letters*, 36(2):150–156, 2008.

[185] Pierre Pinson. Wind energy: Forecasting challenges for its operational management. *Statistical Science*, 28(4):564–585, 11 2013.

[186] Kenneth J. Arrow and Gerard Debreu. Existence of an equilibrium for a competitive economy. *Econometrica: Journal of the Econometric Society*, pages 265–290, 1954.

[187] Nongchao Guo and Chiara Lo Prete. Cross-product manipulation with intertemporal constraints: An equilibrium model. *Energy Policy*, 134:110851, 2019.

[188] Akshaya Jha and Frank A. Wolak. Testing for market efficiency with transactions costs: An application to convergence bidding in wholesale electricity markets. In *Industrial Organization Seminar, Yale University*. Citeseer, 2013.

[189] Rabih A. Jabr. Robust self-scheduling under price uncertainty using conditional value-at-risk. *IEEE Transactions on Power Systems*, 20(4):1852–1858, 2005.

[190] Xiaojia Guo, Alexandros Beskos, and Afzal Siddiqui. The natural hedge of a gas-fired power plant. *Computational Management Science*, 13:63–86, 2016.

[191] Francisco Facchinei and Christian Kanzow. Generalized Nash equilibrium problems. *4or*, 5(3):173–210, 2007.

[192] Ankur A. Kulkarni and Uday V. Shanbhag. On the variational equilibrium as a refinement of the generalized Nash equilibrium. *Automatica*, 48(1):45–55, 2012.

[193] Axel Dreves, Francisco Facchinei, Christian Kanzow, and Simone Sagratella. On the solution of the KKT conditions of generalized Nash equilibrium problems. *SIAM Journal on Optimization*, 21(3):1082–1108, 2011.

Collection of relevant publications

[Paper A] A. Schwele, A. Arrigo, C. Vervaeren, J. Kazempour and F. Vallée, "Coordination of Electricity, Heat, and Natural Gas Systems Accounting for Network Flexibility", in *Proceedings of 21st Power Systems Computation Conference (PSCC)*, Porto, Portugal, June 2020. Published in special issue of *Electric Power Systems Research (EPSR)*, Volume 189, Article No: 106776, December 2020.

[Paper B] A. Schwele, C. Ordoudis, J. Kazempour and P. Pinson, "Coordination of power and natural gas systems: Convexification approaches for linepack modeling", in *Proceedings of IEEE PowerTech Conference*, Milan, Italy, June 2019. Recipient of Basil C. Papadias - Second Best Student Paper Award.

[Paper C] A. Ratha, A. Schwele, J. Kazempour, P. Pinson, S.S. Torbaghan and A. Virag, "Affine Policies for Flexibility Provision by Natural Gas Networks to Power Systems", in *Proceedings of 21st Power Systems Computation Conference (PSCC)*, Porto, Portugal, June 2020. Published in special issue of *Electric Power Systems Research (EPSR)*, Volume 189, Article No: 106565, December 2020.

[Paper D] A. Schwele, C. Ordoudis, P. Pinson and J. Kazempour, "Coordination of Electricity and Natural Gas Markets via Financial Instruments", submitted to *Computational Management Science*, (under review), 2020.

[Paper A] Coordination of Electricity, Heat, and Natural Gas Systems Accounting for Network Flexibility

Authors:
Anna Schwele, Adriano Arrigo, Charlotte Vervaeren, Jalal Kazempour and François Vallée

Published in:
Special issue of Electric Power Systems Research (EPSR) for Proceedings of Power Systems Computation Conference (PSCC) 2020

DOI:
10.1016/j.epsr.2020.106776

Coordination of Electricity, Heat, and Natural Gas Systems Accounting for Network Flexibility

Anna Schwele[1], Adriano Arrigo[2], Charlotte Vervaeren[2], Jalal Kazempour[1] and François Vallée[2]
[1] Department of Electrical Engineering, Technical University of Denmark, Kgs. Lyngby, Denmark
{schwele, seykaz}@elektro.dtu.dk
[2] Electrical Power Engineering Unit, University of Mons, Mons, Belgium
{adriano.arrigo, charlotte.vervaeren, francois.vallee}@umons.ac.be

***Abstract*—Existing energy networks can foster the integration of uncertain and variable renewable energy sources by providing additional operational flexibility. In this direction, we propose a combined power, heat, and natural gas dispatch model to reveal the maximum potential "network flexibility", corresponding to the ability of natural gas and district heating pipelines to store energy. To account for both energy transport and linepack in the pipelines in a computational efficient manner, we explore convex quadratic relaxations of the nonconvex flow dynamics of gas and heat. The resulting model is a mixed-integer second-order cone program. An ex-post analysis ensures feasibility of the heat dispatch, while keeping the relaxation of the gas flow model sufficiently tight. The revealed flexibility is quantified in terms of system cost compared to a dispatch model neglecting the ability of natural gas and district heating networks to store energy.**

***Index Terms*—Combined power-heat-gas dispatch, Convex relaxation, Ex-post feasibility analysis, Multi-energy systems, Second-order cone program.**

I. Introduction

Operational flexibility is required to deal with the uncertainty and variability of growing renewable power generation. Flexibility for power systems is often provided by units interfacing other energy sectors, e.g., gas-fired units, combined heat and power (CHP) plants, and heat pumps. These units link the power system with the natural gas and district heating systems, both physically and economically. The gas-fired units usually provide flexibility thanks to their fast-start and ramping capabilities [1]. Similarly, the CHP units can provide flexibility [2], especially extraction CHPs, as they are able to vary their heat to power ratio. Besides, the heat pumps producing heat from electricity can act as power demand side flexibility. The key point is that a strong coordination between power, heat, and natural gas systems is needed to efficiently utilize those existing sources of flexibility. Unlike the power system, in which supply and demand have to be matched instantaneously, there is potential to use the district heating and natural gas networks as energy storage. The district heating and natural gas networks have the ability to store energy in pipelines in the form of time delays of heat propagation and natural gas linepack. This flexibility, the so-called "network flexibility", is provided through the dynamics of energy flow in pipelines, serving as energy storage (known as "virtual storage"). Accounting for these network dynamics can unlock an additional source of flexibility. The existing energy infrastructure in countries with multi-carrier systems, e.g., Denmark, can help mitigate the uncertainty and variability induced by large-scale renewable power penetration.

It is in general a complex task to holistically model the interdependent multi-energy systems while incorporating the energy flow dynamics of each specific energy network. Although there is an extensive literature on integrated energy systems, the majority of previous works either focused on two out of the three (i.e., power, natural gas, and heat) systems, or discarded the network flexibility in heat and natural gas sides, or provided generalized aggregate models, called "energy hubs". With a focus on network flexibility, we first review the existing works addressing the coordination of power and gas systems, then power and heat systems, and finally energy hubs.

The available works in the literature addressing integrated power and natural gas systems model the gas flow dynamics either through partial differential equations [3] or using a reduced version, resulting in a set of nonlinear and nonconvex steady-state equations [4]. These steady-state equations are still complex and cause computational challenges. Therefore, linear approximations [5], [6] or quadratic relaxation [7], [8] are used to manage the complexity of the natural gas flow dynamics, while accounting for the linepack.

In a similar direction, integrated power and heat dispatch models are introduced in [9], [10], [11], [12], [13]. A proper framework for modeling temperature dynamics in pipelines, time delay of heat transmission, variable supply temperature, and variable mass flow rates will enable exploiting the flexibility from district heating networks. While [9] and [10] consider a constant mass flow rate in pipelines, the heat dispatch models in [11], [12], [13] account for both mass flow rates and inlet temperatures as "control variables", allowing for more degrees of freedom.

The last strand that we explore in the literature is about energy hubs. The concept of energy hubs as a generic ag-

The work was supported by the Danish EUD Programme through the 'Coordinated Operation of Integrated Energy Systems (CORE)' project under the grant 64017-0005. We thank Lesia Mitridati for her thoughtful discussions and inputs for the heat system model.

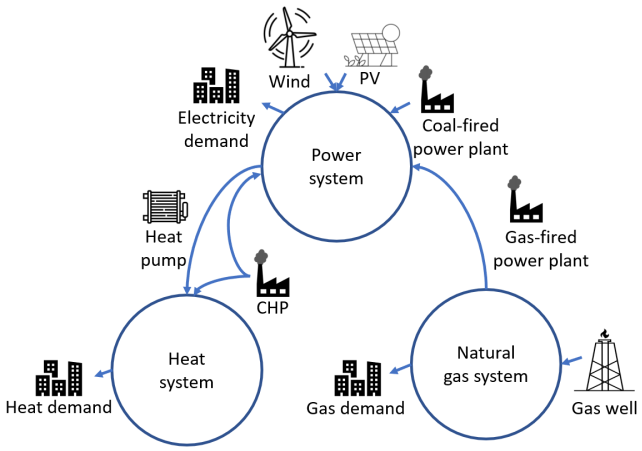

Fig. 1. Interdependent power, natural gas, heat systems.

gregate framework for modeling and optimization of multi-energy systems was firstly proposed in [14]. An energy hub is a unified unit where multiple energy carriers can be converted, conditioned, and stored. However, this generic model fails in accounting for the specific flow dynamics of the energy carriers.

To the best of our knowledge, this is the first work that optimizes the combined dispatch problem for the three energy systems together, accounting for their network and flow dynamics, while dealing with arising nonconvexities. We propose a combined power-heat-gas dispatch that models the interactions of the three energy carriers as well as the network flexibility. As an ideal benchmark, this combined energy dispatch assesses the maximum potential of flexibility that the natural gas and district heating networks can provide for renewable-based power systems. This revealed flexibility is quantified in terms of the reduced operational cost of the entire system compared to a dispatch model neglecting the ability of natural gas and district heating networks to store energy. Since the dynamics of heat and natural gas flow introduce nonconvexities, we explore convex quadratic relaxations of the energy flow model in gas [8], [15] and heat [11] systems, including the gas linepack, variable heat temperature and heat mass flow rates as the three degrees of freedom. We recast the original non-convex model as a mixed-integer second-order cone program (MISOCP), and eventually explore the feasibility of solutions achieved.

II. Interactions of Power, Natural Gas, and Heat Systems

Fig. 1 illustrates the interactions among power, heat, and natural gas systems considered in this paper. The dependency of heat and electricity outputs by CHPs and heat pumps induces strong interdependencies between the heat and electricity systems. The heat pumps produce heat from electricity providing electricity demand side flexibility through power-to-heat (P2H). The CHPs produce both electricity and heat from the combustion of a fuel, e.g., biomass or fossil fuels. These synergies physically link the power and heat systems. On the market perspective, the electricity and heat prices are related and determine the profitability and dispatch decision of CHPs and heat pumps. The cost of heat produced by heat pumps depends on electricity prices while the CHP units need to decide both power and heat dispatch with respect to opportunity cost.

The gas-fired power plants are usually flexible units that operate at the interface of the power and the natural gas systems, yielding both physical and economic interactions. The gas-fired generators produce electricity from the combustion of natural gas. This conversion is characterized by a conversion factor that accounts for the energy losses. The power output of gas-fired units is directly linked to their fuel consumption. An intermittent dispatch of gas-fired units in the power system and thus gas withdrawal from the gas network brings demand fluctuations and uncertainty into the gas system. Economically, the price of natural gas at which gas-fired units acquire fuel impacts the marginal power production cost of these units, and thus the merit-order in the electricity system.

In addition, there is potential of storing energy in the natural gas and district heating pipelines, which are expected to be even more increased through power-to-gas (P2G) and P2H technologies [16]. This additional source of flexibility from existing infrastructure is explored in the next section.

III. Integrated Multi-Energy Dispatch

This section develops an integrated multi-energy dispatch model, co-optimizing the operation of electricity, heat, and natural gas systems.

A. Assumptions

The integrated energy systems assume either a single system operator or a perfect information exchange and timing among the systems. However, in most countries the energy systems are operated independently and sequentially [17]. See [3], [18] and [19] for different levels of coordination among energy sectors. The focus of this paper is set on modeling the flexibility provided by the heat and natural gas networks in an efficient manner. Thus, we aim at accurately modeling the heat and gas flow problems and put less attention to the power side by using a simplified lossless DC power flow model. We assume isothermal energy flow in horizontal heat and gas pipelines. We also consider parallel supply and return pipelines for the heating network with both mass flow rates and temperatures as control variables to account for the energy storage capacity in heat pipelines. The natural gas flow is represented by its steady-state gas flow equation. The dynamics in gas pipelines are approximated by accounting for linepack through varying in- and outflows. Compressor stations and water pumps are modeled with a constant factor, while neglecting their fuel and power consumption.

B. Objective Function

The co-optimization problem aims at minimizing the total cost of operating power, heat, and natural gas systems over

time steps t in the planning horizon $\mathcal{T}$. Accordingly, the objective function reads as

$$\min_{\Theta} \sum_{t\in\mathcal{T}} \Big(\sum_{i\in\mathcal{C}} C_i^{\mathrm{E}}\ p_{i,t} + \sum_{k\in\mathcal{K}} C_k^{\mathrm{G}}\ g_{k,t} + \sum_{i\in\mathcal{HS}} C_i^{\mathrm{H}}\ Q_{i,t} + \sum_{i\in\mathcal{CHP}} C_i(\rho_i^{\mathrm{E}}\ p_{i,t} + \rho_i^{\mathrm{H}}\ Q_{i,t})\Big), \tag{1a}$$

where the set of decision variables is $\Theta = \{p_{i,t},\ w_{j,t},\ \theta_{n,t},\ f_{n,r,t},\ q_{m,u,t},\ q^{\mathrm{in}}_{m,u,t},\ q^{\mathrm{out}}_{m,u,t},\ h_{m,u,t},\ pr_{m,t}, g_{k,t},\ Q_{i,t},\ pr^{\mathrm{S}}_{o,t},\ pr^{\mathrm{R}}_{o,t},\ mf^{\mathrm{HES}}_{o,t},\ mf^{\mathrm{HS}}_{i,t},\ mf^{\mathrm{S}}_{o,v,t},\ mf^{\mathrm{R}}_{o,v,t},\ T^{\mathrm{S}}_{o,t},\ T^{\mathrm{R}}_{o,t},\ T^{\mathrm{S,in}}_{o,v,t},\ T^{\mathrm{R,in}}_{o,v,t},\ T^{\mathrm{S,out}}_{o,v,t},\ T^{\mathrm{R,out}}_{o,v,t},\ \tau^{\mathrm{S}}_{o,v,t},\ \tau^{\mathrm{R}}_{o,v,t},\ u^{\mathrm{S}}_{o,v,\eta,t},\ u^{\mathrm{R}}_{o,v,\eta,t}\}$. The first term of (1a) represents the operating cost of non-gas fired units $i \in \mathcal{C}$ given marginal cost parameters C_i^{E} and power production $p_{i,t}$. The second term corresponds to the cost of gas suppliers $k \in \mathcal{K}$ with marginal gas supply cost parameters C_i^{G} and gas supply $g_{k,t}$. The third term refers to the operating cost of heat boilers $i \in \mathcal{HS}$ given marginal cost parameters C_i^{H} and heat production $Q_{i,t}$. The last term models the operating cost of CHPs $i \in \mathcal{CHP}$ as a linear function of marginal cost C_i, electricity and heat fuel efficiency ρ_i^{E} and ρ_i^{H}, and the respective power and heat production level.

The objective function (1a) is subject to power constraints (2), heat constraints (3), natural gas constraints (4), as well as constraints (5) which couple the three systems. All these constraints are described in the following.

C. Power System Constraints

The power system constraints taking into account a lossless DC power flow model are

$$0 \le p_{i,t} \le \overline{p}_i, \forall i, t, \tag{2a}$$
$$0 \le w_{j,t} \le \overline{w}_{j,t}, \forall j, t, \tag{2b}$$
$$f_{n,r,t} = B_{n,r}(\theta_{n,t} - \theta_{r,t}), \forall (n,r) \in \mathcal{L}, t, \tag{2c}$$
$$-\overline{f}_{n,r} \le f_{n,r,t} \le \overline{f}_{n,r}, \forall (n,r) \in \mathcal{L}, t, \tag{2d}$$
$$-\pi \le \theta_{n,t} \le \pi, \forall n, t,\ \ \theta_{n,t} = 0, \forall n : ref, t, \tag{2e}$$

where parameters $\overline{p}_i$ and $\overline{w}_{j,t}$ in (2a) and (2b) restrict the power production $p_{i,t}$ and $w_{j,t}$ of conventional generators $i \in \mathcal{I}$ and renewable generators $j \in \mathcal{J}$, respectively. Constraints (2c) define the power flow $f_{n,r,t}$ along transmission line (n,r) by line susceptance $B_{n,r}$ and voltage angles $\theta_{n,t}$ at adjacent nodes n and r. The power flow is restricted to transmission line limits $\overline{f}_{n,r}$ by (2d). Constraints (2e) limit the voltage angles, and set the voltage angle to zero at the reference node.

D. Heat System Constraints

Following [11], the heat dispatch model considers both mass flow rates and inlet temperatures as control variables, accounting for temperature dynamics and time delays as

$$D^{\mathrm{H}}_{o,t} = c\ mf^{\mathrm{HES}}_{o,t}(T^{\mathrm{S}}_{o,t} - T^{\mathrm{R}}_{o,t}), \forall o, t, \tag{3a}$$
$$Q_{i,t} = c\ mf^{\mathrm{HS}}_{i,t}(T^{\mathrm{S}}_{o,t} - T^{\mathrm{R}}_{o,t}), \forall o, i \in \mathcal{A}^{\mathrm{HS}}_o, t, \tag{3b}$$
$$0 \le Q_{i,t} \le \overline{Q}_i, \forall i \in \mathcal{HS}, t, \tag{3c}$$
$$\underline{pr}^{\mathrm{HES}}_o \le pr^{\mathrm{S}}_{o,t} - pr^{\mathrm{R}}_{o,t}, \forall o, t, \tag{3d}$$
$$\underline{mf}^{\mathrm{HES}}_o \le mf^{\mathrm{HES}}_{o,t} \le \overline{mf}^{\mathrm{HES}}_o, \forall o, t, \tag{3e}$$
$$\underline{mf}^{\mathrm{HS}}_i \le mf^{\mathrm{HS}}_{i,t} \le \overline{mf}^{\mathrm{HS}}_i, \forall i \in \mathcal{HS}, t, \tag{3f}$$
$$\underline{mf}^{\mathrm{S}}_{o,v} \le mf^{\mathrm{S}}_{o,v,t} \le \overline{mf}^{\mathrm{S}}_{o,v}, \forall (o,v) \in \mathcal{P}, t, \tag{3g}$$
$$\underline{mf}^{\mathrm{R}}_{o,v} \le mf^{\mathrm{R}}_{o,v,t} \le \overline{mf}^{\mathrm{R}}_{o,v}, \forall (o,v) \in \mathcal{P}, t, \tag{3h}$$
$$\sum_{v:(o,v)\in\mathcal{P}} mf^{\mathrm{S}}_{v,o,t} + \sum_{i\in\mathcal{A}^{\mathrm{HS}}_o} mf^{\mathrm{HS}}_{i,t} = \sum_{v:(o,v)\in\mathcal{P}} mf^{\mathrm{S}}_{o,v,t} + mf^{\mathrm{HES}}_{o,t}, \forall o, t, \tag{3i}$$
$$\sum_{v:(o,v)\in\mathcal{P}} mf^{\mathrm{R}}_{v,o,t} + \sum_{i\in\mathcal{A}^{\mathrm{HS}}_o} mf^{\mathrm{HS}}_{i,t} = \sum_{v:(o,v)\in\mathcal{P}} mf^{\mathrm{R}}_{o,v,t} + mf^{\mathrm{HES}}_{o,t}, \forall o, t, \tag{3j}$$
$$L_{o,v}(mf^{\mathrm{S}}_{o,v,t})^2 = pr^{\mathrm{S}}_{o,t} - pr^{\mathrm{S}}_{v,t}, \forall (o,v) \in \mathcal{P}, t, \tag{3k}$$
$$L_{o,v}(mf^{\mathrm{R}}_{o,v,t})^2 = pr^{\mathrm{R}}_{v,t} - pr^{\mathrm{R}}_{o,t}, \forall (o,v) \in \mathcal{P}, t, \tag{3l}$$
$$\underline{pr}^{\mathrm{S}}_o \le pr^{\mathrm{S}}_{o,t} \le \overline{pr}^{\mathrm{S}}_o,\ \ \underline{pr}^{\mathrm{R}}_o \le pr^{\mathrm{R}}_{o,t} \le \overline{pr}^{\mathrm{R}}_o, \forall o, t, \tag{3m}$$
$$\underline{T}^{\mathrm{S}}_o \le T^{\mathrm{S}}_{o,t} \le \overline{T}^{\mathrm{S}}_o,\ \ \underline{T}^{\mathrm{R}}_o \le T^{\mathrm{R}}_o \le \overline{R}^{\mathrm{S}}_o, \forall o, t, \tag{3n}$$
$$T^{\mathrm{S,in}}_{o,v,t} = T^{\mathrm{S}}_{o,t},\ \ T^{\mathrm{R,in}}_{o,v,t} = T^{\mathrm{R}}_{v,t},\ \ \forall (o,v) \in \mathcal{P}, t, \tag{3o}$$
$$T^{\mathrm{S}}_{v,t} = T^{\mathrm{S,out}}_{o,v,t},\ \ T^{\mathrm{R}}_{o,t} = T^{\mathrm{R,out}}_{o,v,t}, \forall (o,v) \in \mathcal{P}, t, \tag{3p}$$
$$T^{\mathrm{S,out}}_{o,v,t} = T^{\mathrm{S,in}}_{o,v,(t-\tau)}(1 - \frac{2\mu_{o,v}}{c\rho R_{o,v}}\tau^{\mathrm{S}}_{o,v,t}), \forall (o,v) \in \mathcal{P}, t, \tag{3q}$$
$$T^{\mathrm{R,out}}_{o,v,t} = T^{\mathrm{R,in}}_{o,v,(t-\tau)}(1 - \frac{2\mu_{o,v}}{c\rho R_{o,v}}\tau^{\mathrm{R}}_{o,v,t}), \forall (o,v) \in \mathcal{P}, t, \tag{3r}$$
$$M(u^{\mathrm{S}}_{o,v,\eta,t} - 1) \le \sum_{\tilde{\eta}=t-\eta}^{t} \frac{mf^{\mathrm{S}}_{o,v,\tilde{\eta}}}{\pi R^2_{o,v}\rho}\Delta t - L_{o,v} \le M\ u^{\mathrm{S}}_{o,v,\eta,t},$$
$$\forall (o,v) \in \mathcal{P}, \eta \in \{0, ..., \overline{\tau}^{\mathrm{S}}_{o,v}\}, t, \tag{3s}$$
$$M(u^{\mathrm{R}}_{o,v,\eta,t} - 1) \le \sum_{\tilde{\eta}=t-\eta}^{t} \frac{mf^{\mathrm{R}}_{o,v,\tilde{\eta}}}{\pi R^2_{o,v}\rho}\Delta t - L_{o,v} \le M\ u^{\mathrm{R}}_{o,v,\eta,t},$$
$$\forall (o,v) \in \mathcal{P}, \eta \in \{0, ..., \overline{\tau}^{\mathrm{R}}_{o,v}\}, t, \tag{3t}$$
$$\tau^{\mathrm{S}}_{o,v,t} = \sum_{\eta=1}^{\overline{\tau}^{\mathrm{S}}_{o,v}} \eta(u^{\mathrm{S}}_{o,v,\eta,t} - u^{\mathrm{S}}_{o,v,(\eta-1),t}), \forall (o,v) \in \mathcal{P}, t, \tag{3u}$$
$$\tau^{\mathrm{R}}_{o,v,t} = \sum_{\eta=1}^{\overline{\tau}^{\mathrm{R}}_{o,v}} \eta(u^{\mathrm{R}}_{o,v,\eta,t} - u^{\mathrm{R}}_{o,v,(\eta-1),t}), \forall (o,v) \in \mathcal{P}, t. \tag{3v}$$

In (3a), the inelastic heat demand $D^{\mathrm{H}}_{o,t}$ in each district heating node o is related to the specific heat capacity of water c, heat exchanger mass flows $mf^{\mathrm{HES}}_{o,t}$ and temperatures at node o of both supply $T^{\mathrm{S}}_{o,t}$ and return network $T^{\mathrm{R}}_{o,t}$. Constraints (3b) relate heat production $Q_{i,t}$, which is limited by its capacity $\overline{Q}_i$ in (3c), to heat station mass flows $mf^{\mathrm{HS}}_{i,t}$ and temperature gradients between supply and return networks at heat stations $i \in \mathcal{A}^{\mathrm{HS}}_o$ located at node o. The minimum pressure gradient $\underline{pr}^{\mathrm{HES}}_o$ between the pressures $pr^{\mathrm{S}}_{o,t}$ and $pr^{\mathrm{R}}_{o,t}$ between supply and return network at heat exchanger station node o is enforced by (3d). The mass flows are restricted in (3e)-(3h) at heat exchange stations by lower bound $\underline{mf}^{\mathrm{HES}}_o$ and upper bound $\overline{mf}^{\mathrm{HES}}_o$, at heat stations $i \in \mathcal{HS}$ by $\underline{mf}^{\mathrm{HS}}_i$ and $\overline{mf}^{\mathrm{HS}}_i$, and supply and return pipelines $(o,v) \in \mathcal{P}$ by $\underline{mf}^{\mathrm{S/R}}_{o,v}$ and $\overline{mf}^{\mathrm{S/R}}_{o,v}$, respectively. Constraints (3i) and (3j) balance mass flow for supply and return network nodes. The Darcy-Weisbach equations (3k) and (3l) relate pressure losses due to friction inside the supply and return pipelines to mass flow

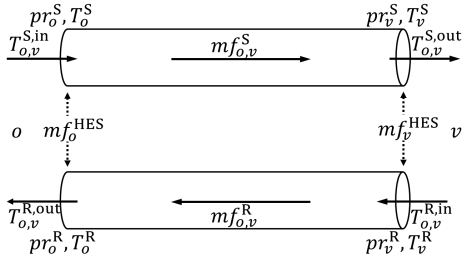

Fig. 2. Heat flow in parallel supply and return pipeline (time index t is dropped for notational clarity).

rates via pressure loss coefficient $L_{o,v}$. Constraints (3m) and (3n) put upper and lower bounds on nodal pressure ($\underline{pr}_o^{\mathrm{S/R}}$, $\overline{pr}_o^{\mathrm{S/R}}$,) and temperature ($\underline{T}_o^{\mathrm{S/R}}$, $\overline{T}_o^{\mathrm{S/R}}$) in both supply and return networks. Pursuing further clarity, the concept of heat flows in these parallel pipelines is shown in Fig. 2.

The temperature at the entrance of the pipe $T_{o,v,t}^{\mathrm{S/R,in}}$ is defined in (3o). Temperature mixing is given by outlet temperatures $T_{o,v,t}^{\mathrm{S/R,out}}$ in (3p). The heat losses are approximated using first-order Taylor series expansion of the heat propagation equations (3q) and (3r) for supply and return pipelines, respectively. The water temperatures at the outlet of a pipe $T_{o,v,t}^{\mathrm{S/R,out}}$ corresponds to past temperatures at the inlet $T_{o,v,(t-\tau)}^{\mathrm{S/R,in}}$ at previous time $t-\tau$ minus heat losses in the pipe. These losses are given by thermal loss coefficient $\mu_{o,v}$, specific water capacity c, water density ρ and the radius of the pipe $R_{o,v}$. We introduce auxiliary binary variables $u_{o,v,\eta,t}^{\mathrm{S/R}} \in \{0,1\}$ and the sufficiently large positive constant M to help define the varying time delays $\tau_{o,v,t}^{\mathrm{S/R}}$. The delay of heat propagation depends on the mass flow rate at each time step and for each pipe and the length of the pipe and is defined by (3s) and (3t). Finally, (3u) and (3v) ensure the minimum delay with the maximum time delay parameters $\overline{\tau}_{o,v}^{\mathrm{S/R}}$, depending on the physical characteristics of the pipelines.

E. Natural Gas System Constraints

Similar to the models in [7] and [8], we dispatch the natural gas system using a steady-state natural gas flow model accounting for linepack in the pipelines. The constraints are

$$0 \le g_{k,t} \le \overline{g}_k, \forall k, t, \tag{4a}$$

$$\underline{pr}_m \le pr_{m,t} \le \overline{pr}_m, \forall m, t, \tag{4b}$$

$$pr_{u,t} \le \Gamma_{m,u}\ pr_{m,t}, \forall (m,u) \in \mathcal{Z}, t, \tag{4c}$$

$$q_{m,u,t} = K_{m,u}\sqrt{pr_{m,t}^2 - pr_{u,t}^2}, \forall (m,u) \in \mathcal{Z}, t, \tag{4d}$$

$$q_{m,u,t} = \frac{q_{m,u,t}^{\mathrm{in}} + q_{m,u,t}^{\mathrm{out}}}{2}, \forall (m,u) \in \mathcal{Z}, t, \tag{4e}$$

$$h_{m,u,t} = S_{m,u}\frac{pr_{m,t} + pr_{u,t}}{2}, \forall (m,u) \in \mathcal{Z}, t, \tag{4f}$$

$$h_{m,u,t} = h_{m,u,(t-1)} + q_{m,u,t}^{\mathrm{in}} - q_{m,u,t}^{\mathrm{out}}, \forall (m,u) \in \mathcal{Z}, t > 1, \tag{4g}$$

$$h_{m,u,t} = H_{m,u}^0 + q_{m,u,t}^{\mathrm{in}} - q_{m,u,t}^{\mathrm{out}}, \forall (m,u) \in \mathcal{Z}, t = 1, \tag{4h}$$

$$H_{m,u}^0 \le h_{m,u,t}, \forall (m,u) \in \mathcal{Z}, t = |\mathcal{T}|, \tag{4i}$$

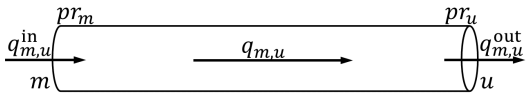

Fig. 3. Natural gas flow along a pipeline (time index t is removed).

where (4a) enforces the capacity $\overline{g}_k$ for gas supply $g_{k,t}$, whereas (4b) imposes the upper and lower limits $\underline{pr}_m$ and $\overline{pr}_m$ for pressure $pr_{m,t}$ at each gas node m. Constraints (4c) provide a linearized representation of compressor stations along pipeline $(m,u) \in \mathcal{Z}$ with fixed compression ratio $\Gamma_{m,u}$. The non-negative natural gas flow $q_{m,u,t} \ge 0$ from node m to u is defined by the Weymouth equation (4d). This equation relates the flow along a pipeline to the difference of squared pressures at beginning node m and ending node u of the pipeline and Weymouth constant $K_{m,u}$. We define this natural gas flow along a pipe as the average of inflows $q_{m,u,t}^{\mathrm{in}}$ into a pipeline and outflows $q_{m,u,t}^{\mathrm{out}}$ out of each pipeline in (4e), see Fig. 3. Constraints (4f) define linepack $h_{m,u,t}$ as a function of pressures at both ends of the pipeline and pipeline characteristics $S_{m,u}$. Constraints (4g) balance in- and outflows with linepack storage in pipelines. Initial linepack $H_{m,u}^0$ at the beginning of the planning horizon and minimum linepack level in the final time period of the optimization horizon are ensured by (4h) and (4i) to avoid depletion of natural gas in the network.

F. Coupling Constraints

The units at the interface, i.e., CHPs, heat pumps, and gas-fired generators, link the three systems, see Fig. 1. The following coupling constraints describe the interdependencies among the energy carriers and how the units at the interfaces link the systems linearly:

$$\sum_{k \in \mathcal{A}_m^{\mathrm{K}}} g_{k,t} - \sum_{i \in \mathcal{A}_m^{\mathrm{G}}} \phi_i\ p_{i,t} - \sum_{u:(m,u)\in\mathcal{Z}} (q_{m,u,t}^{\mathrm{in}} - q_{u,m,t}^{\mathrm{out}}) = D_{m,t}^{\mathrm{G}}, \forall m, t, \tag{5a}$$

$$r_i Q_{i,t} \le p_{i,t}, \forall i \in \mathcal{CHP}, t, \tag{5b}$$

$$0 \le \rho_i^{\mathrm{E}} p_{i,t} + \rho_i^{\mathrm{H}} Q_{i,t} \le \overline{p}_i, \forall i \in \mathcal{CHP}, t, \tag{5c}$$

$$Q_{i,t} = COP_i D_{i,t}^{\mathrm{HP}}, \forall i \in \mathcal{HP}, t, \tag{5d}$$

$$\sum_{i \in \mathcal{A}_n^{\mathrm{I}}} p_{i,t} + \sum_{j \in \mathcal{A}_n^{\mathrm{I}}} w_{j,t} - \sum_{r:(n,r)\in\mathcal{L}} f_{n,r,t} = D_{n,t}^{\mathrm{E}} + \sum_{i \in \mathcal{A}_n^{\mathrm{HP}}} D_{i,t}^{\mathrm{HP}}, \forall n, t. \tag{5e}$$

Constraints (5a) balance gas injection and inelastic demand $D_{m,t}^{\mathrm{G}}$ of units $\mathcal{A}_m^{(.)}$ located at node m with in- and outflow from and to adjacent nodes u of the natural gas network. The fuel consumption of natural gas-fired generators is translated into a nodal, time-varying gas demand $\phi_i\ p_{i,t}$ via fuel conversion factor ϕ_i. Constraints (5b) and (5c) define the joint feasible operating region of an extraction CHP. The heat and electricity outputs $Q_{i,t}$ and $p_{i,t}$ of each CHP are linked through output ratio r_i in (5b). The total capacity limits of CHP units are enforced by (5c). Constraints (5d) translate the heat production of heat pumps $Q_{i,t}$ to power consumption $D_{i,t}^{\mathrm{HP}}$ by the coefficient of performance COP_i. Nodal power balance (5e) matches the inelastic electricity demand $D_{n,t}^{\mathrm{E}}$ and electricity consumption by heat pumps $D_{i,t}^{\mathrm{HP}}$ with the power generation

from conventional, gas-fired, CHP and renewable units $\mathcal{A}_n^{(\cdot)}$ located at node n accounting for power flows along adjacent power transmission lines.

The resulting model (1)-(5) is a mixed-integer non-linear program (MINLP). It is a challenging problem to deal with, as there is no off-the-shelf solver available for a MINLP problem. In the next section, while keeping the binary variables, we convexify the nonlinearities arising from heat and gas flow models. This will eventually result in a MISOCP.

IV. Convexification

The non-convexities of MINLP model (1)-(5) arise from quadratic equality constraints (3k), (3l), and (4d), as well as bilinear terms in (3a), (3b), (3q), and (3r). We first apply quadratic relaxations that allow for modeling both natural gas flow and heat mass flow related to pressure drops. Then, bilinear terms are convexified using a linearization technique [11] and McCormick relaxations [20].

A. Quadratic Relaxation

The steady-state gas flow equation (4d) can be made convex using a second-order cone (SOC) relaxation. We first reformulate (4d) as

$$q_{m,u,t}^2 \leq K_{m,u}^2 (pr_{m,t}^2 - pr_{u,t}^2), \forall (m,u) \in \mathcal{Z}, t, \tag{6a}$$
$$q_{m,u,t}^2 \geq K_{m,u}^2 (pr_{m,t}^2 - pr_{u,t}^2), \forall (m,u) \in \mathcal{Z}, t, \tag{6b}$$

and then drop (6b). Now, (6a) is a SOC constraint, see left plot in Fig. 4. Reference [21] proves the SOC relaxation to be exact under several conditions. The pressure loss equations (3k) and (3l) can be convexified in a similar manner. After reformulating them as

$$L_{o,v}(mf_{o,v,t}^{\text{S/R}})^2 \leq pr_{v,t}^{\text{S/R}} - pr_{o,t}^{\text{S/R}}, \forall (o,v) \in \mathcal{P}, t, \tag{7a}$$
$$L_{o,v}(mf_{o,v,t}^{\text{S/R}})^2 \geq pr_{v,t}^{\text{S/R}} - pr_{o,t}^{\text{S/R}}, \forall (o,v) \in \mathcal{P}, t, \tag{7b}$$

and dropping (7b), the remaining (7a) are SOC constraints, as shown in the middle plot of Fig. 4.

B. Linearization and Relaxation of Bilinear Terms

1) Linearization: The heat propagation equations (3q) and (3r) are non-convex due to the bilinear terms $T_{o,v,(t-\tau_{o,v,t}^{\text{S/R}})}^{\text{S/R,in}} \tau_{o,v,t}^{\text{S/R}}$ and the use of varying time delays $\tau_{o,v,t}^{\text{S/R}}$ as indices. We follow the approach in [11] to linearize these constraints in an exact way using auxiliary binary variables $v_{o,v,\eta,t}^{\text{S/R}} \in \{0,1\}$ as well as a sufficiently large positive constant M. Pursuing linearity of (3q), we include the following constraints:

$$-M\ v_{o,v,\eta,t}^{\text{S}} \leq \tilde{T}_{o,v,\eta,t}^{\text{S,in}} \leq M\ v_{o,v,\eta,t}^{\text{S}}, \quad \forall (o,v) \in \mathcal{P}, \eta \in \{0,...,\overline{\tau}_{o,v}^{\text{S}}\}, t, \tag{8a}$$

$$M(v_{o,v,\eta,t}^{\text{S}} - 1) \leq \tilde{T}_{o,v,\eta,t}^{\text{S,in}} - \tilde{T}_{o,v,(t-\eta)}^{\text{S,in}} \left(1 - \frac{2\mu_{o,v}}{c\rho R_{o,v}}\eta\right) \leq M(1 - v_{o,v,\eta,t}^{\text{S}}), \forall (o,v) \in \mathcal{P}, \eta \in \{0,...,\overline{\tau}_{o,v}^{\text{S}}\}, t, \tag{8b}$$

$$M(v_{o,v,\eta,t}^{\text{S}} - 1) \leq \eta - \tau_{o,v,t}^{\text{S}} \leq M(1 - v_{o,v,\eta,t}^{\text{S}}), \quad \forall (o,v) \in \mathcal{P}, \eta \in \{0,...,\overline{\tau}_{o,v}^{\text{S}}\}, t, \tag{8c}$$

$$\sum_{\eta=0}^{\overline{\tau}^{\text{S}}} v_{o,v,\eta,t}^{\text{S}} = 1, \forall (o,v) \in \mathcal{P}, t, \tag{8d}$$

$$T_{o,v,t}^{\text{S,out}} = \sum_{\eta=0}^{\overline{\tau}_{o,v}^{\text{S}}} \tilde{T}_{o,v,\eta,t}^{\text{S,in}}, \forall (o,v) \in \mathcal{P}, t. \tag{8e}$$

Note that (3r) can be reformulated in the same manner.

2) McCormick Relaxation: Pursuing convexity, bilinear terms $mf(T^{\text{S}} - T^{\text{R}})$ in (3a) and (3b) are linearized using McCormick envelopes [20], illustrated in the right plot of Fig. 4. We can now solve (1)-(3p), (3s)-(4c), (4e)-(5), (6a), (7a), (8) as a MISOCP.

V. Case Study

A. Input Data

We apply the proposed combined power-heat-gas dispatch (1)-(5) with convexified formulation from Section IV on an integrated energy model based on the IEEE 24-bus reliability test system [22], coupled with a 12-node gas network [5] and a 3-node district heating network [11] over a 24-hour scheduling horizon. This integrated energy system is depicted in Fig. 5. All input data can be found in the online appendix [23]. A wind farm, whose power output realization is given in Fig. 6, five non-gas-fired units, six gas-fired units and a biomass-fueled CHP unit are available to supply electricity load. The CHP unit and a heat pump cover the heat demand, while gas fuel is provided by three gas suppliers. The electricity, heat and natural gas loads are shown in Fig. 6.

The optimization problem is solved on an Intel core i5 computer clocking at 2.3 GHz, using Gurobi solver 8.0 with Python, allowing the instance to reach an optimality gap of 0.02% in less than one second.

B. Numerical Results

We first provide the results obtained for the total operational cost of the integrated energy system, i.e., the optimal value of objective function (1a). This cost is achieved under varying levels of wind power penetration, which is defined as the ratio of total wind power capacity to maximum electricity demand. Fig. 7 shows decreasing operational cost of the integrated energy system for increasing levels of wind power penetration. We compare these results to a dispatch that does not account for network flexibility. We replace gas linepack constraints (4f)-(4i) by $q_{m,u,t}^{\text{in}} = q_{m,u,t}^{\text{out}}, \forall (m,u) \in \mathcal{Z}, t$, balancing in- and outflow of gas pipelines neglecting the linepack. The flexibility from the heating network given in constraints (3) is omitted by dispatching heat according to heat production capacity limits (3c) and system-wide heat balance $\sum_{i \in \mathcal{HES}} D_{i,t}^{\text{H}} = \sum_{i \in \mathcal{HS}} Q_{i,t}, \forall t$. Accounting for flow dynamics and storage in gas and heat pipelines decreases the total system cost by 2% on average compared with the case neglecting network flexibility.

Fig. 8 shows the total amount of natural gas and heat supplied and consumed for the entire 24-hour horizon. When modeling linepack, consumption and supply of natural gas and heat do not necessarily need to be matched in each time

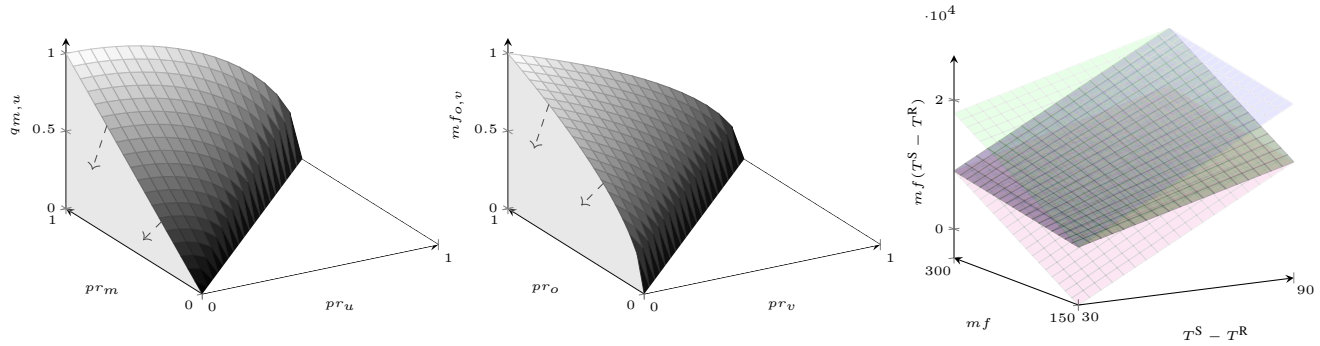

Fig. 4. Three dimensional illustrations of the relaxations. The plots on the left-hand, middle, and right-hand sides show the relaxation corresponding to constraints (6a), (7a), and (3a) and (3b), respectively. The left-hand plot shows the relaxed Weymouth equation (6a) for flow $q_{m,u}$ as a function of pressures at inlet and outlet nodes, i.e., pr_m and pr_u. In the middle, the relaxation of the Darcy-Weisbach equation (7a) is plotted with mass flow $mf_{o,v}$ as a function of pressures at inlet and outlet nodes, i.e., pr_o and pr_v. The dashed arrows in the left and middle plots show the area under the surface added to the feasible space by conic relaxation. McCormick envelopes for bilinear terms $mf(T^S - T^R)$ are illustrated in the right-hand plot. Time index t is dropped for notational clarity.

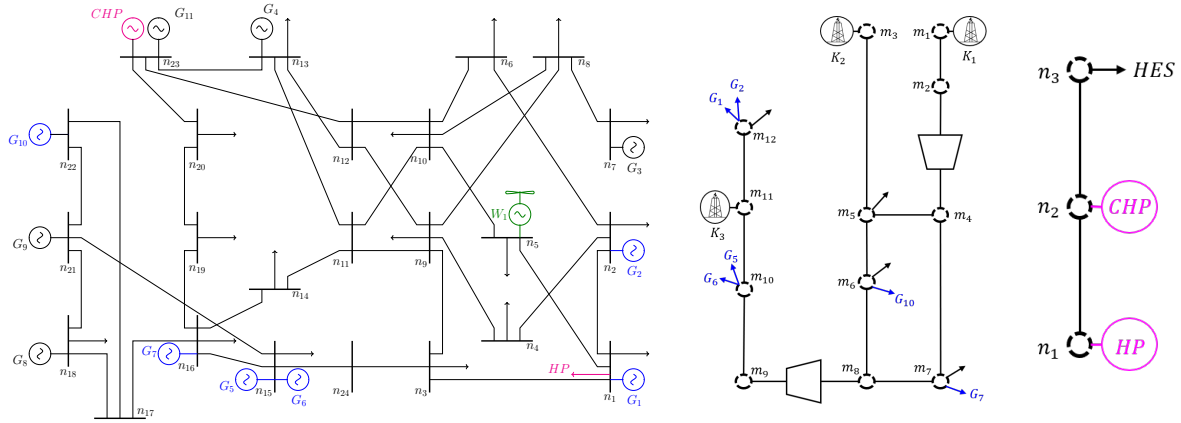

Fig. 5. Illustration of the integrated energy system for the case study. The graphs on the left-hand, middle, and right-hand sides show the topologies corresponding to power, natural gas, and heat networks, respectively. The left-hand plot shows the IEEE 24-bus reliability test system layout. In the middle, the 12-node natural gas network is plotted. The 3-bus heat network is illustrated in the right-hand plot.

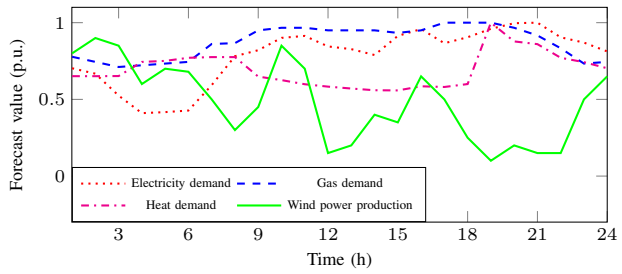

Fig. 6. The hourly inelastic electricity, heat, and gas loads as well as the hourly deterministic wind power forecast, all in per-unit.

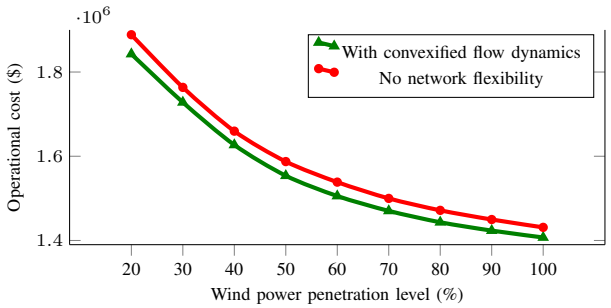

Fig. 7. Total operational cost of the entire integrated energy system in cases with and without considering network flexibility as a function of wind power penetration, i.e., the total wind power capacity divided by the maximum power demand.

period. The amount of energy stored in the pipelines (which is highlighted in shaded zones in Fig. 8) directly impacts the profiles of natural gas and heat supply. When the wind power generation is high in the beginning hours of the time horizon, heat is produced by heat pumps and stored in the district heating system in the first seven hours. Simultaneously, natural gas is accumulated within pipelines until hour 11. During a period of low output from wind power and high power and heat demand in hours 19-23, the linepack stored in gas pipelines is used to fuel electricity production and heat that was previously stored in the district heating network is consumed.

The flexibility provided by energy storage in the networks allows not only to decouple gas supply from consumption and heat production from demand, but also shifting electricity production and consumption. Network flexibility improves uti-

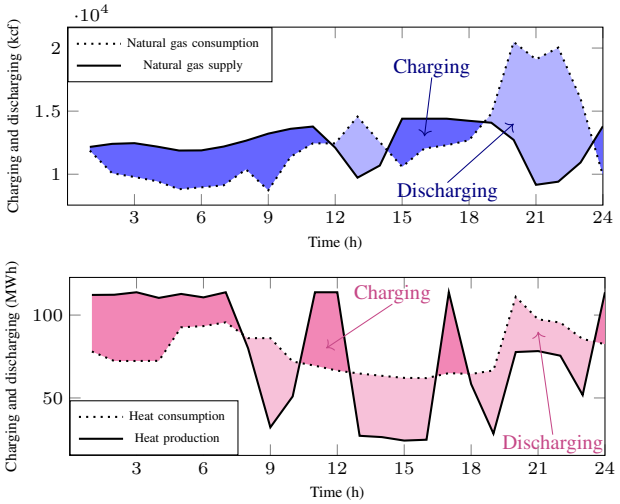

Fig. 8. The hourly profiles of natural gas (upper plot) and heat (lower plot) systems, illustrating the hourly total supply, total consumption, and the charging/discharging energy by network.

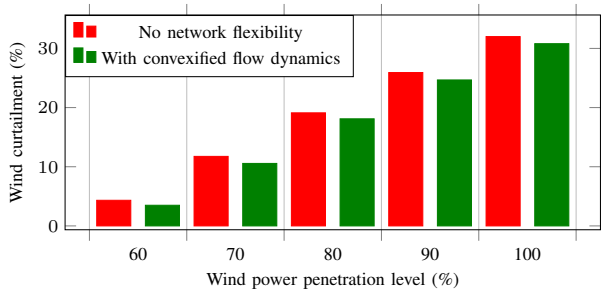

Fig. 9. Comparison of wind curtailment with and without considering network flexibility of natural gas and heat systems.

lization of power production from variable renewable sources. This is evident in reduced wind curtailment over the planning horizon. As shown in Fig. 9, the wind curtailment is reduced by 1.2% on average when accounting for energy storage in networks.

C. Feasibility Verification

Relaxing the original MINLP into a MISOCP enables us to efficiently find an optimal solution. However, this solution is based on relaxations of the original constraints, and therefore, the original constraints might not be hold. Thus, an ex-post evaluation of the results obtained from the MISOCP with respect to the original set of constraints is required.

First, we check the feasibility of results for the heat system. We fix all mass flow rates and binary variables to the optimal value obtained from the MISCOP. We then solve the original set of constraints resulting in a linear set of equations to obtain new values for pressures and temperatures at heat nodes. To solve the resulting system of equations, we adjust the nodal temperature bounds, which results in about 1% increase of the temperature interval. We recover a feasible solution for the real equations of the heat network under this slight parametric change.

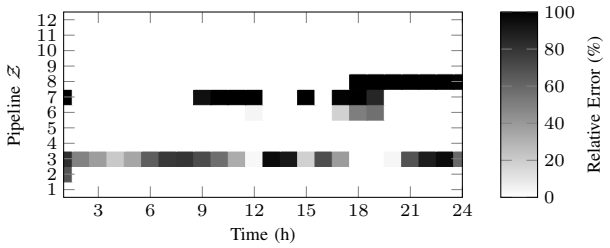

Fig. 10. Matrix plot of the relative error between right-hand and left-hand sides of relaxed Weymouth equations (6a) for each time step (x-axis) and each pipeline (y-axis).

Then, we check the feasibility of solution achieved for the natural gas system. We compute the normalized root mean square error (NRMSE), where the error is defined as the difference between the left-hand and right-hand sides of the relaxed Weymouth equations (6a) for all time steps and pipelines. The average NRMSE for the different wind power penetrations is 1.84%. We observe that there is no mismatch in most pipelines and time steps, but it reaches 100% in pipelines 3, 7 and 8 during particular periods, see Fig. 10. Note that the pipelines in the network loop are prone to mismatch. Since the occurrence rate of error is low, the relaxation seems sufficiently tight.

VI. Conclusion

We introduced an integrated power-heat-gas dispatch accounting for the interactions of the three energy carriers and flow dynamics in an efficient manner using convex relaxations. This ideal benchmark showed the maximum potential of flexibility provided by the existing natural gas and heating infrastructure. We quantified the social value in terms of reduced total system cost that short-term operational flexibility from energy storage in district heating and natural gas networks can provide for the power system. This coordination of energy carriers is an inexpensive solution for increasing the flexibility of the system compared to investing in other storage options and grid reinforcement and interconnections.

As future works, it is of interest to explore the additional alternatives to further tighten the relaxation techniques used. It is also of interest to investigate how the natural gas and heat networks can provide the flexibility without need to solve a co-optimization, and how this flexibility should be monetized and paid. Furthermore, increasing the interactions among all systems, e.g., gas-fueled CHPs, P2G units, natural gas boilers, and multi-generation units, in a larger test case is left for future research.

References

[1] E. Litvinov, F. Zhao, and T. Zheng, "Electricity markets in the United States: Power industry restructuring processes for the present and future," *IEEE Power & Energy Magazine*, vol. 17, no. 1, pp. 32–42, 2019.

[2] X. Chen, C. Kang, M. O'Malley, Q. Xia, J. Bai, C. Liu, R. Sun, W. Wang, and H. Li, "Increasing the flexibility of combined heat and power for wind power integration in China: Modeling and implications," *IEEE Transactions on Power Systems*, vol. 30, no. 4, pp. 1848–1857, 2014.

[3] A. Zlotnik, L. Roald, S. Backhaus, M. Chertkov, and G. Andersson, "Coordinated scheduling for interdependent electric power and natural gas infrastructures," *IEEE Transactions on Power Systems*, vol. 32, no. 1, pp. 600–610, 2017.

[4] L. Bai, F. Li, T. Jiang, and H. Jia, "Robust scheduling for wind integrated energy systems considering gas pipeline and power transmission N–1 contingencies," *IEEE Transactions on Power Systems*, vol. 32, no. 2, pp. 1582–1584, 2017.

[5] C. Ordoudis, P. Pinson, and J. M. Morales, "An integrated market for electricity and natural gas systems with stochastic power producers," *European Journal of Operational Research*, vol. 272, no. 2, pp. 642–654, 2019.

[6] C. M. Correa-Posada and P. Sánchez-Martín, "Integrated power and natural gas model for energy adequacy in short-term operation," *IEEE Transactions on Power Systems*, vol. 30, no. 6, pp. 3347–3355, 2015.

[7] A. Schwele, C. Ordoudis, J. Kazempour, and P. Pinson, "Coordination of power and natural gas systems: Convexification approaches for linepack modeling," in *Proceeding of the 13th IEEE PES PowerTech Conference*.

[8] S. Chen, A. J. Conejo, R. Sioshansi, and Z. Wei, "Unit commitment with an enhanced natural gas-flow model," *IEEE Transactions on Power Systems*, vol. 34, no. 5, pp. 3729–3738, 2019.

[9] C. Lin, W. Wu, B. Zhang, and Y. Sun, "Decentralized solution for combined heat and power dispatch through Benders decomposition," *IEEE Transactions on Sustainable Energy*, vol. 8, no. 4, pp. 1361–1372, 2017.

[10] Y. Zhou, W. Hu, Y. Min, and Y. Dai, "Integrated power and heat dispatch considering available reserve of combined heat and power units," *IEEE Transactions on Sustainable Energy*, vol. 10, no. 3, pp. 1300–1310, 2019.

[11] L. Mitridati and J. A. Taylor, "Power systems flexibility from district heating networks," in *Proceeding of Power Systems Computation Conference (PSCC)*, Dublin, Ireland, 2018.

[12] Z. Li, W. Wu, M. Shahidehpour, J. Wang, and B. Zhang, "Combined heat and power dispatch considering pipeline energy storage of district heating network," *IEEE Transactions on Sustainable Energy*, vol. 7, no. 1, pp. 12–22, 2015.

[13] Y. Chen, Q. Guo, H. Sun, Z. Li, Z. Pan, and W. Wu, "A water mass method and its application to integrated heat and electricity dispatch considering thermal dynamics," *arXiv preprint arXiv:1711.02274*, 2017.

[14] M. Geidl, G. Koeppel, P. Favre-Perrod, B. Klockl, G. Andersson, and K. Frohlich, "Energy hubs for the future," *IEEE Power & Energy Magazine*, vol. 5, no. 1, pp. 24–30, 2006.

[15] G. Byeon and P. Van Hentenryck, "Unit commitment with gas network awareness," *IEEE Transactions on Power Systems*, vol. 35, no. 2, pp. 1327–1339, 2020.

[16] A. Belderbos, E. Delarue, and W. D'haeseleer, "Possible role of power-to-gas in future energy systems," in *Proceeding of International Conference on the European Energy Market (EEM)*, Lisbon, Portugal, 2015.

[17] P. Pinson, L. Mitridati, C. Ordoudis, and J. Østergaard, "Towards fully renewable energy systems: Experience and trends in Denmark," *CSEE Journal of Power and Energy Systems*, vol. 3, no. 1, pp. 26–35, 2017.

[18] L. Mitridati and P. Pinson, "Optimal coupling of heat and electricity systems: A stochastic hierarchical approach," in *Proceeding of the 16th International Conference on Probabilistic Methods Applied to Power Systems (PMAPS)*, Beijing, China, 2016.

[19] L. Mitridati, J. Kazempour, and P. Pinson, "Heat and electricity market coordination: A scalable complementarity approach," *European Journal of Operational Research*, vol. 283, no. 3, pp. 1107–1123, 2020.

[20] G. P. McCormick, "Computability of global solutions to factorable nonconvex programs: Part I – Convex underestimating problems," *Mathmatical Programming*, vol. 10, no. 1, pp. 147–175, 1976.

[21] M. K. Singh and V. Kekatos, "Natural gas flow solvers using convex relaxation," *IEEE Transactions on Control of Network Systems*, 2020, to be published.

[22] C. Ordoudis, P. Pinson, J. M. Morales, and M. Zugno, "An updated version of the IEEE RTS 24-bus system for electricity market and power system operation studies - DTU working paper (available online)," 2016. [Online]. Available: http://orbit.dtu.dk/files/120568114/An

[23] A. Schwele, A. Arrigo, C. Vervaeren, J. Kazempour, and F. Vallée, "Online companion: Coordination of electricity, heat, and natural gas systems accounting for network flexibility," 2020. [Online]. Available: https://doi.org/10.5281/zenodo.3463161

Coordination of Electricity, Heat and Natural Gas Systems Accounting for Network Flexibility

Online Appendix

Anna Schwele, Adriano Arrigo, Charlotte Vervaeren, Jalal Kazempour, François Vallée

This document serves as an electronic companion for the paper "Coordination of Electricity, Heat and Natural Gas Systems Accounting for Network Flexibility". It contains the nomenclature, Section 1 presents the detailed formulation of mixed-integer second-order cone program (MISOCP) from the original manuscript, and Section 2 gives the technical characteristics of power generators, gas suppliers, and heat stations for the case study presented in the paper.

Nomenclature

Sets

$\mathcal{I}$ Set of dispatchable generation units i.
$\mathcal{C}$ Subset of dispatchable power plants excluding natural gas-fired ones ($\mathcal{C} \subset \mathcal{I}$).
$\mathcal{G}$ Subset of natural gas-fired power plants ($\mathcal{G} \subset \mathcal{I}$).
$\mathcal{J}$ Set of wind power units j.
$\mathcal{CHP}$ Subset of combined heat and power plants ($\mathcal{CHP} \subset \mathcal{HS} \subset \mathcal{I}$).
$\mathcal{HP}$ Subset of heat pumps ($\mathcal{HP} \subset \mathcal{HS} \subset \mathcal{I}$).
$\mathcal{HS}$ Subset of heat stations ($\mathcal{HS} \subset \mathcal{I}$).
$\mathcal{HES}$ Set of heat exchange stations o.
$\mathcal{T}$ Set of time periods t.
$\mathcal{L}$ Set of electricity transmission lines (n, r).
$\mathcal{N}$ Set of electricity network nodes n.
$\mathcal{O}$ Set of heat network nodes o.
$\mathcal{P}$ Set of heat pipelines (o, v).
$\mathcal{K}$ Set of natural gas supply units k.
$\mathcal{Z}$ Set of natural gas pipelines (m, u).
$\mathcal{M}$ Set of natural gas network nodes m.
$\mathcal{A}_n^{(\cdot)}$ Set of assets located at electricity network node n.
$\mathcal{A}_o^{(\cdot)}$ Set of assets located at heat network node o.
$\mathcal{A}_m^{(\cdot)}$ Set of assets located at natural gas network node m.
Θ Set of optimization variables.

Variables

$p_{i,t}$ Power dispatch of units i in period t [MW].
$w_{j,t}$ Dispatch of units j in period t [MW].
$Q_{i,t}$ Heat dispatch of units i in period t [MW].
$g_{k,t}$ Dispatch of unit k in period t [kcf/h].
$\theta_{n,t}$ Voltage angle at node n in period t [rad].
$f_{n,r,t}$ Power flow in line (n, r) in period t [MW].
$pr_{m,t}$ Pressure at node m in period t [psig].
$h_{m,u,t}$ Average mass of natural gas (linepack) in pipeline (m, u) in period t [kcf].
$q_{m,u,t}^{\text{in/out}}$ Inflow/outflow natural gas rate of pipeline (m, u) in period t [kcf/h].
$q_{m,u,t}$ Natural gas flow in pipeline (m, u) in period t [kcf/h].
$mf_{o,t}^{\text{HES}}$ Heat exchanger mass flows at network node o in period t [kg m^{-3}].
$mf_{i,t}^{\text{HS}}$ Mass flows at heat station i in period t [kg m^{-3}].

$T^{\mathsf{S}}_{o,t}$ Temperature at supply network node o in period t [K].
$T^{\mathsf{R}}_{o,t}$ Temperature at return network node o in period t [K].
$T^{\mathsf{S,in}}_{o,v,t}$ Temperature at the entrance of the pipe (o,v) in period t [K].
$T^{\mathsf{R,in}}_{o,v,t}$ Temperature at the entrance of the pipe (o,v) in period t [K].
$T^{\mathsf{S,out}}_{o,v,t}$ Temperature at the outlet of the pipe (o,v) in period t [K].
$T^{\mathsf{R,out}}_{o,v,t}$ Temperature at the outlet of the pipe (o,v) in period t [K].
$pr^{\mathsf{S}}_{o,t}$ Pressure at supply network node o in period t [psig].
$pr^{\mathsf{R}}_{o,t}$ Pressure at return network node o in period t [psig].
$D^{\mathsf{HP}}_{i,t}$ Power consumption of heat pump i in period t [MWh].
$\tau^{\mathsf{S/R}}_{o,v,t}$ Time delay of heat propagation in supply and return pipeline (o,v) in period t [h].
$u^{\mathsf{S/R}}_{o,v,\eta,t}$ Auxiliary binary variable defining varying time delays in pipeline (o,v) in period t {0,1}.
$v^{\mathsf{S/R}}_{o,v,\eta,t}$ Auxiliary binary variable defining varying time delays in pipeline (o,v) in period t {0,1}.

Parameters

$D^{\mathsf{E}}_{n,t}$ Electricity demand at node n in period t [MWh].
$D^{\mathsf{H}}_{o,t}$ Heat demand at node o in period t [MWh].
$D^{\mathsf{G}}_{m,t}$ Natural gas demand at node m in period t [kcf/h].
C^{E}_{i} Power production cost of unit i [$/MWh].
C^{H}_{i} Heat production cost of unit i [$/MWh].
C_i Marginal production cost of unit i [$/MWh].
C^{G}_{k} Supply cost of unit k [$/kcf].
$\overline{p}_i$ Capacity of dispatchable unit i [MW].
$\overline{Q}_i$ Capacity of dispatchable unit i [MW].
ρ^{E}_i Electricity fuel efficiency of CHP unit $i \in \mathcal{CHP}$.
ρ^{H}_i Heat fuel efficiency of CHP unit $i \in \mathcal{CHP}$.
$\underline{pr}^{\mathsf{HES}}_{o}$ Minimum pressure gradient at heat exchanger station node o [psig].
r_i Output ratio of unit $i \in \mathcal{CHP}$.
COP_i Coefficient of performance of unit $i \in \mathcal{HP}$.
ϕ_i Power conversion factor of natural gas unit $i \in \mathcal{G}$ [kcf/MWh].
$\overline{w}_{j,t}$ Wind power realization for unit j in period t [MW].
$\overline{g}_k$ Capacity of natural gas unit k [kcf].
$B_{n,r}$ Susceptance of line (n,r) [S].
$\overline{f}_{n,r}$ Transmission capacity of line (n,r) [MW].
$K_{m,u}$ Natural gas flow constant of pipeline (m,u) [kcf/psig].
$S_{m,u}$ Linepack constant of pipeline (m,u) [kcf/(psig h)].
$H^{0}_{m,u}$ Initial linepack in pipeline (m,u) [kcf].
$\underline{pr}^{\mathsf{S}}_{o}$ Minimum pressure at supply network node o [psig].
$\overline{pr}^{\mathsf{S}}_{o}$ Maximum pressure at supply network node o [psig].
$\underline{pr}^{\mathsf{R}}_{o}$ Minimum pressure at return network node o [psig].
$\overline{pr}^{\mathsf{R}}_{o}$ Maximum pressure at return network node o [psig].
$\underline{T}^{\mathsf{S}}_{o}$ Minimum temperature at supply network node o [K].
$\overline{T}^{\mathsf{S}}_{o}$ Maximum temperature at supply network node o [K].
$\underline{T}^{\mathsf{R}}_{o}$ Minimum temperature at return network node o [K].
$\overline{T}^{\mathsf{R}}_{o}$ Maximum temperature at return network node o [K].
$\underline{mf}^{\mathsf{HES}}_{o}$ Minimum mass flow at heat exchange station o [kg/h].
$\overline{mf}^{\mathsf{HES}}_{o}$ Maximum mass flow at heat exchange station o [kg/h].
$\underline{mf}^{\mathsf{HS}}_{i}$ Minimum mass flow at heat station $i \in \mathcal{HS}$ [kg/h].
$\overline{mf}^{\mathsf{HS}}_{i}$ Maximum mass flow at heat station $i \in \mathcal{HS}$ [kg/h].
$\underline{mf}^{\mathsf{S}}_{o,v}$ Minimum mass flow in supply pipeline $(o,v) \in \mathcal{P}$ [kg/h].
$\overline{mf}^{\mathsf{S}}_{o,v}$ Maximum mass flow in supply pipeline $(o,v) \in \mathcal{P}$ [kg/h].
$\underline{mf}^{\mathsf{R}}_{o,v}$ Minimum mass flow in return pipeline $(o,v) \in \mathcal{P}$ [kg/h].
$\overline{mf}^{\mathsf{R}}_{o,v}$ Maximum mass flow in return pipeline $(o,v) \in \mathcal{P}$ [kg/h].

$L_{o,v}$ Pressure loss coefficient pipeline $(o,v) \in \mathcal{P}$.
$\underline{pr}_m$ Minimum pressure limit at node m [psig].
$\overline{pr}_m$ Maximum pressure limit at node m [psig].
$\Gamma_{m,u}$ Compressor factor at natural gas pipeline (m,u).
c Specific heat capacity of water [J kg^{-1}K^{-1}].
$\mu_{o,v}$ Thermal loss coefficient [J m^{-2}s^{-2}K^{-1}].
ρ Water density [kg m^{-3}].
$R_{o,v}$ Radius of the pipeline (o,v) [m].
$\overline{\tau}^{\mathsf{S/R}}_{o,v}$ Maximum time delay parameters of pipeline (o,v).
M A sufficiently large positive constant.

1. MISOCP for the Integrated Multi-energy Dispatch

$$\min_{\Theta} \sum_{t\in\mathcal{T}} \Big(\sum_{i\in\mathcal{C}} C^{\mathrm{E}}_i \; p_{i,t} + \sum_{k\in\mathcal{K}} C^{\mathrm{G}}_k \; g_{k,t} + \sum_{i\in\mathcal{HS}} C^{\mathrm{H}}_i \; Q_{i,t} + \sum_{i\in\mathcal{CHP}} C_i(\rho^{\mathrm{E}}_i \; p_{i,t} + \rho^{\mathrm{H}}_i \; Q_{i,t}) \Big), \tag{1a}$$

subject to

$$0 \le p_{i,t} \le \overline{p}_i, \forall i, t, \tag{1b}$$
$$0 \le w_{j,t} \le \overline{w}_{j,t}, \forall j, t, \tag{1c}$$
$$f_{n,r,t} = B_{n,r}(\theta_{n,t} - \theta_{r,t}), \forall (n,r) \in \mathcal{L}, t, \tag{1d}$$
$$-\overline{f}_{n,r} \le f_{n,r,t} \le \overline{f}_{n,r}, \forall (n,r) \in \mathcal{L}, t, \tag{1e}$$
$$-\pi \le \theta_{n,t} \le \pi, \forall n, t, \;\; \theta_{n,t} = 0, \forall n : ref, t, \tag{1f}$$
$$D^{\mathrm{H}}_{o,t} \ge c\, \overline{mf}^{\mathrm{HES}}_o (T^{\mathrm{S}}_{o,t} - T^{\mathrm{R}}_{o,t}) + c\, mf^{\mathrm{HES}}_{o,t} (\overline{T}^{\mathrm{S}}_o - \underline{T}^{\mathrm{R}}_o) - c\, \overline{mf}^{\mathrm{HES}}_o (\overline{T}^{\mathrm{S}}_o - \underline{T}^{\mathrm{R}}_o), \forall o, t, \tag{1g}$$
$$D^{\mathrm{H}}_{o,t} \ge c\, \underline{mf}^{\mathrm{HES}}_o (T^{\mathrm{S}}_{o,t} - T^{\mathrm{R}}_{o,t}) + c\, mf^{\mathrm{HES}}_{o,t} (\underline{T}^{\mathrm{S}}_o - \overline{T}^{\mathrm{R}}_o) - c\, \underline{mf}^{\mathrm{HES}}_o (\underline{T}^{\mathrm{S}}_o - \overline{T}^{\mathrm{R}}_o), \forall o, t, \tag{1h}$$
$$D^{\mathrm{H}}_{o,t} \le c\, \overline{mf}^{\mathrm{HES}}_o (T^{\mathrm{S}}_{o,t} - T^{\mathrm{R}}_{o,t}) + c\, mf^{\mathrm{HES}}_{o,t} (\underline{T}^{\mathrm{S}}_o - \overline{T}^{\mathrm{R}}_o) - c\, \overline{mf}^{\mathrm{HES}}_o (\underline{T}^{\mathrm{S}}_o - \overline{T}^{\mathrm{R}}_o), \forall o, t, \tag{1i}$$
$$D^{\mathrm{H}}_{o,t} \le c\, \underline{mf}^{\mathrm{HES}}_o (T^{\mathrm{S}}_{o,t} - T^{\mathrm{R}}_{o,t}) + c\, mf^{\mathrm{HES}}_{o,t} (\overline{T}^{\mathrm{S}}_o - \underline{T}^{\mathrm{R}}_o) - c\, \underline{mf}^{\mathrm{HES}}_o (\overline{T}^{\mathrm{S}}_o - \underline{T}^{\mathrm{R}}_o), \forall o, t, \tag{1j}$$
$$Q_{i,t} \ge c\, \overline{mf}^{\mathrm{HS}}_i (T^{\mathrm{S}}_{o,t} - T^{\mathrm{R}}_{o,t}) + c\, mf^{\mathrm{HS}}_{i,t} (\overline{T}^{\mathrm{S}}_o - \underline{T}^{\mathrm{R}}_o) - c\, \overline{mf}^{\mathrm{HS}}_i (\overline{T}^{\mathrm{S}}_o - \underline{T}^{\mathrm{R}}_o), \forall o, i \in \mathcal{A}^{\mathrm{HS}}_o, t, \tag{1k}$$
$$Q_{i,t} \ge c\, \underline{mf}^{\mathrm{HS}}_i (T^{\mathrm{S}}_{o,t} - T^{\mathrm{R}}_{o,t}) + c\, mf^{\mathrm{HS}}_{i,t} (\underline{T}^{\mathrm{S}}_o - \overline{T}^{\mathrm{R}}_o) - c\, \underline{mf}^{\mathrm{HS}}_i (\overline{T}^{\mathrm{S}}_o - \overline{T}^{\mathrm{R}}_o), \forall o, i \in \mathcal{A}^{\mathrm{HS}}_o, t, \tag{1l}$$
$$Q_{i,t} \le c\, \overline{mf}^{\mathrm{HS}}_i (T^{\mathrm{S}}_{o,t} - T^{\mathrm{R}}_{o,t}) + c\, mf^{\mathrm{HS}}_{i,t} (\underline{T}^{\mathrm{S}}_o - \overline{T}^{\mathrm{R}}_o) - c\, \overline{mf}^{\mathrm{HS}}_i (\underline{T}^{\mathrm{S}}_o - \overline{T}^{\mathrm{R}}_o), \forall o, i \in \mathcal{A}^{\mathrm{HS}}_o, t, \tag{1m}$$
$$Q_{i,t} \le c\, \underline{mf}^{\mathrm{HS}}_i (T^{\mathrm{S}}_{o,t} - T^{\mathrm{R}}_{o,t}) + c\, mf^{\mathrm{HS}}_{i,t} (\overline{T}^{\mathrm{S}}_o - \underline{T}^{\mathrm{R}}_o) - c\, \underline{mf}^{\mathrm{HS}}_i (\overline{T}^{\mathrm{S}}_o - \underline{T}^{\mathrm{R}}_o), \forall o, i \in \mathcal{A}^{\mathrm{HS}}_o, t, \tag{1n}$$
$$0 \le Q_{i,t} \le \overline{Q}_i, \forall i \in \mathcal{HS}, t, \tag{1o}$$
$$\underline{pr}^{\mathrm{HES}}_o \le pr^{\mathrm{S}}_{o,t} - pr^{\mathrm{R}}_{o,t}, \forall o, t, \tag{1p}$$
$$\underline{mf}^{\mathrm{HES}}_o \le mf^{\mathrm{HES}}_{o,t} \le \overline{mf}^{\mathrm{HES}}_o, \forall o, t, \tag{1q}$$
$$\underline{mf}^{\mathrm{HS}}_{i,} \le mf^{\mathrm{HS}}_{i,t} \le \overline{mf}^{\mathrm{HS}}_i, \forall i \in \mathcal{HS}, t, \tag{1r}$$
$$\underline{mf}^{\mathrm{S}}_{o,v} \le mf^{\mathrm{S}}_{o,v,t} \le \overline{mf}^{\mathrm{S}}_{o,v}, \forall (o,v) \in \mathcal{P}, t, \tag{1s}$$
$$\underline{mf}^{\mathrm{R}}_{o,v} \le mf^{\mathrm{R}}_{o,v,t} \le \overline{mf}^{\mathrm{R}}_{o,v}, \forall (o,v) \in \mathcal{P}, t, \tag{1t}$$
$$\sum_{v:(o,v)\in\mathcal{P}} mf^{\mathrm{S}}_{v,o,t} + \sum_{i\in\mathcal{A}^{\mathrm{HS}}_o} mf^{\mathrm{HS}}_{i,t} = \sum_{v:(o,v)\in\mathcal{P}} mf^{\mathrm{S}}_{o,v,t} + mf^{\mathrm{HES}}_{o,t}, \forall o, t, \tag{1u}$$
$$\sum_{v:(o,v)\in\mathcal{P}} mf^{\mathrm{R}}_{v,o,t} + \sum_{i\in\mathcal{A}^{\mathrm{HS}}_o} mf^{\mathrm{HS}}_{i,t} = \sum_{v:(o,v)\in\mathcal{P}} mf^{\mathrm{R}}_{o,v,t} + mf^{\mathrm{HES}}_{o,t}, \forall o, t, \tag{1v}$$
$$L_{o,v}(mf^{\mathrm{S}}_{o,v,t})^2 \le pr^{\mathrm{S}}_{v,t} - pr^{\mathrm{S}}_{o,t}, \forall (o,v) \in \mathcal{P}, t, \tag{1w}$$

$$L_{o,v}(mf^{\mathrm{R}}_{o,v,t})^2 \leq pr^{\mathrm{R}}_{v,t} - pr^{\mathrm{R}}_{o,t}, \forall (o,v) \in \mathcal{P}, t, \tag{1x}$$

$$\underline{pr}^{\mathrm{S}}_{o} \leq pr^{\mathrm{S}}_{o,t} \leq \overline{pr}^{\mathrm{S}}_{o},\ \ \underline{pr}^{\mathrm{R}}_{o} \leq pr^{\mathrm{R}}_{o,t} \leq \overline{pr}^{\mathrm{R}}_{o}, \forall o, t, \tag{1y}$$

$$\underline{T}^{\mathrm{S}}_{o} \leq T^{\mathrm{S}}_{o,t} \leq \overline{T}^{\mathrm{S}}_{o},\ \ \underline{T}^{\mathrm{R}}_{o} \leq T^{\mathrm{R}}_{o,t} \leq \overline{R}^{\mathrm{S}}_{o}, \forall o, t, \tag{1z}$$

$$T^{\mathrm{S,in}}_{o,v,t} = T^{\mathrm{S}}_{o,t},\ \ T^{\mathrm{R,in}}_{o,v,t} = T^{\mathrm{R}}_{v,t},\ \ \forall (o,v) \in \mathcal{P}, t, \tag{1aa}$$

$$T^{\mathrm{S}}_{v,t} = T^{\mathrm{S,out}}_{o,v,t},\ \ T^{\mathrm{R}}_{o,t} = T^{\mathrm{R,out}}_{o,v,t}, \forall (o,v) \in \mathcal{P}, t, \tag{1ab}$$

$$-M\ v^{\mathrm{S}}_{o,v,\eta,t} \leq \tilde{T}^{\mathrm{S,in}}_{o,v,\eta,t} \leq M\ v^{\mathrm{S}}_{o,v,\eta,t}, \forall (o,v) \in \mathcal{P}, \eta \in \{0, ..., \overline{\tau}^{\mathrm{S}}_{o,v}\}, t, \tag{1ac}$$

$$M(v^{\mathrm{S}}_{o,v,\eta,t} - 1) \leq \tilde{T}^{\mathrm{S,in}}_{o,v,\eta,t} - \tilde{T}^{\mathrm{S,in}}_{o,v,(t-\eta)} \left(1 - \frac{2\mu_{o,v}}{c\rho R_{o,v}}\eta\right) \leq M(1 - v^{\mathrm{S}}_{o,v,\eta,t}), \forall (o,v) \in \mathcal{P}, \eta \in \{0, ..., \overline{\tau}^{\mathrm{S}}_{o,v}\}, t, \tag{1ad}$$

$$M(v^{\mathrm{S}}_{o,v,\eta,t} - 1) \leq \eta - \tau^{\mathrm{S}}_{o,v,t} \leq M(1 - v^{\mathrm{S}}_{o,v,\eta,t}), \forall (o,v) \in \mathcal{P}, \eta \in \{0, ..., \overline{\tau}^{\mathrm{S}}_{o,v}\}, t, \tag{1ae}$$

$$\sum_{\eta=0}^{\overline{\tau}^{\mathrm{S}}} v^{\mathrm{S}}_{o,v,\eta,t} = 1, \forall (o,v) \in \mathcal{P}, t, \tag{1af}$$

$$T^{\mathrm{S,out}}_{o,v,t} = \sum_{\eta=0}^{\overline{\tau}^{\mathrm{S}}_{o,v}} \tilde{T}^{\mathrm{S,in}}_{o,v,\eta,t}, \forall (o,v) \in \mathcal{P}, t. \tag{1ag}$$

$$-M\ v^{\mathrm{S}}_{o,v,\eta,t} \leq \tilde{T}^{\mathrm{S,in}}_{o,v,\eta,t} \leq M\ v^{\mathrm{S}}_{o,v,\eta,t}, \forall (o,v) \in \mathcal{P}, \eta \in \{0, ..., \overline{\tau}^{\mathrm{S}}_{o,v}\}, t, \tag{1ah}$$

$$M(v^{\mathrm{S}}_{o,v,\eta,t} - 1) \leq \tilde{T}^{\mathrm{S,in}}_{o,v,\eta,t} - \tilde{T}^{\mathrm{S,in}}_{o,v,(t-\eta)} \left(1 - \frac{2\mu_{o,v}}{c\rho R_{o,v}}\eta\right) \leq M(1 - v^{\mathrm{S}}_{o,v,\eta,t}), \forall (o,v) \in \mathcal{P}, \eta \in \{0, ..., \overline{\tau}^{\mathrm{S}}_{o,v}\}, t, \tag{1ai}$$

$$M(v^{\mathrm{S}}_{o,v,\eta,t} - 1) \leq \eta - \tau^{\mathrm{S}}_{o,v,t} \leq M(1 - v^{\mathrm{S}}_{o,v,\eta,t}), \forall (o,v) \in \mathcal{P}, \eta \in \{0, ..., \overline{\tau}^{\mathrm{S}}_{o,v}\}, t, \tag{1aj}$$

$$\sum_{\eta=0}^{\overline{\tau}^{\mathrm{S}}} v^{\mathrm{S}}_{o,v,\eta,t} = 1, \forall (o,v) \in \mathcal{P}, t, \tag{1ak}$$

$$T^{\mathrm{S,out}}_{o,v,t} = \sum_{\eta=0}^{\overline{\tau}^{\mathrm{S}}_{o,v}} \tilde{T}^{\mathrm{S,in}}_{o,v,\eta,t}, \forall (o,v) \in \mathcal{P}, t, \tag{1al}$$

$$M(u^{\mathrm{S}}_{o,v,\eta,t} - 1) \leq \sum_{\tilde{\eta}=t-\eta}^{t} \frac{mf^{\mathrm{S}}_{o,v,\tilde{\eta}}}{\pi R^2_{o,v}\rho}\Delta t - L_{o,v} \leq M\ u^{\mathrm{S}}_{o,v,\eta,t}, \forall (o,v) \in \mathcal{P}, \eta \in \{0, ..., \overline{\tau}^{\mathrm{S}}_{o,v}\}, t, \tag{1am}$$

$$M(u^{\mathrm{R}}_{o,v,\eta,t} - 1) \leq \sum_{\tilde{\eta}=t-\eta}^{t} \frac{mf^{\mathrm{R}}_{o,v,\tilde{\eta}}}{\pi R^2_{o,v}\rho}\Delta t - L_{o,v} \leq M\ u^{\mathrm{R}}_{o,v,\eta,t}, \forall (o,v) \in \mathcal{P}, \eta \in \{0, ..., \overline{\tau}^{\mathrm{R}}_{o,v}\}, t, \tag{1an}$$

$$\tau^{\mathrm{S}}_{o,v,t} = \sum_{\eta=1}^{\overline{\tau}^{\mathrm{S}}_{o,v}} \eta(u^{\mathrm{S}}_{o,v,\eta,t} - u^{\mathrm{S}}_{o,v,(\eta-1),t}), \forall (o,v) \in \mathcal{P}, t, \tag{1ao}$$

$$\tau^{\mathrm{R}}_{o,v,t} = \sum_{\eta=1}^{\overline{\tau}^{\mathrm{R}}_{o,v}} \eta(u^{\mathrm{R}}_{o,v,\eta,t} - u^{\mathrm{R}}_{o,v,(\eta-1),t}), \forall (o,v) \in \mathcal{P}, t, \tag{1ap}$$

$$0 \leq g_{k,t} \leq \overline{g}_k, \forall k, t, \tag{1aq}$$

$$\underline{pr}_{m} \leq pr_{m,t} \leq \overline{pr}_{m}, \forall m, t, \tag{1ar}$$

$$pr_{u,t} \leq \Gamma_{m,u}\ pr_{m,t}, \forall (m,u) \in \mathcal{Z}, t, \tag{1as}$$

$$q^2_{m,u,t} \leq K^2_{m,u}(pr^2_{m,t} - pr^2_{u,t}), \forall (m,u) \in \mathcal{Z}, t, \tag{1at}$$

$$q_{m,u,t} = \frac{q^{\mathrm{in}}_{m,u,t} + q^{\mathrm{out}}_{m,u,t}}{2}, \forall (m,u) \in \mathcal{Z}, t, \tag{1au}$$

$$h_{m,u,t} = S_{m,u}\frac{pr_{m,t} + pr_{u,t}}{2}, \forall (m,u) \in \mathcal{Z}, t, \tag{1av}$$

$$h_{m,u,t} = h_{m,u,(t-1)} + q^{\text{in}}_{m,u,t} - q^{\text{out}}_{m,u,t}, \forall (m,u) \in \mathcal{Z}, t > 1, \tag{1aw}$$

$$h_{m,u,t} = H^{0}_{m,u} + q^{\text{in}}_{m,u,t} - q^{\text{out}}_{m,u,t}, \forall (m,u) \in \mathcal{Z}, t = 1, \tag{1ax}$$

$$H^{0}_{m,u} \leq h_{m,u,t}, \forall (m,u) \in \mathcal{Z}, t = |\mathcal{T}|, \tag{1ay}$$

$$\sum_{k \in \mathcal{A}^{K}_{m}} g_{k,t} - \sum_{i \in \mathcal{A}^{G}_{m}} \phi_i \; p_{i,t} - \sum_{u:(m,u)\in\mathcal{Z}} (q^{\text{in}}_{m,u,t} - q^{\text{out}}_{u,m,t}) = D^{\text{G}}_{m,t}, \forall m, t, \tag{1az}$$

$$r_i Q_{i,t} \leq p_{i,t}, \forall i \in \mathcal{CHP}, t, \tag{1ba}$$

$$0 \leq \rho^{\text{E}}_i p_{i,t} + \rho^{\text{H}}_i Q_{i,t} \leq \overline{p}_i, \forall i \in \mathcal{CHP}, t, \tag{1bb}$$

$$Q_{i,t} = COP_i D^{\text{HP}}_{i,t}, \forall i \in \mathcal{HP}, t, \tag{1bc}$$

$$\sum_{i \in \mathcal{A}^{I}_{n}} p_{i,t} + \sum_{j \in \mathcal{A}^{J}_{n}} w_{j,t} - \sum_{r:(n,r)\in\mathcal{L}} f_{n,r,t} = D^{\text{E}}_{n,t} + \sum_{i \in \mathcal{A}^{HP}_{n}} D^{\text{HP}}_{i,t}, \forall n, t. \tag{1bd}$$

2. Input Data

Table 1 gives the technical characteristics of power generators and transmission lines, Table 2 provides the technical characteristics of the gas system and Table 3 contains the input data for the heat network.

Generator i	1	2	3	4	5	6	7	8	9	10	11	12						
Located at bus n	1	2	7	13	15	15	16	18	21	22	23	23						
Connected to gas node m	12	12	-	-	10	10	7	-	-	6	-	-						
Connected to heat node o	-	-	-	-	-	-	-	-	-	-	-	2						
C^{E}_i [$/MWh]	-	-	65.61	30.82	-	-	-	20.84	26.9	-	32.22	-						
C_i [$/MWh]	-	-	-	-	-	-	-	-	-	-	-	17.5						
$\overline{p}_i$ [MW]	152	152	300	591	60	155	155	400	400	300	350	1000						
Type	$\mathcal{G}$	$\mathcal{G}$	$\mathcal{C}$	$\mathcal{C}$	$\mathcal{G}$	$\mathcal{G}$	$\mathcal{G}$	$\mathcal{C}$	$\mathcal{C}$	$\mathcal{G}$	$\mathcal{C}$	$\mathcal{CHP}$						
ϕ_i [kcf/MWh]	12.65	20.25	-	-	11.12	15.1	14.88	-	-	13.3	-	-						
Wind farm j	1																	
Located at bus n	5																	
$\overline{W}_j$ [MW]	2100																	
Power load	1	2	3	4	5	6	7	8	9	10	11	12	13	14	15	16	17	18
At bus n	1	2	3	4	5	6	7	8	9	10	13	14	15	16	18	19	20	23
Share of total load	0.038	0.044	0.063	0.026	0.025	0.048	0.044	0.060	0.061	0.068	0.093	0.073	0.111	0.035	0.117	0.014	0.04	0.04
Line $(n,r) \in \mathcal{L}$	1	2	3	4	5	6	7	8	9	10	11	12	13	14	15	16	17	18
n	1	1	1	2	2	3	3	4	5	6	7	8	8	9	9	10	10	11
r	2	3	5	4	6	9	24	9	10	10	8	9	10	11	12	11	12	13
$1/B_{n,r}$ [pu]	0.0146	0.2253	0.0907	0.1356	0.205	0.1271	0.084	0.111	0.094	0.0642	0.0652	0.1762	0.1762	0.084	0.084	0.084	0.084	0.0488
$\overline{f}_{n,r}$ [MW]	175	175	350	175	175	175	400	175	350	175	350	175	175	400	400	400	400	500
Line $(n,r) \in \mathcal{L}$	19	20	21	22	23	24	25	26	27	28	29	30	31	32	33	34		
n	11	12	12	13	14	15	15	15	16	16	17	17	18	19	20	21		
r	14	13	23	23	16	16	21	24	17	19	18	22	21	20	23	22		
$1/B_{n,r}$ [pu]	0.0426	0.0488	0.0985	0.0884	0.0594	0.0172	0.0249	0.0529	0.0263	0.0234	0.0143	0.1069	0.0132	0.0203	0.0112	0.0692		
$\overline{f}_{n,r}$ [MW]	500	500	500	250	250	500	400	500	500	500	500	500	1000	1000	1000	500		

Table 1. Power system input data for generators, wind farms, loads and transmission lines

Gas supplier k	1	2	3									
Located at node m	1	3	11									
$\overline{g}_k$ [kcf]	7200	7200	18000									
C_k^{G} [$/kcf]	2	2.4	3.2									
Demand	1	2	3	4								
At node m	5	6	7	12								
Share of total demand	0.25	0.35	0.25	0.15								
Pipeline $(m,u) \in \mathcal{Z}$	1	2	3	4	5	6	7	8	9	10	11	12
m	1	2	3	4	5	4	6	7	8	9	10	11
u	2	4	5	5	6	7	8	8	9	10	11	12
$K_{m,u}$ [kcf/psig h]	28	28	28	21	21	21	28	21	28	28	28	28
$\Gamma_{m,u}$	-	1.2	-	-	-	-	-	-	1.3	-	-	-
$S_{m,u}$ [kcf/psig]	121	121	150	186	189	184	150	179	149	148	150	130
$H^0_{m,u}$ [kcf]	39300	39300	49300	59300	54300	54300	39300	44300	39300	39300	39300	29300

TABLE 2. Input data for gas system. Note that minimum and maximum pressure limits $\underline{pr}_m$ and $\overline{pr}_m$ are 100 psig and 500 psig for all nodes m, respectively.

Heat unit i	$\mathcal{CHP}$	$\mathcal{HP}$	
Located at node o	1	2	
$\overline{Q}_i$ [MW]	250	150	
$\underline{mf}_i^{\mathrm{HS}}$ [kg/h]	0	0	
$\overline{mf}_i^{\mathrm{HS}}$ [kg/h]	300	300	
COP_i	-	2.5	
r_i	0.6	-	
ρ_i^{E}	2.4	-	
ρ_i^{H}	0.25	-	
C_i [$/MWh]	17.5	-	
Node o	1	2	3
$\underline{mf}_o^{\mathrm{HES}}$ [kg/h]	-	-	50
$\overline{mf}_o^{\mathrm{HES}}$ [kg/h]	-	-	300
$\underline{T}_o^{\mathrm{R}}$ [C]	30	30	30
$\overline{T}_o^{\mathrm{R}}$ [C]	60	60	60
$\underline{T}_o^{\mathrm{S}}$ [C]	90	90	90
$\overline{T}_o^{\mathrm{S}}$ [C]	120	120	120
$\underline{pr}_o^{\mathrm{S/R}}$ [psig]	0	0	0
$\overline{pr}_o^{\mathrm{S/R}}$ [psig]	100	100	100
Pipeline $(o,v) \in \mathcal{P}$	1	2	
o	1	2	
v	2	3	
$R_{o,v}$ [m]	2	3	
$\mu_{o,v}$ [MW m^{-2} K^{-1}]	20	20	
$\nu_{o,v}$ [10^{-3}]	1.93	1.93	
$\underline{mf}_{o,v}^{\mathrm{S/R}}$ [kg/h]	50	50	
$\overline{mf}_{o,v}^{\mathrm{S/R}}$ [kg/h]	300	300	

TABLE 3. District heating system characteristics. Note that c=1.17 Wh/(kg K), ρ=988 kg/m^3.

[Paper B] Coordination of power and natural gas systems: Convexification approaches for linepack modeling

Authors:
Anna Schwele, Christos Ordoudis, Jalal Kazempour and Pierre Pinson

Published in:
Proceedings of IEEE Milan PowerTech Conference 2019

DOI:
10.1109/PTC.2019.8810632

Coordination of Power and Natural Gas Systems: Convexification Approaches for Linepack Modeling

Anna Schwele, Christos Ordoudis, Jalal Kazempour, Pierre Pinson
Center for Electric Power and Energy, Technical University of Denmark, Kgs. Lyngby, Denmark
{schwele, chror, seykaz, ppin}@elektro.dtu.dk

***Abstract*—Utilizing operational flexibility from natural gas networks can foster the integration of uncertain and variable renewable power production. We model a combined power and natural gas dispatch to reveal the maximum potential of linepack, i.e., energy storage in the pipelines, as a source of flexibility for the power system. The natural gas flow dynamics are approximated by a combination of steady-state equations and varying incoming and outgoing flows in the pipelines to account for both natural gas transport and linepack. This steady-state natural gas flow results in a nonlinear and nonconvex formulation. To cope with the computational challenges, we explore convex quadratic relaxations and linear approximations. We propose a novel mixed-integer second-order cone formulation including McCormick relaxations to model the bidirectional natural gas flow accounting for linepack. Flexibility is quantified in terms of system cost compared to a dispatch model that either neglects linepack or assumes infinite storage capability.**

***Index Terms*—Combined power and natural gas dispatch, convexification, McCormick relaxation, second-order cone program, steady-state gas flow.**

NOMENCLATURE

Sets

$\mathcal{I}$	Set of dispatchable power plants i.
$\mathcal{C}$	Subset of dispatchable power plants excluding natural gas-fired ones ($\mathcal{C} \subset \mathcal{I}$).
$\mathcal{G}$	Subset of natural gas-fired power plants ($\mathcal{G} \subset \mathcal{I}$).
$\mathcal{J}$	Set of wind power units j.
$\mathcal{T}$	Set of time periods t.
$\mathcal{L}$	Set of electricity transmission lines (n, r).
$\mathcal{N}$	Set of electricity network nodes n.
$\mathcal{K}$	Set of natural gas supply units k.
$\mathcal{Z}$	Set of natural gas pipelines (m, u).
$\mathcal{M}$	Set of natural gas network nodes m.
$\mathcal{V}$	Set of fixed pressure points v.
$\mathcal{A}_n^{(.)}$	Set of assets located at electricity network node n.
$\mathcal{A}_m^{(.)}$	Set of assets located at natural gas network node m.
Θ	Set of optimization variables.

Variables

$p_{i,t}, w_{j,t}$	Dispatch of units i and j in period t, respectively [MW].
$g_{k,t}$	Dispatch of unit k in period t [kcf/h].
$\theta_{n,t}$	Voltage angle at node n in period t [rad].
$f_{n,r,t}$	Power flow in line (n, r) in period t [MW].
$pr_{m,t}$	Pressure at node m in period t [psig].
$h_{m,u,t}$	Average mass of natural gas (linepack) in pipeline (m, u) in period t [kcf].
$q^{\text{in/out}}_{m,u,t}$	Inflow/outflow natural gas rate of pipeline (m, u) in period t [kcf/h].
$q_{m,u,t}$	Natural gas flow in pipeline (m, u) in period t [kcf/h].
$q^{+/-}_{m,u,t}$	Natural gas flow in pipeline (m, u) from node m to u/from node u to m in period t [kcf/h].
$y_{m,u,t}$	Binary variable defining the direction of the natural gas flow in pipeline (m, u) in period t {0,1}.

Parameters

$D^{\text{E}}_{n,t}$	Electricity demand at node n in period t [MW].
$D^{\text{G}}_{m,t}$	Natural gas demand at node m in period t [kcf/h].
C^{E}_i	Production cost of unit i [$/MWh].
C^{G}_k	Supply cost of unit k [$/kcf].
P^{max}_i	Capacity of dispatchable unit i [MW].
ϕ_i	Power conversion factor of natural gas unit $i \in \mathcal{G}$ [kcf/MWh].
$W_{j,t}$	Wind power forecast for unit j in period t [MW].
G^{max}_k	Capacity of natural gas unit k [kcf].
$B_{n,r}$	Susceptance of line (n, r) [S].
$F^{\text{max}}_{n,r}$	Transmission capacity of line (n, r) [MW].
$K_{m,u}$	Natural gas flow constant of pipeline (m, u) [kcf/(psig h)].
$S_{m,u}$	Linepack constant of pipeline (m, u) [kcf/psig].
$H^0_{m,u}$	Initial linepack in pipeline (m, u) [kcf].
PR^{min}_m	Minimum pressure limit at node m [psig].
PR^{max}_m	Maximum pressure limit at node m [psig].
$\Gamma_{m,u}$	Compressor factor at natural gas pipeline (m, u).
M	A sufficiently large constant.

I. INTRODUCTION

The growing share of stochastic renewable energy sources that introduce uncertainty and variability into the operation of power system increases the need for flexible resources. Natural gas-fired power plants (NGFPP) typically provide operational flexibility in systems with high share of renewable energy penetration [1], thus linking the power and natural gas systems [2]. In power system operations, security and network constraints related to the natural gas system are becoming important for generation scheduling [3], unit commitment [4], and reserve scheduling decisions [5] to ensure fuel availability for NGFPPs. Apart from ensuring technical feasibility of short-term operations, accounting for the natural gas network unlocks its inherent flexibility in order to facilitate the integration of renewables and deal with uncertainties and variability from large-scale wind power penetration [6], [7]. This necessitates a proper *coordination* between power and natural gas systems.

Several works in the literature have investigated different coordination levels of power and natural gas systems in terms of short-term operational integration, proving the advantages of such coupling for the whole system, see [6]–[9]. A full coupling (co-optimization) of the two energy systems is not compatible with the current market regulations in most countries which usually require decoupled operations on different temporal scales [10]. The full coupling requires a single entity to operate the whole integrated system. This is the case in Denmark, where Energinet.dk is operating both systems, but separately [11]. The co-optimization model yields an *ideal*

benchmark showing the maximum potential flexibility that can be unlocked, obtaining the minimum overall cost for the two systems [12]. This benchmark, though not directly implementable in practice, is highly useful, since it provides a lower bound for system cost, and can be used to assess the performance of any other coordination scheme that aligns with current market regulations.

The ability to store natural gas in the pipelines is referred to as *linepack*, and can provide short-term flexibility to the power system. Unlocking linepack flexibility requires accurate modeling of natural gas flow dynamics along pipelines as well as efficient solution methods. Different integrated natural gas and power flow models are presented in [8] using dynamic natural gas flow models, while [13] models steady-state gas flow constraints. It is worth mentioning that modeling *bidirectional* gas flow is crucial, since the direction of natural gas flow in the pipeline may change due to sudden off-take from NGFPPs to compensate for variability from renewable generation.

Several works have aimed at convexifying the steady-state natural gas flow via linear approximation or convex relaxation techniques. Reference [14] introduces a semidefinite programming (SDP) relaxation for the natural gas flow, assuming that the flow direction is known. Similarly, [15] proposes a second-order cone (SOC) relaxation for modeling optimal power and natural gas flows, assuming fixed flow directions and ignoring compressors, linepack and storage. A mixed-integer second-order cone programming (MISOCP) relaxation is proposed in [16] to represent natural gas flows for expansion planning of natural gas and power systems with unidirectional gas flow, while the expansion planning model in [17] allows for varying flow directions along a pipeline. Reference [18] proposes a MISOCP relaxation model treating gas flow direction in each pipeline as a variable, proving the uniqueness and exactness of the solution, but ignoring linepack. The piecewise linear approximation model in [19] also considers bidirectional gas flows but neglects linepack. The mixed-integer linear programming (MILP) models proposed in [6] and [7] yield improved flexibility and reliability when accounting for the bidirectional gas flows and linepack. More specifically, the models in [6] and [7] are able to incorporate linepack dynamics while allowing for bidirectional natural gas flow using an outer linear approximation and a piecewise linear approximation, respectively. Table I summarizes the convexification approaches for steady-state natural gas flow models in the literature, and compares them with the proposed model in this paper.

To the best of our knowledge, the existing quadratic and semidefinite relaxation models either assume known flow directions or neglect the ability of pipelines to store natural gas, see [14]–[18]. Thus, we propose a novel MISOCP model including McCormick relaxations of the steady-state natural gas flow to incorporate both linepack and bidirectional flow. Similar to the approach in [20], which investigates the linepack flexibility provided by district heating networks for the power system, our work evaluates the social value of short-term operational flexibility that the natural gas network can provide to the electricity system. The objective of this paper is to present a methodology for a combined electricity and natural gas dispatch as an ideal benchmark that appropriately models the dynamics of gas flow. We use this model to assess the ability of the natural gas network to react to changes in the power system due to intermittent renewables. In order to evaluate the modeling of the linepack properties to account for inherent flexibility of the natural gas system, we compare the proposed MISOCP relaxation of the bidirectional nonconvex steady-state natural gas flow under different levels of wind penetration to the MILP approximation proposed in [6]. Finally, the value of linepack flexibility provided by the gas network is quantified in terms of system cost compared to the coupled dispatch of the electricity and natural gas systems either without linepack modeling or with infinite storage capability.

TABLE I
COMPARISON OF NATURAL GAS FLOW CONVEXIFICATION APPROACHES

Reference	Natural gas flow model	Bidirectional flow	Linepack
[14]	Relaxation (SDP)	No	No
[15]	Relaxation (SOCP)	No	No
[16]	Relaxation (MISOCP)	No	No
[17], [18]	Relaxation (MISOCP)	Yes	No
[19]	Approximation (MILP)	Yes	No
[6], [7]	Approximation (MILP)	Yes	Yes
This paper	Relaxation (MISOCP)	Yes	Yes

The paper is organized as follows. Section II introduces the formulation of the combined power and natural gas dispatch model. In Section III, we explore two convexification approaches for efficiently solving the natural gas flow model, which are compared in Section IV for a case study quantifying the value of natural gas network flexibility for the power system. Section V draws the conclusion.

II. COMBINED POWER AND NATURAL GAS DISPATCH

A. Model framework and assumptions

We propose a fully coupled electricity and natural gas dispatch that co-optimizes the operations in both systems. Both wind power production and wind spillage costs are assumed to be zero. Since the focus of this paper is modeling the flexibility provided by the natural gas network, we aim at accurately modeling the gas flow problem, while we use a lossless DC model for the power flows on the electricity side. Under the assumption of isothermal natural gas flow in horizontal pipelines, the natural gas flow is represented by its steady-state gas flow equation. The dynamics in pipelines are approximated by accounting for the energy storage capacity of gas networks in the form of linepack through varying in- and outflows. Compressor stations are modeled with a constant compressor factor neglecting fuel and power consumption of compressors [3].

B. Co-optimization Model

The original combined dispatch problem, which is mixed-integer and nonconvex, is formulated by the following optimization problem (1):

$$\min_{\Theta} \sum_{t\in\mathcal{T}} \Big(\sum_{i\in\mathcal{C}} C_i^{\mathrm{E}}\ p_{i,t} + \sum_{k\in\mathcal{K}} C_k^{\mathrm{G}}\ g_{k,t} \Big) \tag{1a}$$

subject to

$$0 \le p_{i,t} \le P_i^{\max}, \forall i, t, \tag{1b}$$
$$0 \le w_{j,t} \le W_{j,t}, \forall j, t, \tag{1c}$$
$$f_{n,r,t} = B_{n,r}(\theta_{n,t} - \theta_{r,t}), \forall (n,r) \in \mathcal{L}, t, \tag{1d}$$
$$-F_{n,r}^{\max} \le f_{n,r,t} \le F_{n,r}^{\max}, \forall (n,r) \in \mathcal{L}, t, \tag{1e}$$
$$-\pi \le \theta_{n,t} \le \pi, \forall n, t, \;\; \theta_{n,t} = 0, \forall n{:}\text{ref}, t, \tag{1f}$$
$$\sum_{i \in \mathcal{A}_n^I} p_{i,t} + \sum_{j \in \mathcal{A}_n^J} w_{j,t} - \sum_{(n,r) \in \mathcal{L}} f_{n,r,t} = D_{n,t}^{\mathrm{E}}, \forall n, t, \tag{1g}$$
$$0 \le g_{k,t} \le G_k^{\max}, \forall k, t, \tag{1h}$$
$$PR_m^{\min} \le pr_{m,t} \le PR_m^{\max}, \forall m, t, \tag{1i}$$
$$pr_{u,t} \le \Gamma_{m,u}\ pr_{m,t}, \forall (m,u) \in \mathcal{Z}, t, \tag{1j}$$
$$q_{m,u,t}|q_{m,u,t}| = K_{m,u}^2(pr_{m,t}^2 - pr_{u,t}^2), \forall (m,u) \in \mathcal{Z}, t, \tag{1k}$$
$$q_{m,u,t} = q_{m,u,t}^+ - q_{m,u,t}^-, \forall (m,u) \in \mathcal{Z}, t, \tag{1l}$$
$$0 \le q_{m,u,t}^+ \le M\ y_{m,u,t}, \forall (m,u) \in \mathcal{Z}, t, \tag{1m}$$
$$0 \le q_{m,u,t}^- \le M(1 - y_{m,u,t}), \forall (m,u) \in \mathcal{Z}, t, \tag{1n}$$
$$q_{m,u,t}^+ = \frac{q_{m,u,t}^{\text{in}} + q_{m,u,t}^{\text{out}}}{2}, \forall (m,u) \in \mathcal{Z}, t, \tag{1o}$$
$$q_{m,u,t}^- = \frac{q_{u,m,t}^{\text{in}} + q_{u,m,t}^{\text{out}}}{2}, \forall (m,u) \in \mathcal{Z}, t, \tag{1p}$$
$$h_{m,u,t} = S_{m,u}\frac{pr_{m,t} + pr_{u,t}}{2}, \forall (m,u) \in \mathcal{Z}, t, \tag{1q}$$
$$h_{m,u,t} = h_{m,u,(t-1)} + q_{m,u,t}^{\text{in}} - q_{m,u,t}^{\text{out}} + q_{u,m,t}^{\text{in}} - q_{u,m,t}^{\text{out}}, \quad \forall (m,u) \in \mathcal{Z}, t > 1, \tag{1r}$$
$$h_{m,u,t} = H_{m,u}^0 + q_{m,u,t}^{\text{in}} - q_{m,u,t}^{\text{out}} + q_{u,m,t}^{\text{in}} - q_{u,m,t}^{\text{out}}, \quad \forall (m,u) \in \mathcal{Z}, t = 1, \tag{1s}$$
$$H_{m,u}^0 \le h_{m,u,t}, \forall (m,u) \in \mathcal{Z}, t = |\mathcal{T}|, \tag{1t}$$
$$\sum_{k \in \mathcal{A}_m^K} g_{k,t} - \sum_{i \in \mathcal{A}_m^G} \phi_i\ p_{i,t} - \sum_{u:(m,u) \in \mathcal{Z}} (q_{m,u,t}^{\text{in}} - q_{u,m,t}^{\text{out}}) = D_{m,t}^{\mathrm{G}}, \forall m, t, \tag{1u}$$

where the set of optimization variables is $\Theta = \{q_{m,u,t}, y_{m,u,t}, q_{m,u,t}^+, q_{m,u,t}^-, q_{m,u,t}^{\text{in}}, q_{m,u,t}^{\text{out}}, h_{m,u,t}, pr_{m,t}, g_{k,t}, p_{i,t}, w_{j,t}, \theta_{n,t}, f_{n,r,t}\}$. Objective function (1a) minimizes the total cost of operating the power and natural gas systems, i.e., the production cost of non-NGFPPs and natural gas supply cost. The model contains two sets of constraints: (1b)-(1g) correspond to the power system while (1h)-(1u) pertain to the natural gas system. The two systems are coupled through (1u) translating the dispatch of NGFPPs into a time-varying nodal demand for natural gas by $\sum_{i \in \mathcal{A}_m^G} \phi_i\ p_{i,t}, \forall m, t$. Constraints (1b) and (1c) impose capacity limits of the power plants and wind farms, respectively. Constraints (1d) and (1e) define power flows along each transmission line and bound them to transmission capacity. In (1f) the voltage angles are restricted and that of the reference node is set to zero. Constraint (1g) enforces the power balance at each node. Constraints (1h) and (1i) impose limits on capacity of natural gas supply and nodal pressure, respectively. Pipelines with compressors relate the inlet and outlet pressures between two adjacent nodes via compressor factor $\Gamma_{m,u}$ in (1j). The piecewise quadratic and nonconvex constraint (1k), known as Weymouth equation, describes the steady-state gas flow between nodes m and u, which depends on the pressure at the adjacent nodes and the physical properties of the pipeline reflected in parameter $K_{m,u}$. The natural gas flow in each pipeline is decomposed in (1l) to two non-negative variables $q_{m,u,t}^+$ and $q_{m,u,t}^-$, which are required to determine the direction of flow using binary variable $y_{m,u,t}$ in (1m) and (1n). Note that the big constant M is set to the maximum gas flow along a pipeline to ensure that either (1m) or (1n) is active. The flow in each pipeline is defined as the average of inflow and outflow according to (1o) and (1p), see Fig. 1. The average mass in each pipeline is given by (1q) which determines the linepack on pipelines based on pressures at adjacent nodes and parameter $S_{m,u}$ reflecting the pipeline properties. The mass conservation at each pipeline is enforced by (1r). Constraint (1s) sets the initial amount of linepack, while (1t) imposes a minimum linepack level at the end of time period to ensure that the natural gas in the network is not depleted. Finally, constraint (1u) imposes the nodal natural gas balance, and couples the power and natural gas systems through fuel consumption of NGFPPs.

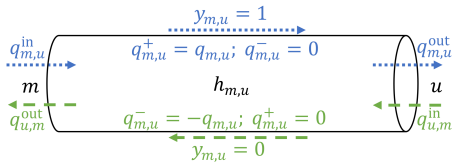

Fig. 1. Bidirectional flow along a pipeline (time index t is dropped for notational clarity)

Note that the resulting mixed-integer and nonlinear programming (MINLP) model (1) is computationally challenging, since there is currently no off-the-shelf solver to efficiently solve such a problem. In the next section, we investigate the two options to convexify the nonlinearities of this model.

III. Linepack Convexification Approaches

We first propose a novel MISOCP relaxation that allows for modeling both bidirectional natural gas flow and convexified dynamics of linepack in pipelines. Then, for comparison purposes, another convexification alternative based on a linear approximation method proposed in [6] is briefly explained.

A. Proposed MISOCP Relaxation

Weymouth equation (1k) can be equivalently written as:

$$q_{m,u,t}|q_{m,u,t}| \le K_{m,u}^2(pr_{m,t}^2 - pr_{u,t}^2), \forall (m,u) \in \mathcal{Z}, t, \tag{2a}$$
$$q_{m,u,t}|q_{m,u,t}| \ge K_{m,u}^2(pr_{m,t}^2 - pr_{u,t}^2), \forall (m,u) \in \mathcal{Z}, t. \tag{2b}$$

We drop (2b) and then replace (2a) by the following set of constraints in (3). Compared to (2a), note that the absolute function is omitted in (3) but the bidirectional flows along pipelines are still modeled by additional terms related to binary variable $y_{m,u,t}$ [18].

$$\Big\{ -M(1 - y_{m,u,t}) \le q_{m,u,t} \le M\ y_{m,u,t}, \tag{3a}$$

$$q^2_{m,u,t} \le K^2_{m,u}(pr^2_{m,t} - pr^2_{u,t}) + M^2(1 - y_{m,u,t}), \quad (3b)$$
$$q^2_{m,u,t} \le K^2_{m,u}(pr^2_{u,t} - pr^2_{m,t}) + M^2\ y_{m,u,t}, \Big\} \quad (3c)$$
$$\forall (m,u) \in \mathcal{Z}, t.$$

While (3a) is a linear constraint, (3b) and (3c) are still not in the form of SOC constraints. We introduce two auxiliary variables $\varphi^+_{m,u,t} = pr_{m,t} + pr_{u,t}$ and $\varphi^-_{m,u,t} = pr_{m,t} - pr_{u,t}$, so that $\varphi^+_{m,u,t}\ \varphi^-_{m,u,t} = pr^2_{m,t} - pr^2_{u,t}$. Accordingly, we reformulate (3b) and (3c) as

$$\Big\{ q^2_{m,u,t} \le K^2_{m,u}(\varphi^+_{m,u,t}\ \varphi^-_{m,u,t}) + M^2(1 - y_{m,u,t}), \quad (4a)$$
$$q^2_{m,u,t} \le K^2_{m,u}(-\varphi^+_{m,u,t}\ \varphi^-_{m,u,t}) + M^2\ y_{m,u,t}, \Big\} \quad (4b)$$
$$\forall (m,u) \in \mathcal{Z}, t.$$

Similarly, constraints (1j) and (1q) in the original problem are replaced by

$$\Big\{ \frac{1}{2}(\varphi^+_{m,u,t} - \varphi^-_{m,u,t}) \le \Gamma_{m,u}\ \frac{1}{2}(\varphi^+_{m,u,t} + \varphi^-_{m,u,t}), \quad (5a)$$
$$h_{m,u,t} = S_{m,u}\frac{\varphi^+_{m,u,t}}{2}, \Big\}\ \forall (m,u) \in \mathcal{Z}, t. \quad (5b)$$

Since $pr_{m,t}$ is substituted by auxiliary variables, we drop the pressure bounds (1i), and then introduce parameters $\underline{\varphi}^+_{m,u,t} = PR^{\min}_m + PR^{\min}_u$, $\overline{\varphi}^+_{m,u,t} = PR^{\max}_m + PR^{\max}_u$, $\underline{\varphi}^-_{m,u,t} = PR^{\min}_m - PR^{\max}_u$, and $\overline{\varphi}^-_{m,u,t} = PR^{\max}_m - PR^{\min}_u$ to limit those auxiliary variables as

$$\Big\{ \underline{\varphi}^+_{m,u,t} \le \varphi^+_{m,u,t} \le \overline{\varphi}^+_{m,u,t}, \quad (6a)$$
$$\underline{\varphi}^-_{m,u,t} \le \varphi^-_{m,u,t} \le \overline{\varphi}^-_{m,u,t}, \Big\}\ \forall (m,u) \in \mathcal{Z}, t. \quad (6b)$$

We still need to rephrase (4a) and (4b) due to the bilinear term $\varphi^+_{m,u,t}\ \varphi^-_{m,u,t}$. Therefore, we use McCormick relaxation technique by introducing a new auxiliary variable, denoted as $\psi_{m,u,t}$, and defining the McCormick envelopes [21]. For notional clarity, we drop subscripts m, u and n from all variables and parameters. These envelopes are:

$$\psi \ge \underline{\varphi}^+\ \varphi^- + \varphi^+\ \underline{\varphi}^- - \underline{\varphi}^+\ \underline{\varphi}^- \quad (7a)$$
$$\psi \ge \overline{\varphi}^+\ \varphi^- + \varphi^+\ \overline{\varphi}^- - \overline{\varphi}^+\ \overline{\varphi}^- \quad (7b)$$
$$\psi \le \overline{\varphi}^+\ \varphi^- + \varphi^+\ \underline{\varphi}^- - \overline{\varphi}^+\ \underline{\varphi}^- \quad (7c)$$
$$\psi \le \underline{\varphi}^+\ \varphi^- + \varphi^+\ \overline{\varphi}^- - \underline{\varphi}^+\ \overline{\varphi}^-. \quad (7d)$$

Now, (4a) and (4b) are expressed by mixed-integer second-order cone constraints:

$$\Big\{ q^2_{m,u,t} \le K^2_{m,u}\ \psi_{m,u,t} + M^2(1 - y_{m,u,t}), \quad (8a)$$
$$q^2_{m,u,t} \le -K^2_{m,u}\ \psi_{m,u,t} + M^2\ y_{m,u,t}, \Big\} \quad (8b)$$
$$\forall (m,u) \in \mathcal{Z}, t.$$

Note that if $y_{m,u,t} = 0$, then (8a) is satisfied trivially, while (8b) becomes $q^2_{m,u,t} \le -K^2_{m,u}\psi_{m,u,t}$. Similarly, (8b) is non-binding when $y_{m,u,t} = 1$, while (8b) reads as $q^2_{m,u,t} \le K^2_{m,u}\psi_{m,u,t}$. The resulting MISOCP model includes (1a)-(1h), (1l)-(1p), (1r)-(1u), (3a), and (5)-(8).

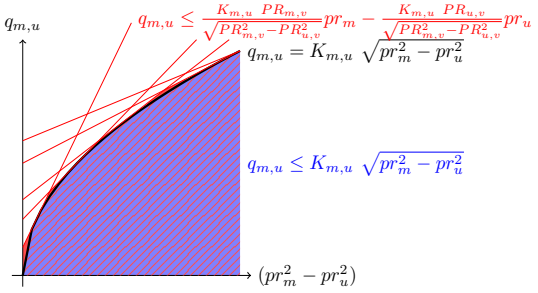

Fig. 2. SOC relaxation and outer linear approximation of (1k)

B. MILP Approximation

We compare the proposed MISOCP relaxation to the outer approximation approach based on the Taylor series expansion around fixed pressure points from [6]. This tractable MILP formulation of bidirectional gas flow model accounts for linepack flexibility. Instead of relaxing the solution space described by the Weymouth equation into a SOC as in (2a), the approach in [6] defines a number of planes tangent to the cone described by (1k), see Fig. 2. Each equality constraint (1k) is replaced by a set of linear inequalities (9), that linearly approximate the Weymouth equation around fixed pressure points $PR_{m,v}, PR_{u,v}, \forall (m,u) \in \mathcal{Z}, v \in \mathcal{V}$:

$$q^+_{m,u,t} \le \frac{K_{m,u}\ PR_{m,v}}{\sqrt{PR^2_{m,v} - PR^2_{u,v}}} pr_{m,t} - \frac{K_{m,u}\ PR_{u,v}}{\sqrt{PR^2_{m,v} - PR^2_{u,v}}} pr_{u,t}$$
$$+ M(1 - y_{m,u,t}), \forall \{(m,u) \in \mathcal{Z} | m > u\}, v, t, \quad (9a)$$
$$q^-_{m,u,t} \le \frac{K_{m,u}\ PR_{u,v}}{\sqrt{PR^2_{u,v} - PR^2_{m,v}}} pr_{u,t} - \frac{K_{m,u}\ PR_{m,v}}{\sqrt{PR^2_{u,v} - PR^2_{m,v}}} pr_{m,t}$$
$$+ M\ y_{m,u,t}, \forall \{(m,u) \in \mathcal{Z} | m < u\}, v, t. \quad (9b)$$

Table II summarizes the introduced models. Note that the solutions obtained from both MISOCP and MILP approaches may not be necessarily feasible for the original model (1). However, these models are still useful as benchmarks to assess the value of linepack flexibility.

IV. Numerical Study

We compare the convexification approaches presented in Section III using an integrated energy system consisting of a 12-node natural gas system and the IEEE 24-node reliability test system [6]. The forecast profiles of total electricity load and wind power production over the 24-hour scheduling horizon are illustrated in Fig. 3. We solve all models using an Intel CoreTM i7-7820HQ with four processors clocking at 2.70 GHz and 16 GB of RAM in Python using Gurobi solver

TABLE II
Summary of Combined Power and Natural Gas Dispatch Models

Model	Properties
MINLP	Original model; no off-the-shelf solver
MISOCP	Quadratic relaxation of the original MINLP model
MILP	Linear approximation of the original MINLP model

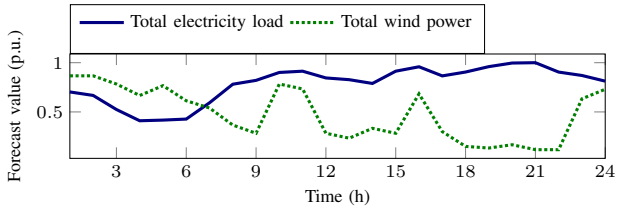

Fig. 3. Demand and wind power forecasts

package 7.5.2. All input data and codes used are available in [22].

We now present our results. Fig. 4 shows the total system cost, which is the optimal value obtained for (1a), under different levels of wind power penetration, i.e., the total installed wind power capacity divided by total demand of power system. We first quantify the value of modeling the linepack by comparing the total system cost obtained in MISOCP and MILP models with that of a case neglecting linepack (green curve in Fig. 4). This comparison indicates that the flexibility revealed from the pipelines decreases the total system cost. This cost reduction in MISOCP and MILP models is 2% and 1% on average across different levels of wind penetration, respectively. In order to quantify the amount of flexibility unveiled from linepack, we now compare the results achieved with a case including an ideal electricity storage. This storage has infinite capacity, charging and discharging rates allowing for the most cost-efficient shift of the electricity demand over hours. According to a performance ratio defined as $\frac{\text{cost}^{\text{No linepack}} - \text{cost}^{\text{MISOCP}}}{\text{cost}^{\text{No linepack}} - \text{cost}^{\text{Ideal storage}}}$, the MISOCP model yields on average a cost saving equal to 25.5% of that in the ideal storage case, while this value is 13.1% for the MILP model.

For the case of 50% wind penetration, Fig. 5 shows the daily profiles of total charging and discharging of energy in the natural gas pipelines as well as the total amount of natural gas supplied and consumed by NGFPPs. The total linepack increases from the initial 526,600 kcf to maximum 570,193 kcf and 572,578 kcf in the MISOCP and MILP models, respectively. For the two convexification approaches the charging and discharging profiles of the natural gas network are slightly different, see Figs. 5(a) and 5(b). Compared to the case neglecting linepack (Figs. 5(c) and 5(f)), both approaches result in shifting the natural gas demand profile in a more cost-efficient manner and thus, utilizing less expensive natural gas supply for electricity production (Figs. 5(d) and 5(e)). The amount of energy stored in the pipelines directly impacts the profiles of natural gas supply and consumption by NGFPPs, see Figs. 5(d)-5(f). According to these plots, the gas supply curve in the model neglecting linepack is highly volatile (Fig. 5(f)), while it is entirely flat in the MISOCP model (Fig. 5(d)). This profile is also flat during the most hours of the day considered (i.e., from hour 1 to 17) in the MILP model (Fig. 5(e)).

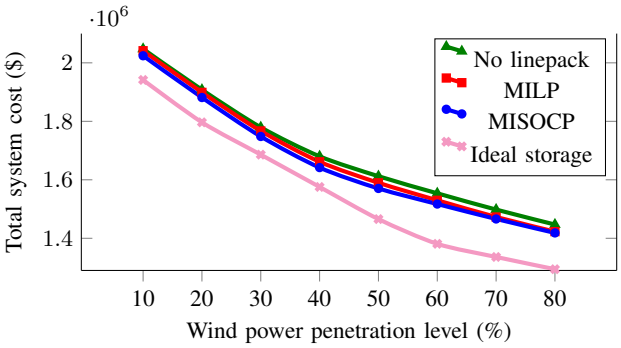

Fig. 4. Total system cost as a function of wind power penetration

To gain better insight into the impacts of modeling linepack, we focus on hours 18-22 with comparatively low wind power production (Fig. 3). During these hours, the NGFPPs need to consume more natural gas to compensate the lack of wind power production. In the MISOCP model the increased need for natural gas during these hours is fully supplied by linepack, while keeping the gas supply profile still flat (Fig. 5(d)). Compared to the MISOCP model, linepack in the MILP model is not sufficient to fuel the increased power production of NGFPPs in hours 18 to 21. Therefore, the natural gas supply is increased (Fig. 5(e)). Without modeling linepack, the natural gas consumption and supply need to be matched in each time period as illustrated in Fig. 5(f).

Based on the above results, the MISOCP model seems to reveal more linepack flexibility than the MILP model. However, compared to the MILP approximation, the MISOCP relaxation is less accurate in modeling the original constraints (1k). For both convexification models, we check the potential mismatch between the values obtained for the right- and left-hand sides of each equality constraint (1k). We quantify this mismatch using the normalized root mean squared error (NRMSE) with respect to the average flow. This error is 0.95% in the MISOCP model, while it is 0.03% only in the MILP model. A potential interpretation for the lower accuracy of the MISOCP model is that we used one relaxation technique (i.e., McCormick) within the process to achieve another relaxation, i.e., SOC constraints.

Regarding the computational aspects of the two models, the MISOCP model is solved on average within 10 seconds, while the MILP model requires 1,000 seconds to be solved with an optimality gap tolerance of 0.02%. This implies that there is a trade-off between computational efficiency and accuracy of the flow representation in the two convexification approaches.

V. Conclusion

This paper proposed a new MISOCP model for efficiently solving a combined power and natural gas dispatch problem, while accounting for both linepack and bidirectional flow in pipelines. The performance of the proposed model was compared against three models: (i) a similar problem but with MILP approximations of the linepack, (ii) a model neglecting the linepack, and (iii) a benchmark model with an ideal electric storage. Our results showed that the proposed model can be solved faster than the MILP model, but is less accurate. As potential future works, it is of interest to improve the accuracy of the MISOCP model by tightening

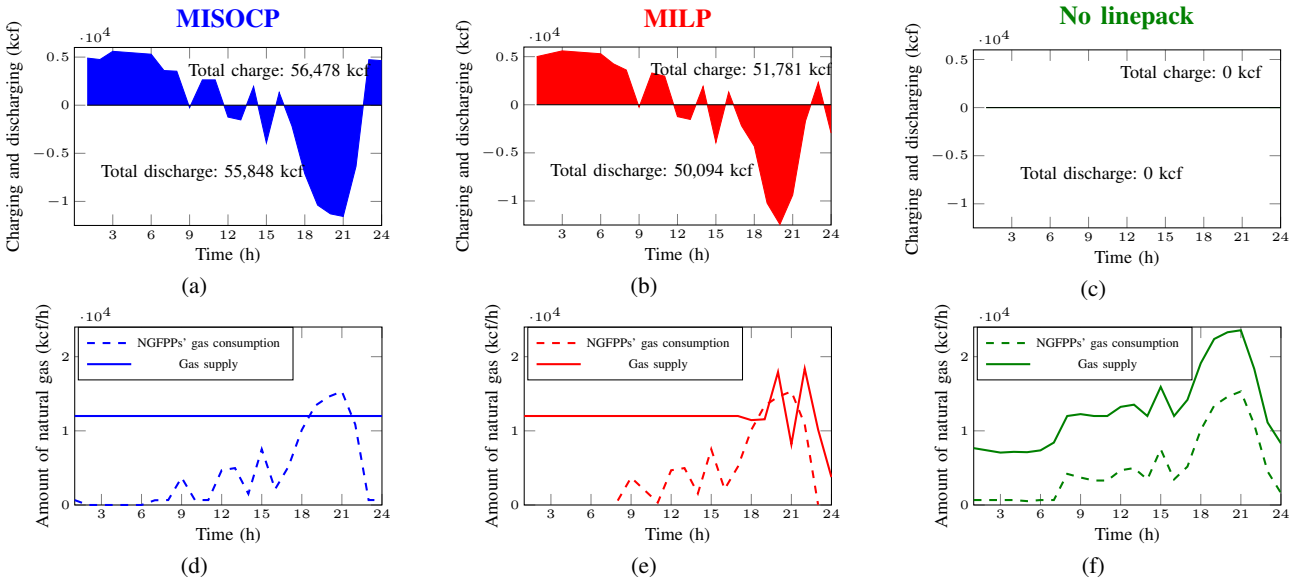

Fig. 5. Comparison of the results obtained from convexification approaches over 24 hours for 50% wind penetration. Plots (a) and (d) correspond to the MISOCP model, illustrating the hourly charging/discharging profile of linepack storage and the hourly profile of natural gas supply/consumption, respectively. The similar results for the MILP model are presented in plots (b) and (e), while they are depicted in plots (c) and (f) for a case ignoring linepack

McCormick relaxation [23], to investigate the possibility of adding sufficient conditions to tighten the SOC relaxation [18], and to explore alternatives for ex-post feasibility recovery [24].

Acknowledgment

This work was supported by the Danish Energy Technology Development and Demonstration Programme (EUDP) through the CORE project (12500/EUDP).

References

[1] J. Gil, A. Caballero, and A. J. Conejo, "Power cycling: CCGTs: The critical link between the electricity and natural gas markets," *IEEE Power and Energy Magazine*, vol. 12, no. 6, pp. 40–48, 2014.

[2] M. Gil, P. Dueñas, and J. Reneses, "Electricity and natural gas interdependency: Comparison of two methodologies for coupling large market models within the European regulatory framework," *IEEE Transactions on Power Systems*, vol. 31, no. 1, pp. 361–369, 2016.

[3] C. M. Correa-Posada and P. Sanchez-Martin, "Security-constrained optimal power and natural-gas flow," *IEEE Transactions on Power Systems*, vol. 29, no. 4, pp. 1780–1787, 2014.

[4] A. Antenucci and G. Sansavini, "Gas-constrained secure reserve allocation with large renewable penetration," *IEEE Transactions on Sustainable Energy*, vol. 9, no. 2, pp. 685–694, 2018.

[5] S. Clegg and P. Mancarella, "Integrated electrical and gas network flexibility assessment in low-carbon multi-energy systems," *IEEE Transactions on Sustainable Energy*, vol. 7, no. 2, pp. 718–731, 2016.

[6] C. Ordoudis, P. Pinson, and J. M. Morales, "An integrated market for electricity and natural gas systems with stochastic power producers," *European Journal of Operational Research*, vol. 272, no. 2, pp. 642–654, 2019.

[7] C. M. Correa-Posada and P. Sánchez-Martín, "Integrated power and natural gas model for energy adequacy in short-term operation," *IEEE Transactions on Power Systems*, vol. 30, no. 6, pp. 3347–3355, 2015.

[8] A. Zlotnik, L. Roald, S. Backhaus, M. Chertkov, and G. Andersson, "Coordinated scheduling for interdependent electric power and natural gas infrastructures," *IEEE Transactions on Power Systems*, vol. 32, no. 1, pp. 600–610, 2017.

[9] C. Ordoudis, S. Delikaraoglou, P. Pinson, and J. Kazempour, "Exploiting flexibility in coupled electricity and natural gas markets: A price-based approach," in *IEEE PowerTech*, Manchester, UK, 2017.

[10] R. D. Tabors, S. Englander, and R. Stoddard, "Who's on first? The coordination of gas and power scheduling," *The Electricity Journal*, vol. 25, no. 5, pp. 8–15, 2012.

[11] P. Pinson, L. Mitridati, C. Ordoudis, and J. Ostergaard, "Towards fully renewable energy systems: Experience and trends in denmark," *CSEE Journal of Power and Energy Systems*, vol. 3, no. 1, pp. 26–35, 2017.

[12] A. Zlotnik, A. Rudkevich, R. Carter, P. Ruiz, S. Backhaus, and J. Tafl, "Grid architecture at the gas–electric interface," *Los Alamos Natl. Lab., Santa Fe, NM, USA, Rep. LA-UR-17-23662*, 2017.

[13] L. Bai, F. Li, T. Jiang, and H. Jia, "Robust scheduling for wind integrated energy systems considering gas pipeline and power transmission N–1 contingencies," *IEEE Transactions on Power Systems*, vol. 32, no. 2, pp. 1582–1584, 2017.

[14] S. D. Manshadi and M. E. Khodayar, "Coordinated operation of electricity and natural gas systems: A convex relaxation approach," *IEEE Transactions on Smart Grid*, to be published, 2018.

[15] Y. He, M. Shahidehpour, Z. Li, C. Guo, and B. Zhu, "Robust constrained operation of integrated electricity-natural gas system considering distributed natural gas storage," *IEEE Transactions on Sustainable Energy*, vol. 9, pp. 1061–1071, 2018.

[16] C. Borraz-Sánchez, R. Bent, S. Backhaus, H. Hijazi, and P. V. Hentenryck, "Convex relaxations for gas expansion planning," *INFORMS Journal on Computing*, vol. 28, no. 4, pp. 645–656, 2016.

[17] C. B. Sanchez, R. Bent, S. Backhaus, S. Blumsack, H. Hijazi, and P. Van Hentenryck, "Convex optimization for joint expansion planning of natural gas and power systems," in *2016 49th Hawaii International Conference on System Sciences (HICSS)*. IEEE, 2016, pp. 2536–2545.

[18] M. K. Singh and V. Kekatos, "Natural gas flow equations: Uniqueness and an MI-SOCP solver," *arXiv preprint arXiv:1809.09025*, 2018.

[19] C. Shao, X. Wang, M. Shahidehpour, X. Wang, and B. Wang, "An MILP-based optimal power flow in multicarrier energy systems," *IEEE Transactions on Sustainable Energy*, vol. 8, no. 1, pp. 239–248, 2017.

[20] L. Mitridati and J. A. Taylor, "Power systems flexibility from district heating networks," in *2018 Power Systems Computation Conference (PSCC)*, Dublin, Ireland, 2018.

[21] G. P. McCormick, "Computability of global solutions to factorable nonconvex programs: Part I – Convex underestimating problems," *Mathematical Programming*, vol. 10, no. 1, pp. 147–175, 1976.

[22] A. Schwele, C. Ordoudis, J. Kazempour, and P. Pinson, "Electronic companion: Coordination of power and natural gas systems: Convexification approaches for linepack modeling," 2018. [Online]. Available: https://zenodo.org/badge/latestdoi/161356114

[23] M. Bynum, A. Castillo, J.-P. Watson, and C. D. Laird, "Tightening McCormick relaxations toward global solution of the ACOPF problem," *IEEE Transactions on Power Systems*, vol. 34, no. 1, pp. 814–817, 2019.

[24] L. Halilbašić, P. Pinson, and S. Chatzivasileiadis, "Convex relaxations and approximations of chance-constrained AC-OPF problems," *IEEE Transactions on Power Systems*, vol. 34, no. 2, pp. 1459–1470, 2019.

[Paper C] Affine Policies for Flexibility Provision by Natural Gas Networks to Power Systems

Authors:
Anubhav Ratha, Anna Schwele, Jalal Kazempour, Pierre Pinson, Shahab Shariat Torbaghan and Ana Virag

Published in:
Special issue of Electric Power Systems Research (EPSR) for Proceedings of Power Systems Computation Conference (PSCC) 2020

DOI:
10.1016/j.epsr.2020.106565

Affine Policies for Flexibility Provision by Natural Gas Networks to Power Systems

Anubhav Ratha*†, Anna Schwele*, Jalal Kazempour*, Pierre Pinson*, Shahab Shariat Torbaghan† and Ana Virag†
* Center for Electric Power and Energy, Technical University of Denmark, Kgs. Lyngby, Denmark
{arath, schwele, seykaz, ppin}@elektro.dtu.dk
† Flemish Institute of Technological Research (VITO), Boeretang 200, 2400 Mol, Belgium
{anubhav.ratha, shahab.shariattorbaghan, ana.virag}@vito.be

***Abstract*—Using flexibility from the coordination of power and natural gas systems helps with the integration of variable renewable energy in power systems. To include this flexibility into the operational decision-making problem, we propose a distributionally robust chance-constrained co-optimization of power and natural gas systems considering flexibility from short-term gas storage in pipelines, i.e., linepack. Recourse actions in both systems, based on linear decision rules, allow adjustments to the dispatch and operating set-points during real-time operation when the uncertainty in wind power production is revealed. We convexify the non-linear and non-convex power and gas flow equations using DC power flow approximation and second-order cone relaxation, respectively. Our coordination approach enables a study of the mitigation of short-term uncertainty propagated from the power system to the gas side. We analyze the results of the proposed approach on a case study and evaluate the solution quality via out-of-sample simulations performed *ex-ante*.**

***Index Terms*—Linear decision rules, Distributionally robust chance constraints, Linepack flexibility, Power and natural gas coordination, Second-order cone program.**

I. Introduction

Natural gas-fired power plants (NGFPPs) typically provide operational flexibility to power systems with a high share of intermittent renewable energy. Short-term gas storage in natural gas pipelines, known as linepack, provides an additional source of flexibility [1] at no extra investment cost. Efficient procurement of flexibility from the natural gas system during day-ahead scheduling of power systems requires consideration of the operational constraints of the natural gas system. Further, with the increasing share of intermittent renewable energy sources in the power system, the need for flexibility and thereby, the interdependence between power and natural gas systems is becoming stronger [2]. As a result, the coordination between power and natural gas systems during the day-ahead dispatch has been a topic of research interest in recent years. For example, various levels of coordination and information exchange between the systems are discussed in [3], [4], while [5], [6], [7], [8], [9] model full integration of the power with the natural gas system. The value of gas system related flexibility for the power system is quantified in [6] and [7] in a deterministic manner.

Increasing interactions between power and natural gas systems, however, result in the propagation of short-term uncertainty faced by power systems to the gas side. Prior works on the coordinated operation of power and natural gas systems have largely ignored this short-term uncertainty. This may result in additional recourse actions necessary during the real-time operation stage when the flexibility from the natural gas system is not correctly anticipated. Affine policies, built on the theory of linear decision rules, have been a preferred choice for day-ahead decision making, wherein nominal dispatch schedules along with the recourse actions for real-time operation are optimally decided [10]. In this paper, we introduce a unified framework to elicit flexibility based on affine policies from agents, e.g., power producers, natural gas suppliers as well as the network assets, i.e., linepack. Our affine policies are decided based on the features of uncertainty drawn from the historical measurements, with no distributional restriction imposed on the random variables.

Previous works discussing uncertainty-aware coordination between power and natural gas systems use stochastic programming approaches such as scenario-based [5], robust [8], and chance-constrained optimization [9]. Reference [5] proposes a two-stage stochastic program for the day-ahead and real-time operations of integrated power and natural gas system under uncertainty from renewable generation. In a similar direction, a robust dispatch framework is proposed in [8] which models uncertainty through intervals and extreme scenario approximation. Chance-constraints are introduced into the planning problem of the integrated power and natural gas system [9]. While scenario-based approaches [5] incur a high computational expense due to a large number of scenarios needed to characterize the uncertainty properly, robust approaches [8] often suffer from over-conservativeness of the solution due to the design objective to minimize worst-case cost. Distributionally robust chance-constrained formulation of the problem [11] allows for a tunable probabilistic violation of operational limits when facing extreme realizations of uncertainty which is characterized by an ambiguity set.

The work of A. Ratha was supported by a Ph.D. grant provided by the Flemish Institute for Technological Research (VITO) and scholarship from Technical University of Denmark (DTU). The work of A. Schwele and J. Kazempour was supported by the Danish EUD Programme through the Coordinated Operation of Integrated Energy Systems (CORE) project under the grant 64017-0005.

In this work, we adopt a distributionally robust chance-constrained optimization technique, considering its advantages over other stochastic programming approaches [11], to introduce a coordinated day-ahead dispatch of power and natural gas systems taking the flexibility provided by linepack into account. To the best of our knowledge, this is the first paper to bring linepack flexibility to the day-ahead dispatch problem, while modeling and mitigating the short-term uncertainty propagated from the power system to the natural gas system. Studying this uncertainty propagation opens new pathways for the endogenous valuation of the natural gas network as a provider of short-term flexibility to power systems. This could potentially result in the design of new market-based coordination mechanisms and market products enabling gas system agents and the network to play an active role in providing flexibility to the power system. From a methodological perspective, our main contribution is a tractable reformulation of distributionally robust chance constraints for the combined power and gas dispatch problem considering linepack.

The rest of this paper is organized as follows: Section II presents the distributionally robust chance-constrained power and natural gas dispatch problem. Section III discusses the solution methodology, which is then applied to a case study in Section IV. Finally, conclusions are drawn and the avenues for future work are discussed in Section V.

II. Problem Formulation

A. Preliminaries

In the following, we introduce the operation of a coupled power and natural gas system, wherein power generated from dispatchable power plants $i \in \mathcal{I}$ and wind farms $j \in \mathcal{J}$ is used to meet the inelastic electricity demand from a set of loads $d \in \mathcal{D}$. The dispatchable generators comprise of NGFPPs $i \in \mathcal{G}$ and non-NGFPPs $i \in \mathcal{C}$, such that $\mathcal{G} \cap \mathcal{C} = \emptyset$ and $\mathcal{G} \cup \mathcal{C} = \mathcal{I}$. On the gas side, natural gas suppliers $k \in \mathcal{K}$, together with available linepack in the gas network, are dispatched to meet the natural gas demand from inelastic gas loads and the fuel needed by NGFPPs. The non-linear and non-convex power and gas flow equations are convexified using DC power flow approximation and second-order cone relaxation, respectively. We assume that wind power is available at zero marginal cost of production. Power produced by wind farms during real-time operation is the sole uncertainty source considered.

B. Uncertainty Model

For wind farm j, the day-ahead point forecast for time period $t \in \mathcal{T}$ is given by $W^{\text{PF}}_{j,t}$. The forecast error observed in real-time is assumed to be a random variable $\delta_{j,t}$, such that the overall system uncertainty can be characterized by $\Omega = [\delta_{11}\ \delta_{21}\ \dots\ \delta_{|\mathcal{J}|t}\ \dots\ \delta_{|\mathcal{J}||\mathcal{T}|}]^\top \in \mathbb{R}^{|\mathcal{J}||\mathcal{T}|}$, where $\mathbb{R}$ is the set of real numbers and $|\cdot|$ is the cardinality operator over a set. We consider that Ω follows an unknown multivariate probability distribution $\mathbb{P} \in \Pi$, where Π is an ambiguity set defined as

$$\Pi = \{\mathbb{P} \in \Pi_0(\mathbb{R}^{|\mathcal{J}|}) : \mathbb{E}_{\mathbb{P}}[\Omega] = \boldsymbol{\mu}^{\Pi}, \mathbb{E}_{\mathbb{P}}[\Omega\Omega^\top] = \boldsymbol{\Sigma}^{\Pi}\}, \quad (1)$$

such that the family of distributions, $\Pi_0(\mathbb{R}^{|\mathcal{J}|})$ contains all probability distributions whose first and second-order moments are given by known parameters $\boldsymbol{\mu}^{\Pi} \in \mathbb{R}^{|\mathcal{J}||\mathcal{T}|}$ and $\boldsymbol{\Sigma}^{\Pi} \in \mathbb{R}^{|\mathcal{J}||\mathcal{T}|\times|\mathcal{J}||\mathcal{T}|}$, respectively. Further, $\mathbb{E}_{\mathbb{P}}[\cdot]$ denotes expectation with respect to the distribution $\mathbb{P}$ and $(\cdot)^\top$ is the transpose operator. Without any loss of generality, we assume that the mean $\boldsymbol{\mu}^{\Pi} = 0$ and that the covariance matrix $\boldsymbol{\Sigma}^{\Pi}$ can be empirically estimated from historical record of wind forecast errors. The structure of the positive semi-definite covariance matrix, $\boldsymbol{\Sigma}^{\Pi}$ is such that its diagonal blocks, comprised of sub-matrices, $\boldsymbol{\Sigma}^{\Pi}_t \in \mathbb{R}^{|\mathcal{J}|\times|\mathcal{J}|}, \forall t \in \mathcal{T}$, capture the spatial correlation among the wind forecast errors in period t, while the off-diagonal blocks contain information about spatio-temporal correlation of the uncertain parameters.

With this description of uncertain wind forecast errors, the net deviation from the point forecasts of all wind farms in the time period t is $\mathbf{e}^\top \Omega_t$ where $\mathbf{e} \in \mathbb{R}^{|\mathcal{J}|}$ is a vector of all ones. The temporally collapsed random vector is formed as: $\Omega_t = F_t \Omega$, where $F_t \in \mathbb{R}^{|\mathcal{J}|\times|\mathcal{J}||\mathcal{T}|}$ is a *selector matrix* formed by blocks of null matrices $\mathbf{0} \in \mathbb{R}^{|\mathcal{J}|\times|\mathcal{J}|}$ and a single block of identity matrix $\mathbf{1} \in \mathbb{R}^{|\mathcal{J}|\times|\mathcal{J}|}$, starting at column $(|\mathcal{J}|(t-1)+1),\ \forall t \in \mathcal{T}$. As a sign convention, $\mathbf{e}^\top \Omega_t > 0$ implies deficit of wind power available in the system during real-time operation stage as compared to the day-ahead forecast.

C. Uncertainty-Aware Power and Natural Gas Coordination

The proposed day-ahead coordinated electricity and natural gas model is a stochastic program, presented in (2) in the following. The objective function has a min-max structure such that the total *expected* system dispatch cost is minimized while the uncertain variable Ω draws from a probability distribution $\mathbb{P} \in \Pi$ that results in maximizing the expected cost of dispatch, i.e., the *worst-case* probability distribution.

$$\min_{\Theta_1}\ \max_{\mathbb{P}\in\Pi}\ \mathbb{E}_{\mathbb{P}}\left[\sum_{t\in\mathcal{T}}\Big(\sum_{i\in\mathcal{C}} C^{\text{E}}_i\ \tilde{p}_{i,t} + \sum_{k\in\mathcal{K}} C^{\text{G}}_k\ \tilde{g}_{k,t}\Big)\right] \quad (2a)$$

subject to

$$\mathbf{e}^\top\tilde{\mathbf{p}}_t + \mathbf{e}^\top(\mathbf{W}^{\text{PF}}_t - \Omega_t) = \mathbf{e}^\top\mathbf{D}^{\text{E}}_t,\ \forall t, \quad (2b)$$

$$\tilde{\mathbf{P}}^{\text{inj}}_t = \boldsymbol{\Psi}_{\text{I}}\tilde{\mathbf{p}}_t + \boldsymbol{\Psi}_{\text{J}}(\mathbf{W}^{\text{PF}}_t - \Omega_t) - \boldsymbol{\Psi}_{\text{D}}\mathbf{D}^{\text{E}}_t,\ \forall t, \quad (2c)$$

$$\min_{\mathbb{P}\in\Pi}\ \mathbb{P}[\{\boldsymbol{\Psi}\tilde{\mathbf{P}}^{\text{inj}}_t\}_{(n,r)} \geq -\{\overline{\mathbf{F}}\}_{(n,r)}] \geq (1-\epsilon_{nr}),\ \forall (n,r) \in \mathcal{L},\ \forall t, \quad (2d)$$

$$\min_{\mathbb{P}\in\Pi}\ \mathbb{P}[\{\boldsymbol{\Psi}\tilde{\mathbf{P}}^{\text{inj}}_t\}_{(n,r)} \leq \{\overline{\mathbf{F}}\}_{(n,r)}] \geq (1-\epsilon_{nr}),\ \forall (n,r) \in \mathcal{L},\ \forall t, \quad (2e)$$

$$\min_{\mathbb{P}\in\Pi}\ \mathbb{P}[\tilde{p}_{i,t} \geq \underline{P}_i] \geq (1-\epsilon_i),\ \forall i,\ \forall t, \quad (2f)$$

$$\min_{\mathbb{P}\in\Pi}\ \mathbb{P}[\tilde{p}_{i,t} \leq \overline{P}_i] \geq (1-\epsilon_i),\ \forall i,\ \forall t, \quad (2g)$$

$$\min_{\mathbb{P}\in\Pi}\ \mathbb{P}[\tilde{g}_{k,t} \geq \underline{G}_k] \geq (1-\epsilon_k),\ \forall k,\ \forall t, \quad (2h)$$

$$\min_{\mathbb{P}\in\Pi}\ \mathbb{P}[\tilde{g}_{k,t} \leq \overline{G}_k] \geq (1-\epsilon_k),\ \forall k,\ \forall t, \quad (2i)$$

$$\min_{\mathbb{P}\in\Pi}\ \mathbb{P}[\tilde{pr}_{m,t} \geq \underline{PR}_m] \geq (1-\epsilon_m),\ \forall m,\ \forall t, \quad (2j)$$

$$\min_{\mathbb{P}\in\Pi}\ \mathbb{P}[\tilde{pr}_{m,t} \leq \overline{PR}_m] \geq (1-\epsilon_m),\ \forall m,\ \forall t, \quad (2k)$$

$$\min_{\mathbb{P}\in\Pi} \mathbb{P}[\tilde{pr}_{u,t} \leq \Gamma_{m,u}\ \tilde{pr}_{m,t}] \geq (1-\epsilon_{mu}), \quad \forall (m,u) \in \mathcal{Z}_c,\ \forall t, \tag{2l}$$

$$\min_{\mathbb{P}\in\Pi} \mathbb{P}[\tilde{q}_{m,u,t} \geq 0] \geq (1-\epsilon_{mu}),\ \forall (m,u) \in \mathcal{Z},\ \forall t, \tag{2m}$$

$$\min_{\mathbb{P}\in\Pi} \mathbb{P}[\tilde{q}^{\text{in}}_{m,u,t} \geq 0] \geq (1-\epsilon_{mu}),\ \forall (m,u) \in \mathcal{Z},\ \forall t, \tag{2n}$$

$$\min_{\mathbb{P}\in\Pi} \mathbb{P}[\tilde{q}^{\text{out}}_{m,u,t} \geq 0] \geq (1-\epsilon_{mu}),\ \forall (m,u) \in \mathcal{Z},\ \forall t, \tag{2o}$$

$$\tilde{q}^2_{m,u,t} = K^2_{m,u}(\tilde{pr}^2_{m,t} - \tilde{pr}^2_{u,t}),\ \forall (m,u) \in \mathcal{Z},\ \forall t, \tag{2p}$$

$$\tilde{q}_{m,u,t} = \frac{\tilde{q}^{\text{in}}_{m,u,t} + \tilde{q}^{\text{out}}_{m,u,t}}{2},\ \forall (m,u) \in \mathcal{Z},\ \forall t, \tag{2q}$$

$$\tilde{h}_{m,u,t} = S_{m,u}\frac{\tilde{pr}_{m,t} + \tilde{pr}_{u,t}}{2},\ \forall (m,u) \in \mathcal{Z},\ \forall t, \tag{2r}$$

$$\tilde{h}_{m,u,t} = H^0_{m,u} + \tilde{q}^{\text{in}}_{m,u,t} - \tilde{q}^{\text{out}}_{m,u,t}, \forall (m,u) \in \mathcal{Z}, t = 1, \tag{2s}$$

$$\tilde{h}_{m,u,t} = \tilde{h}_{m,u,(t-1)} + \tilde{q}^{\text{in}}_{m,u,t} - \tilde{q}^{\text{out}}_{m,u,t}, \quad \forall (m,u) \in \mathcal{Z}, t > 1, \tag{2t}$$

$$\min_{\mathbb{P}\in\Pi} \mathbb{P}[\tilde{h}_{m,u,t} \geq H^0_{m,u}] \geq (1-\epsilon_{mu}), \quad \forall (m,u) \in \mathcal{Z}, t = |\mathcal{T}|, \tag{2u}$$

$$\sum_{k\in\mathcal{A}^{\text{K}}_m} \tilde{g}_{k,t} - \sum_{i\in\mathcal{A}^{\text{G}}_m} \phi_i\ \tilde{p}_{i,t} - \sum_{u:(m,u)\in\mathcal{Z}} (\tilde{q}^{\text{in}}_{m,u,t} - \tilde{q}^{\text{out}}_{u,m,t}) = D^{\text{G}}_{m,t},\ \forall m,\ \forall t, \tag{2v}$$

where the set of stochastic variables is Θ_1=$\{\tilde{p}_{i,t},\ \tilde{g}_{k,t},\ \tilde{pr}_{m,t},\ \tilde{q}_{m,u,t},\ \tilde{q}^{\text{in}}_{m,u,t},\ \tilde{q}^{\text{out}}_{m,u,t},\ \tilde{h}_{m,u,t}\}$. The terms in objective (2a) are the expected cost of power generation by non-NGFPPs and the cost of natural gas supply by gas suppliers derived from marginal production cost C^{E}_i and C^{G}_k, respectively.

The inequalities (2d)-(2o) and (2u) are modeled as distributionally robust chance constraints. This means that at the optimal solution to problem (2), the probability of meeting each individual constraint inside the square brackets $\mathbb{P}[\cdot]$ is modeled to have a confidence level of at least $(1-\epsilon_{(\cdot)})$, where each $\epsilon_{(\cdot)}$ lies within 0 and 1, i.e., $\epsilon_{(\cdot)} \in [0,1]$. Subscripts $(\cdot)$ take the appropriate indices from the set $\{i,\ (n,r),\ k,\ m,\ (m,u)\}$ depending on the individual constraint.

Constraints (2b)-(2g) pertain to the power system. These constraints include the power balance (2b), limits on the stochastic power flows in the transmission lines (2c)-(2e) and the upper ($\underline{P}_i$) and lower bounds ($\overline{P}_i$) on the stochastic power production of generators (2f) and (2g). Vectors $\tilde{\mathbf{p}}_t \in \mathbb{R}^{|\mathcal{I}|}$, $\mathbf{W}^{\text{PF}}_t \in \mathbb{R}^{|\mathcal{J}|}$ and $\mathbf{D}^{\text{E}}_t \in \mathbb{R}^{|\mathcal{D}|}$ represent the power produced by generators, wind forecasts for wind farms and electricity demand from loads in period t, while Ω_t is the random vector of forecast errors, as previously defined. Vector coefficients, $\mathbf{e}$ in (2b) are of appropriate dimensions such that the total supply and demand are balanced in each period t. The matrix $\mathbf{\Psi} \in \mathbb{R}^{|\mathcal{L}|\times|\mathcal{N}|}$ represents the Power Transfer Distribution Factor (PTDF) matrix, derived from the reactances of power transmission lines [12], which maps the injections $\tilde{\mathbf{P}}^{\text{inj}}_t \in \mathbb{R}^{|\mathcal{N}|}$ at the electricity nodes to the power flows in each of the power lines $(n,r) \in \mathcal{L}$ respecting capacity limits $\overline{\mathbf{F}}$ in the network. Similarly, matrices $\mathbf{\Psi}_{\text{I}} \in \mathbb{R}^{|\mathcal{N}|\times|\mathcal{I}|}$, $\mathbf{\Psi}_{\text{J}} \in \mathbb{R}^{|\mathcal{N}|\times|\mathcal{J}|}$, and $\mathbf{\Psi}_{\text{D}} \in \mathbb{R}^{|\mathcal{N}|\times|\mathcal{D}|}$ map generators, wind farms and loads to the electricity nodes, such that (2c) gives the nodal power injections for all electricity nodes in the system.

Natural gas system constraints are given in (2h)-(2u). While constraints (2h) and (2i) limit the stochastic gas supply $\tilde{g}_{k,t}$ by supplier k in time period t to $\underline{G}_k$ and $\overline{G}_k$, (2j) and (2k) limit the nodal gas pressure $\tilde{pr}_{m,t}$ at each gas node $m \in \mathcal{M}$ to be within the physical limits $\underline{PR}_m$ and $\overline{PR}_m$. For the natural gas pipelines with compressors, $\mathcal{Z}_c \subset \mathcal{Z}$, compression is modeled linearly in (2l), which relate the inlet and outlet pressures of two adjacent nodes through compression factor $\Gamma_{m,u}$. We consider that the direction of gas flow in each pipeline $(m,u) \in \mathcal{Z}$ is predetermined and (2m)-(2o) enforce this flow direction in real-time. As remarked in [1], this assumption is non-limiting for the high-pressure, gas transmission networks when considering day-ahead operational problems. On the contrary, it can be a limiting assumption while considering a network expansion planning problem or a gas distribution system wherein injections from distributed gas producers (e.g., biogas plants) cannot be neglected[1]. Equality constraints (2p), known as Weymouth equation, describe the flow $\tilde{q}_{m,u,t}$ (given by (2q) as the average of inflow, $\tilde{q}^{\text{in}}_{m,u,t}$ and outflow, $\tilde{q}^{\text{out}}_{m,u,t}$) along pipeline (m,u) as a quadratic non-convex function of the pressures $\tilde{pr}_{m,t}$ and $\tilde{pr}_{u,t}$ at the inlet (m) and outlet (u) nodes of the pipeline scaled by the pipeline resistance constant $K_{m,u}$. Constraints (2r) define the amount of linepack in the pipelines as the average of inlet and outlet pressures, scaled by the pipeline parameter $S_{m,u}$. Following the modeling approach in [7], (2s)-(2u) describe the evolution of the amount of linepack $\tilde{h}_{m,u,t}$ in a pipeline over time, with (2u) ensuring that the linepack is not depleted at the end of the simulation horizon beyond initial linepack amount $H^0_{m,u}$. Supply-demand balance of natural gas at each node is ensured in real-time by equality constraints (2v) which also couple the power and natural gas systems through the fuel consumed by the NGFPPs scaled by a fuel conversion factor ϕ_i. The sets $\mathcal{A}^{\text{K}}_m \subset \mathcal{K}$ and $\mathcal{A}^{\text{G}}_m \subset \mathcal{G}$ collect gas suppliers and NGFPPs that are located at node m, respectively, while $D^{\text{G}}_{m,t}$ is the nodal gas demand.

The requirement to solve the stochastic program (2) during the day-ahead stage renders the problem infinite dimensional, as the optimization variables are a function of uncertain parameters that are only revealed during real-time operation on the next day. To enable solvability of the problem, we adopt recourse actions based on linear decision rules [13] for the sources of flexibility in the coupled system, i.e., flexible power generation and natural gas supply and linepack. The assumption of affine response to uncertainty by flexible agents, although somewhat limiting in light of the non-linear dynamics of natural gas flow in the network, provides an intuitive understanding of the methodology behind uncertainty propagation from power system to natural gas system at a lower complexity of exposition. Generalized decision rules, for instance as discussed in [14], are left for future work.

[1]The assumptions on fixed gas flow directions may be violated in extreme uncertainty realizations.

D. Affine Policies

When solving the day-ahead dispatch problem, flexible and adjustable agents in the coupled system, i.e., power producers and gas suppliers, are assigned optimal affine policies in addition to the nominal schedule. These affine policies govern their response to the realizations of uncertainty in wind forecast errors during the real-time operation.

a) Power producers: The affine response from dispatchable power plants (NGFPPs and non-NGFPPs) is given by

$$\tilde{p}_{i,t} = p_{i,t} + (\mathbf{e}^\top \Omega_t)\alpha_{i,t},\ \forall i \in \mathcal{I},\ \forall t \tag{3}$$

where $\tilde{p}_{i,t}$ is the stochastic power production of unit i in real-time, $p_{i,t}$ is the nominal power production schedule if the uncertainty were absent (perfect forecasts) and $\alpha_{i,t} \in [-1, 1]$ denotes the *participation factor* of the unit towards mitigation of the deviation.

b) Gas suppliers: The stochastic natural gas supply by supplier k is given by

$$\tilde{g}_{k,t} = g_{k,t} + (\mathbf{e}^\top \Omega_t)\beta_{k,t},\ \forall k \in \mathcal{K},\ \forall t \tag{4}$$

where $g_{k,t}$ is the nominal gas supply and $\beta_{k,t}$ is the participation factor of the supplier towards uncertainty mitigation.

The response to uncertainty by flexible network asset, i.e., linepack, is not directly adjustable as it depends on the allocation of the above affine policies, subject to the topology of the gas network and the physical gas flow constraints.

E. Uncertainty Response by Power and Gas Networks

Here, we discuss how uncertainty affects the flows in the power and gas networks. We consider the case of imperfect forecasts, i.e., $\mathbf{e}^\top \Omega_t \neq 0$.

During the real-time operation, power flows in the transmission lines, modeled by (2c)-(2e) change depending on the realized uncertainty Ω_t, the affine responses of power producers $\alpha_{i,t}$, and the spatial configuration of wind farms and power producers. Moreover, given the response from dispatchable power plants $\alpha_{i,t}$, the power balance constraint (2b) holds true for any realization of uncertainty Ω_t iff

$$\mathbf{e}^\top \mathbf{p}_t + \mathbf{e}^\top \mathbf{W}_t^{\text{PF}} = \mathbf{e}^\top \mathbf{D}_t^{\text{E}},\ \forall t, \tag{5a}$$

$$\mathbf{e}^\top \boldsymbol{\alpha}_t = 1,\ \forall t. \tag{5b}$$

Constraints (5) are derived from (2b) by separating the nominal and uncertainty-dependent terms.

On the gas side, the uncertainty in gas flows, in response to changes in gas supply $\beta_{k,t}$ and in fuel demand from NGFPPs $\phi_i \alpha_{i,t},\ \forall i \in \mathcal{G}$, is mitigated by the flexibility provided by linepack. It is vital to note that the real-time natural gas flows and nodal pressures are functions of $\beta_{k,t}$ and $\alpha_{i,t},\ \forall i \in \mathcal{G}$. However, the analytical derivation of this relationship is not straightforward, given the non-linear gas flow dynamics and the inter-temporal linkages associated with the linepack model. As a simplification, we model the flow and pressure changes as affine functions of uncertainty[2]. We model the real-time natural gas flows in the pipelines as

$$\tilde{q}_{m,u,t} = q_{m,u,t} + (\mathbf{e}^\top \Omega_t)\gamma_{m,u,t},\ \forall (m,u) \in \mathcal{Z},\ \forall t, \tag{6a}$$

$$\tilde{q}^{\text{in}}_{m,u,t} = q^{\text{in}}_{m,u,t} + (\mathbf{e}^\top \Omega_t)\gamma^{\text{in}}_{m,u,t},\ \forall (m,u) \in \mathcal{Z},\ \forall t, \tag{6b}$$

$$\tilde{q}^{\text{out}}_{m,u,t} = q^{\text{out}}_{m,u,t} + (\mathbf{e}^\top \Omega_t)\gamma^{\text{out}}_{m,u,t},\ \forall (m,u) \in \mathcal{Z},\ \forall t, \tag{6c}$$

where $q_{m,u,t},\ q^{\text{in}}_{m,u,t},\ q^{\text{out}}_{m,u,t}$ denote the average flow rate, inflow and outflow rate of natural gas in the pipeline connecting nodes m and u, in absence of forecast errors and the variables $\gamma_{m,u,t},\ \gamma^{\text{in}}_{m,u,t},\ \gamma^{\text{out}}_{m,u,t}$ represent the auxiliary variables which model changes in these flow rates during real-time.

Consequently, the nodal balance constraint for natural gas (2v) holds true for any realization of uncertainty Ω_t iff

$$\sum_{k \in \mathcal{A}^{\text{K}}_m} g_{k,t} - \sum_{i \in \mathcal{A}^{\text{G}}_m} \phi_i\ p_{i,t} - \sum_{u:(m,u)\in\mathcal{Z}} (q^{\text{in}}_{m,u,t} - q^{\text{out}}_{u,m,t}) = D^{\text{G}}_{m,t},\ \forall m,\ \forall t, \tag{7a}$$

$$\sum_{k \in \mathcal{A}^{\text{K}}_m} \beta_{k,t} - \sum_{i \in \mathcal{A}^{\text{G}}_m} \phi_i \alpha_{i,t} - \sum_{u:(m,u)\in\mathcal{Z}} (\gamma^{\text{in}}_{m,u,t} - \gamma^{\text{out}}_{u,m,t}) = 0\ \forall m,\ \forall t. \tag{7b}$$

Constraints (7) are derived by separating the nominal and uncertainty-dependent terms in (2v). Following a similar approach, (2q), $\forall (m,u) \in \mathcal{Z},\ \forall t$, decomposes into

$$q_{m,u,t} = \frac{q^{\text{in}}_{m,u,t} + q^{\text{out}}_{m,u,t}}{2};\ \gamma_{m,u,t} = \frac{\gamma^{\text{in}}_{m,u,t} + \gamma^{\text{out}}_{m,u,t}}{2}. \tag{8}$$

We model real-time pressures at gas nodes as

$$\tilde{pr}_{m,t} = pr_{m,t} + (\mathbf{e}^\top \Omega_t)\rho_{m,t},\ \forall m,\ \forall t, \tag{9}$$

where $pr_{m,t}$ and $\rho_{m,t}$ denote the nominal pressure and the auxiliary variable that models the change in pressure at node m in real-time, respectively. This allows us to expand the Weymouth equation in (2p) as, $\forall (m,u) \in \mathcal{Z},\ \forall t$,

$$\begin{aligned}(q^2_{m,u,t} + (\mathbf{e}^\top \boldsymbol{\Omega}_t)^2 \gamma^2_{m,u,t} + 2(\mathbf{e}^\top \boldsymbol{\Omega}_t)\gamma_{m,u,t} q_{m,u,t}) = \\ K^2_{m,u}(pr^2_{m,t} - pr^2_{u,t}) + (\mathbf{e}^\top \boldsymbol{\Omega}_t)^2 K^2_{m,u}(\rho^2_{m,t} - \rho^2_{u,t}) \\ + 2(\mathbf{e}^\top \boldsymbol{\Omega}_t) K^2_{m,u}(\rho_{m,t} pr_{m,t} - \rho_{u,t} pr_{u,t}).\end{aligned} \tag{10}$$

Separating terms that are independent of, quadratically- and linearly-dependent on uncertainty in (10), it can be replaced by the equalities (11) that must hold true for any realization of the uncertainty[3]. For pipelines $\forall (m,u) \in \mathcal{Z},\ \forall t$,

$$q^2_{m,u,t} = K^2_{m,u}(pr^2_{m,t} - pr^2_{u,t}), \tag{11a}$$

$$\gamma^2_{m,u,t} = K^2_{m,u}(\rho^2_{m,t} - \rho^2_{u,t}), \tag{11b}$$

$$\gamma_{m,u,t} q_{m,u,t} = K^2_{m,u}(\rho_{m,t} pr_{m,t} - \rho_{u,t} pr_{u,t}). \tag{11c}$$

[2]In future works, the simplified approach adopted in this paper must be enhanced by considering the true, non-linear analytical relationship of changes in real-time flows and nodal pressures to the affine policies.

[3]Modeling of uncertainty propagation to physical variables such as $\tilde{q}_{m,u,t}$ and $\tilde{pr}_{m,t}$ by estimating sensitivities using Taylor series expansion around the forecast has recently been applied to AC optimal power flow (see, e.g., [15]). Since we solve the dispatch problem in day-ahead, wherein uncertainty around the forecast point is non-negligible, we cannot justify such a sensitivity-based approach.

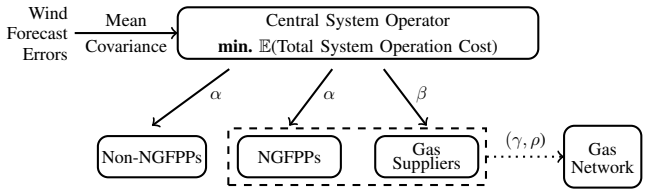

Fig. 1. Coordinated power and natural gas day-ahead dispatch

In addition to the Weymouth equations, the auxiliary variables for flow changes ($\gamma_{m,u,t},\ \gamma^{\text{in}}_{m,u,t},\ \gamma^{\text{out}}_{m,u,t}$) and pressure changes ($\rho_{m,t}$) are coupled by the equality constraints (2r)-(2t) that govern the amount of linepack and evolution of linepack in the pipelines. On separating nominal and uncertainty-dependent terms, these constraints should hold true for any realization of Ω_t iff the equalities (12) hold. For pipelines $\forall(m,u) \in \mathcal{Z}$,

$$h_{m,u,t} = H^0_{m,u} + q^{\text{in}}_{m,u,t} - q^{\text{out}}_{m,u,t},\ \ t = 1, \tag{12a}$$

$$h_{m,u,t} = h_{m,u,(t-1)} + (q^{\text{in}}_{m,u,t} - q^{\text{out}}_{m,u,t}),\ \ t > 1, \tag{12b}$$

$$\frac{S_{m,u}}{2}(\rho_{m,t} + \rho_{u,t} - \rho_{m,(t-1)} - \rho_{u,(t-1)}) = (\gamma^{\text{in}}_{m,u,t} - \gamma^{\text{out}}_{m,u,t}),\ \ t > 1, \tag{12c}$$

where $h_{m,u,t}$ is the nominal linepack in the pipeline in case perfect forecasts of wind power production were to be realized. It is worth noting that, considering the initial linepack amount $H^0_{m,u}$ is uncertainty-independent, constraint (2s) decomposes solely as (12a). Whereas the linepack amount in hours $t > 1$, given by (2t), decomposes as nominal (12b) and uncertainty-dependent (12c) equalities, which govern the change in nominal linepack amount and the response to uncertainty during real-time operation, respectively.

F. Power and Natural Gas Coordination with Affine Policies

In the following we present a finite-dimensional solvable approximation of the stochastic program (2), under the strategy of affine response to uncertainty. As shown in Fig. 1, this day-ahead problem is solved by a central system operator.

$$\min_{\Theta_2} \sum_{t\in\mathcal{T}} \Big(\sum_{i\in\mathcal{C}} C^{\text{E}}_i\ p_{i,t} + \sum_{k\in\mathcal{K}} C^{\text{G}}_k\ g_{k,t} \Big) \tag{13a}$$

subject to

$$\min_{\mathbb{P}\in\Pi} \mathbb{P}[p_{i,t} + (\mathbf{e}^\top\Omega_t)\alpha_{i,t} \geq \underline{P}_i] \geq (1-\epsilon_i),\ \ \forall i,\ \forall t, \tag{13b}$$

$$\min_{\mathbb{P}\in\Pi} \mathbb{P}[p_{i,t} + (\mathbf{e}^\top\Omega_t)\alpha_{i,t} \leq \overline{P}_i] \geq (1-\epsilon_i),\ \ \forall i,\ \forall t, \tag{13c}$$

$$\min_{\mathbb{P}\in\Pi} \mathbb{P}[g_{k,t} + (\mathbf{e}^\top\Omega_t)\beta_{k,t} \geq \underline{G}_k] \geq (1-\epsilon_k),\ \ \forall k,\ \forall t, \tag{13d}$$

$$\min_{\mathbb{P}\in\Pi} \mathbb{P}[g_{k,t} + (\mathbf{e}^\top\Omega_t)\beta_{k,t} \leq \overline{G}_k] \geq (1-\epsilon_k),\ \ \forall k,\ \forall t, \tag{13e}$$

$$\min_{\mathbb{P}\in\Pi} \mathbb{P}[pr_{m,t} + (\mathbf{e}^\top\Omega_t)\rho_{m,t} \geq \underline{PR}_m] \geq (1-\epsilon_m), \forall m, \forall t, \tag{13f}$$

$$\min_{\mathbb{P}\in\Pi} \mathbb{P}[pr_{m,t} + (\mathbf{e}^\top\Omega_t)\rho_{m,t} \leq \overline{PR}_m] \geq (1-\epsilon_m),\ \ \forall m,\ \forall t, \tag{13g}$$

$$\min_{\mathbb{P}\in\Pi} \mathbb{P}[(pr_{u,t} - \Gamma_{m,u}\ pr_{m,t}) + (\mathbf{e}^\top\Omega_t)(\rho_{u,t} - \Gamma_{m,u}\ \rho_{m,t}) \leq 0] \geq (1-\epsilon_{mu}),\ \ \forall(m,u) \in \mathcal{Z}_c,\ \forall t, \tag{13h, 13i}$$

$$\min_{\mathbb{P}\in\Pi} \mathbb{P}[q_{m,u,t} + (\mathbf{e}^\top\Omega_t)\gamma_{m,u,t} \geq 0] \geq (1-\epsilon_{mu}),\ \ \forall(m,u) \in \mathcal{Z},\ \forall t, \tag{13j}$$

$$\min_{\mathbb{P}\in\Pi} \mathbb{P}[q^{\text{in}}_{m,u,t} + (\mathbf{e}^\top\Omega_t)\gamma^{\text{in}}_{m,u,t} \geq 0] \geq (1-\epsilon_{mu}),\ \ \forall(m,u) \in \mathcal{Z},\ \forall t, \tag{13k}$$

$$\min_{\mathbb{P}\in\Pi} \mathbb{P}[q^{\text{out}}_{m,u,t} + (\mathbf{e}^\top\Omega_t)\gamma^{\text{out}}_{m,u,t} \geq 0] \geq (1-\epsilon_{mu}),\ \ \forall(m,u) \in \mathcal{Z},\ \forall t, \tag{13l}$$

$$\min_{\mathbb{P}\in\Pi} \mathbb{P}[h_{m,u,t} + S_{m,u}(\mathbf{e}^\top\Omega_t)\frac{\rho_{m,t} + \rho_{u,t}}{2} \geq H^0_{m,u}] \geq (1-\epsilon_{mu}),\ \ \forall(m,u) \in \mathcal{Z},\ t = |\mathcal{T}|, \tag{13m}$$

$$\text{(2c) - (2e), (5), (7), (8), (11), (12),} \tag{13n}$$

where the optimization variables are $\Theta_2 = \{\ p_{i,t},\ \alpha_{i,t},\ g_{k,t},\ \beta_{k,t},\ pr_{m,t},\ \rho_{m,t},\ q_{m,u,t},\ \gamma_{m,u,t},\ q^{\text{in}}_{m,u,t},\ \gamma^{\text{in}}_{m,u,t},\ q^{\text{out}}_{m,u,t},\ \gamma^{\text{out}}_{m,u,t},\ h_{m,u,t}\}$. The expectation term in objective (2a) reduces to (13a) on account of the zero-mean assumption of Ω_t. As discussed in [16] for programs with a similar structure, the stochastic program (13) is computationally intractable due to the probabilistic distributionally robust chance constraints. To achieve tractability, a convex second-order cone (SOC) approximation of the non-convex individual distributionally robust chance constraints is adopted. Furthermore, the non-convex quadratic equality constraints (11) representing the Weymouth equation for the uncertainty-aware gas flows require convexification. The approach towards solving (13) along with its final tractable form is discussed in the next section.

III. Solution Approach

A. SOC Reformulation of Probabilistic Constraints

For distributionally robust individual chance constraints under the assumption of known first and second-order moments of the underlying probability distribution, [17, Theorem 2.2] provides a SOC approximation based on a variant of Chebyshev's Inequality. While interested readers are directed to [17] for a proof, convex reformulation of constraint (13c) is presented below as an illustration.

With $\mathbf{\Sigma}^{\Pi}_t \in \mathbb{R}^{|\mathcal{J}|\times|\mathcal{J}|}$ as the t-th diagonal sub-matrix of the covariance matrix $\mathbf{\Sigma}^{\Pi}$ in time period t and $\mathbf{e} \in \mathbb{R}^{|\mathcal{J}|}$ denoting a vector of all ones, the probabilistic chance constraints (13c) can be approximated by the following SOC constraints:

$$\sqrt{\frac{1-\epsilon_i}{\epsilon_i}}\Big\|\alpha_{i,t}\mathbf{e}^\top(\mathbf{\Sigma}^{\Pi}_t)^{1/2}\Big\|_2 \leq -p_{i,t} + \overline{P}_i,\ \ \forall i,\ \forall t. \tag{14}$$

Similar reformulation is performed for the other distributionally robust chance constraints in (13). References [18] and [19] remark that such conic reformulation based on Chebyshev's Inequality results in over-conservative solutions as $\epsilon_i \to 0$ while approaching infeasibility for $\epsilon_i \approx 0$. Exact reformulation of such chance constraints improving on this issue has been recently proposed in [18]. However, since the focus of this work is on uncertainty-aware coordination between electricity and natural gas systems, our formulation is limited to the conic approximation. We ensure that large enough risk measures $\epsilon_{(\cdot)}$ are considered in the case study (Section IV) such that infeasibility is avoided.

TABLE I
VARIABLE BOUNDS FOR MCCORMICK RELAXATION.

Variable	Lower bound	Upper bound
$pr_{m,t}$	$\underline{PR}_m$	$\overline{PR}_m$
$\rho_{m,t}$	$-(\overline{PR}_m - \underline{PR}_m)/\widehat{W}$	$(\overline{PR}_m - \underline{PR}_m)/\widehat{W}$
$q_{m,u,t}$	0	$\overline{Q}$
$\gamma_{m,u,t}$	$-\overline{Q}/\widehat{W}$	$\overline{Q}/\widehat{W}$

B. Convex Relaxation of Weymouth Equation

The non-convex quadratic equality constraints in (11a) can be equivalently written as

$$q^2_{m,u,t} \leq K^2_{m,u}(pr^2_{m,t} - pr^2_{u,t}),\ \forall(m,u) \in \mathcal{Z},\ \forall t, \quad (15a)$$
$$q^2_{m,u,t} \geq K^2_{m,u}(pr^2_{m,t} - pr^2_{u,t}),\ \forall(m,u) \in \mathcal{Z},\ \forall t. \quad (15b)$$

To relax (11a), we adopt the convex SOC constraints (15a) and drop the non-convex constraints (15b)[4]. The tightness of this relaxation is analyzed in [20] and will be further examined in Section IV. Note that (11b) can be convexified in the same manner. However, this convexification strategy cannot be applied to (11c). We adopt McCormick relaxation [21], defining rectangular envelopes around the bi-linear terms in (11c) based on the known and estimated bounds on variables. We first define auxiliary variables $\nu_{m,t}$ for gas nodes $m \in \mathcal{M}$ and $\lambda_{m,u,t}$ for the pipelines $(m,u) \in \mathcal{Z},\ \forall t$ and then replace (11c) by the following set of constraints:

$$\lambda_{m,u,t} - K^2_{m,u}\nu_{m,t} + K^2_{m,u}\nu_{u,t} = 0,\ \forall(m,u) \in \mathcal{Z},\ \forall t, \quad (16a)$$
$$\lambda_{m,u,t} = q_{m,u,t}\gamma_{m,u,t}, \forall(m,u) \in \mathcal{Z}, \forall t, \quad (16b)$$
$$\nu_{m,t} = pr_{m,t}\rho_{m,t},\ \forall m,\ \forall t, \quad (16c)$$
$$\nu_{u,t} = pr_{u,t}\rho_{u,t},\ \forall u : (m,u) \in \mathcal{Z},\ \forall t. \quad (16d)$$

To illustrate the McCormick relaxation, the inequalities that replace the non-convex constraints (16c) are

$$\forall m,t \begin{cases} \rho^L_{m,t}pr_{m,t} + pr^L_{m,t}\rho_{m,t} \leq \nu_{m,t} + pr^L_{m,t}\rho^L_{m,t} \\ \rho^U_{m,t}pr_{m,t} + pr^U_{m,t}\rho_{m,t} \leq \nu_{m,t} + pr^U_{m,t}\rho^U_{m,t} \\ \rho^L_{m,t}pr_{m,t} + pr^U_{m,t}\rho_{m,t} \geq \nu_{m,t} + pr^U_{m,t}\rho^L_{m,t} \\ \rho^U_{m,t}pr_{m,t} + pr^L_{m,t}\rho_{m,t} \geq \nu_{m,t} + pr^L_{m,t}\rho^U_{m,t}, \end{cases} \quad (17)$$

where superscripts L and U indicate lower and upper bounds of the variables, respectively. Constraints (16b) and (16d) are treated similarly. The variable bounds used to construct the McCormick envelopes are listed in Table I. Parameter $\widehat{W}$ is the total installed wind capacity in the system and parameter $\overline{Q}$ denotes the upper bound on gas flow in the pipelines, which we obtain by solving a deterministic version of problem (2) with $\mathbf{e}^\top\Omega_t = 0$. The bounds for network response variables, $\gamma_{m,u,t}$ and $\rho_{m,u,t}$ are trivially deduced from equations (6a) and (9), respectively.

Following the convex approximation of probabilistic constraints and relaxation of Weymouth equations, the tractable form of the distributionally robust chance-constrained day-ahead coordinated power and natural gas dispatch is presented in Appendix A. Problem (20) is a convex second-order cone program (SOCP) and is solvable using off-the-shelf convex optimization solvers.

[4]Linear approximations of the dropped non-convex constraints, as proposed by [1] in a deterministic setting, may also be included to the problem.

IV. CASE STUDY

A. Input Data

A coupled power and natural gas system consisting of a 12-node gas network connected to the IEEE 24-bus reliability test system [5] is used to evaluate our proposed coordinated dispatch. The installed wind capacity reaches one-thirds of the peak demand in the simulation horizon of 24 hours. Data for the parameters of the power and natural gas networks and for the operational characteristics of all assets in the system are provided in online appendix [22]. A dataset of 1,000 zero-mean wind forecast error scenarios based on actual measurements recorded in Western Denmark [23] is used to empirically estimate the covariance matrix $\mathbf{\Sigma}^{\Pi}$. The parameters $\epsilon_{(\cdot)}$ for all distributionally robust chance constraints in (20) are set to identical values.

The problem is implemented in Julia v1.1.1 modeled with JuMP v0.2 and solved to optimality by Mosek v9.0 with an average CPU time of 1.67 seconds on a personal computer with 8GB memory running on Intel Core i5 clocked at 2.3 GHz. The optimal solution provides nominal dispatch schedule as well as affine policies that quantify the response to uncertain wind realizations during real-time.

B. Optimal Affine Policies

In Fig. 2, we show the optimal allocations from the distributionally robust chance-constrained day-ahead coordinated power and natural gas model (20) for violation probabilities $\epsilon_{(\cdot)}$ set to 0.05. Fig. 2(a) shows the nominal dispatch of NGFPPs and non-NGFPPS to meet the forecasted net electricity demand, i.e., load minus wind production forecast, while Fig. 2(b) shows their affine responses to uncertainty. Similarly, Figs. 2(c)-(d) present the nominal schedule and the response policies for the three gas suppliers. We highlight our main observations in the following.

First, when power producers and gas suppliers are either dispatched not at all or at full capacity, they are not eligible to adjust their output to mitigate uncertainty. Thus, the response policies for these units are zero. As a result, expensive generators, which are not dispatched in hours with low net demand, are assigned zero α_i in these hours. Similarly, the most expensive gas supplier ($k3$) is not expected to respond to uncertainty in hours 1-13, while not dispatched. On the other hand, the least expensive gas supplier ($k1$) cannot provide a response to uncertainty in hours 1-10, because her nominal dispatch is already at maximum capacity.

Second, NGFPPs are the main providers of flexibility in response to wind uncertainty during hours 8-24, see Fig. 2(b). Although the volatility of gas demand from NGFPPs can be mitigated by linepack, gas suppliers are also required to respond to uncertainty, especially in hours 14-24, see Fig. 2(d).

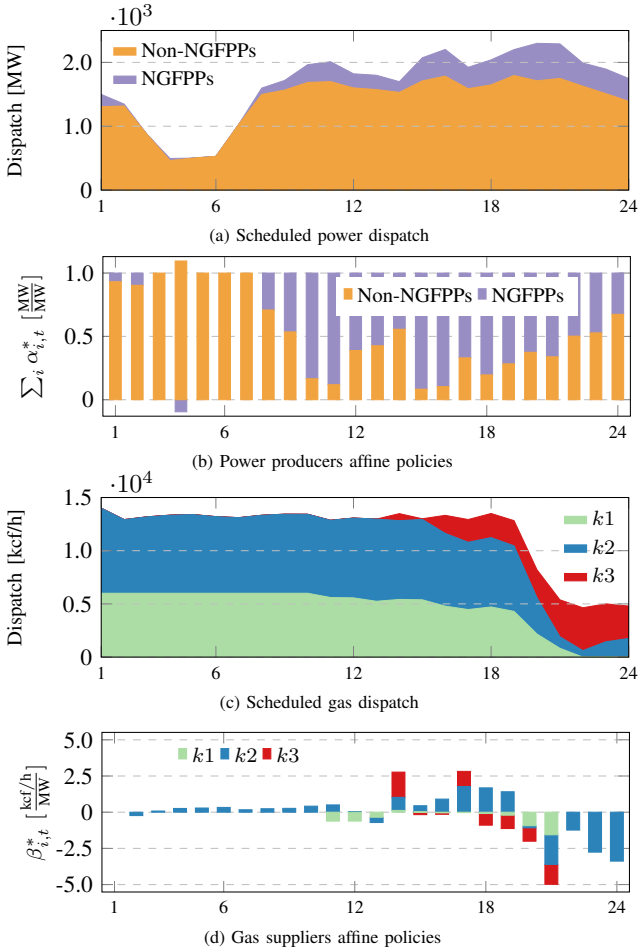

Fig. 2. Optimal dispatch and affine policies for $\epsilon_{(\cdot)} = 0.05$ for the simulation horizon of 24 hours.

Not only the availability and cost structure of power and gas supply, but also network effects impact the optimal response. The spatial correlations of uncertain wind forecasts and location of flexibility providers in both power and gas networks affect the response policies. An example of network effects is the allocation of affine policies in hour 4 in Fig. 2(b). Here, flexibility is provided not only with respect to cost efficiency, but also considering locational benefits and preferable energy flow effects.

C. Choice of Violation Probabilities $\epsilon_{(\cdot)}$

To evaluate the quality of the solution obtained and to make an informed choice for $\epsilon_{(\cdot)}$, we perform *ex-ante* simulations using a test dataset of wind realization scenarios, distinct from those used to estimate the covariance matrix. With fixed day-ahead decisions, i.e., nominal production schedules and affine policies, we compute the violation probability of the distributionally robust chance constraints (13b)-(13m) and (2d)-(2e) for a choice of $\epsilon_{(\cdot)}$ as

$$\eta_\epsilon = \frac{1}{N_s} \sum_{s=1}^{N_s} \mathbb{I}_s. \tag{18}$$

The indicator function $\mathbb{I}_s$ takes a value 1 if at least one of these

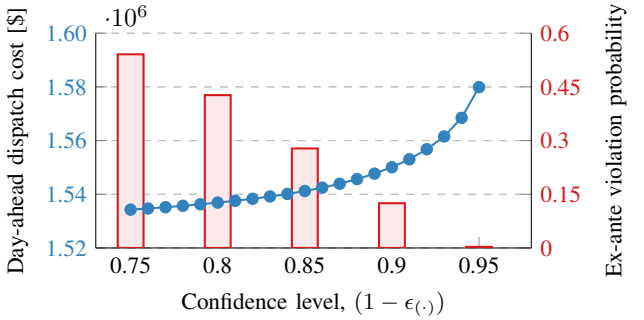

Fig. 3. Day-ahead dispatch cost (left y-axis) with values of $\epsilon_{(\cdot)}$ chosen for the distributionally robust chance constraints is shown by line with markers ●. The ex-ante violation probability (right y-axis) of these constraints, evaluated for 1,000 test samples, is shown in bars.

constraints is violated for the wind realization that corresponds to scenario s. Referring to the left-hand y-axis, the lineplot in Fig. 3 shows the expected cost of day-ahead dispatch at various values of confidence levels $(1 - \epsilon_{(\cdot)})$ imposed on the probabilistic constraints. With a higher confidence of meeting the constraints, the expected cost of day-ahead dispatch increases. The bars, which refer to the right-hand y-axis, show the ex-ante violation probability computed at selected confidence level values. For $\epsilon_{(\cdot)} = 0.05$, an ex-ante violation probability of 0.003 is expected at a day-ahead expected dispatch cost of $1,580,000.

D. Ex-Ante Violation Probabilities

Next, we analyse the violation probabilities (18) for each of the following chance-constraints: I. generator bounds (13b) and (13c), II. line flow limits (2d) and (2e), III. non-depletion of linepack in pipelines requirement (13m), IV. natural gas flow direction constraints (13j)-(13l), V. nodal gas pressure bounds (13f) and (13g), and VI. gas supplier bounds (13d) and (13e). Fig. 4 shows the probability of violation of these individual constraints for different choices of $\epsilon_{(\cdot)}$.

Power generation limits (13b) and (13c) are most susceptible to violation at all values of $\epsilon_{(\cdot)}$. Power transmission lines are not prone to reaching their operational limits. We do not observe any violation probability of power flow limits until decreasing the confidence level to 0.75. On the gas side, the constraints of gas flow directions (13j)-(13l) are susceptible to violations, causing the dependent nodal pressure limits (13f) and (13g) to be violated as well. On the one hand, this can be explained by the relaxation gap for the gas flow equations, which is discussed in detail in the following. On the other hand, this motivates future work to consider bi-directional gas flows, specially in the context of flexibility provision by linepack, albeit at the cost of losing convexity due to introduction of integer variables. The non-depletion of linepack constraints are, however, satisfied even at $\epsilon_{(\cdot)} = 0.25$. This indicates that there is enough short-term gas storage available in the gas pipelines such that they are not depleted at the end of the day while providing flexibility to the power system. Notably, these outcomes and resulting inferences are system-specific.

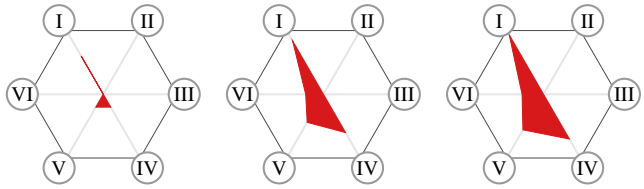

(a) $\epsilon_{(\cdot)} = 0.05$ (b) $\epsilon_{(\cdot)} = 0.10$ (c) $\epsilon_{(\cdot)} = 0.15$

Fig. 4. Ex-ante violation probabilities by constraint type. Corners of the hexagons represent a violation probability of 0.005, 0.15 and 0.3 for (a), (b) and (c), respectively.

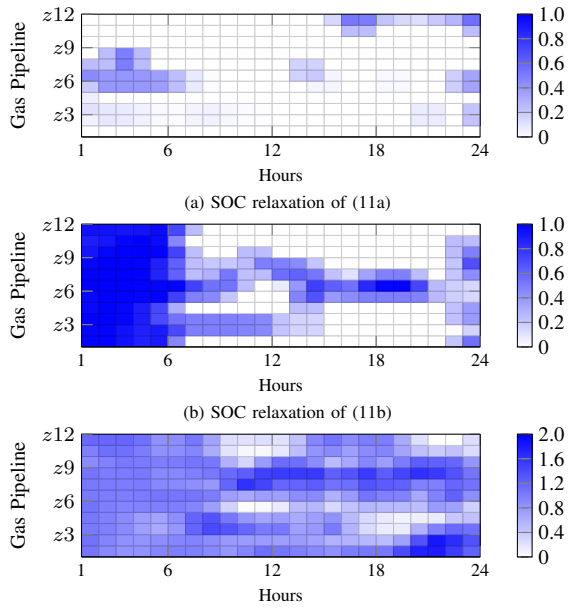

(a) SOC relaxation of (11a)

(b) SOC relaxation of (11b)

(c) McCormick Relaxation of (11c)

Fig. 5. Normalized relaxation gap for the convex relaxations adopted for Weymouth equation in (11) for $\epsilon_{(\cdot)} = 0.05$.

E. Tightness of Convex Relaxations

We examine the tightness of the relaxation for the non-convex Weymouth equation (11) by comparing the left-hand and right-hand sides of each of these equality constraints. We define the normalized root mean square relaxation gap Ξ for the original equality constraint $X_{m,u,t} = Y_{m,u,t}, \forall (m,u) \in \mathcal{Z},\ \forall t$ relaxed to $X_{m,u,t} \leq Y_{m,u,t}, \forall (m,u) \in \mathcal{Z},\ \forall t$ as

$$\Xi = \left[\frac{1}{|\mathcal{Z}||\mathcal{T}|} \sum_{t \in \mathcal{T}} \sum_{z \in \mathcal{Z}} \left(\frac{Y^*_{m,u,t} - X^*_{m,u,t}}{Y^*_{m,u,t}} \right)^2 \right]^{\frac{1}{2}}, \qquad (19)$$

where superscript $*$ indicates values obtained at optimality. For $\epsilon_{(\cdot)} = 0.05$, we observe a Ξ-value of 0.78, 1.67 and 2.87 for (11a), (11b) and (11c), respectively.

Fig. 5 presents heatmaps of the normalized root mean square relaxation gap Ξ for each gas pipeline in each hour of the simulation horizon for $\epsilon_{(\cdot)} = 0.05$. The occurrence of relaxation gap is lower for constraint (11a) than for (11b). While the relaxation of constraint (11a) seems to be sufficiently tight in Fig. 5(a), the relaxation of (11b) is not always exact, see Fig. 5(b). The relaxation gap is particularly extant in hours 1-6. The structure of the gas network, which is non-radial and cyclical, and the inter-temporal dynamics of linepack contribute to the lack of tightness of the relaxations. Conditions for exactness of the relaxation of the Weymouth equation can be found in [20] and [24], while approaches for tightening these SOC relaxations are proposed in [1] and [25]. For the McCormick relaxation of constraint (11c) the relaxation gap occurs very frequently and with high severity, see Fig. 5(c). Adversely negative values of γ and/or ρ in the bilinear terms lead to normalized relaxation gaps even larger than 1. Improvements on this approach, such as iterative tightening of the bounds or by convex quadratic enhancement of McCormick relaxation as proposed in [26], will be considered in future works. However, in the context of the proposed coordinated day-ahead dispatch, the tightness of the relaxation is of limited importance, since an additional gas flow feasibility problem [24] is expected to be solved closer to real-time by the gas network operator.

V. Conclusion and Future Perspectives

A. Conclusion

We proposed a distributionally robust chance-constrained coordination of power and natural gas systems to study the propagation of uncertainty from the power to the gas side. Our tractable reformulation of the stochastic program, using recourse actions from the flexible agents in the coupled system and adopting a simplified model for real-time gas flows and nodal pressures, results in a convex SOCP. Ex-ante out-of-sample evaluations are used to demonstrate the quality of the solution while highlighting a trade-off between dispatch cost and violation probability, which influences the choice of allowable violation probabilities. The proposed coordination model enables efficient harnessing of short-term flexibility from the assets in natural gas networks for power systems facing uncertainty. Analysis of the optimal affine policies highlights that our proposed approach enables cost-efficient dispatch and allocation of flexibility across energy sectors facing spatio-temporal effects of uncertainty.

B. Future Perspectives

For future works, detailed out-of-sample simulation studies should be undertaken to better understand the quality of optimal affine responses. Studying the impact of the response policies on the feasibility of the physical constraints of power and natural gas networks in real-time operation and testing the severity of allowed constraint violations are of interest. Convexity-preserving algorithms that tighten the relaxation of gas flow equations can be employed in future works. Further, power-to-gas units that provide additional inter-sectoral flexibility could be included in the model.

Analyzing the proposed coordination in a market context wherein payments for the provision of flexibility-as-a-service are considered, is an interesting topic to investigate in future. Moreover, the impact of limited information sharing among sectors as opposed to the central dispatch considered in this work would be highly insightful. Finally, a market clearing mechanism involving auctions that elicit flexibility from the natural gas sector is a viable pathway towards real-world implementation that is opened up by this paper.

APPENDIX A

The final tractable form of the proposed distributionally robust chance-constrained coordination of power and natural gas systems is the SOCP presented below:

$$\min_{\Theta_2 \cup \{\lambda_{m,u,t},\ \nu_{m,t}\}} \sum_{t\in\mathcal{T}} \Big(\sum_{i\in\mathcal{C}} C_i^{\mathrm{E}}\ p_{i,t} + \sum_{k\in\mathcal{K}} C_k^{\mathrm{G}}\ g_{k,t} \Big) \tag{20a}$$

subject to

$$\xi_i \Big\| -\alpha_{i,t}\mathbf{e}^\top (\mathbf{\Sigma}_t^{\Pi})^{1/2} \Big\|_2 \le p_{i,t} - \underline{P}_i,\ \ \forall i,\ \forall t, \tag{20b}$$

$$\xi_i \Big\| \alpha_{i,t}\mathbf{e}^\top (\mathbf{\Sigma}_t^{\Pi})^{1/2} \Big\|_2 \le -p_{i,t} + \overline{P}_i,\ \ \forall i,\ \forall t, \tag{20c}$$

$$\xi_{nr} \Big\| \{\mathbf{\Psi}(\mathbf{\Psi}_{\mathrm{I}}\boldsymbol{\alpha}_t\mathbf{e}^\top - \mathbf{\Psi}_{\mathrm{J}})\}_{(n,r)} (\mathbf{\Sigma}_t^{\Pi})^{1/2} \Big\|_2 \le \{\overline{\mathbf{F}} + \mathbf{\Psi}(\mathbf{\Psi}_{\mathrm{D}}\mathbf{D}_t^{\mathrm{E}} - \mathbf{\Psi}_{\mathrm{I}}\mathbf{p}_t - \mathbf{\Psi}_{\mathrm{J}}\mathbf{W}_t^{\mathrm{PF}})\}_{(n,r)},\ \ \forall (n,r)\in\mathcal{L},\ \forall t, \tag{20d}$$

$$\xi_{nr} \Big\| -\{\mathbf{\Psi}(\mathbf{\Psi}_{\mathrm{I}}\boldsymbol{\alpha}_t\mathbf{e}^\top - \mathbf{\Psi}_{\mathrm{J}})\}_{(n,r)} (\mathbf{\Sigma}_t^{\Pi})^{1/2} \Big\|_2 \le \{\overline{\mathbf{F}} - \mathbf{\Psi}(\mathbf{\Psi}_{\mathrm{D}}\mathbf{D}_t^{\mathrm{E}} - \mathbf{\Psi}_{\mathrm{I}}\mathbf{p}_t - \mathbf{\Psi}_{\mathrm{J}}\mathbf{W}_t^{\mathrm{PF}})\}_{(n,r)},\ \ \forall (n,r)\in\mathcal{L},\ \forall t, \tag{20e}$$

$$\xi_k \Big\| -\beta_{k,t}\mathbf{e}^\top (\mathbf{\Sigma}_t^{\Pi})^{1/2} \Big\|_2 \le g_{k,t} - \underline{G}_i,\ \ \forall k,\ \forall t, \tag{20f}$$

$$\xi_k \Big\| \beta_{k,t}\mathbf{e}^\top (\mathbf{\Sigma}_t^{\Pi})^{1/2} \Big\|_2 \le -g_{k,t} + \overline{G}_i,\ \ \forall k,\ \forall t, \tag{20g}$$

$$\xi_m \Big\| -\rho_{m,t}\mathbf{e}^\top (\mathbf{\Sigma}_t^{\Pi})^{1/2} \Big\|_2 \le pr_{m,t} - \underline{PR}_m,\ \ \forall m,\ \forall t, \tag{20h}$$

$$\xi_m \Big\| \rho_{m,t}\mathbf{e}^\top (\mathbf{\Sigma}_t^{\Pi})^{1/2} \Big\|_2 \le -pr_{m,t} + \overline{PR}_m,\ \ \forall m,\ \forall t, \tag{20i}$$

$$\xi_{mu} \Big\| (\rho_{u,t} - \Gamma_{m,u}\rho_{m,t})\mathbf{e}^\top (\mathbf{\Sigma}_t^{\Pi})^{1/2} \Big\|_2 \le \Gamma_{m,u} pr_{m,t} - pr_{u,t},\ \ \forall (m,u)\in\mathcal{Z}_c,\ \forall t, \tag{20j}$$

$$\xi_{mu} \Big\| -\gamma_{m,u,t}\mathbf{e}^\top (\mathbf{\Sigma}_t^{\Pi})^{1/2} \Big\|_2 \le q_{m,u,t}, \forall (m,u)\in\mathcal{Z}, \forall t, \tag{20k}$$

$$\xi_{mu} \Big\| -\gamma_{m,u,t}^{\mathrm{in}}\mathbf{e}^\top (\mathbf{\Sigma}_t^{\Pi})^{1/2} \Big\|_2 \le q_{m,u,t}^{\mathrm{in}}, \forall (m,u)\in\mathcal{Z}, \forall t, \tag{20l}$$

$$\xi_{mu} \Big\| -\gamma_{m,u,t}^{\mathrm{out}}\mathbf{e}^\top (\mathbf{\Sigma}_t^{\Pi})^{1/2} \Big\|_2 \le q_{m,u,t}^{\mathrm{out}}, \forall (m,u)\in\mathcal{Z}, \forall t, \tag{20m}$$

$$\gamma_{m,u,t}^2 \le K_{m,u}^2 (\rho_{m,t}^2 - \rho_{u,t}^2),\ \ \forall (m,u)\in\mathcal{Z},\ \forall t, \tag{20n}$$

$$\xi_{mu} \Big\| -(\rho_{m,t} + \rho_{u,t}) (\frac{S_{m,u}}{2})^{\frac{1}{2}} \mathbf{e}^\top (\mathbf{\Sigma}_t^{\Pi})^{1/2} \Big\|_2 \le h_{m,u,t} - H_{m,u}^0,\ \ \forall (m,u)\in\mathcal{Z},\ t = |\mathcal{T}|, \tag{20o}$$

McCormick envelopes of (16b) and (16d), (20p)

(12), (7), (5), (15a), (16a), (17), (20q)

where $\xi_i = \sqrt{\frac{1-\epsilon_i}{\epsilon_i}}$, $\xi_{nr} = \sqrt{\frac{1-\epsilon_{nr}}{\epsilon_{nr}}}$, $\xi_k = \sqrt{\frac{1-\epsilon_k}{\epsilon_k}}$, $\xi_m = \sqrt{\frac{1-\epsilon_m}{\epsilon_m}}$, $\xi_{mu} = \sqrt{\frac{1-\epsilon_{mu}}{\epsilon_{mu}}}$ are parameters.

REFERENCES

[1] S. Chen, A. J. Conejo, R. Sioshansi, and Z. Wei, "Unit commitment with an enhanced natural gas-flow model," *IEEE Transactions on Power Systems*, vol. 34, no. 5, pp. 3729–3738, 2019.

[2] P. Pinson, L. Mitridati, C. Ordoudis, and J. Østergaard, "Towards fully renewable energy systems: Experience and trends in Denmark," *CSEE Journal of Power and Energy Systems*, vol. 3, no. 1, pp. 26–35, 2017.

[3] G. Byeon and P. Van Hentenryck, "Unit commitment with gas network awareness," *IEEE Transactions on Power Systems*, vol. 35, no. 2, pp. 1327–1339, 2020.

[4] A. Zlotnik, L. Roald, S. Backhaus, M. Chertkov, and G. Andersson, "Coordinated scheduling for interdependent electric power and natural gas infrastructures," *IEEE Transactions on Power Systems*, vol. 32, no. 1, pp. 600–610, 2017.

[5] C. Ordoudis, P. Pinson, and J. M. Morales, "An integrated market for electricity and natural gas systems with stochastic power producers," *European Journal of Operational Research*, vol. 272, no. 2, pp. 642–654, 2019.

[6] H. Ameli, M. Qadrdan, and G. Strbac, "Coordinated operation strategies for natural gas and power systems in presence of gas-related flexibilities," *Energy Systems Integration*, vol. 1, no. 1, pp. 3–13, 2019.

[7] A. Schwele, C. Ordoudis, J. Kazempour, and P. Pinson, "Coordination of power and natural gas systems: Convexification approaches for linepack modeling," in *Proc. 13th IEEE PES PowerTech Conference*, Milan, 2019.

[8] C. Wang, W. Wei, J. Wang, and T. Bi, "Convex optimization based adjustable robust dispatch for integrated electric-gas systems considering gas delivery priority," *Applied Energy*, vol. 239, pp. 70–82, 2019.

[9] B. Odetayo, J. MacCormack, W. Rosehart, and H. Zareipour, "A chance constrained programming approach to integrated planning of distributed power generation and natural gas network," *Electric Power Systems Research*, vol. 151, pp. 197–207, 2017.

[10] A. Ratha, J. Kazempour, A. Virag, and P. Pinson, "Exploring market properties of policy-based reserve procurement for power systems," in *2019 IEEE 58th Conference on Decision and Control (CDC)*, 2019, pp. 7498–7505.

[11] W. Wiesemann, D. Kuhn, and M. Sim, "Distributionally robust convex optimization," *Operations Research*, vol. 62, no. 6, pp. 1358–1376, 2014.

[12] R. D. Christie, B. F. Wollenberg, and I. Wangensteen, "Transmission management in the deregulated environment," *Proceedings of the IEEE*, vol. 88, no. 2, pp. 170–195, 2000.

[13] A. Georghiou, D. Kuhn, and W. Wiesemann, "The decision rule approach to optimization under uncertainty: Methodology and applications," *Computational Management Science*, vol. 16, no. 4, pp. 545–576, 2019.

[14] A. Georghiou, W. Wiesemann, and D. Kuhn, "Generalized decision rule approximations for stochastic programming via liftings," *Mathematical Programming*, vol. 152, no. 1, pp. 301–338, 2015.

[15] L. Roald and G. Andersson, "Chance-constrained AC optimal power flow: Reformulations and efficient algorithms," *IEEE Transactions on Power Systems*, vol. 33, no. 3, pp. 2906–2918, 2018.

[16] S. Zymler, D. Kuhn, and B. Rustem, "Distributionally robust joint chance constraints with second-order moment information," *Mathematical Programming*, vol. 137, no. 1, pp. 167–198, 2013.

[17] M. R. Wagner, "Stochastic 0-1 linear programming under limited distributional information," *Operations Research Letters*, vol. 36, no. 2, pp. 150 – 156, 2008.

[18] W. Xie and S. Ahmed, "Distributionally robust chance constrained optimal power flow with renewables: A conic reformulation," *IEEE Transactions on Power Systems*, vol. 33, no. 2, pp. 1860–1867, 2018.

[19] Y. Dvorkin, "A chance-constrained stochastic electricity market," *IEEE Transactions on Power Systems (Early Access)*, 2019.

[20] C. Borraz-Sánchez, R. Bent, S. Backhaus, H. Hijazi, and P. Van Hentenryck, "Convex relaxations for gas expansion planning," *INFORMS Journal on Computing*, vol. 28, no. 4, pp. 645–656, 2016.

[21] G. P. McCormick, "Computability of global solutions to factorable nonconvex programs: Part I - Convex underestimating problems," *Mathematical Programming*, vol. 10, no. 1, pp. 147–175, 1976.

[22] A. Ratha, A. Schwele, J. Kazempour, P. Pinson, S. S. Torbaghan, and A. Virag, "Online appendix for paper: Affine policies for flexibility provision by natural gas networks to power systems," 2020. [Online]. Available: https://doi.org/10.5281/zenodo.3755120

[23] P. Pinson, "Wind energy: Forecasting challenges for its operational management," *Statistical Science*, vol. 28, no. 4, pp. 564–585, 11 2013.

[24] M. K. Singh and V. Kekatos, "Natural gas flow equations: Uniqueness and an MI-SOCP solver," in *2019 American Control Conference (ACC)*, 2019, pp. 2114–2120.

[25] C. Coffrin, H. L. Hijazi, and P. Van Hentenryck, "Strengthening the SDP relaxation of AC power flows with convex envelopes, bound tightening, and valid inequalities," *IEEE Transactions on Power Systems*, vol. 32, no. 5, pp. 3549–3558, 2017.

[26] J. E. Mitchell, J.-S. Pang, and B. Yu, "Convex quadratic relaxations of nonconvex quadratically constrained quadratic programs," *Optimization Methods and Software*, vol. 29, no. 1, pp. 120–136, 2014.

[Paper D] Coordination of Electricity and Natural Gas Markets via Financial Instruments

Authors:
Anna Schwele, Christos Ordoudis, Pierre Pinson and Jalal Kazempour

Submitted to:
Computational Management Science

Coordination of Power and Natural Gas Markets via Financial Instruments

Anna Schwele · Christos Ordoudis · Pierre Pinson · Jalal Kazempour

Abstract Current electricity and natural gas markets operate in a temporally and sectorally decoupled way. However, increasing integration of stochastic renewable energy sources challenges the current energy market designs in two ways. First, the need for exchanging operational flexibility between energy sectors is increasing, which requires improving *sectoral coordination* between electricity and gas markets. Second, the dispatch of flexible units needs to be made in a more informed manner, requiring to strengthen *temporal coordination* between day-ahead and real-time energy markets. This paper presents two-stage stochastic equilibrium and optimization models to explore financial instruments in the form of *virtual bidding* as a market-based solution to enhance both sectoral and temporal coordination in energy markets. Explicit virtual bidding by purely financial players enhances temporal coordination, while the implicit one by physical players improves sectoral coordination, too.

The work was supported by the EUD Programme through the 'Coordinated Operation of Integrated Energy Systems (CORE)' project under the grant 64017-0005.

Anna Schwele
Center for Electric Power and Energy, Technical University of Denmark, Kongens Lyngby, Denmark,
E-mail: schwele@elektro.dtu.dk

Christos Ordoudis
Center for Electric Power and Energy, Technical University of Denmark, Kongens Lyngby, Denmark,
E-mail: chror@elektro.dtu.dk

Pierre Pinson
Center for Electric Power and Energy, Technical University of Denmark, Kongens Lyngby, Denmark,
E-mail: ppin@elektro.dtu.dk

Jalal Kazempour
Center for Electric Power and Energy, Technical University of Denmark, Kongens Lyngby, Denmark,
E-mail: seykaz@elektro.dtu.dk

By exploiting a fully stochastic co-optimization model as an ideal benchmark, we numerically illustrate the benefits of virtual bidding for increasing market efficiency in terms of reduced expected operational cost of the energy system. We show that flexible resources in electricity and gas markets are dispatched more efficiently in the day-ahead stage when virtual bidding exists.

Keywords OR in energy · electricity and natural gas markets · generalized Nash equilibrium (GNE) · scenario-based stochastic programming · operational flexibility · sectoral and temporal coordination · virtual bidding

1 Introduction

The growing share of power production from stochastic renewable energy sources, e.g., wind and solar power units, increases the need for operational flexibility[1] to deal with their variability and uncertainty (NERC, 2010). Natural gas-fired power plants are usually flexible units and are able to compensate for the production variability and uncertainty caused by stochastic renewable sources (Gil et al., 2014). These gas-fired power plants operate at the interface of the electricity and the natural gas systems, yielding both physical and economic interactions (Fleten and Nasakkala, 2010). The natural gas system is crucial for ensuring fuel availability and technical feasibility, while it is also able to provide flexibility for power systems through stored gas in the pipelines (Ordoudis et al., 2019; Correa-Posada and Sánchez-Martín, 2015; Yang et al., 2018). An increasingly volatile dispatch of gas-fired power plants to offset wind intermittency introduces demand fluctuations and uncertainty into the gas market (Heinen et al., 2017; Dall'Anese et al., 2017; Nicholson and Quinn, 2019). The subsequent trend towards increasing volumes in gas trading in short-term spot markets like Gaspoint Nordic (Hibbard and Schatzki, 2012; Pinson et al., 2017) will become more important as natural gas demand profiles become more uncertain. Electricity and natural gas markets in many countries are cleared sequentially and separately (Hibbard and Schatzki, 2012; Tabors et al., 2012). However, the increasing operation of natural gas-fired power plants as one of the main sources of flexibility in power systems as well as the need for exchanging operational flexibility among the sectors lead to the growing interaction of power and natural gas systems. Therefore, *sectoral coordination* between electricity and natural gas markets is crucial for renewable-based energy systems (Meibom et al., 2013). Furthermore, the majority of current electricity markets throughout the world clear several *sequential* markets in short run, e.g., in day-ahead (DA) and real-time (RT) stages, with a *deterministic* description of uncertain supply (Daraeepour et al., 2019). There is a similar sequential deterministic market design for natural gas systems. Despite the recent advances in forecasting tools, the deterministic forecast of stochastic renewable energy sources used at the DA stage can be erroneous, which

[1] By operational flexibility, we refer to the capability of a power system to modify its output or state in response to a change in renewable power production (Zhao et al., 2016).

may cause wrong unit commitment and dispatch decisions (Jonsson et al., 2010). This eventually results in market inefficiency, i.e., a comparatively high operational cost for the system. To resolve such an inefficiency, *temporal coordination* between DA and RT markets in both power and natural gas systems is required (Morales and Pineda, 2017).

The market-based mechanisms for improving both sectoral and temporal coordination of power and natural gas systems range from an extremely disruptive choice of designing a fully stochastic integrated energy market (Correa-Posada and Sánchez-Martín, 2015; Zlotnik et al., 2016) to less-disruptive solutions that preserve the current regulatory framework with separate and sequential clearing of markets. The latter, i.e., less disruptive market mechanisms, is the focus of this paper, while the former, i.e., the fully stochastic integrated energy market, is used as an *ideal benchmark* to assess the performance of the proposed mechanisms. Among others, the less-disruptive (or "soft") market-based mechanisms for power and natural gas coordination can be achieved by information exchange among the markets (Byeon and Van Hentenryck, 2020), defining new market products (Chen et al., 2017; Warrington et al., 2013; Wang and Hobbs, 2016; Godoy-Gonzalez et al., 2020), prescribing new bidding formats (Liu et al., 2015; O'Connell et al., 2016; Savelli et al., 2018), and introducing new market players which act as coordinators at the interface of different sectors.

In this paper, we propose financial instruments to enhance the coordination of power and natural gas markets. Specifically, we explore the effect of *virtual bidding* (Hogan, 2016), also called "convergence bidding" (Li et al., 2015) in the literature, as a soft market-based mechanism for improving both temporal and sectoral coordination of power and natural gas systems under uncertainty. Virtual bidding (VB) exists today in U.S. markets, such as PJM (Birge et al., 2018), and refers to the financial arbitrage between two trading floors in an energy market, e.g., between DA and RT electricity markets. The virtual bidder may earn profit due to price difference in DA and RT markets by performing arbitrage. This virtual bidder can be a purely financial player who has no physical asset, the so-called *explicit VB*, or she can be one of the existing physical market players, the so-called *implicit VB*. An example of an implicit virtual bidder is a generator, who does arbitrage between DA and RT markets by selling electricity in DA more than her installed capacity (Isemonger, 2006; Mather et al., 2017). It is known in the literature that VB has potential to improve the market efficiency of electricity markets by enhancing the temporal coordination between deterministic DA and RT markets (Kazempour and Hobbs, 2018; Morales and Pineda, 2017). The reason for such an improvement is that VB increases market liquidity and brings additional information to the DA market. It is worth noting that such an improved market efficiency may not be fully realized under some circumstances (Parsons et al., 2015) or may have some limits (Birge et al., 2018; Ito and Reguant, 2016). An example of such conditions is markets where virtual bidders behave strategically (Lo Prete et al., 2019a,b).

In this paper, we aim at quantifying the maximum potential of VB for improving both sectoral and temporal coordination of electricity and natural gas markets under supply uncertainty. For this purpose, we model renewable generation uncertainty via a finite set of scenarios, and develop three stochastic generalized Nash equilibrium (GNE) problems (Facchinei and Kanzow, 2007), whose solution existence can be mathematically ensured under some assumptions. These stochastic equilibrium models serve as simulation tools for deriving policy implications to explore how much VB can improve the sectoral and temporal coordination in renewable-based electricity and natural gas markets. We also provide analytical insights by comparing the GNE problems and the ideal benchmark, i.e., the two-stage stochastic co-optimization problem (Zakeri et al., 2019; Zavala et al., 2017; Pritchard et al., 2010). It is important to highlight that these stochastic equilibrium models should be seen as policy tools, since they are not intended to be used for market clearing in practice.

As the core contribution of this paper, we first integrate explicit VB to electricity and natural gas markets, which achieves temporal coordination between DA and RT markets in each energy sector. Then, we investigate the possibility of natural gas-fired power plants, who are at the interface of power and natural gas, to behave as implicit virtual bidders. We illustrate that such implicit virtual bidders have potential to achieve both temporal and sectoral coordination in electricity and natural gas markets.

The manuscript is organized as follows. In Section 2 we provide more details about temporal and sectoral market coordination, the concept of VB and our modeling assumptions. Sections 3 and 4 contain the mathematical formulations of GNE models with explicit and implicit VB, respectively. The formulation of the ideal benchmark model is included in Section 5. In Section 6, we show the numerical results for a case study, and finally Section 7 concludes the paper. For clarity purposes, we maintain the generic representation of optimization problems throughout the paper, and include their detailed representations in the online appendix (Schwele et al., 2020).

2 Preliminaries

This section first highlights the temporal and sectoral coordination of power and natural gas markets under uncertainty. Then, it further describes both types of VB (explicit and implicit). Finally, it summarizes the modeling assumptions made in this paper.

2.1 Two-dimensional Coordination: Temporal and Sectoral

The independent market operators clear each trading stage (DA and RT) separately and sequentially for electricity and natural gas markets. The current market-clearing framework for electricity and natural gas systems is illustrated in Fig. 1, including four market-clearing sequences. First, the electricity market is cleared in a DA auction 12-36 hours before actual energy delivery using

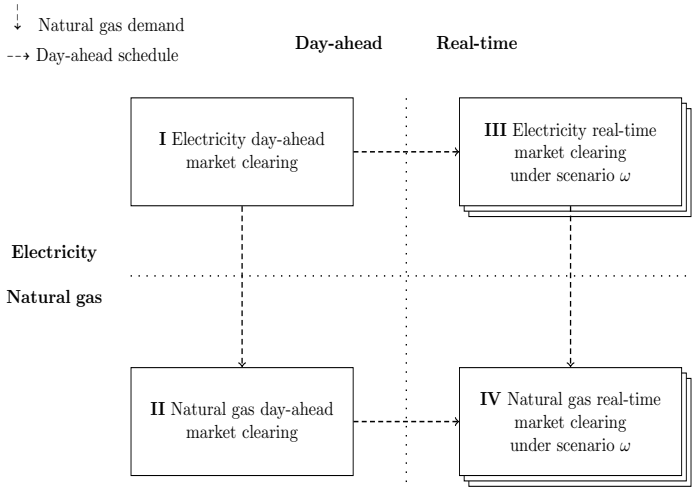

Fig. 1 Sequential setup of electricity and natural gas markets, including four market-clearing sequences I to IV.

a deterministic forecast of uncertain parameters, e.g., renewable power generation and natural gas prices. Note that future natural gas prices directly impact the marginal production cost of natural gas-fired power plants and consequently the merit order[2] in the electricity market. Second, the natural gas DA market is cleared for given natural gas demand of gas-fired power plants determined by their dispatch in the electricity market. Third, once the uncertainty is realized (e.g., scenario ω occurs), the RT electricity market is cleared to adjust imbalances under fixed DA unit commitment and dispatch decisions. Fourth, the natural gas market is cleared in RT, while the dispatch of gas suppliers in DA and the demand of natural gas-fired power plants in RT are given.

The sequential setup in Fig. 1, even though aligned with current practice, is totally uncoordinated in both temporal and sectoral dimensions. This setup is temporally uncoordinated since both electricity and gas markets in DA are cleared based on the available deterministic forecast in that stage, without foresight into the potential deviations that may realize in RT. It is also sectorally uncoordinated because the electricity market is cleared based on an estimation of natural gas price, and the gas market is cleared afterwards. As it is common in practice, the integration of operating reserve as an extra market product is able to potentially enhance the temporal coordination between DA and RT markets. However it may bring extra inefficiencies if the value assigned for the minimum reserve requirement in the DA market is not properly selected (Doherty and O'Malley, 2005; Zugno and Conejo, 2015). This can be an even more challenging issue in European markets, where energy and

[2] The merit order refers to placing the power plants with an ascending order of marginal production costs.

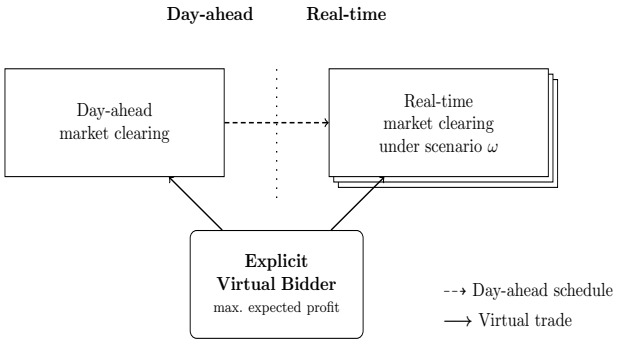

Fig. 2 Explicit virtual bidding by arbitraging electricity between the DA and RT electricity markets (or by arbitraging gas between DA and RT natural gas markets). This type of virtual bidding has potential to enhance temporal coordination between DA and RT markets.

reserve markets are cleared sequentially (Dominguez et al., 2019). Note that we exclude the reserve market as it is not the focus of this study.

While the share of stochastic renewable energy sources is growing, the lack of temporal and sectoral coordination in electricity and natural gas markets may cause market inefficiency. In other words, the overall operational cost of electricity and natural gas systems in DA and RT might be comparatively higher than that cost in the ideal co-optimization benchmark. The reason for such an inefficiency is non-optimal DA dispatch decisions made due to uncoordinated DA market clearing. If flexible sources are dispatched in the DA stage inefficiently, they will not be available in RT to cope with imbalances. As a consequence, more expensive actions, e.g., load curtailment, might be required. Therefore, it is desirable to dispatch the flexible sources in DA in an efficient manner while preserving the current sequential market-clearing framework. This requires soft market-based mechanisms for enhancing the temporal and sectoral coordination of power and natural gas markets, which is the focus of this paper.

2.2 Virtual Bidding

Virtual bidding is a purely financial instrument, existing in the U.S. electricity markets, e.g., CAISO, PJM, and MISO (Hogan, 2016; Li et al., 2015; Birge et al., 2018). It allows market players to profit from anticipated price differences between the DA and RT markets by performing arbitrage Kovacevic (2016). We explain below both explicit and implicit VB (Isemonger, 2006; Mather et al., 2017).

An *explicit* virtual bidder is a purely financial player who does not own any physical assets. Therefore, her positions in DA and RT need to even out to zero. For example, an explicit virtual bidder may buy 10 MWh in the DA electricity market in a specific hour at the DA market price in that hour,

and then sells the same 10 MWh back in the RT electricity market at the same hour but at the price of the RT market. Therefore, her payoff is equal to the difference between the DA and RT prices times the amount of virtually traded power. Assuming that this virtual bidder is a price-taker with perfect foresight into the distribution of DA and RT prices, she is supposed to enhance informational and productive efficiency of the two-settlement market by bringing more competitiveness, liquidity and transparency to wholesale energy markets. Fig. 2 illustrates how such an explicit VB is integrated into the two-settlement market-clearing setup. While DA and RT energy markets are cleared deterministically and sequentially, the explicit virtual bidder solves a stochastic program maximizing her own expected profit. The outcomes of the stochastic program of virtual bidders, i.e., virtual trades, are exogenous in DA and RT markets. In other words, these virtual bidders act as *self-scheduling* market players.[3] On the other hand, the DA and RT market-clearing prices are exogenous in the stochastic program of virtual bidder. It is obvious from Fig. 2 that a set of interrelated optimization problems (one for DA market clearing, one for RT market clearing per scenario, and one for explicit virtual bidder) is required to explore the performance of explicit VB. This clarifies the need for developing a stochastic equilibrium model. It is demonstrated in (Kazempour and Hobbs, 2018) that this setup can bring temporal coordination between DA and RT electricity markets. This is an interesting insight for market operators since they can keep the market clearing deterministic, while leaving the correction of market inefficiency to virtual bidders. However, VB may not always work in such a desirable way, as discussed in (Parsons et al., 2015) and (Birge et al., 2018).

Unlike the explicit VB, the *implicit* virtual bidder is a physical market player. An example of such a player is a natural gas-fired power plant who is at the interface of power and natural gas systems, as illustrated in Fig. 3. This power plant has potential to enhance both temporal and sectoral coordination in electricity and natural gas markets. Although the presence of explicit VB may eliminate the motivation for physical players to perform arbitrage, physical players may still find self-scheduling profitable to forgo the market and dispatch their production/consumption themselves outside the market. For example, assume a natural gas-fired power plant that has perfect foresight into future DA and RT power and gas prices, and realizes that her profit is not maximized when she participates in deterministic electricity and natural gas markets. In other words, she has the opportunity to gain a higher profit in expectation by self-scheduling outside the market (Guo et al., 2016; Sioshansi et al., 2010). Note that the power production and gas consumption of this power plant are exogenous in the market-clearing problems, while she still pays/is paid based on the market-clearing prices (Jha and Wolak, 2015; Papavasiliou et al., 2015). An implicit virtual bidder may benefit from self-scheduling by solving her own stochastic program with better representation

[3] By self-scheduling market players, we refer to those players who make their DA dispatch decisions internally, rather than submitting price-quantity bids to the DA market.

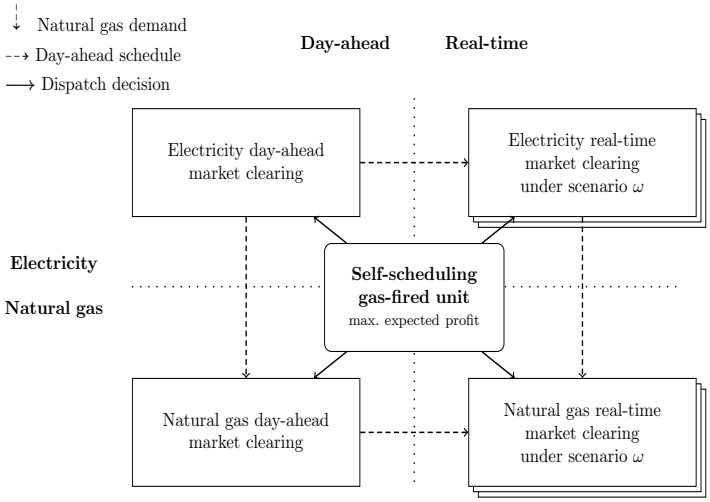

Fig. 3 Implicit virtual bidding by a natural gas-fired power plant, who is on the interface of electricity and natural gas systems. This power plant self-schedules her power productions and gas consumptions in DA and RT electricity and natural gas markets. This type of virtual bidding has potential to enhance temporal and sectoral coordination between DA and RT electricity and natural gas markets.

of uncertainty and technical constraints for a longer time horizon. However, these self-schedulers take on the full risk of RT price uncertainty. The influence of risk aversion and price volatility on the decision of generators to do self-scheduling is discussed in (Papavasiliou et al., 2015) and (Conejo et al., 2004).

2.3 Modeling Framework and Assumptions

Wind power production is assumed as the only source of uncertainty. Note that the wind power forecast in DA is a single point (deterministic), while different scenarios may occur in RT, i.e., we are not sure about the actual outcome of the uncertain parameter. Wind power uncertainty is represented using a finite set of scenarios. We consider two trading floors (DA and RT) only, and other potential floors, e.g., intra-day adjustment markets, are excluded. We also consider simple price-quantity bids only, discarding any other types of bids, e.g., bid curves, block bids, etc. The wind power production cost is zero, and can be spilled at zero cost. Both electricity and natural gas demands are inelastic to price. All demand and supply in both energy sectors are assumed to be located at a single node, neglecting the transmission systems. Trading of natural gas takes place according to the entry-exit model (Vazquez and Hallack, 2015). On the power side, a multi-period unit commitment scheduling model is used. We relax the binary nature of commitment status of conventional generators to lie within zero and one, but in a tight manner (Hua and Baldick, 2017). This relaxation ensures convexity, which is

required to solve the stochastic equilibrium model as a mixed complementarity problem, while providing more accurate cost estimates than pure dispatch models. The production cost of generators is assumed to be a linear function. We assume all market players including virtual bidders (either explicit or implicit) to act competitively, non-strategically, and in a risk-neutral manner when participating in the markets, so they offer at prices identical to their marginal costs. We assume a "perfect" virtual bidder, assuming that she can always zero out her position in RT. These assumptions enable us to quantify the full potential of VB in enhancing temporal and sectoral coordination in the proposed simulation tool.

Notation: We denote by $\mathbb{R}$ and $\mathbb{R}_+$ free and non-negative real numbers, respectively. We use upper case letters for matrices and lower case letters for vectors. Bold lower case letters denote vectors of variables. Note that e is the vector of ones and $(.)^\top$ is the transpose operator. We use functions $h(.)$ and $g(.)$ to show equality and inequality constraints in every optimization problem, but note that these constraints for different optimization problems are not necessarily identical.

3 Temporal Coordination

In this section, we first explore temporal coordination between electricity DA and RT markets via explicit VB. We then argue such a coordination in DA and RT natural gas markets. The sectoral coordination will be discussed later in Section 4.

3.1 Temporal Coordination Between DA and RT Electricity Markets

We present below optimization problems for explicit electricity virtual bidder as well as DA and RT electricity markets. These optimization problems are interrelated and construct a stochastic equilibrium problem.

3.1.1 Explicit Electricity Virtual Bidder:

The expected profit-maximization problem of each explicit electricity virtual bidder $r \in \mathcal{R}$ over the time horizon $\mathcal{T}$ writes as

$$\left\{ \max_{\mathbf{v}_r^{\mathrm{E}}, \boldsymbol{\Delta}\mathbf{v}_r^{\mathrm{E}}} \ \boldsymbol{\lambda}^{\mathrm{DA,E}\top} \ \mathbf{v}_r^{\mathrm{E}} + \left(\sum_{\omega} \pi_\omega \ \boldsymbol{\lambda}_{\boldsymbol{\omega}}^{\mathrm{RT,E}} \right)^\top \boldsymbol{\Delta}\mathbf{v}_r^{\mathrm{E}} \right. \tag{1a}$$

$$\left. \text{subject to } \ \mathbf{v}_r^{\mathrm{E}} + \boldsymbol{\Delta}\mathbf{v}_r^{\mathrm{E}} = 0 \right\} \ \forall r. \tag{1b}$$

Note that (1) is a two-stage stochastic linear program. The virtual bidder decides her DA position $\mathbf{v}_r^{\mathrm{E}} \in \mathbb{R}^{\mathcal{T}}$ given the DA electricity prices $\boldsymbol{\lambda}^{\mathrm{DA,E}} \in \mathbb{R}^{\mathcal{T}}$ as well as the distribution of RT electricity prices $\boldsymbol{\lambda}_{\omega}^{\mathrm{RT,E}} \in \mathbb{R}^{\mathcal{T}}$ $\forall \omega$ weighted

by probability π_ω over the set of scenarios $\omega \in \Omega$. This virtual bidder is a purely financial player without physical assets, and therefore is obliged to offset her DA position by her RT position $\mathbf{\Delta v}_r^{\mathrm{E}} \in \mathbb{R}^{\mathcal{T}}$ in each scenario. Objective function (1a) maximizes the expected profit of explicit virtual bidder who arbitrages between the DA and RT electricity markets. Constraint (1b) ensures that the virtual bidder sells (buys) the same amount back in the RT market that was bought (sold) in the DA market. One important observation about this explicit virtual bidder is that she enforces the convergence of DA and expected RT electricity prices (Kazempour and Hobbs, 2018). Derived from Karush–Kuhn–Tucker (KKT) optimality conditions associated with (1), the virtual bidder enforces the DA and the expected RT electricity prices to be equal, i.e., $\boldsymbol{\lambda}^{\mathrm{DA,E}} = \sum_\omega \pi_\omega \boldsymbol{\lambda}_\omega^{\mathrm{RT,E}}$. See online appendix (Schwele et al., 2020) for further details. Note that market operators treat the dispatch decision of virtual bidders as fixed input into the market-clearing problem presented in the following section.

3.1.2 DA Electricity Market:

Consider $\mathcal{G}$ number of gas-fired generators and $\mathcal{C}$ number of non gas-fired generators, such that $\mathcal{G} \cup \mathcal{C} = \mathcal{I}$. Besides, consider $\mathcal{J}$ number of wind power units. For given production cost of non gas-fired generators $\mathbf{C}^{\mathrm{E}} \in \mathbb{R}_+^{\mathcal{C}}$, estimation of natural gas prices $\tilde{\boldsymbol{\lambda}}^{\mathrm{G}} \in \mathbb{R}^{\mathcal{T}}$ to compute the production cost $C(\tilde{\boldsymbol{\lambda}}^{\mathrm{G}}) \in \mathbb{R}^{\mathcal{G}\times\mathcal{T}}$ for gas-fired generators, and fixed dispatch of virtual bidders $\mathbf{v}_r^{\mathrm{E}}$ obtained from (1), the electricity market operator clears the market in DA to minimize the total operational cost of the power system as

$$\min_{\mathbf{p},\mathbf{u},\mathbf{s},\mathbf{w}} \quad e^\top \mathbf{p}^{\mathrm{C}}\ \mathbf{C}^{\mathrm{E}} + e^\top \mathbf{p}^{\mathrm{G}}\ C(\tilde{\boldsymbol{\lambda}}^{\mathrm{G}})\ e + e^\top \mathbf{s}\ e \tag{2a}$$

$$\text{subject to} \quad h(\mathbf{p}, \mathbf{w}, \mathbf{v}_r^{\mathrm{E}}) = 0 : \boldsymbol{\lambda}^{\mathrm{DA,E}}, \tag{2b}$$

$$g(\mathbf{p}, \mathbf{w}, \mathbf{u}, \mathbf{s}) \leq 0. \tag{2c}$$

Note that (2) is a deterministic linear program. Variables $\mathbf{p}, \mathbf{u}, \mathbf{s} \in \mathbb{R}_+^{\mathcal{T}\times\mathcal{I}}$ are the dispatch, commitment status, and start-up cost of conventional generators in DA, respectively. In particular, $\mathbf{p}^{\mathrm{C}} \in \mathbb{R}_+^{\mathcal{T}\times\mathcal{C}}$ and $\mathbf{p}^{\mathrm{G}} \in \mathbb{R}_+^{\mathcal{T}\times\mathcal{G}}$ are the DA dispatch of non gas- and gas-fired generators, respectively. The commitment status $\mathbf{u}$ is relaxed to lie within zero and one. Besides, $\mathbf{w} \in \mathbb{R}_+^{\mathcal{T}\times\mathcal{J}}$ refers to the DA dispatch of wind power units, limited by their deterministic forecast in DA.

Objective function (2a) minimizes the total system cost in DA, including the operational and start-up costs of conventional generators. Equality constraint (2b) enforces the balance between power production and consumption in DA with inelastic demand. The virtual DA positions $\mathbf{v}_r^{\mathrm{E}}$ are treated as given inputs. The dual variable associated with power balance (2b), i.e., $\boldsymbol{\lambda}^{\mathrm{DA,E}} \in \mathbb{R}^{\mathcal{T}}$, provides the DA electricity price. Recall that this vector of dual variables was treated as exogenous values in the problem of virtual bidders (1). Inequality constraints (2c) enforce lower and upper bounds on the DA dispatch of

wind and conventional generation, impose ramping limits of conventional generators, represent the tight relaxation of unit commitment, and compute the start-up cost of each conventional generator. The detailed representation of all equality and inequality constraints is given in the online appendix (Schwele et al., 2020).

3.1.3 RT Electricity Market:

The actual wind power production is realized in RT, which might not be necessarily identical to the deterministic wind power forecast in DA. Therefore, the electricity market operator clears the RT market to make the necessary adjustments in order to keep the system balanced. The balancing actions are the power adjustment of generators and the two extreme actions, i.e., wind spillage and load shedding. The (relaxed) commitment status of fast-starting conventional generators $\mathcal{F} \subset \mathcal{I}$ and therefore their start-up cost can be updated in RT, while that is not the case for the slow-starting generators $\mathcal{S} \subset \mathcal{I}$. Note that $\mathcal{F} \cup \mathcal{S} = \mathcal{I}$. For given production costs of non gas-fired and gas-fired generators $\mathbf{C}^{\mathrm{E}} \in \mathbb{R}_{+}^{\mathcal{C}}$ and $C(\tilde{\boldsymbol{\lambda}}^{\mathrm{G}}) \in \mathbb{R}^{\mathcal{G} \times \mathcal{T}}$, load shedding cost $\mathbf{C}^{\mathrm{sh,E}} \in \mathbb{R}_{+}^{\mathcal{T}}$, fixed dispatch of explicit virtual bidders $\boldsymbol{\Delta}\mathbf{v}_r^{\mathrm{E}}$ achieved from (1) and fixed DA electricity market-clearing outcomes $\mathbf{p}$ and $\mathbf{u}$ obtained from (2), the RT electricity market clearing under scenario $\omega \in \Omega$ writes as

$$\left\{ \min_{\substack{\boldsymbol{\Delta}\mathbf{p}_\omega, \boldsymbol{\Delta}\mathbf{u}_\omega, \boldsymbol{\Delta}\mathbf{s}_\omega, \\ \boldsymbol{\Delta}\mathbf{w}_\omega, \boldsymbol{\Delta}\mathbf{d}_\omega^{\mathrm{E}}}} \; e^\top \boldsymbol{\Delta}\mathbf{p}_\omega^{\mathrm{C}} \; \mathbf{C}^{\mathrm{E}} + e^\top \boldsymbol{\Delta}\mathbf{p}_\omega^{\mathrm{G}} \; C(\tilde{\boldsymbol{\lambda}}^{\mathrm{G}}) \; e + e^\top \boldsymbol{\Delta}\mathbf{s}_\omega \; e + \mathbf{C}^{\mathrm{sh,E}^\top} \; \boldsymbol{\Delta}\mathbf{d}_\omega^{\mathrm{E}} \right. \tag{3a}$$

$$\text{subject to} \;\; h(\boldsymbol{\Delta}\mathbf{p}_\omega, \boldsymbol{\Delta}\mathbf{w}_\omega, \boldsymbol{\Delta}\mathbf{d}_\omega^{\mathrm{E}}, \boldsymbol{\Delta}\mathbf{v}_r^{\mathrm{E}}) = 0 : \boldsymbol{\lambda}_{\boldsymbol{\omega}}^{\mathrm{RT,E}}, \tag{3b}$$

$$\left. g(\boldsymbol{\Delta}\mathbf{p}_\omega, \boldsymbol{\Delta}\mathbf{w}_\omega, \boldsymbol{\Delta}\mathbf{d}_\omega^{\mathrm{E}}, \boldsymbol{\Delta}\mathbf{u}_\omega, \boldsymbol{\Delta}\mathbf{s}_\omega, \mathbf{p}, \mathbf{u}) \leq 0, \right\} \forall \omega. \tag{3c}$$

Note that (3), one per scenario, is a deterministic linear program. We denote by $\boldsymbol{\Delta}\mathbf{p}_\omega \in \mathbb{R}^{\mathcal{T} \times \mathcal{I}}$ the power adjustment of conventional generators. In addition, $\boldsymbol{\Delta}\mathbf{u}_\omega \in \mathbb{R}^{\mathcal{T} \times \mathcal{F}}$ and $\boldsymbol{\Delta}\mathbf{s}_\omega \in \mathbb{R}^{\mathcal{T} \times \mathcal{F}}$ refer to the adjusted relaxed commitment decision and the adjusted start-up cost of fast-starting units, respectively. Wind spillage and load shedding actions are denoted by $\boldsymbol{\Delta}\mathbf{w}_\omega \in \mathbb{R}_{+}^{\mathcal{T} \times \mathcal{J}}$ and $\boldsymbol{\Delta}\mathbf{d}_\omega^{\mathrm{E}} \in \mathbb{R}_{+}^{\mathcal{T}}$, respectively.

Objective function (3a) minimizes the total balancing cost for underlying scenario ω. Equality constraint (3b) balances the wind power deviations in RT from the DA schedule with the position of virtual bidders $\boldsymbol{\Delta}\mathbf{v}_r^{\mathrm{E}}$ as fixed input. The dual variable vector $\boldsymbol{\lambda}_{\boldsymbol{\omega}}^{\mathrm{RT,E}} \in \mathbb{R}^{\mathcal{T}}$ represents the RT electricity prices under scenario ω. Recall that this vector was exogenous in the problem of virtual bidders (1). Inequality constraints (3c) enforce lower and upper bounds on the load shedding and power adjustment of wind power units, conventional slow- and fast-starting generators, restrict the ramp-rate limits of conventional

generators, enforce the adjusted unit commitment, and calculate the start-up cost for fast-starting units. The detailed representation of constraints is provided in the online appendix (Schwele et al., 2020).

3.2 Temporal Coordination within DA and RT Natural Gas Markets

Similar to Section 3.1, we present here the optimization problems for explicit natural gas virtual bidder, and DA and RT natural gas markets, which define a stochastic equilibrium problem together.

3.2.1 Explicit Natural Gas Virtual Bidder:

Similarly to the electricity VB, the profit-maximization problem of each explicit natural gas virtual bidder $q \in \mathcal{Q}$ participating in the natural gas DA and RT markets is given by the following two-stage stochastic linear program:

$$\left\{ \max_{\mathbf{v}_q^{\mathrm{G}}, \boldsymbol{\Delta}\mathbf{v}_q^{\mathrm{G}}} \ \boldsymbol{\lambda}^{\mathrm{DA,G}\top} \mathbf{v}_q^{\mathrm{G}} + \left(\sum_{\omega} \pi_\omega \ \boldsymbol{\lambda}_{\boldsymbol{\omega}}^{\mathrm{RT,G}} \right)^{\top} \boldsymbol{\Delta}\mathbf{v}_q^{\mathrm{G}} \right. \tag{4a}$$

$$\left. \text{subject to } \ \mathbf{v}_q^{\mathrm{G}} + \boldsymbol{\Delta}\mathbf{v}_q^{\mathrm{G}} = 0 \right\} \ \forall q. \tag{4b}$$

For given DA and RT natural gas market prices $\boldsymbol{\lambda}^{\mathrm{DA,G}} \in \mathbb{R}^{\mathcal{T}}$ and $\boldsymbol{\lambda}_{\boldsymbol{\omega}}^{\mathrm{RT,G}} \in \mathbb{R}^{\mathcal{T}}$ $\forall \omega$, the virtual bidder solves (4) to maximize her expected profit stemming from the price differences in DA and RT natural gas markets. Her decision variables are DA positions, i.e., $\mathbf{v}_q^{\mathrm{G}} \in \mathbb{R}^{\mathcal{T}}$ and RT positions, i.e., $\boldsymbol{\Delta}\mathbf{v}_q^{\mathrm{G}} \in \mathbb{R}^{\mathcal{T}}$. Recall that we assume that the virtual bidder has a perfect foresight into future DA and distribution of RT prices over scenarios. Equality constraint (4b) zeros out the DA and RT trades of the explicit virtual bidder. As an important observation, this explicit virtual bidder enforces the DA and the expected RT natural gas prices to be equal, i.e., $\boldsymbol{\lambda}^{\mathrm{DA,G}} = \sum_\omega \boldsymbol{\lambda}_{\boldsymbol{\omega}}^{\mathrm{RT,G}}$. This observation can be derived by the KKT optimality conditions associated with (4).

3.2.2 DA Natural Gas Market:

For given scheduled natural gas consumption of gas-fired generators as a function of $\mathbf{p}^{\mathrm{G}}$ obtained from the DA electricity market (2) and the DA trade of virtual bidders $\mathbf{v}_q^{\mathrm{G}}$ determined in (4), the natural gas market operator clears the DA market with $\mathcal{K}$ number of gas suppliers as

$$\min_{\mathbf{g}} \ e^{\top} \mathbf{C}^{\mathrm{G}} \mathbf{g} \ e \tag{5a}$$

$$\text{subject to } \ h(\mathbf{g}, \mathbf{p}^{\mathrm{G}}, \mathbf{v}_q^{\mathrm{G}}) = 0 : \boldsymbol{\lambda}^{\mathrm{DA,G}} \tag{5b}$$

$$g(\mathbf{g}) \leq 0, \tag{5c}$$

where (5) is a deterministic linear program. Parameters in the vector $\mathbf{C}^{\mathrm{G}} \in \mathbb{R}_{+}^{\mathcal{K}}$ represent the supply cost of gas suppliers, and variables in the matrix $\mathbf{g} \in \mathbb{R}_{+}^{\mathcal{T}\times\mathcal{K}}$ are the DA schedule of those suppliers. Objective function (5a) minimizes the total gas supply cost. Equality constraint (5b) represents the DA natural gas supply balance with inelastic demand including given gas demand for power production and virtual trade $\mathbf{v}_q^{\mathrm{G}}$. The "actual" natural gas prices are derived through dual variables $\boldsymbol{\lambda}^{\mathrm{DA,G}} \in \mathbb{R}^{\mathcal{T}}$, which are not necessarily identical to the estimated prices $\tilde{\boldsymbol{\lambda}}^{\mathrm{G}}$ used in the electricity market-clearing problems (2) and (3). Constraint (5c) enforces the lower and upper bounds on the gas supply. The detailed representation of constraints is provided in the online appendix (Schwele et al., 2020).

3.2.3 RT Natural Gas Market:

The natural gas operator clears the RT natural gas market to offset the change in fuel consumption of gas-fired generators $\boldsymbol{\Delta}\mathbf{p}_{\omega}^{\mathrm{G}}$ occurred under scenario ω. This deterministic linear problem writes as

$$\left\{ \min_{\boldsymbol{\Delta}\mathbf{g}_{\omega},\boldsymbol{\Delta}\mathbf{d}_{\omega}^{\mathrm{G}}} \; e^{\top}\mathbf{C}^{\mathrm{G}}\boldsymbol{\Delta}\mathbf{g}_{\omega}\; e + \mathbf{C}^{\mathrm{sh,G}^{\top}}\; \boldsymbol{\Delta}\mathbf{d}_{\omega}^{\mathrm{G}} \right. \tag{6a}$$

$$\text{subject to } \; h(\boldsymbol{\Delta}\mathbf{g}_{\omega}, \boldsymbol{\Delta}\mathbf{p}_{\omega}^{\mathrm{G}}, \boldsymbol{\Delta}\mathbf{d}_{\omega}^{\mathrm{G}}, \boldsymbol{\Delta}\mathbf{v}_{q}^{\mathrm{G}}) = 0 : \boldsymbol{\lambda}_{\boldsymbol{\omega}}^{\mathrm{RT,G}} \tag{6b}$$

$$\left. g(\boldsymbol{\Delta}\mathbf{g}_{\omega}, \boldsymbol{\Delta}\mathbf{d}_{\omega}^{\mathrm{G}}, \mathbf{g}) \leq 0 \right\} \forall\omega, \tag{6c}$$

where objective function (6a) minimizes the total balancing cost. The first balancing action is gas supply adjustment $\boldsymbol{\Delta}\mathbf{g}_{\omega} \in \mathbb{R}^{\mathcal{T}\times\mathcal{K}}$ whose cost is $\mathbf{C}^{\mathrm{G}} \in \mathbb{R}_{+}^{\mathcal{K}\times\mathcal{T}}$. The second but extreme balancing action is the natural gas load shedding $\boldsymbol{\Delta}\mathbf{d}_{\omega}^{\mathrm{G}} \in \mathbb{R}_{+}^{\mathcal{T}}$ at the comparatively high cost of $\mathbf{C}^{\mathrm{sh,G}} \in \mathbb{R}_{+}^{\mathcal{T}}$. Equality constraint (6b) balances the gas supply adjustments in RT. The actual natural gas RT prices under scenario ω are the vector of dual variables $\boldsymbol{\lambda}_{\boldsymbol{\omega}}^{\mathrm{RT,G}} \in \mathbb{R}^{\mathcal{T}}$. Constraints (6c) enforce the lower and upper bounds on gas supply, gas adjustments and gas load shedding. The detailed representation of constraints is given in the online appendix (Schwele et al., 2020).

3.3 Analysis of Stochastic Equilibrium Problems

In order to achieve temporal coordination, the profit-maximization problem of explicit virtual bidders as well as the DA and RT market-clearing optimization problems need to be solved simultaneously. Note that the explicit virtual bidders do not link the electricity and natural gas markets, but they will be linked later in Section 4 with implicit VB. For now, we can identify two stochastic equilibrium problems, one per energy sector. The first stochastic equilibrium problem related to the electricity sector includes optimization problems (1) $\forall r$, (2) and (3) $\forall\omega$. The second stochastic equilibrium problem corresponding

to the natural gas sector consists of (4) $\forall q$, (5) and (6) $\forall \omega$. Note that these two stochastic equilibrium problems should be solved sequentially, i.e., one should first solve (1)-(3), and then for given natural gas demands, (4)-(6) can be solved.

Remark 1 Each linear optimization problem (2), (3), (5) and (6) related to DA and RT market-clearing problems can be equivalently reformulated as a pure Nash equilibrium problem, wherein price-taking agents maximize their profit in a perfectly competitive market.

The KKT optimality conditions of each optimization problem (2), (3), (5) and (6) and its corresponding pure Nash equilibrium problem are identical – See Appendix A for more details.[4]

Remark 2 Both stochastic equilibrium problems (1)-(3) and (4)-(6) are GNE problems.

In both stochastic equilibrium problems, the feasible set of players depends on the decision of other players. For example, decisions of virtual bidders in (1), i.e., $\mathbf{v}_r^{\mathrm{E}}$ and $\boldsymbol{\Delta}\mathbf{v}_r^{\mathrm{E}}$, appear within the power balance constraints in (2) and (3). Replacing (2) and (3) with their equivalent Nash equilibrium problems (as mentioned in Remark 1) will not change the GNE nature of the overall problem, as the DA power schedule of generators affects the feasible set of those generators in their RT problem. This is a challenging issue, because a GNE problem is formulated as a quasi-variational inequality Pang and Fukushima (2005), which is generally hard to solve and admits multiple or even infinite solutions (Facchinei and Kanzow, 2007). (Facchinei and Kanzow, 2007; Harker and Pang, 1990; Harker, 1991; Schiro et al., 2013; Krawczyk, 2007; Fukushima, 2011) and (Kulkarni and Shanbhag, 2012) explore a specific class of GNE problems with *shared constraints*. However, the coupling constraints in our proposed stochastic equilibrium problems, i.e., (1)-(3), and (4)-(6), are not shared constraints.

Remark 3 Existence of a solution to the proposed stochastic GNE problems can be mathematically proven under some circumstances.

The basis of this proof relies upon (Harker, 1991, Theorem 1) and (Harker, 1991, Theorem 2), provided that the feasible set of every agent in the GNE problems is non-empty, convex and compact. In our case, this condition will be fulfilled only if we assume bounds on market prices, i.e., by imposing price floors and caps, and bounds on virtual trades, e.g., by imposing a budget constraint for each virtual bidder. The investigation of solution uniqueness for these GNE problems is not straightforward (Harker, 1991; Fukushima, 2011).

[4] As explained in Remark 1 and illustrated in Appendix A, each optimization problem (2), (3), (5) and (6) can be replaced by a set of optimization problems that constitute the corresponding Nash equilibrium problem. However, solving these problems simultaneously as the equilibrium problems (1)-(3) and (4)-(6) leads to coupled strategy sets and jeopardizes integrability of the equilibrium (Facchinei and Pang, 2007).

4 Sectoral and Temporal Coordination

In order to enhance the sectoral coordination between electricity and natural gas markets, this section extends the model in Section 3 and allows natural gas-fired generators to act as implicit virtual bidders. In other words, they are allowed to self-schedule outside the markets to optimally allocate their operational flexibility in the electricity market and their fuel consumption in the natural gas market. Each self-scheduler, i.e., implicit virtual bidder[5], maximizes her own expected profit. Similar to the explicit virtual bidders, we assume that each self-scheduler has a perfect foresight into DA and distribution of RT prices over scenarios in both electricity and natural gas markets. Note that including these self-schedulers in the model links the power and natural gas markets, so that a single stochastic equilibrium problem is achieved.

We consider both slow- and fast-starting types of gas-fired generators as potential self-schedulers. The difference between these two types of generators is that the slow-starting gas-fired units fix their unit commitment status in DA and cannot change it in the RT, while the fast-start units can. The expected profit maximization problem of each self-scheduling slow-starting gas-fired unit $\mathcal{G} \cap \mathcal{S}$ participating in both electricity and natural gas markets is

$$\max_{\mathbf{p},\mathbf{u},\mathbf{s},\boldsymbol{\Delta}\mathbf{p}_\omega} \quad \left(\boldsymbol{\lambda}^{\mathrm{DA,E}} - C(\boldsymbol{\lambda}^{\mathrm{DA,G}})\right)^\top \mathbf{p} - e^\top \mathbf{s} + \sum_\omega \pi_\omega \Big[\left(\boldsymbol{\lambda}^{\mathrm{RT,E}}_{\boldsymbol{\omega}} - C(\boldsymbol{\lambda}^{\mathrm{RT,G}}_{\boldsymbol{\omega}})\right) \Big]^\top \boldsymbol{\Delta}\mathbf{p}_\omega \tag{7a}$$

$$\text{subject to} \quad g(\mathbf{p},\mathbf{u},\mathbf{s}) \le 0 : \boldsymbol{\mu}, \tag{7b}$$

$$g(\boldsymbol{\Delta}\mathbf{p}_\omega,\mathbf{p},\mathbf{u}) \le 0 : \boldsymbol{\nu}_\omega, \ \ \forall\omega, \tag{7c}$$

where (7) is a two-stage stochastic linear program, whose objective function (7a) maximizes the expected profit of the underlying self-scheduling gas-fired generator. Note that this objective function includes the actual DA and RT gas prices $\boldsymbol{\lambda}^{\mathrm{DA,G}}$ and $\boldsymbol{\lambda}^{\mathrm{RT,G}}_{\boldsymbol{\omega}}$ from models (5) and (6), and not the estimated gas price $\tilde{\boldsymbol{\lambda}}^{\mathrm{G}}$. This problem is subject to the DA (7b) and RT operational constraints (7c), so that the final production of gas-fired units in RT have to lie within their feasible operational limits.

Similarly, each fast-start self-scheduling gas-fired unit $\mathcal{G} \cap \mathcal{F}$ solves a two-stage stochastic linear program to maximize her expected profit as

$$\max_{\substack{\mathbf{p},\mathbf{u},\mathbf{s},\boldsymbol{\Delta}\mathbf{p}_\omega,\\ \boldsymbol{\Delta}\mathbf{u}_\omega,\boldsymbol{\Delta}\mathbf{s}_\omega}} \quad \left(\boldsymbol{\lambda}^{\mathrm{DA,E}} - C(\boldsymbol{\lambda}^{\mathrm{DA,G}})\right)^\top \mathbf{p} - e^\top \mathbf{s} + \sum_\omega \pi_\omega \Big[\left(\boldsymbol{\lambda}^{\mathrm{RT,E}}_{\boldsymbol{\omega}} - C(\boldsymbol{\lambda}^{\mathrm{RT,G}}_{\boldsymbol{\omega}})\right)^\top \boldsymbol{\Delta}\mathbf{p}_\omega + e^\top \boldsymbol{\Delta}\mathbf{s}_\omega \Big] \tag{8a}$$

$$\text{subject to} \quad g(\mathbf{p},\mathbf{u},\mathbf{s}) \le 0 : \boldsymbol{\mu}, \tag{8b}$$

$$g(\boldsymbol{\Delta}\mathbf{p}_\omega,\boldsymbol{\Delta}\mathbf{u}_\omega,\boldsymbol{\Delta}\mathbf{s}_\omega,\mathbf{p},\mathbf{u}) \le 0 : \boldsymbol{\nu}_\omega, \ \ \forall\omega. \tag{8c}$$

[5] In the rest of the manuscript we use the terms implicit virtual bidder and self-scheduler interchangeably.

The resulting stochastic GNE problem includes optimization problems (2), (3) $\forall\omega$, (5), (6) $\forall\omega$, (7) and (8). Note that in this stochastic equilibrium problem, the decisions of self-schedulers $\mathbf{p}$, and $\mathbf{\Delta p}_\omega$ in (7) and (8) are exogenous values within the market-clearing problems (2), (3), (5) and (6).

Remark 4 In a case including both implicit and explicit VB, if the dispatch of self-schedulers in DA is restricted by constraint (7b) or (8b), then the stochastic equilibrium problem will be feasible if and only if such DA constraints are inactive. Any non-zero dual variable corresponding to the DA constraints of self-schedulers will make the stochastic equilibrium problem infeasible.

Proposition 1 *Self-scheduling in* (7) *and* (8) *respecting both DA and RT operational constraints and explicit VB according to* (1) *and* (4) *are mutually exclusive, i.e. cannot coincide or exist together.*

Proof. The KKT optimality conditions of the problem of each virtual bidder (1) and (4) enforce DA and expected RT prices to be equal, i.e., $\boldsymbol{\lambda}^{\mathrm{DA,E}} = \sum_\omega \pi_\omega \, \boldsymbol{\lambda}_\omega^{\mathrm{RT,E}}$ and $\boldsymbol{\lambda}^{\mathrm{DA,G}} = \sum_\omega \pi_\omega \, \boldsymbol{\lambda}_\omega^{\mathrm{RT,G}}$. The KKT optimality conditions of each self-scheduler if her DA dispatch is restricted enforce $C(\boldsymbol{\lambda}^{\mathrm{DA,G}}) - \boldsymbol{\lambda}^{\mathrm{DA,E}} + \boldsymbol{\mu} + \sum_\omega \boldsymbol{\nu}_\omega = 0$ and $C(\boldsymbol{\lambda}_\omega^{\mathrm{RT,G}}) - \boldsymbol{\lambda}_\omega^{\mathrm{RT,E}} + \boldsymbol{\nu}_\omega = 0, \forall\omega$. Consequently, these KKTs enforce that $\boldsymbol{\lambda}^{\mathrm{DA,E}} + \boldsymbol{\mu} = \sum_\omega \boldsymbol{\lambda}_\omega^{\mathrm{RT,E}}$, so that if both explicit virtual bidders and self-schedulers are included at the same time, the problem is feasible only if $\boldsymbol{\mu} = 0$. This implies that DA constraints of self-schedulers are inactive. See online appendix (Schwele et al., 2020) for more details. □

Including explicit and implicit VB requires solving (1)-(8) as a GNE problem by neglecting the operational bounds of self-schedulers in DA, i.e., (7b) and (8b). Self-schedulers can submit physical and virtual bids as long as their positions in RT adhere to their feasible operational limits, thus acting as implicit virtual bidders.

5 Ideal Benchmark

We compare the proposed "soft" market-based mechanism for power and natural gas coordination to the ideal benchmark of a fully stochastic integrated energy market clearing. This ideal benchmark is indeed a disruptive solution to achieve a full temporal and sectoral coordination, which ignores the current market sequences. Assuming that the given set of scenarios is a good representation of the probability distribution of uncertainty, the stochastic market clearing efficiently makes informed DA decisions by anticipating the potential recourse actions in RT (Pritchard et al., 2010; Morales et al., 2012; Zakeri et al., 2019; Zavala et al., 2017). In this benchmark, the fully integrated power and natural gas system is co-optimized under complete exchange of operational information. The resulting two-stage stochastic linear program aims at minimizing the total expected operational cost of both sectors in DA and RT,

and writes as

$$\min_{\substack{\mathbf{p},\mathbf{u},\mathbf{s},\mathbf{w},\mathbf{g},\boldsymbol{\Delta}\mathbf{p}_\omega,\\ \boldsymbol{\Delta}\mathbf{u}_\omega,\boldsymbol{\Delta}\mathbf{s}_\omega,\boldsymbol{\Delta}\mathbf{w}_\omega,\\ \boldsymbol{\Delta}\mathbf{d}^{\mathrm{E}}_\omega,\boldsymbol{\Delta}\mathbf{g}_\omega,\boldsymbol{\Delta}\mathbf{d}^{\mathrm{G}}_\omega}} \; e^\top \mathbf{p}^{\mathrm{C}}\mathbf{C}^{\mathrm{E}} + e^\top \mathbf{s}\; e + e^\top \mathbf{C}^{\mathrm{G}}\mathbf{g}\; e + \sum_\omega \pi_\omega \Big(e^\top \boldsymbol{\Delta}\mathbf{p}_\omega \mathbf{C}^{\mathrm{E}} + e^\top \boldsymbol{\Delta}\mathbf{s}_\omega\; e$$

$$+ \mathbf{C}^{\mathrm{sh,E}^\top}\; \boldsymbol{\Delta}\mathbf{d}^{\mathrm{E}}_\omega + e^\top \mathbf{C}^{\mathrm{G}} \boldsymbol{\Delta}\mathbf{g}_\omega\; e + \mathbf{C}^{\mathrm{sh,G}^\top}\; \boldsymbol{\Delta}\mathbf{d}^{\mathrm{G}}_\omega \Big) \Big] \tag{9a}$$

$$\text{subject to} \;\; (2\mathrm{b}), (2\mathrm{c}), (5\mathrm{b}), (5\mathrm{c}), \tag{9b}$$

$$(3\mathrm{b}), (3\mathrm{c}), (6\mathrm{b}), (6\mathrm{c}), \;\; \forall \omega. \tag{9c}$$

Objective function (9a) minimizes the total DA system cost for power production and gas supply as well as the expected RT balancing costs in both sectors, while respecting the operational constraints in DA (9b) and in RT (9c) for each scenario. The stochastic optimization problem (9) can be equivalently reformulated as a pure Nash equilibrium problem, wherein each market player is a stochastic decision-maker, who maximizes her expected profit with respect to DA and RT operational constraints with perfect information regarding uncertainty and prices in both sectors.

Remark 5 The GNE problem (1)-(8) defined in Section 4 including explicit and implicit VB is not necessarily equal to the ideal benchmark (9), since their KKTs are different.

Recall that the GNE problem enforces convergence of DA and expected RT prices in both power and natural gas sectors through the optimality conditions of explicit virtual bidders. On the contrary, in the stochastic market clearing problem (9), the DA and RT prices converge in expectation *only if* all DA operational inequalities are non-binding, i.e., every market player acts as an unrestrained arbitrager between DA and RT markets. This can be easily explored by checking the KKT optimality conditions associated with (9).

The co-optimization of power and natural gas system correctly accounts for the impact of natural gas prices on the merit order of the electricity supply curve. Allowing all gas-fired units to self-schedule in the sequential setup with perfect knowledge over both natural gas and electricity prices approximates system integration. This is further explored in the following proposition.

Proposition 2 *If DA operational bounds on* $\mathbf{p}, \mathbf{u}, \mathbf{w}, \mathbf{g}$ *in the stochastic optimization problem* (9) *are non-binding, the DA and the RT prices converge in expectation (i.e.,* $\boldsymbol{\lambda}^{E,DA} = \sum_\omega \pi_\omega \boldsymbol{\lambda}^{E,RT}_{\boldsymbol{\omega}}$ *and* $\boldsymbol{\lambda}^{G,DA} = \sum_\omega \pi_\omega \boldsymbol{\lambda}^{G,RT}_{\boldsymbol{\omega}}$*) and the outcomes of* (9) *are equal to the GNE problem* (1)-(8) *when all gas-fired units are implicit virtual bidders.*

Proof. This is proven by demonstrating that the KKT optimality conditions of the two problems above under the conditions mentioned are identical – See online appendix (Schwele et al., 2020) for more details. □

Table 1 summarizes all models introduced. While sequential and ideal benchmark can be solved as linear programs (LP), all other models are recast as mixed complementarity problems (MCP) by concatenating all KKT conditions from the respective optimization models.

Table 1 Summary of market setup models.

Market setup	Name	Model	Optimization	Equilibrium	Model type
Sequential	*Seq*	(2)	✓	−*	LP
		(5)	✓	−*	LP
		(3) $\forall\omega$	✓	−*	LPs
		(6) $\forall\omega$	✓	−*	LPs
Sequential with explicit virtual bidding	*Seq+eVB*	(1) $\forall r$, (2), (3) $\forall\omega$	−	GNE	MCP
		(4) $\forall q$, (5), (6) $\forall\omega$	−	GNE	MCP
Sequential with implicit virtual bidding	*Seq+iVB*	(2), (3) $\forall\omega$, (5), (6) $\forall\omega$, (7), (8)	−	GNE	MCP
Sequential with both explicit and implicit virtual bidding	*Seq+VB*	(1) $\forall r$, (2), (3) $\forall\omega$, (4) $\forall q$, (5), (6) $\forall\omega$, (7a), (7c) , (8a), (8c)	−	GNE	MCP
Ideal benchmark	*Ideal*	(9)	✓	−*	LP

*There exists a pure Nash equilibrium (NE) which is equivalent to the optimization problem, see Appendix.

6 Numerical Results

This section provides a case study to analyze and compare the proposed market setups presented in Sections 3, 4 and 5, which are summarized in Table 1. We solve all models using an Intel CoreTM i7-7820HQ with four processors clocking at 2.70 GHz and 16 GB of RAM in GAMS using PATH and CPLEX solver for MCP and LP models, respectively. The CPU time for LP models is below 1 second, while that time for different MCPs varies between 1 and 800 seconds. See online appendix (Schwele et al., 2020) for further details.

6.1 Input Data

This case study contains a power system with 6 non gas-fired generators (namely, $\mathcal{C}^1$ to $\mathcal{C}^6$) and 4 gas-fired generators (namely, $\mathcal{G}^1$ to $\mathcal{G}^4$). These gas-fired generators connect the power system to a natural gas system with four gas suppliers, namely $\mathcal{K}_1$ to $\mathcal{K}_4$. We consider a 24-hour time horizon. All technical details of generators and natural gas suppliers as well as the total hourly demand in both power and natural gas sectors are provided in the online appendix (Schwele et al., 2020). Note that the demand in both sectors is certain, and the only source of uncertainty is assumed to be the wind power. Wind forecast and scenarios are also given in the online appendix. The natural gas supply curve is shown in Fig. 4, which is the same throughout all 24 hours. Fig. 5 illustrates the shifting of the electricity merit order curve due to a potential change in the natural gas price. The reason for this shift is that the gas price affects the marginal production cost of the gas-fired generators. Since in both DA and RT stages, the electricity market is cleared before the natural gas market, the electricity market operator needs an estimation of the gas price. In the following, we assume that the electricity market operator uses the average gas supply cost, i.e., \$2.5/kcf, as a deterministic and static estimation of the natural gas prices in both DA and RT. The value of lost load in the electricity and natural gas sectors are set to \$600/MWh and \$300/kcf, respectively. The wind power penetration, i.e., total wind power capacity installed divided by the total electricity demand, is 34%. The next subsections provide the market outcomes obtained from different setups.

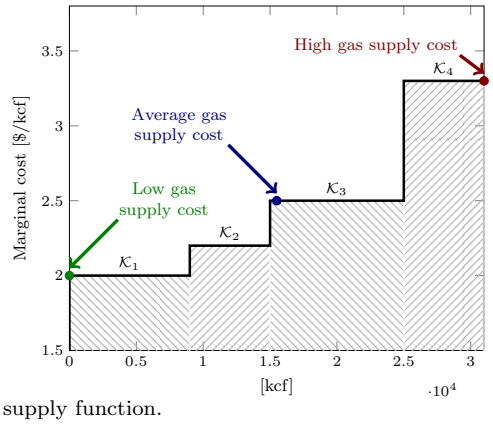

Fig. 4 Natural gas supply function.

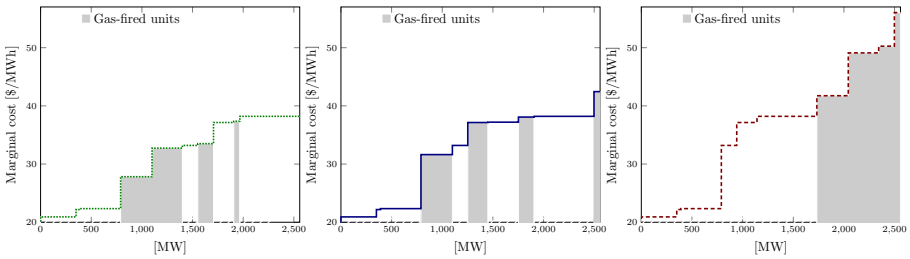

Fig. 5 Electricity merit order depending on natural gas price. The plots on the left-hand, middle, and right-hand sides show the merit order corresponding to the low, average and high prices for natural gas (as illustrated in Fig. 4), respectively.

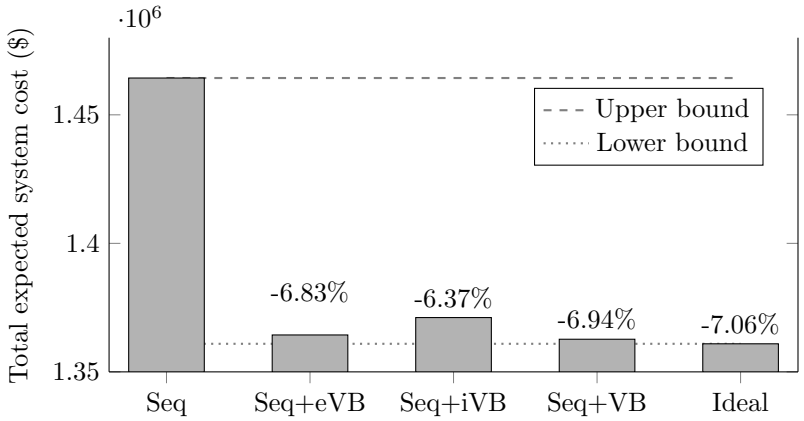

Fig. 6 Total expected cost of the electricity and natural gas systems calculated by (9a) under different market setups. The percentages show the reduction in the total expected system cost compared to that cost in the fully uncoordinated sequential setup (first bar).

6.2 Main Results: Total Expected System Cost

The total expected cost of electricity and natural gas systems achieved under different market setups is shown in Fig. 6. As expected, the highest system

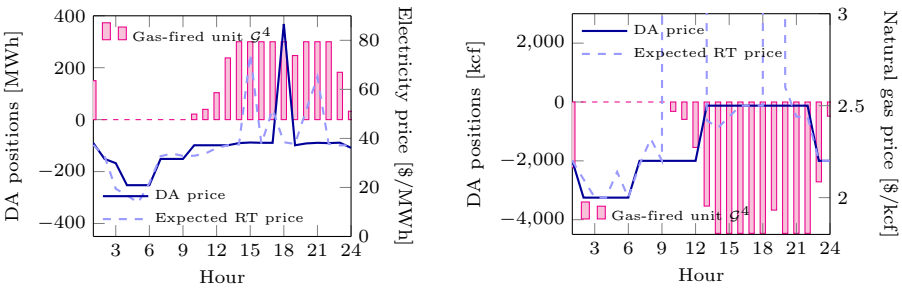

Fig. 7 Hourly DA schedule of slow-start gas-fired generator $\mathcal{G}^4$ as well as DA and expected RT market-clearing prices obtained from fully uncoordinated sequential market setup *Seq*. The left- and right-hand side plots correspond to the electricity and natural gas market outcomes, respectively.

cost corresponds to the sequential setup *Seq* (first bar in Fig. 6), which is a fully uncoordinated model. On the other hand, the fully coordinated ideal model (i.e., last bar in Fig. 6) yields the lowest cost. In this case study, the full temporal and sectoral coordination results in a 7.06% cost reduction. The three proposed setups *Seq+eVB*, *Seq+iVB* and *Seq+VB* provide partial coordination, and therefore, the system cost achieved in those setups is between the upper and lower bounds. Among these three market setups, *Seq+VB* with both implicit and explicit VB yields the highest cost saving, which is 6.94% (fourth bar in Fig. 6). Out-of-sample simulation relaxes our assumptions of perfect knowledge of virtual bidders. An analysis of out-of-sample performance can be found in the online appendix (Schwele et al., 2020). In the following three subsections, we discuss in details how each market setup impacts the DA schedules. For clarity, we focus on DA dispatch of one of the slow-start gas-fired generators, i.e., $\mathcal{G}^4$, and analyze how each market setup affects her dispatch, and therefore her individual expected profit.

6.3 Upper Bound: Sequential Market Setup (*Seq*)

The corresponding market-clearing outcomes of the fully uncoordinated sequential market setup *Seq* are given in Fig. 7. The DA schedules in this setup have no foresight into uncertainty in the RT operation and sectoral interactions between the two systems. Thus, the DA and expected RT prices can significantly differ. An example of such case is the electricity market price during hours 14 to 22 in the left-hand side plot and the natural gas market price during hours 9 to 13 and 18 to 20 in the right-hand side plot of Fig. 7. The slow-start gas-fired generator $\mathcal{G}^4$ is dispatched in the DA electricity market myopically, without considering the volatility of the actual hourly natural gas price and the need for flexibility provided by $\mathcal{G}^4$ in RT. This generator is scheduled in hours 10 to 13 relying on the comparatively low estimated gas price, while her real production cost is higher due to comparatively high natural gas market prices. When power system flexibility is required, which is evident from the

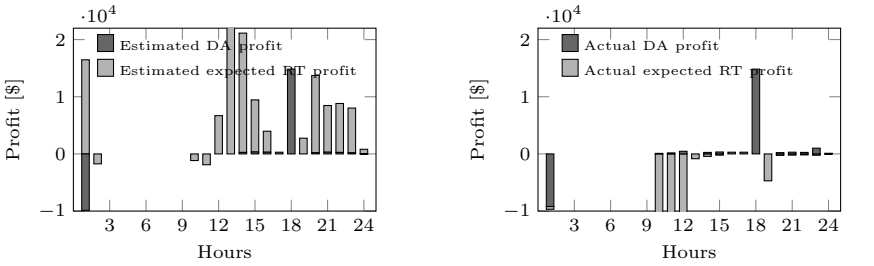

Fig. 8 Hourly profit in DA and in expectation in RT of slow-start gas-fired generator $\mathcal{G}^4$ obtained from fully uncoordinated sequential market setup *Seq*. The left-hand plot shows the estimated profits using natural gas price estimations while the actual profits for realized natural gas prices are depicted on the right-hand side.

	Seq	*Seq+eVB*	*Seq+iVB* (self-scheduling by $\mathcal{G}^4$)	*Seq+VB* (implicit VB by $\mathcal{G}^4$)	*Ideal*
$\mathcal{C}^1$	14,078	13,693	13,499	13,411	12,410
$\mathcal{C}^2$	18,713	18,180	22,330	17,623	16,362
$\mathcal{C}^3$	26,029	8,673	36,920	11,099	8,673
$\mathcal{C}^4$	711	254	693	494	0
$\mathcal{C}^5$	134,062	126,703	127,079	123,956	115,180
$\mathcal{C}^6$	90,417	85,375	81,230	84,315	76,314
$\mathcal{G}^1$	-198,988	6,608	10,661	8,003	8,960
$\mathcal{G}^2$	1,267	0	-809	0	0
$\mathcal{G}^3$	11,127	6,332	5,564	5,535	4,177
$\mathcal{G}^4$	-529,059	4,878	11,415	8,319	8,833

Table 2 Expected profit of each generator under different market setups

high expected RT electricity prices in hours 14 and 20, generator $\mathcal{G}^4$ is unable to provide upward adjustment since she is already dispatched at full capacity in DA. Apart from the high expected system cost, this inefficient DA dispatch results in a negative expected profit (-$529,059) for $\mathcal{G}^4$, as given in Table 2. The faulty estimation of natural gas prices when clearing the electricity market leads to underestimating power generation costs and overestimating the profits of $\mathcal{G}^4$ in RT, such that $\mathcal{G}^4$ actually operates at negative profits in RT, see Fig. 8. This illustrates the need for market coordination, and specifically the potential of scheduling power generators in DA more efficiently.

6.4 Lower Bound: Ideal Benchmark (*Ideal*)

In this ideal stochastic co-optimization model, the DA decisions are made while perfectly foreseeing uncertainty in RT as well as the sectoral interdependencies. As given in Fig. 9, the DA and expected RT prices converge in both power and natural gas sectors. The fully efficient DA dispatch in this ideal market setup ends up to a non-negative expected profit for all generators (see Table 2), including $\mathcal{G}^4$ whose expected profit is $8,833.

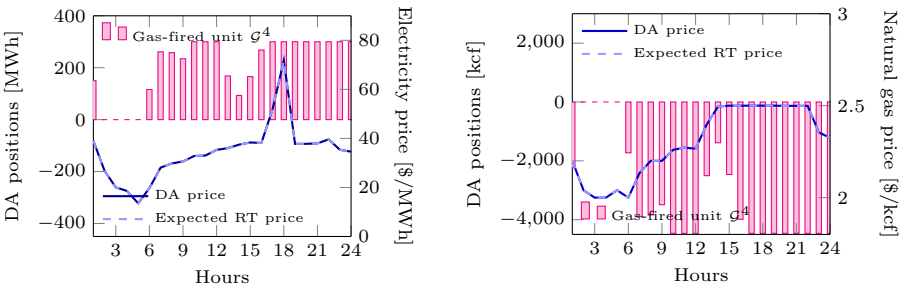

Fig. 9 Hourly DA schedule of slow-start gas-fired generator $\mathcal{G}^4$ as well as DA and expected RT market-clearing prices obtained from fully coordinated market setup *Ideal*. The left- and right-hand side plots correspond to the electricity and natural gas market outcomes, respectively.

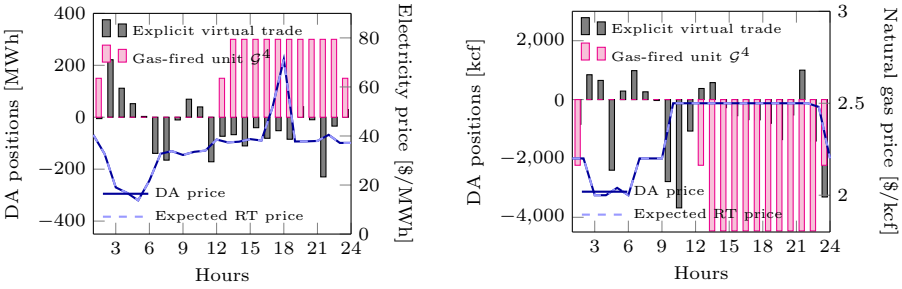

Fig. 10 Hourly DA schedule of explicit virtual bidder (i.e., the purely financial player) and slow-start gas-fired generator $\mathcal{G}^4$ as well as DA and expected RT market-clearing prices obtained from market setup *Seq+eVB*. The left- and right-hand side plots correspond to the electricity and natural gas market outcomes, respectively.

6.5 Temporal Coordination: *Seq+eVB*

Recall that the market setup *Seq+eVB* provides the DA-RT temporal (but not sectoral) coordination by allowing explicit VB in both electricity and natural gas markets. Note that it is sufficient to consider a single explicit virtual bidder only in each sector since the transmission network is not considered. The hourly amount of DA virtual bids in both sectors is shown in Fig. 10. The virtual bidders act as either buyers or sellers over the 24 hours in the DA market. For example, the virtual bidder in DA electricity market acts as a seller in hours 3-6, 10, 11, 20, and 24, while as a buyer in the rest of hours as illustrated in the left-hand plot of Fig. 10. The DA positions of this player are going to be zeroed out by her RT actions. Practically, this means that every MWh the virtual bidder sells in DA in hours 3-6, 10, 11, 20, and 24 will be bought back in the same hours in RT. The right-hand plot of Fig. 10 shows that in the DA natural gas market, the virtual bidder acts as a supplier in most hours. She behaves as a natural gas consumer only in hours 5, 10, 11 and 24. Note that allowing explicit VB achieves full convergence of DA and expected RT prices

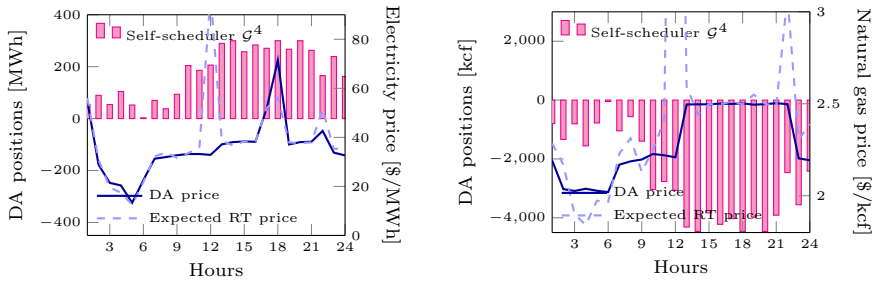

Fig. 11 Hourly DA schedule of slow-start gas-fired generator $\mathcal{G}^4$ as well as DA and expected RT market-clearing prices obtained from market setup *Seq+iVB*. Generator $\mathcal{G}^4$ does self-scheduling. The left- and right-hand side plots correspond to the electricity and natural gas market outcomes, respectively.

in both power and gas markets. Explicit VB also impacts the DA dispatch of generators. For example, the slow-start gas-fired generator $\mathcal{G}^4$ is no longer dispatched between hours 2 and 11, while she is fully dispatched in hours 13 to 22. Explicit VB alone decreases the total expected system cost, but to the disadvantage of several individual generators. For example, the expected profit most generators decreases compared to the fully coordinated sequential model and only gas-fired generators $\mathcal{G}^1$ and $\mathcal{G}^4$ are better off.

6.6 Temporal and Sectoral Coordination: *Seq+iVB* and *Seq+VB*

The efficient dispatch of market players operating on the interface of electricity and natural gas sectors can enhance the sectoral coordination. A foresighted schedule of gas-fired generators in the DA electricity market may improve not only the temporal coordination with the RT electricity market, but also the sectoral coordination with the DA natural gas market. We analyze below the two market setups *Seq+iVB* and *Seq+VB* separately.

6.6.1 Self-scheduling Gas-fired Generators: Seq+iVB

As realized in the previous subsections, the DA dispatch of gas-fired generator $\mathcal{G}^4$ in setup *Seq* is inefficient, such that she ends up to a negative expected profit. This shows the significant potential for this generator to do self-schedule, rather than participating in the markets relied upon a deterministic sequential clearing procedure. Fig. 11 shows the DA dispatch and market outcomes when generator $\mathcal{G}^4$ acts as an implicit virtual bidder. Note that in this setup, the implicit virtual bidder has to still respect her operational constraints in both DA and RT stages. This restriction will be relaxed later in setup *Seq+VB*. According to Fig. 11, generator $\mathcal{G}^4$ increases her production during hours 1 to 13 when the actual natural gas price is comparatively low, whereas she reduces her power production and consequently natural gas consumption when the gas price is comparatively high in hours 14 to 24. As

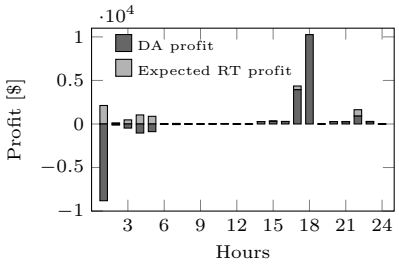

Fig. 12 Hourly profit in DA and in expectation in RT of slow-start gas-fired generator $\mathcal{G}^4$ self-scheduling in the sequential market setup *Seq+iVB*.

presented in Fig. 12, allowing this gas-fired generator to self-schedule alone increases her expected profit to \$11,415. Moreover, the total social welfare is improved in terms of reducing the non-negative expected profits for other generators and reducing the total expected system cost by 6.37% (third bar in Fig. 6). Another important observation is that the self-scheduling by $\mathcal{G}^4$ causes shrinking the price spread between DA and expected RT prices in both power and gas sectors.

6.6.2 Explicit and Implicit Virtual Bidding: Seq+VB

This setup allows explicit VB by purely financial players and implicit VB by gas-fired generator $\mathcal{G}^4$. Fig. 13 shows that the explicit and implicit VBs together achieve full price convergence in expectation in both power and natural gas markets. When generator $\mathcal{G}^4$ is allowed to submit virtual bids in the electricity and natural gas markets, the amount of explicit virtual trade decreases significantly in the electricity market and almost disappears in the natural gas market compared to Fig. 10. Note that $\mathcal{G}^4$ extends her bidding behaviour in the DA electricity and natural gas markets beyond her operational constraints acting as an implicit virtual bidder. For example, virtual bids are submitted to act as an electricity consumer and natural gas producer in the DA markets, e.g., in hours 3, 4 and 9. More specifically, she bids in DA below her operational capacity in hours 3, 4 and 9 and above her capacity in hours 12, 13, and 19-21. The convergence of DA and expected RT prices indicates full temporal coordination. Moreover, the additional system cost reduction compared to the case with explicit VB only (see second and fourth bars in Fig. 6) suggests improved sectoral coordination. All generators can expect a non-negative expected profit in this market setup with both implicit and explicit VB. The implicit virtual bidder $\mathcal{G}^4$ expects to earn \$8,319. Although this generator can extend her bidding activity beyond her operational constraints in DA, her expected profit is lower than that in a case when $\mathcal{G}^4$ is the only self-scheduler in the market setup without explicit VB (*Seq+iVB*). However, when explicit VB is allowed (*Seq+iVB* and *Seq+VB*), generator $\mathcal{G}^4$ is better off by submitting virtual bids, see Table 2.

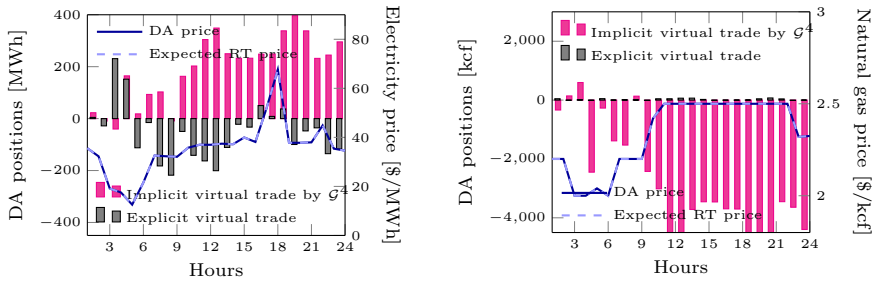

Fig. 13 Hourly DA schedule of explicit (i.e., purely financial player) and implicit virtual bidder (i.e., generator $\mathcal{G}^4$) as well as DA and expected RT market-clearing prices obtained from market setup *Seq+VB*. The left- and right-hand side plots correspond to the electricity and natural gas market outcomes, respectively.

6.7 Main Observations

Based on the above results, allowing market players to arbitrage seems to enhance the coordination of sectors and trading floors. The inclusion of explicit VB results in generating better price signals that reflect the uncertainties inherent in the RT stages. These price signals improve DA schedules so that the existing flexibility is allocated and utilized more efficiently. The VB improves the temporal coordination of the sequential DA and RT markets in the electricity and natural gas sectors. The self-scheduling gas-fired generator strengthens the temporal coordination of DA and RT markets by decreasing the price spread and improves the sectoral coordination by making use of her superior information of natural gas prices. In the same manner, the implicit VB by gas-fired generators helps sectoral coordination between the electricity and natural gas markets and improves the temporal coordination between DA and RT markets. Such a gas-fired generator is able to arbitrage both between the trading floors and between the sectors by submitting virtual bids in the electricity and natural gas markets. That way the coordination between the sectors flourishes via better information exchange. More specifically, better price signals and improved DA schedules help allocate and utilize the existing flexibility more efficiently. The DA schedules are improved through bidding activities that better reflect the uncertainties and that take into account the interactions of power and gas sectors.

7 Conclusion

This work explores the capability of financial instruments via VB either by purely financial players (explicit VB) or by physical players like gas-fired generators (implicit VB) in improving the temporal and sectoral coordination in two-stage (DA and RT) electricity and natural gas markets under uncertainty. We use two models as benchmarks: a fully uncoordinated sequential model which achieves an upper bound for the total expected system cost, and

a stochastic ideal co-optimization which provides full temporal and sectoral coordination and yields a lower bound for the total expected system cost. The resulting models with VB are equilibrium problems, including the deterministic market-clearing problems in DA and RT in both power and gas sectors, and the two-stage stochastic optimization problems of virtual bidders, who maximize their expected profit.

Our results reveal that competitive virtual bidders who have prefect insight into the probability distribution of RT prices in power and natural gas markets increase the efficiency of deterministic sequential markets, such that the resulting total expected system cost is between the lower and upper bounds. In our case study, it is illustrated that the inclusion of virtual bidding can result in an expected system cost that is very close to the lower bound. In particular, the explicit VB provides a temporal coordination of the DA and RT stages in power and natural gas markets. Moreover, implicit VB by gas-fired generators brings both temporal and sectoral coordination. This implies that the sequential market with VB may approximate the stochastic ideal integrated energy system, and help reveal and exploit the existing flexibility in the systems more efficiently.

The main policy implication is that a disruptive market re-design to a stochastic and integrated energy market might not be necessarily crucial for unlocking the existing flexibility. Instead, this can be done to some extent via financial instruments by allowing VB, while preserving the current sequential market-clearing setup.

As potential future works, it is of high interest to relax the assumption that explicit and implicit virtual bidders have perfect knowledge of the probability distribution of real-time prices. This requires modeling the potential information asymmetry in the equilibrium model (Lo Prete et al., 2019b; Dvorkin Jr et al., 2019). It is also important to analyze the cases where virtual bidders behave as strategic and/or risk-averse players. The proposed equilibrium may become computationally hard to solve if more players and scenarios are considered, and thus more efficient solution techniques might be required. One potential solution can be distributed optimization by solving the problem as an iterative Walrasian auction, e.g., similar to the methods used in (Mays et al., 2019; Höschle et al., 2018), but the GNE nature of the model may bring some computational challenges. The other potential extension is to include network constraints, especially in the natural gas sector as it allows modeling linepack (stored gas in the pipelines). However, it will need either approximation (Ordoudis et al., 2019; Correa-Posada and Sánchez-Martín, 2015) or relaxation (Schwele et al., 2019) methods to convexify the linepack model.

Appendix

The linear optimization problem (2) can be equivalently reformulated as a pure Nash equilibrium problem of profit maximizing agents, namely (10). For given market prices $\boldsymbol{\lambda}^{\mathrm{DA,E}}$, each non gas-fired generator $\mathcal{C}$ maximizes her DA

profit with respect to her operational constraints as

$$\max_{\mathbf{p}^{\mathrm{C}},\mathbf{u}^{\mathrm{C}},\mathbf{s}^{\mathrm{C}}} \quad \left(\boldsymbol{\lambda}^{\mathrm{DA,E}} - \boldsymbol{C}^{\mathrm{E}}\right)^{\top} \mathbf{p}^{\mathrm{C}} - e^{\top}\mathbf{s}^{\mathrm{C}} \tag{10a}$$

$$\text{subject to} \quad g(\mathbf{p}^{\mathrm{C}}, \mathbf{u}^{\mathrm{C}}, \mathbf{s}^{\mathrm{C}}) \leq 0. \tag{10b}$$

Similarly, each gas-fired generator $\mathcal{G}$ maximizes her DA profit as:

$$\max_{\mathbf{p}^{\mathrm{G}},\mathbf{u}^{\mathrm{G}},\mathbf{s}^{\mathrm{G}}} \quad \left(\boldsymbol{\lambda}^{\mathrm{DA,E}} - C(\tilde{\boldsymbol{\lambda}}^{\mathrm{G}})\right)^{\top} \mathbf{p}^{\mathrm{G}} - e^{\top}\mathbf{s}^{\mathrm{G}} \tag{10c}$$

$$\text{subject to} \quad g(\mathbf{p}^{\mathrm{G}}, \mathbf{u}^{\mathrm{G}}, \mathbf{s}^{\mathrm{G}}) \leq 0. \tag{10d}$$

Likewise, each wind farm $\mathcal{J}$ maximizes her DA profit limited by her deterministic wind forecast in DA as

$$\max_{\mathbf{w}} \quad \boldsymbol{\lambda}^{\mathrm{DA,E}^{\top}} \mathbf{w} \tag{10e}$$

$$\text{subject to} \quad g(\mathbf{w}) \leq 0, \tag{10f}$$

and eventually, for given production decisions of conventional and wind generators and dispatch of virtual bidders, a price-setting agent determines the DA electricity price $\boldsymbol{\lambda}^{\mathrm{DA,E}}$ as

$$\min_{\boldsymbol{\lambda}^{\mathrm{DA,E}}} \quad \boldsymbol{\lambda}^{\mathrm{DA,E}^{\top}} h(\mathbf{p}, \mathbf{w}, \mathbf{v}_r^{\mathrm{E}}). \tag{10g}$$

The Karush-Kuhn-Tucker (KKT) optimality conditions of optimization problem (2) and pure Nash equilibrium problem (10) are identical – See online appendix (Schwele et al., 2020) for more details.

In the same manner, the RT market-clearing optimization problem (3) under scenario ω can be equivalently reformulated as a pure Nash equilibrium problem. Note that in such an equilibrium problem, each agent's DA schedule is fixed. For example, the slow-starting non gas-fired generators $\mathcal{C} \cap \mathcal{S}$ maximize their profit in RT with respect to their DA commitment decisions as

$$\left\{ \max_{\boldsymbol{\Delta}\mathbf{p}_{\omega}^{\mathrm{C}}} \quad \left(\boldsymbol{\lambda}_{\boldsymbol{\omega}}^{\mathrm{RT,E}} - \mathbf{C}^{\mathrm{E}}\right)^{\top} \boldsymbol{\Delta}\mathbf{p}_{\omega}^{\mathrm{C}} \right. \tag{11a}$$

$$\left. \text{subject to} \quad g(\boldsymbol{\Delta}\mathbf{p}_{\omega}^{\mathrm{C}}, \mathbf{p}^{\mathrm{C}}, \mathbf{u}^{\mathrm{C}}) \leq 0, \right\} \forall \omega. \tag{11b}$$

Optimization problems (5) and (6) can also be equivalently reformulated as pure Nash equilibrium problems, in which every agent maximizes her own profit and a price-setter agent determines the price, similar to Proposition 1 – see online appendix (Schwele et al., 2020) for more details.

Acknowledgements We thank Benjamin F. Hobbs and Stefanos Delikaraoglou for thoughtful discussions about the initial model. We also thank Kenneth Bruninx and Anubhav Ratha for providing constructive feedback on previous drafts. We are very grateful to Uday V. Shanbhag, Maryam Kamgarpour and Jong Shi Pang for their fruitful inputs on generalized Nash equilibrium model. Finally, we thank Yves Smeers and Ibrahim Abada for their helpful comments at the 23rd International Symposium on Mathematical Programming (ISMP 2018). The work was supported by the EUD Programme through the 'Coordinated Operation of Integrated Energy Systems (CORE)' project under the grant 64017-0005.

References

Birge J, Hortaçsu A, Mercadal I, Pavlin M (2018) Limits to arbitrage in electricity markets: A case study of MISO. Energy Economics 75:518–533

Byeon G, Van Hentenryck P (2020) Unit commitment with gas network awareness. IEEE Transactions on Power Systems 35(2):1327–1339

Chen R, Wang J, Sun H (2017) Clearing and pricing for coordinated gas and electricity day-ahead markets considering wind power uncertainty. IEEE Transactions on Power Systems 33:2496–2508

Conejo AJ, Nogales FJ, Arroyo JM, García-Bertrand R (2004) Risk-constrained self-scheduling of a thermal power producer. IEEE Transactions on Power Systems 19(3):1569–1574

Correa-Posada CM, Sánchez-Martín P (2015) Integrated power and natural gas model for energy adequacy in short-term operation. IEEE Transactions on Power Systems 30(6):3347–3355

Dall'Anese E, Mancarella P, Monti A (2017) Unlocking flexibility: Integrated optimization and control of multienergy systems. IEEE Power and Energy Magazine 15(1):43–52

Daraeepour A, Patino-Echeverri D, Conejo AJ (2019) Economic and environmental implications of different approaches to hedge against wind production uncertainty in two-settlement electricity markets: A PJM case study. Energy Economics 80:336–354

Doherty R, O'Malley M (2005) A new approach to quantify reserve demand in systems with significant installed wind capacity. IEEE Transactions on Power Systems 20:587–595

Dominguez R, Oggioni G, Smeers Y (2019) Reserve procurement and flexibility services in power systems with high renewable capacity: Effects of integration on different market designs. International Journal of Electrical Power & Energy Systems 113:1014–1034

Dvorkin Jr V, Kazempour J, Pinson P (2019) Electricity market equilibrium under information asymmetry. Operations Research Letters 47(6):521–526

Facchinei F, Kanzow C (2007) Generalized Nash equilibrium problems. 4OR 5(3):173–210

Facchinei F, Pang JS (2007) Finite-dimensional variational inequalities and complementarity problems. Springer Science & Business Media

Fleten SF, Nasakkala E (2010) Gas-fired power plants: Investment timing, operating flexibility and CO2 capture. Energy Economics 32(4):805–816

Fukushima M (2011) Restricted generalized Nash equilibria and controlled penalty algorithm. Computational Management Science 8:201–218

Gil J, Caballero A, Conejo AJ (2014) Power cycling: CCGTs: The critical link between the electricity and natural gas markets. IEEE Power and Energy Magazine 12(6):40–48

Godoy-Gonzalez D, Gil E, Gutierrez-Alcaraz G (2020) Ramping ancillary service for cost-based electricity markets with high penetration of variable renewable energy. Energy Economics 85:104556

Guo X, Beskos A, Siddiqui A (2016) The natural hedge of a gas-fired power plant. Computational Management Science 13:63–86

Harker PT (1991) Generalized Nash games and quasi-variational inequalities. European Journal of Operational Research 54(1):81–94

Harker PT, Pang JS (1990) Finite-dimensional variational inequality and nonlinear complementarity problems: A survey of theory, algorithms and applications. Mathematical Programming 48(1-3):161–220

Heinen S, Hewicker C, Jenkins N, McCalley J, O'Malley M, Pasini S, Simoncini S (2017) Unleashing the flexibility of gas: Innovating gas systems to meet the electricity system's flexibility requirements. IEEE Power and Energy Magazine 15(1):16–24

Hibbard PJ, Schatzki T (2012) The interdependence of electricity and natural gas: Current factors and future prospects. The Electricity Journal 25(4):6–17

Hogan WW (2016) Virtual bidding and electricity market design. The Electricity Journal 29(5):33–47

Höschle H, Le Cadre H, Smeers Y, Papavasiliou A, Belmans R (2018) An ADMM-based method for computing risk-averse equilibrium in capacity markets. IEEE Transactions on Power Systems 33:4819–4830

Hua B, Baldick R (2017) A convex primal formulation for convex hull pricing. IEEE Transactions on Power Systems 32:3814–3823

Isemonger AG (2006) The benefits and risks of virtual bidding in multi-settlement markets. The Electricity Journal 19(9):26–36

Ito K, Reguant M (2016) Sequential markets, market power, and arbitrage. American Economic Review 106:1921–1957

Jha A, Wolak FA (2015) Testing for market efficiency with transaction costs: An application to financial trading in wholesale electricity markets. `https://web.stanford.edu/group/fwolak/cgi-bin/sites/default/files/CAISO_VB_draft_VNBER_final_V2.pdf`, Stanford Working Paper

Jonsson T, Pinson P, Madsen H (2010) On the market impact of wind energy forecasts. Energy Economics 32(2):313–320

Kazempour J, Hobbs BF (2018) Value of flexible resources, virtual bidding, and self–scheduling in two–settlement electricity markets with wind generation– Part I: Principles and competitive model. IEEE Transactions on Power Systems 33(1):749–759

Kovacevic RM (2016) Arbitrage conditions for electricity markets with production and storage. Computational Management Science 16:671–696

Krawczyk J (2007) Numerical solutions to coupled-constraint (or generalised Nash) equilibrium problems. Computational Management Science 4:183–204

Kulkarni AA, Shanbhag UV (2012) On the variational equilibrium as a refinement of the generalized Nash equilibrium. Automatica 48(1):45–55

Li R, Svoboda AJ, Oren SS (2015) Efficiency impact of convergence bidding in the California electricity market. Journal of Regulatory Economics 48(3):245–284

Liu Y, Holzer JT, Ferris MC (2015) Extending the bidding format to promote demand response. Energy Policy 86:82–92

Lo Prete C, Guo N, Shanbhag UV (2019a) Virtual bidding and financial transmission rights: An equilibrium model for cross-product manipulation in electricity markets. IEEE Transactions on Power Systems 34:953–967

Lo Prete C, Hogan WW, Liu B, Wang J (2019b) Cross-product manipulation in electricity markets, microstructure models and asymmetric information. The Energy Journal 50:1–43

Mather J, Bitar E, Poolla K (2017) Virtual bidding: Equilibrium, learning, and the wisdom of crowds. IFAC-PapersOnLine 50(1):225–232

Mays J, Morton D, O'Neill R (2019) Asymmetric risk and fuel neutrality in capacity markets. Nature Energy 4:948–956

Meibom P, Hilger KB, Madsen H, Vinther D (2013) Energy comes together in Denmark: The key to a future fossil–free Danish power system. IEEE Power and Energy Magazine 11(5):46–55

Morales JM, Pineda S (2017) On the inefficiency of the merit order in forward electricity markets with uncertain supply. European Journal of Operational Research 261:789–799

Morales JM, Conejo A, Liu K, Zhong J (2012) Pricing electricity in pools with wind producers. IEEE Transactions on Power Systems 27(3):1366–1376

NERC (2010) Flexibility requirements and metrics for variable generation: Implications for system planning studies. `https://www.nerc.com/files/IVGTF_Task_1_4_Final.pdf`, Technical Report of North American Electric Reliability Corporation

Nicholson E, Quinn A (2019) Wholesale electricity markets in the united states: Identifying future challenges facing commercial energy. IEEE Power and Energy Magazine 17(1):67–72

O'Connell N, Pinson P, Madsen H, O'Malley M (2016) Economic dispatch of demand response balancing through asymmetric block offers. IEEE Transactions on Power Systems 31:2999–3007

Ordoudis C, Pinson P, Morales JM (2019) An integrated market for electricity and natural gas systems with stochastic power producers. European Journal of Operational Research 272(2):642–654

Pang JS, Fukushima M (2005) Quasi-variational inequalities, generalized Nash equilibria, and multi-leader-follower games. Computational Management Science 2:21–56

Papavasiliou A, He Y, Svoboda A (2015) Self-commitment of combined cycle units under electricity price uncertainty. IEEE Transactions on Power Systems 30(4):1690–1701

Parsons JE, Colbert C, Larrieu J, Martin T, Mastrangelo E (2015) Financial arbitrage and efficient dispatch in wholesale electricity markets. http://www.mit.edu/~jparsons/publications/20150300_Financial_Arbitrage_and_Efficient_Dispatch.pdf, MIT Center for Energy and Environmental Policy Research

Pinson P, Mitridati L, Ordoudis C, Ostergaard J (2017) Towards fully renewable energy systems: Experience and trends in Denmark. CSEE Journal of Power and Energy Systems 3(1):26–35

Pritchard G, Zakeri G, Philpott A (2010) A single-settlement, energy-only electric power market for unpredictable and intermittent participants. Operations Research 58:1210–1219

Savelli I, Cornelusse B, Giannitrapani A, Paoletti S, Vicino A (2018) A new approach to electricity market clearing with uniform purchase price and curtailable block orders. Applied Energy 226:618–630

Schiro DA, Pang JS, Shanbhag UV (2013) On the solution of affine generalized Nash equilibrium problems with shared constraints by Lemke's method. Mathematical Programming 142(1-2):1–46

Schwele A, Ordoudis C, Kazempour J, Pinson P (2019) Coordination of power and natural gas systems: Convexification approaches for linepack modeling. IEEE PES PowerTech Conference 2019 pp 1–6

Schwele A, Ordoudis C, Kazempour J, Pinson P (2020) Electronic companion: Virtual bidding for coordination of electricity and natural gas markets under uncertainty: A stochastic equilibrium analysis. URL https://zenodo.org/badge/latestdoi/293420700

Sioshansi R, Oren S, O'Neill R (2010) Three-part auctions versus self-commitment in day-ahead electricity markets. Utilities Policy 18:165–173

Tabors RD, Englander S, Stoddard R (2012) Who's on first? The coordination of gas and power scheduling. The Electricity Journal 25(5):8–15

Vazquez M, Hallack M (2015) Interaction between gas and power market designs. Utilities Policy 33:23–33

Wang B, Hobbs BF (2016) Real-time markets for flexiramp: A stochastic unit commitment-based analysis. IEEE Transactions on Power Systems 31:846–860

Warrington J, Goulart P, Marithoz S, Morari M (2013) Policy-based reserves for power systems. IEEE Transactions on Power Systems 28:4427–4437

Yang J, Zhang N, Kang C, Xia Q (2018) Effect of natural gas flow dynamics in robust generation scheduling under wind uncertainty. IEEE Transactions on Power Systems 33:2087–2097

Zakeri G, Pritchard G, Bjorndal M, Bjorndal E (2019) Pricing wind: A revenue adequate, cost recovering uniform price auction for electricity markets with intermittent generation. INFORMS Journal on Optimization 1(1):35–48

Zavala VM, Kim K, Anitescu M, Birge J (2017) A stochastic electricity market clearing formulation with consistent pricing properties. Operations Research

65(3):557–576

Zhao J, Zheng T, Litvinov E (2016) A unified framework for defining and measuring flexibility in power system. IEEE Transactions on Power Systems 31:339–347

Zlotnik A, Roald L, Backhaus S, Chertkov M, Andersson G (2016) Control policies for operational coordination of electric power and natural gas transmission systems. In: American Control Conference (ACC), 2016, pp 7478–7483

Zugno M, Conejo AJ (2015) A robust optimization approach to energy and reserve dispatch in electricity markets. European Journal of Operational Research 247(2):659–671

Coordination of Power and Natural Gas Markets via Financial Instruments

Anna Schwele, Christos Ordoudis, Pierre Pinson, Jalal Kazempour

This document serves as an electronic companion for the paper "Coordination of Power and Natural Gas Markets via Financial Instruments". It contains seven sections: The input data for the case study is shown in Section 1. Section 2 analyses the impact of our assumption of perfect knowledge of virtual bidders. Section 3 presents the detailed formulation of all optimization problems from the original manuscript including the equivalent equilibrium problems following Remark 1. The Karush Kuhn Tucker (KKT) conditions of all optimization and equilibrium problems are provided in Section 4. Sections 5 and 6 show the proofs of Propositions 1 and 2, respectively. Section 7 contains an overview over computational performance.

Nomenclature

Sets

$\mathcal{I}$	Set of dispatchable power production units i.
$\mathcal{C}$	Subset of non-gas power plants ($\mathcal{C} \subset \mathcal{I}$).
$\mathcal{G}$	Subset of natural gas-fired power plants ($\mathcal{G} \subset \mathcal{I}$).
$\mathcal{S}$	Subset of slow-start power plants ($\mathcal{S} \subset \mathcal{I}$).
F	Subset of fast-start power plants ($\mathcal{F} \subset \mathcal{I}$).
$\mathcal{SS}$	Subset of self-scheduling power plants ($\mathcal{SS} \subset \mathcal{I}$).
$\mathcal{J}$	Set of wind power units j.
$\mathcal{K}$	Set of natural gas supply units k.
$\mathcal{R}$	Set of electricity virtual bidders r.
$\mathcal{Q}$	Set of natural gas virtual bidders q.
Ω	Set of wind power scenarios ω.
$\mathcal{T}$	Set of time periods t.
	Note that $\mathcal{C} \cup \mathcal{G} = \mathcal{I}$, $\mathcal{F} \cap \mathcal{S} = \emptyset$, $\mathcal{F} \cap \mathcal{SS} = \emptyset$ and $\mathcal{S} \cap \mathcal{SS} = \emptyset$.

Variables

$p^{\mathrm{DA}}_{i,t}, w^{\mathrm{DA}}_{j,t}$	Day-ahead dispatch of units i and j in period t, respectively [MW].
$p^{\mathrm{RT}}_{i,t,\omega}$	Power production adjustment of unit i in scenario ω, period t [MW].
$w^{\mathrm{RT}}_{j,t,\omega}$	Wind power production adjustment of unit j in scenario ω, period t [MW].
$l^{\mathrm{sh,E}}_{t,\omega}, l^{\mathrm{sh,G}}_{t,\omega}$	Electricity and natural gas load shedding under scenario ω, period t [MW, kcf/h].
$g^{\mathrm{DA}}_{k,t}$	Day-ahead dispatch of unit k in period t [kcf/h].

$g^{\mathrm{RT}}_{k,t,\omega}$ Natural gas adjustment by unit k in scenario ω, period t [kcf/h].
$\hat{\lambda}^{\mathrm{E}}_{t}$ Day-ahead electricity price in period t [$/MWh].
$\tilde{\lambda}^{\mathrm{E}}_{t,\omega}$ Probability-weighted real-time electricity price in period t, scenario ω [$/MWh].
$\hat{\lambda}^{\mathrm{G}}_{t}$ Day-ahead natural gas price in period t [$/kcf].
$\tilde{\lambda}^{\mathrm{G}}_{t,\omega}$ Probability-weighted real-time natural gas price in period t, scenario ω [$/kcf].
μ, ν Set of dual variables in day-ahead and real-time markets, respectively.
$c^{\mathrm{DA}}_{i,t}$ Start-up cost of dispatchable unit i in period t [$].
$c^{\mathrm{RT}}_{i,t,\omega}$ Start-up cost adjustment of dispatchable fast-start unit i in period t under scenario s [$].
$u^{\mathrm{DA}}_{i,t}$ Relaxed unit commitment status of dispatchable unit i in period t.
$u^{\mathrm{RT}}_{i,t,\omega}$ Relaxed unit commitment adjustment of fast-start unit i in period t, scenario ω.
$v^{\mathrm{DA,E}}_{r,t}$ Day-ahead trade of electricity virtual bidder r in period t [MW].
$v^{\mathrm{RT,E}}_{r,t}$ Real-time trade of electricity virtual bidder r in period t [MW].
$v^{\mathrm{DA,G}}_{q,t}$ Day-ahead trade of natural gas virtual bidder q in period t [kcf/h].
$v^{\mathrm{RT,G}}_{q,t}$ Real-time trade of natural gas virtual bidder q in period t [kcf/h].

Parameters

D^{E}_{t} Electricity demand in period t [MWh].
D^{G}_{t} Natural gas demand in period t [kcf/h].
C^{E}_{i} Production cost of unit i [$/MWh].
$C^{\mathrm{sh,E}}$ Value of electricity lost load [$/MWh].
C^{G}_{k} Day-ahead offer price of unit k [$/kcf].
$C^{\mathrm{sh,G}}$ Value of natural gas lost load [$/kcf].
$P^{\max}_{i}$ Capacity of dispatchable unit i [MW].
$P^{\min}_{i}$ Minimum production level of dispatchable unit i [MW].
ϕ_i Power conversion factor of natural gas unit $i \in G$ [kcf/MWh].
$W_{j,t,\omega}$ Wind power realization of unit j in period t, scenario ω [MW].
$W^{\mathrm{DA}}_{j,t}$ Day-ahead wind power forecast for unit j in period t [MW].
$\overline{W}_{j}$ Capacity of wind power unit j [MW].
$G^{\max}_{k}$ Capacity of natural gas unit k [kcf].
G^{adj}_{k} Adjustment limit of natural gas unit k [kcf/h].
π_ω Probability of scenario ω.
C^{SU}_{i} Start-up cost of dispatchable unit i [$].
U^{ini}_{i} Initial commitment status of dispatchable unit i [0/1].
P^{ini}_{i} Initial dispatch of unit i [MW].
R_i Up/down ramping limit of dispatchable unit i [MW/h].

1. Input Data

Table 3 gives the technical characteristics of power generators, whose columns one to ten show the unit name, minimum power production ($P^{\min}_{i}$), capacity ($P^{\max}_{i}$), ramp rate (R_i), start-up cost

Unit	$P_i^{\min}$ [MW]	$P_i^{\max}$ [MW]	R_i [MW/h]	C_i^{SU} [$]	U^{ini} [0/1]	P_i^{ini} [MWh]	Type	C_i^{E} [$/MWh]	ϕ_i [kcf/MWh]
$\mathcal{C}^1$	0	40	20	17,462	1	40	non gas-fired	22.18	-
$\mathcal{C}^2$	0	152	50	13,207	1	100	non gas-fired	33.2	-
$\mathcal{C}^3$	0	300	195	22,313	0	0	non gas-fired	37.14	-
$\mathcal{C}^4$	100	591	230	28,272	0	0	non gas-fired	38.2	-
$\mathcal{C}^5$	400	400	400	50,000	1	400	non gas-fired	22.34	-
$\mathcal{C}^6$	0	350	80	33,921	0	0	non gas-fired	20.92	-
$\mathcal{G}^1$	0	155	100	21,450	1	100	gas-fired	-	15.23
$\mathcal{G}^2$	0	60	60	10,721	0	0	gas-fired	-	16.98
$\mathcal{G}^3$	0	310	200	42,900	0	0	gas-fired	-	12.65
$\mathcal{G}^4$	0	300	150	10,000	0	0	gas-fired	-	14.88

Table 1 Technical characteristics of power generators

Supplier	$G_k^{\min}$ [kcf]	$G_k^{\max}$ [kcf]	G_k^{adj} [kcf/h]	C_k^{G} [$/kcf]
$\mathcal{K}^1$	0	9,000	1,000	2
$\mathcal{K}^2$	0	6,000	1,000	2.2
$\mathcal{K}^3$	0	15,000	1,000	2.5
$\mathcal{K}^4$	0	15,000	1,000	3.3

Table 2 Technical characteristics of gas suppliers

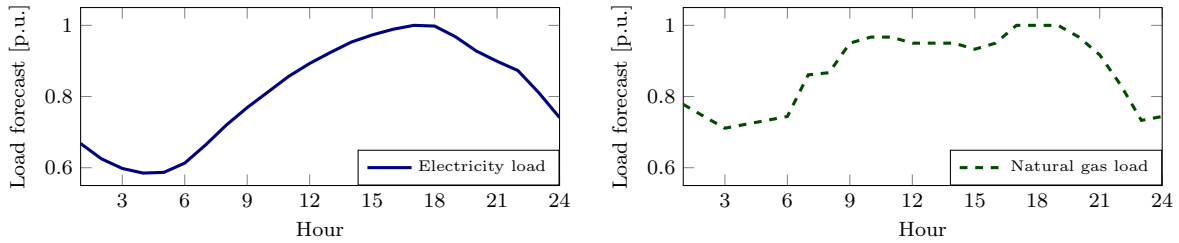

Figure 1 Electricity and natural gas demand. The plots on the left- and right-hand sides show the total hourly demand for power and natural gas, respectively.

(C_i^{SU}), initial commitment status at the beginning of time horizon (U^{ini}), initial dispatch (P^{ini}), type, production cost for non gas-fired generators (C_i^{E}), and gas-to-power conversion ratio for gas-fired generators (ϕ_i), respectively. In addition, Table 4 provides the technical characteristics of four gas suppliers, including minimum and maximum gas capacity ($G_k^{\min}$ and $G_k^{\max}$), ramp rate (G_k^{adj}), and supply cost (C_k^{G}). The total hourly demand in both power and natural gas sectors is shown in Fig. 1. The profile of deterministic wind power forecast (in per-unit) in day-ahead is illustrated by a solid curve in the left-hand side plot of Fig. 2, while the right-hand side plot provides the five equiprobable wind scenarios that may realize in real-time. Due to potential forecast error in day-ahead, observe that the day-ahead deterministic forecast (solid curve in the left-hand side plot) is not necessarily identical to the expected wind power realization in real-time (dashed curve in the same plot). In this case, the day-ahead wind forecast underestimates the available wind power production during hours 1 to 6 and 19 to 23, while overestimates it from hour 7 to 18.

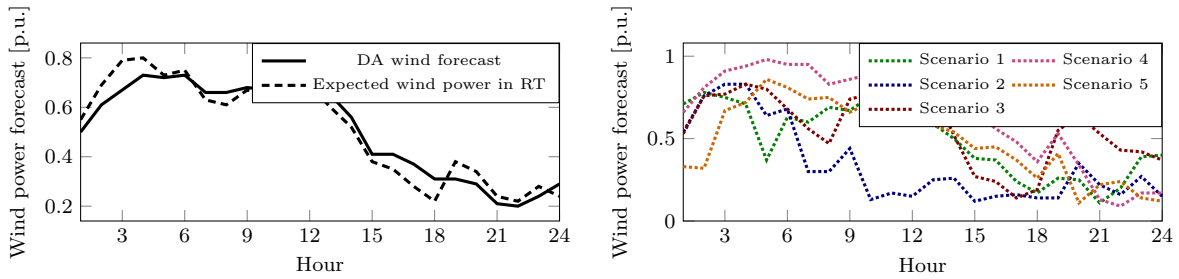

Figure 2 **Wind power forecast in day-ahead (DA) and potential scenarios in real-time (RT): The upper plot shows the deterministic wind power forecast in DA and the expected value of five wind power scenarios in RT. These five equiprobable scenarios in RT are depicted in the lower plot.**

		Seq	*Seq+eVB*	*Seq+iVB*	*Seq+VB*	*Ideal*
In-sample		$1,464,320	-6.83%	-6.37%	-6.94%	-7.06%
Out-of-sample	Same distribution	$1,360,886	-4.49%	-3.36%	-4.29%	-5.33%
	Higher first moments	$1.344.285	-3.91%	-3.06%	-3.73%	-4.76%
	Lower first moments	$1,410,223	-5.24%	-3.45%	-4.85%	-6.12%
	Different distribution	$1,252.643	-3.30%	-3.99%	-3.79%	-4.60%

Table 3 **Total expected cost of the electricity and natural gas systems under different market setups for in-sample and out-of-sample scenarios. The percentages show the differences in the total expected system cost compared to that cost in the fully uncoordinated sequential setup Seq.**

2. Out-of-sample Analysis

This section presents an ex-post out-of-sample analysis to evaluate the performance of the proposed market setups against our assumption of perfect knowledge of virtual bidders and against estimations of natural gas prices. For this purpose, we test the impact of unseen scenarios on the market setups. To assess the impact of the assumption of perfect knowledge of virtual bidders on market outcomes, we generate a set of 100 new scenarios from the same distribution and 100 scenarios from a distribution with different first and second moments. Fixing the day-ahead schedules to those obtained with the original in-sample simulations, we solve a real-time electricity market and then a real-time gas market for each out-of-sample scenario. The expected total system costs achieved with the sequential setup *Seq* decrease compared to those in the in-sample simulation, due to the updated expected electricity and gas adjustment costs under the previously unseen scenarios, as exhibited in Table 3. The fully coordinated ideal model *Ideal* still provides a lower bound for the expected total system cost. The setups including soft coordination via financial instruments consistently achieve lower expected system costs compared to the fully sequential setup *Seq*. The effectiveness of virtual bidders to improve sectoral and temporal coordination and make day-ahead schedules more efficient is not overly sensitive to the quality of information of these agents.

3. Optimization Problems

3.1. Explicit Electricity Virtual Bidder

The profit maximization problem of each virtual bidder r participating in the electricity market given the day-ahead and expectation of real-time prices $\hat{\lambda}_t^{\mathrm{E}}$ and $\tilde{\lambda}_{t,\omega}^{\mathrm{E}}$, respectively, is given below:

$$\left\{ \max_{v_{r,t}^{\mathrm{DA,E}}, v_{r,t}^{\mathrm{RT,E}}} \; \sum_{t\in\mathcal{T}} \left(\hat{\lambda}_t^{\mathrm{E}} \; v_{r,t}^{\mathrm{DA,E}} + \sum_{\omega\in\Omega} \tilde{\lambda}_{t,\omega}^{\mathrm{E}} \right) \; v_{r,t}^{\mathrm{RT,E}} \right. \tag{1a}$$

$$\left. \text{subject to } \; v_{r,t}^{\mathrm{DA,E}} + v_{r,t}^{\mathrm{RT,E}} = 0 : \rho_{r,t}, \;\; \forall t, \right\}, \;\; \forall r \in \mathcal{R}, \tag{1b}$$

where $\Theta^{\mathrm{VBE}} = \{v_{r,t}^{\mathrm{DA,E}}, v_{r,t}^{\mathrm{RT,E}}, \forall r, t\}$ is the set of primal optimization variables. Objective function (1a) maximizes the expected profit of arbitraging in the day-ahead and real-time electricity markets. Equation (1b) ensures that each virtual bidder sells (buys) the same amount back in the real-time market that was bought (sold) in the day-ahead market. The market operators treat the virtual bidders' dispatch decision as fixed input into the market clearing in the following.

3.2. Day-Ahead Electricity Market

The day-ahead electricity market clears with given day-ahead positions of virtual trade as:

$$\min_{\Theta^{\mathrm{EDA}}} \; \sum_{t\in\mathcal{T}} \Big(\sum_{i\in\mathcal{C}} C_i^{\mathrm{E}} \; p_{i,t}^{\mathrm{DA}} + \sum_{i\in\mathcal{G}} \hat{\lambda}_t^{\mathrm{G}} \; \phi_i \; p_{i,t}^{\mathrm{DA}} + \sum_{i\in\mathcal{I}} c_{i,t}^{\mathrm{DA}} \Big) \tag{2a}$$

$$\text{subject to } \; \sum_{i\in\mathcal{I}} p_{i,t}^{\mathrm{DA}} + \sum_{j\in\mathcal{J}} w_{j,t}^{\mathrm{DA}} - D_t^{\mathrm{E}} + \sum_{r\in\mathcal{R}} v_{r,t}^{\mathrm{DA,E}} = 0 : \hat{\lambda}_t^{\mathrm{E}}, \forall t, \tag{2b}$$

$$0 \le w_{j,t}^{\mathrm{DA}} \le W_{j,t}^{\mathrm{DA}} : \underline{\mu}_{j,t}^{\mathrm{W}}, \overline{\mu}_{j,t}^{\mathrm{W}}, \;\; \forall j, t, \tag{2c}$$

$$u_{i,t}^{\mathrm{DA}} \; P_i^{\min} \le p_{i,t}^{\mathrm{DA}} \le u_{i,t}^{\mathrm{DA}} \; P_i^{\max} : \underline{\mu}_{i,t}^{\mathrm{P}}, \overline{\mu}_{i,t}^{\mathrm{P}}, \;\; \forall i \in \mathcal{I}, t, \tag{2d}$$

$$-u_{i,(t-1)}^{\mathrm{DA}} \; R_i \le \left(p_{i,t}^{\mathrm{DA}} - p_{i,(t-1)}^{\mathrm{DA}} \right) \le u_{i,t}^{\mathrm{DA}} \; R_i : \underline{\mu}_{i,t}^{\mathrm{R}}, \overline{\mu}_{i,t}^{\mathrm{R}}, \;\; \forall i \in \mathcal{I}, t > 1, \tag{2e}$$

$$-U_i^{\mathrm{ini}} \; R_i \le \left(p_{i,t}^{\mathrm{DA}} - P_i^{\mathrm{ini}} \right) \le u_{i,t}^{\mathrm{DA}} \; R_i : \underline{\mu}_{i,t}^{\mathrm{R}}, \overline{\mu}_{i,t}^{\mathrm{R}}, \;\; \forall i \in \mathcal{I}, t = 1, \tag{2f}$$

$$0 \le u_{i,t}^{\mathrm{DA}} \le 1 : \underline{\mu}_{i,t}^{\mathrm{B}}, \overline{\mu}_{i,t}^{\mathrm{B}}, \;\; \forall i \in \mathcal{I}, t, \tag{2g}$$

$$C_i^{\mathrm{SU}} \;\; \left(u_{i,t}^{\mathrm{DA}} - u_{i,(t-1)}^{\mathrm{DA}} \right) \le c_{i,t}^{\mathrm{DA}} : \overline{\mu}_{i,t}^{\mathrm{SU}}, \;\; \forall i \in \mathcal{I}, t > 1, \tag{2h}$$

$$C_i^{\mathrm{SU}} \left(u_{i,t}^{\mathrm{DA}} - U_i^{\mathrm{ini}} \right) \le c_{i,t}^{\mathrm{DA}} : \overline{\mu}_{i,t}^{\mathrm{SU}}, \;\; \forall i \in \mathcal{I}, t = 1, \tag{2i}$$

$$0 \le c_{i,t}^{\mathrm{DA}} : \underline{\mu}_{i,t}^{\mathrm{SU}}, \;\; \forall i \in \mathcal{I}, t, \tag{2j}$$

where $\Theta^{\mathrm{EDA}} = \{p_{i,t}^{\mathrm{DA}}, c_{i,t}^{\mathrm{DA}}, u_{i,t}^{\mathrm{DA}}, \forall i \in \mathcal{I}, t; w_{j,t}^{\mathrm{DA}}, \forall j, t\}$ is the set of primal optimization variables. The objective (2a) of the deterministic day-ahead market-clearing problem is to minimize the day-ahead generation cost. The total cost stems from the cost of non-gas and gas-fired power plants. These units are assumed to bid in the market truthfully, i.e., offer at prices equal to their marginal cost of production. For the case of gas-fired units, we assume that the marginal cost of production is described by a linear function of the estimated natural gas price, i.e., $C_i = \hat{\lambda}_t^{\mathrm{G}} \phi_i, \forall i \in \mathcal{G}$. Constraint

(2b) is the day-ahead power balance with inelastic demand treating the virtual day-ahead positions $\sum_{r\in\mathcal{R}} v_{r,t}^{\mathrm{DA,E}}$ as given inputs. Constraints (2c) and (2d) enforce lower and upper bounds on the day-ahead dispatch of wind and conventional generation. Constraints (2e), (2f) ensure the ramping limits of conventional generators and represent in combination with (2g) the tight relaxation of unit commitment. Constraints (2h), (2i), and (2j) enforce the start-up cost of each generator.

The optimization problem for day-ahead electricity market clearing can be equivalently formulated as the following equilibrium model with each unit maximizing her profit and a price-setting agent according to Remark 1. Each non gas-fired generator $\mathcal{C}$ maximizes her day-ahead profit with respect to her operational constraints according to

$$\left\{ \max_{p_{i,t}^{\mathrm{DA}}, c_{i,t}^{\mathrm{DA}}, u_{i,t}^{\mathrm{DA}}} \sum_{t\in\mathcal{T}} \left[\left(\hat{\lambda}_t^{\mathrm{E}} - C_i^{\mathrm{E}} \right) p_{i,t}^{\mathrm{DA}} - c_{i,t}^{\mathrm{DA}} \right] \right. \tag{3a}$$

$$\left. \text{subject to } (2\mathrm{d}) - (2\mathrm{j}) \right\} \ \forall (i \in \mathcal{C}). \tag{3b}$$

Similarly, gas-fired generator $\mathcal{G}$ decides her day-ahead dispatch based on estimated marginal cost via natural gas price forecast $\hat{\lambda}_t^{\mathrm{G}}$:

$$\left\{ \max_{p_{i,t}^{\mathrm{DA}}, c_{i,t}^{\mathrm{DA}}, u_{i,t}^{\mathrm{DA}}} \sum_{t\in\mathcal{T}} \left[\left(\hat{\lambda}_t^{\mathrm{E}} - \hat{\lambda}_t^{\mathrm{G}} \ \phi_i \right) p_{i,t}^{\mathrm{DA}} - c_{i,t}^{\mathrm{DA}} \right] \right. \tag{4a}$$

$$\left. \text{subject to } (2\mathrm{d}) - (2\mathrm{j}) \right\} \ \forall (i \in \mathcal{G}). \tag{4b}$$

Wind farm $\mathcal{J}$ maximizes her profit according to the day-ahead wind forecast $W_{j,t}^{\mathrm{DA}}$ as

$$\left\{ \max_{w_{j,t}^{\mathrm{DA}}} \sum_{t\in\mathcal{T}} \hat{\lambda}_t^{\mathrm{E}} \ w_{j,t}^{\mathrm{DA}} \right. \tag{5a}$$

$$\left. \text{subject to } (2\mathrm{c}) \right\} \ \forall j \in \mathcal{J}. \tag{5b}$$

A price setting agent decides the day-ahead electricity price $\hat{\lambda}_t^{\mathrm{E}}$ according to

$$\min_{\hat{\lambda}_t^{\mathrm{E}}} \sum_{t\in\mathcal{T}} \hat{\lambda}_t^{\mathrm{E}} \Big(\sum_{i\in\mathcal{I}} p_{i,t}^{\mathrm{DA}} + \sum_{j\in\mathcal{J}} w_{j,t}^{\mathrm{DA}} - D_t^{\mathrm{E}} + \sum_{r\in\mathcal{R}} v_{r,t}^{\mathrm{DA,E}}. \Big) \tag{6a}$$

The equilibrium problem (3)-(6) is equivalent to the day-ahead market optimization problem (2), since the Karush-Kuhn-Tucker (KKT) conditions are identical, see Section 4.

3.3. Real-Time Electricity Market

In real-time operation, wind power production $W_{j,t,\omega}$ is realized and the real-time markets are cleared to adjust for imbalances. The day-ahead schedule is treated as fixed parameters in the following formulation. The RT market-clearing problem for wind generation scenario ω is formulated as

$$\left\{ \min_{\Theta^{\mathrm{ERT}}} \ \pi_\omega \sum_{t\in\mathcal{T}} \Big(\sum_{i\in\mathcal{C}} C_i^{\mathrm{E}}\ p_{i,t,\omega}^{\mathrm{RT}} + \sum_{i\in\mathcal{G}} \tilde{\lambda}_{t,\omega}^{\mathrm{G}}\ \phi_i\ p_{i,t,\omega}^{\mathrm{RT}} + C^{\mathrm{sh,E}}\ l_{t,\omega}^{\mathrm{sh,E}} + \sum_{i\in\mathcal{F}} c_{i,t,\omega}^{\mathrm{RT}} \Big) \right. \tag{7a}$$

$$\text{subject to} \ \sum_{i\in\mathcal{I}} p_{i,t,\omega}^{\mathrm{RT}} + l_{t,\omega}^{\mathrm{sh,E}} + \sum_{r\in\mathcal{R}} v_{r,t}^{\mathrm{RT,E}} + \sum_{j\in\mathcal{J}} w_{j,t,\omega}^{\mathrm{RT}} = 0 : \tilde{\lambda}_{t,\omega}^{\mathrm{E}},\ \forall t, \tag{7b}$$

$$0 \le l_{t,\omega}^{\mathrm{sh,E}} \le D_t^{\mathrm{E}} : \underline{\nu}_{t,\omega}^{\mathrm{DE}}, \overline{\nu}_{t,\omega}^{\mathrm{DE}},\ \ \forall t, \tag{7c}$$

$$0 \le \left(w_{j,t}^{\mathrm{DA}} + w_{j,t,\omega}^{\mathrm{RT}}\right) \le W_{j,t,\omega} : \underline{\nu}_{j,t,\omega}^{\mathrm{W}}, \overline{\nu}_{j,t,\omega}^{\mathrm{W}},\ \ \forall j,t, \tag{7d}$$

$$u_{i,t}^{\mathrm{DA}}\ P_i^{\min} \le \left(p_{i,t}^{\mathrm{DA}} + p_{i,t,\omega}^{\mathrm{RT}}\right) \le u_{i,t}^{\mathrm{DA}}\ P_i^{\max} : \underline{\nu}_{i,t,\omega}^{\mathrm{P}}, \overline{\nu}_{i,t,\omega}^{\mathrm{P}},\ \ \forall i\in\mathcal{S}, t, \tag{7e}$$

$$-u_{i,(t-1)}^{\mathrm{DA}}\ R_i \le \left(p_{i,t}^{\mathrm{DA}} + p_{i,t,\omega}^{\mathrm{RT}} - p_{i,(t-1)}^{\mathrm{DA}} - p_{i,(t-1),\omega}^{\mathrm{RT}}\right) \le u_{i,t}^{\mathrm{DA}}\ R_i : \underline{\nu}_{i,t,\omega}^{\mathrm{R}}, \overline{\nu}_{i,t,\omega}^{\mathrm{R}},\ \ \forall i\in\mathcal{S}, t>1, \tag{7f}$$

$$-U_i^{\mathrm{ini}}\ R_i \le \left(p_{i,t}^{\mathrm{DA}} + p_{i,t,\omega}^{\mathrm{RT}} - P_i^{\mathrm{ini}}\right) \le u_{i,t}^{\mathrm{DA}}\ R_i : \underline{\nu}_{i,t,\omega}^{\mathrm{R}}, \overline{\nu}_{i,t,\omega}^{\mathrm{R}},\ \ \forall i\in\mathcal{S}, t=1, \tag{7g}$$

$$\left(u_{i,t}^{\mathrm{DA}} + u_{i,t,\omega}^{\mathrm{RT}}\right) P_i^{\min} \le \left(p_{i,t}^{\mathrm{DA}} + p_{i,t,\omega}^{\mathrm{RT}}\right) \le \left(u_{i,t}^{\mathrm{DA}} + u_{i,t,\omega}^{\mathrm{RT}}\right) P_i^{\max} : \underline{\nu}_{i,t,\omega}^{\mathrm{P}}, \overline{\nu}_{i,t,\omega}^{\mathrm{P}},\ \ \forall i\in\mathcal{F}, t, \tag{7h}$$

$$-\left(u_{i,(t-1)}^{\mathrm{DA}} + u_{i,(t-1),\omega}^{\mathrm{RT}}\right) R_i \le \left(p_{i,t}^{\mathrm{DA}} + p_{i,t,\omega}^{\mathrm{RT}} - p_{i,(t-1)}^{\mathrm{DA}} - p_{i,(t-1),\omega}^{\mathrm{RT}}\right) \le \left(u_{i,t}^{\mathrm{DA}} + u_{i,t,\omega}^{\mathrm{RT}}\right) R_i$$
$$: \underline{\nu}_{i,t,\omega}^{\mathrm{R}}, \overline{\nu}_{i,t,\omega}^{\mathrm{R}},\ \ \forall i\in\mathcal{F}, t>1, \tag{7i}$$

$$-U_i^{\mathrm{ini}}\ R_i \le \left(p_{i,t}^{\mathrm{DA}} + p_{i,t,\omega}^{\mathrm{RT}} - P_i^{\mathrm{ini}}\right) \le \left(u_{i,t}^{\mathrm{DA}} + u_{i,t,\omega}^{\mathrm{RT}}\right)\ R_i : \underline{\nu}_{i,t,\omega}^{\mathrm{R}}, \overline{\nu}_{i,t,\omega}^{\mathrm{R}},\ \ \forall i\in\mathcal{F}, t=1, \tag{7j}$$

$$0 \le \left(u_{i,t}^{\mathrm{DA}} + u_{i,t,\omega}^{\mathrm{RT}}\right) \le 1 : \underline{\nu}_{i,t,\omega}^{\mathrm{B}}, \overline{\nu}_{i,t,\omega}^{\mathrm{B}},\ \ \forall i\in\mathcal{F}, t, \tag{7k}$$

$$C_i^{\mathrm{SU}}\ \left(u_{i,t}^{\mathrm{DA}} + u_{i,t,\omega}^{\mathrm{RT}} - u_{i,(t-1)}^{\mathrm{DA}} - u_{i,(t-1),\omega}^{\mathrm{RT}}\right) \le \left(c_{i,t}^{\mathrm{DA}} + c_{i,t,\omega}^{\mathrm{RT}}\right) : \overline{\nu}_{i,t,\omega}^{\mathrm{SU}},\ \ \forall i\in\mathcal{F}, t, \tag{7l}$$

$$C_i^{\mathrm{SU}}\ \left(u_{i,t}^{\mathrm{DA}} + u_{i,t,\omega}^{\mathrm{RT}} - U_i^{\mathrm{ini}}\right) \le \left(c_{i,t}^{\mathrm{DA}} + c_{i,t,\omega}^{\mathrm{RT}}\right) : \overline{\nu}_{i,t,\omega}^{\mathrm{SU}},\ \ \forall i\in\mathcal{F}, t=1, \tag{7m}$$

$$\left. 0 \le \left(c_{i,t}^{\mathrm{DA}} + c_{i,t,\omega}^{\mathrm{RT}}\right) : \underline{\nu}_{i,t,\omega}^{\mathrm{SU}},\ \ \forall i\in\mathcal{F}, t \right\} \forall\omega, \tag{7n}$$

where $\Theta^{\mathrm{ERT}} = \{p_{i,t,\omega}^{\mathrm{RT}}, \forall i\in\mathcal{I}, t, \omega; w_{j,t,\omega}^{\mathrm{RT}}, \forall j, t, \omega;\ l_{t,\omega}^{\mathrm{sh,E}},\ \forall t, \omega;\ u_{i,t,\omega}^{\mathrm{RT}},\ c_{i,t,\omega}^{\mathrm{RT}}\ \ \forall i\in\mathcal{F}, t, \omega\}$ is the set of primal optimization variables. The objective of (7) is to minimize the probability-weighted system cost in the real-time market under scenarios ω. Objective function (7a) describes the real-time cost of power adjustments to cover excess or deficit of wind power production. Electricity load shedding cost is also taken into account. Constraint (7b) balances the deviations in real-time from the day-ahead schedule with the position of virtual bidders $\sum_{r\in\mathcal{R}} v_{r,t}^{\mathrm{RT,E}}$ as fixed input. Constraints (7c),(7d), (7e), and (7h) enforce lower and upper bounds on the real-time adjustment of load levels, wind generation, and conventional slow- and fast-starting generators, respectively. Constraints (7f),(7g),(7i), and (7j) ensure the ramp-rate limits of conventional slow- and fast-starting generators

and represent in combination with (7k) the tight relaxation of unit commitment for fast-starting units. Constraints (7l), (7m), and (7n) enforce the start-up cost of fast-starting generators.

Following Remark 1, optimization problem (7) can be equivalently formulated as the following equilibrium problem. Slow-starting non gas-fired generator $\mathcal{C} \cap \mathcal{S}$ maximizes her profit in real-time with respect to her day-ahead commitment decision as

$$\left\{ \max_{p^{\mathrm{RT}}_{i,t,\omega}} \; \sum_{t \in \mathcal{T}} \left(\tilde{\lambda}^{\mathrm{E}}_{t,\omega} - \pi_\omega \; C^{\mathrm{E}}_i \right) p^{\mathrm{RT}}_{i,t,\omega} \right. \tag{8a}$$

$$\left. \text{subject to } \; (7\mathrm{e}) - (7\mathrm{g}) \right\} \forall (i \in \mathcal{C} \cap \mathcal{S}), \omega, \tag{8b}$$

while each fast-starting generator $\mathcal{C} \cap \mathcal{F}$ can update her commitment decision in real-time according to

$$\left\{ \max_{p^{\mathrm{RT}}_{i,t,\omega}, c^{\mathrm{RT}}_{i,t,\omega}, u^{\mathrm{RT}}_{i,t,\omega}} \; \sum_{t \in \mathcal{T}} \left[\left(\tilde{\lambda}^{\mathrm{E}}_{t,\omega} - \pi_\omega \; C^{\mathrm{E}}_i \right) p^{\mathrm{RT}}_{i,t,\omega} - \pi_\omega \; c^{\mathrm{RT}}_{i,t,\omega} \right] \right. \tag{9a}$$

$$\left. \text{subject to } \; (7\mathrm{h}) - (7\mathrm{n}) \right\} \forall (i \in \mathcal{C} \cap \mathcal{F}), \omega. \tag{9b}$$

Similarly, gas-fired generators optimize their dispatch decisions in real-time based on real-time natural gas price estimation $\tilde{\lambda}^{\mathrm{G}}_{t,\omega}$ as slow-starters $\mathcal{G} \cap \mathcal{S}$ according to

$$\left\{ \max_{p^{\mathrm{RT}}_{i,t,\omega}} \; \sum_{t \in \mathcal{T}} \left(\tilde{\lambda}^{\mathrm{E}}_{t,\omega} - \pi_\omega \; \tilde{\lambda}^{\mathrm{G}}_{t,\omega} \; \phi_i \right) p^{\mathrm{RT}}_{i,t,\omega} \right. \tag{10a}$$

$$\left. \text{subject to } \; (7\mathrm{e}) - (7\mathrm{g}) \right\} \forall (i \in \mathcal{G} \cap \mathcal{S}), \omega \tag{10b}$$

and as fast-starters $\mathcal{G} \cap \mathcal{F}$, as

$$\left\{ \max_{p^{\mathrm{RT}}_{i,t,\omega}, c^{\mathrm{RT}}_{i,t,\omega}, u^{\mathrm{RT}}_{i,t,\omega}} \; \sum_{t \in \mathcal{T}} \left[\left(\tilde{\lambda}^{\mathrm{E}}_{t,\omega} - \pi_\omega \; \tilde{\lambda}^{\mathrm{G}}_{t,\omega} \; \phi_i \right) p^{\mathrm{RT}}_{i,t,\omega} - \pi_\omega \; c^{\mathrm{RT}}_{i,t,\omega} \right] \right. \tag{11a}$$

$$\left. \text{subject to } \; (7\mathrm{h}) - (7\mathrm{n}) \right\} \forall (i \in \mathcal{G} \cap \mathcal{F}), \omega. \tag{11b}$$

Wind farm $\mathcal{J}$ adjusts her dispatch in real-time according to the actual wind power realization $W_{j,t,\omega}$:

$$\left\{ \max_{w^{\mathrm{RT}}_{j,t,\omega}} \; \sum_{t \in \mathcal{T}} \tilde{\lambda}^{\mathrm{E}}_{t,\omega} \; w^{\mathrm{RT}}_{j,t,\omega} \right. \tag{12a}$$

$$\left. \text{subject to } \; (7\mathrm{d}) \right\} \forall j, \omega. \tag{12b}$$

Power demand is able to shed load in real-time incurring cost as

$$\left\{ \min_{l^{\mathrm{sh,E}}_{t,\omega}} \sum_{t\in\mathcal{T}} \left(\pi_\omega \; C^{\mathrm{sh,E}} \; - \tilde{\lambda}^{\mathrm{E}}_{t,\omega} \right) l^{\mathrm{sh,E}}_{t,\omega} \right) \tag{13a}$$

$$\text{subject to } (7c) \Big\} \forall \omega. \tag{13b}$$

For each scenario, the real-time electricity price $\tilde{\lambda}^{\mathrm{E}}_{t,\omega}$ is set according to

$$\left\{ \min_{\tilde{\lambda}^{\mathrm{E}}_{t,\omega}} \; \sum_{t\in\mathcal{T}} \tilde{\lambda}^{\mathrm{E}}_{t,\omega} \Big(\sum_{i\in\mathcal{I}} p^{\mathrm{RT}}_{i,t,\omega} + l^{\mathrm{sh,E}}_{t,\omega} + \sum_{j\in\mathcal{J}} w^{\mathrm{RT}}_{j,t,\omega} + \sum_{r\in\mathcal{R}} v^{\mathrm{RT,E}}_{r,t} \Big) \right\} \forall \omega. \tag{14a}$$

The equilibrium problem (8)-(14) is equivalent to the real-time market optimization problem (7) for each scenario ω.

3.4. Explicit Natural Gas Virtual Bidder

We also introduce virtual bidding in natural gas markets. Similarly to electricity virtual bidding, the profit maximization problem of each virtual bidder q participating in the natural gas market is given below for day-ahead and real-time distribution of natural gas spot price $\hat{\lambda}^{\mathrm{G}}_t$ and $\tilde{\lambda}^{\mathrm{G}}_{t,\omega}$, respectively:

$$\left\{ \max_{\Theta^{\mathrm{VBG}}} \; \sum_{t\in\mathcal{T}} \left(\hat{\lambda}^{\mathrm{G}}_t \; v^{\mathrm{DA,G}}_{q,t} + \sum_{\omega\in\Omega} \tilde{\lambda}^{\mathrm{G}}_{t,\omega} \; v^{\mathrm{RT,G}}_{q,t} \right) \right. \tag{15a}$$

$$\left. \text{subject to } \; v^{\mathrm{DA,G}}_{q,t} + v^{\mathrm{RT,G}}_{q,t} = 0 : \psi_{q,t}, \;\; \forall t, \right\}, \;\; \forall q \in \mathcal{Q}, \tag{15b}$$

where $\Theta^{\mathrm{VBG}} = \{ v^{\mathrm{DA,G}}_{q,t}, v^{\mathrm{RT,G}}_{q,t}, \forall q, t \}$ is the set of primal optimization variables. Objective function (15a) maximizes the expected profit of virtual bidder participating in the day-ahead and real-time natural gas markets and equation (15b) balances the virtual bidders day-ahead and real-time trade.

3.5. Day-Ahead Natural Gas Market

Both the day-ahead dispatch of virtual bidders and gas-fired units are inputs into the natural gas day-ahead market clearing problem. The power dispatch of gas-fired units is translated into a time-varying demand for natural gas by $\sum_{i\in\mathcal{G}} \phi_i \; p^{\mathrm{DA}}_{i,t}, \forall t$. Operating cost of the natural gas system in day-ahead is minimized according to

$$\min_{\Theta^{\mathrm{GD}}} \; \sum_{t\in\mathcal{T}} \Big(\sum_{k\in\mathcal{K}} C^{\mathrm{G}}_k \; g^{\mathrm{DA}}_{k,t} \Big) \tag{16a}$$

$$\text{subject to } \; \sum_{k\in\mathcal{K}} g^{\mathrm{DA}}_{k,t} - \sum_{i\in\mathcal{G}} \phi_i \; p^{\mathrm{DA}}_{i,t} - D^{\mathrm{G}}_t + \sum_{q\in\mathcal{Q}} v^{\mathrm{DA,G}}_{q,t} = 0 : \hat{\lambda}^{\mathrm{G}}_t, \;\; \forall t, \tag{16b}$$

$$0 \le g^{\mathrm{DA}}_{k,t} \le G^{\max}_k : \underline{\mu}^{\mathrm{G}}_{k,t}, \overline{\mu}^{\mathrm{G}}_{k,t}, \;\; \forall k, t, \tag{16c}$$

where $\Theta^{\mathrm{GD}} = \{g^{\mathrm{DA}}_{k,t}, \forall k, t\}$ is the set of primal optimization variables. Objective function (16a) gives the cost of natural gas supply. Equation (16b) represents the day-ahead gas supply balance with inelastic demand including fixed gas demand for power production $\sum_{i\in\mathcal{G}} \phi_i \; p^{\mathrm{DA}}_{i,t}$ and amount of virtual trade $\sum_{q\in\mathcal{Q}} v^{\mathrm{DA,G}}_{q,t}$. Constraint (16c) enforces lower and upper bounds on the gas supply.

The optimization problem for day-ahead gas market clearing can be equivalently formulated as the following equilibrium model with each supplier maximizing their profit and a price-setting agent. Each natural gas supplier or producer maximizes her day-ahead profit with respect to her operational constraints according to

$$\left\{ \max_{\Theta^{\mathrm{GD}}} \; \sum_{t\in\mathcal{T}} \left(\hat{\lambda}^{\mathrm{G}}_t - C^{\mathrm{G}}_k \right) g^{\mathrm{DA}}_{k,t} \tag{17a}$$

$$\text{subject to } (16\mathrm{c}) \Big\} \; \forall k, \tag{17b}$$

with the day-ahead price for natural gas $\hat{\lambda}^{\mathrm{G}}_t$ set by

$$\min_{\hat{\lambda}^{\mathrm{G}}_t} \; \sum_{t\in\mathcal{T}} \hat{\lambda}^{\mathrm{G}}_t \Big(\sum_{k\in\mathcal{K}} g^{\mathrm{DA}}_{k,t} - \sum_{i\in\mathcal{G}} \phi_i \; p^{\mathrm{DA}}_{i,t} - D^{\mathrm{G}}_t + \sum_{q\in\mathcal{Q}} v^{\mathrm{DA,G}}_{q,t} \Big) \tag{18a}$$

The KKT conditions of optimization problem (16) are equivalent to those of equilibrium problem (17)-(18).

3.6. Real-Time Natural Gas Market

The real-time natural gas market is cleared for adjusted fuel consumption by gas-fired units converted to a time-varying demand deviation via $\sum_{i\in\mathcal{G}} \phi_i \; p^{\mathrm{RT}}_{i,t,\omega}, \forall t, \omega$. The day-ahead schedule of the natural gas system as well as real-time electricity adjustments of gas-fired units and dispatch decisions by virtual bidders are treated as fixed parameters in the following formulation:

$$\left\{ \min_{\Theta^{\mathrm{GR}}} \; \pi_\omega \sum_{t\in\mathcal{T}} \Big(\sum_{k\in\mathcal{K}} C^{\mathrm{G}}_k \; g^{\mathrm{RT}}_{k,t,\omega} + C^{\mathrm{sh,G}} \; l^{\mathrm{sh,G}}_{t,\omega} \Big) \tag{19a}$$

$$\text{subject to } \sum_{k\in\mathcal{K}} g^{\mathrm{RT}}_{k,t,\omega} - \sum_{i\in\mathcal{G}} \phi_i \; p^{\mathrm{RT}}_{i,t,\omega} + l^{\mathrm{sh,G}}_{t,\omega} + \sum_{q\in\mathcal{Q}} v^{\mathrm{RT,G}}_{q,t} = 0 : \tilde{\lambda}^{\mathrm{G}}_{t,\omega}, \; \forall t, \tag{19b}$$

$$0 \le \left(g^{\mathrm{DA}}_{k,t} + g^{\mathrm{RT}}_{k,t,\omega} \right) \le G^{\max}_k : \underline{\nu}^{\mathrm{G}}_{k,t,\omega}, \overline{\nu}^{\mathrm{G}}_{k,t,\omega}, \;\; \forall k, t, \tag{19c}$$

$$g^{\mathrm{RT}}_{k,t,\omega} \le G^{\mathrm{adj}}_k : \underline{\nu}^{\mathrm{GR}}_{t,\omega}, \overline{\nu}^{\mathrm{GR}}_{t,\omega}, \;\; \forall k, t, \tag{19d}$$

$$0 \le l^{\mathrm{sh,G}}_{t,\omega} \le D^{\mathrm{G}}_t : \underline{\nu}^{\mathrm{DG}}_{t,\omega}, \overline{\nu}^{\mathrm{DG}}_{t,\omega}, \;\; \forall t, \Big\} \forall \omega \tag{19e}$$

where $\Theta^{\mathrm{GR}} = \{g^{\mathrm{RT}}_{k,t,\omega}, \forall k, t, \omega; l^{\mathrm{sh,G}}_{t,\omega}, \forall t, \omega\}$ is the set of primal optimization variables. The real-time cost of the natural gas system is given in objective function (19a). The probability-weighted cost of natural gas adjustments along with natural gas load shedding is minimized in (19a)under scenarios

ω. Constraint (19b) represents the balance of gas supply adjustments in real-time including fixed amount of virtual trade $\sum_{q\in\mathcal{Q}} v_{q,t}^{\mathrm{RT,G}}$. Constraints (19c), (19d), and (19e) enforce lower and upper bounds on gas supply, gas adjustments and gas load shedding, respectively.

Market-clearing problem (19) is equivalent to the following equilibrium problem (20)-(22). Each gas supplier updates her supply in real-time as

$$\left\{ \max_{\Theta^{\mathrm{GR}}} \ \sum_{t\in\mathcal{T}} \left(\tilde{\lambda}_{t,\omega}^{\mathrm{G}} - \pi_\omega \ C_k^{\mathrm{G}} \right) g_{k,t,\omega}^{\mathrm{RT}} \right. \tag{20a}$$

$$\left. \text{subject to } \ (19c), (19d) \right\} \forall k, \omega, \tag{20b}$$

and cost incurred by gas demand curtailment is minimized according to

$$\left\{ \min_{\Theta^{\mathrm{GR}}} \ \sum_{t\in\mathcal{T}} \left(\pi_\omega \ C^{\mathrm{sh,G}} - \tilde{\lambda}_{t,\omega}^{\mathrm{G}} \right) l_{t,\omega}^{\mathrm{sh,G}} \right. \tag{21a}$$

$$\left. \text{subject to } \ (19e) \right\} \forall \omega. \tag{21b}$$

The real-time natural gas price is determined for each scenario ω as

$$\left\{ \min_{\tilde{\lambda}_{t,\omega}^{\mathrm{G}}} \ \sum_{t\in\mathcal{T}} \tilde{\lambda}_{t,\omega}^{\mathrm{G}} \left(\sum_{k\in\mathcal{K}} g_{k,t,\omega}^{\mathrm{RT}} - \sum_{i\in\mathcal{G}} \phi_i \ p_{i,t,\omega}^{\mathrm{RT}} + l_{t,\omega}^{\mathrm{sh,G}} + \sum_{q\in\mathcal{Q}} v_{q,t}^{\mathrm{RT,G}} \right) \right\} \forall \omega. \tag{22a}$$

3.7. Self-Scheduling Gas-Fired Generators

For improving the sectoral coordination, we allow natural gas-fired units to self-schedule outside the markets for optimally allocating their flexibility in the power and natural gas markets. Each gas-fired unit maximizes its expected profit given a perfect anticipation of the distribution of both electricity and natural gas real-time market prices.

3.7.1. Self-scheduling slow-starting gas-fired unit The profit maximization problem of each self-scheduling gas-fired unit $\mathcal{G}\cap\mathcal{S}$ participating in the electricity and natural gas market is given below:

$$\left\{ \max_{\Theta^{\mathrm{SSS}}} \ \sum_{t\in\mathcal{T}} \left[p_{i,t}^{\mathrm{DA}} \left(\hat{\lambda}_t^{\mathrm{E}} - \phi_i \ \hat{\lambda}_t^{\mathrm{G}} \right) - c_{i,t}^{\mathrm{DA}} + \sum_{\omega\in\Omega} p_{i,t,\omega}^{\mathrm{RT}} \left(\tilde{\lambda}_{t,\omega}^{\mathrm{E}} - \phi_i \ \tilde{\lambda}_{t,\omega}^{\mathrm{G}} \right) \right] \right. \tag{23a}$$

$$\text{subject to} (2d) - (2j) \tag{23b}$$

$$\left. (7e) - (7g) \forall \omega \right\} \ \forall i \in (\mathcal{G}\cap\mathcal{S}), \tag{23c}$$

where $\Theta^{\mathrm{SSS}} = \{p_{i,t}^{\mathrm{DA}}, u_{i,t}^{\mathrm{DA}}, c_{i,t}^{\mathrm{DA}}, \forall i \in (\mathcal{G}\cap\mathcal{S}), t; p_{i,t,\omega}^{\mathrm{RT}}, \forall i \in (\mathcal{G}\cap\mathcal{S}), t, \omega\}$ is the set of primal optimization variables. Objective function (23a) maximizes the expected profit of self-scheduling gas-fired generators and simultaneously considering the day-ahead (2d)-(2j) and real-time (7e)-(7g) constraints

for all scenarios $\omega \in \Omega$. Note that the self-scheduler's dispatch decisions $p_{i,t}^{\mathrm{DA}}, u_{i,t}^{\mathrm{DA}}$, $p_{i,t,\omega}^{\mathrm{RT}}$ are fixed input in the market-clearing problems (2), (7), (16), and (19).

3.7.2. Self-scheduling fast-starting gas-fired unit The profit maximization problem of each fast-start self-scheduling gas-fired unit $\mathcal{G} \cap \mathcal{F}$ participating in the electricity and natural gas market is given below:

$$\left\{ \max_{\Theta^{\mathrm{SSF}}} \sum_{t \in \mathcal{T}} \left[p_{i,t}^{\mathrm{DA}} \left(\hat{\lambda}_t^{\mathrm{E}} - \phi_i \, \hat{\lambda}_t^{\mathrm{G}} \right) - c_{i,t}^{\mathrm{DA}} + \sum_{\omega \in \Omega} p_{i,t,\omega}^{\mathrm{RT}} \left(\tilde{\lambda}_{t,\omega}^{\mathrm{E}} - \phi_i \, \tilde{\lambda}_{t,\omega}^{\mathrm{G}} \right) - \pi_\omega \, c_{i,t,\omega}^{\mathrm{RT}} \right] \right. \tag{24a}$$

$$\text{subject to } (2\mathrm{d}) - (2\mathrm{j}) \tag{24b}$$

$$\left. (7\mathrm{h}) - (7\mathrm{n}) \forall \omega \right\} \; \forall i \in (\mathcal{G} \cap \mathcal{F}), \tag{24c}$$

where $\Theta^{\mathrm{SSF}} = \{p_{i,t}^{\mathrm{DA}}, u_{i,t}^{\mathrm{DA}}, c_{i,t}^{\mathrm{DA}}, \forall i \in (\mathcal{G} \cap \mathcal{F}), t; p_{i,t,\omega}^{\mathrm{RT}}, u_{i,t,\omega}^{\mathrm{RT}}, c_{i,t,\omega}^{\mathrm{RT}}, \forall i \in (\mathcal{G} \cap \mathcal{F}), t, \omega\}$ is the set of primal optimization variables. Objective function (24a) maximizes the expected profit of self-scheduling gas-fired generators and simultaneously considering the day-ahead (2d)-(2j) and real-time (7h)-(7n) constraints for all scenarios $\omega \in \Omega$.

3.8. Ideal Benchmark: Stochastic Integrated Electricity and Natural Gas Market

The stochastic and fully-coupled dispatch model simulates the integrated power and natural system by jointly modeling the day-ahead and real-time stages. The problem is formulated as a two-stage stochastic program aiming to minimize the total expected cost and writes as follows,

$$\begin{aligned} \min_{\Theta^{\mathrm{SC}}} \sum_{t \in \mathcal{T}} \Big[& \sum_{i \in \mathcal{C}} \left(C_i^{\mathrm{E}} \, p_{i,t}^{\mathrm{DA}} \right) + \sum_{i \in \mathcal{I}} c_{i,t}^{\mathrm{DA}} + \sum_{k \in \mathcal{K}} C_k^{\mathrm{G}} \, g_{k,t}^{\mathrm{DA}} + \sum_{\omega \in \Omega} \pi_\omega \\ & \Big(\sum_{i \in \mathcal{C}} C_i^{\mathrm{E}} \, p_{i,t,\omega}^{\mathrm{RT}} + \sum_{i \in \mathcal{F}} c_{i,t}^{\mathrm{RT}} + \sum_{k \in \mathcal{K}} C_k^{\mathrm{G}} \, g_{k,t,\omega}^{\mathrm{RT}} + C^{\mathrm{sh,E}} \, l_{t,\omega}^{\mathrm{sh,E}} + C^{\mathrm{sh,G}} \, l_{t,\omega}^{\mathrm{sh,G}} \Big) \Big] \end{aligned} \tag{25a}$$

subject to

$$(2\mathrm{d}) - (2\mathrm{g}), \;\; \forall i, \;\; (16\mathrm{c}), (16\mathrm{b}), \tag{25b}$$

$$(7\mathrm{e}) - (7\mathrm{k}), \;\; \forall i, \omega, \;\; (19\mathrm{c}) - (19\mathrm{b}), \;\; \forall \omega, \tag{25c}$$

where $\Theta^{\mathrm{SC}} = \{\Theta^{\mathrm{ED}}, \Theta^{\mathrm{GD}}, \Theta^{\mathrm{ER}}, \Theta^{\mathrm{GR}}\}$ is the set of primal optimization variables. In this model, the temporal coordination of the two trading floors is taken into account by anticipating the real-time constraints (25c) for all scenarios $\omega \in \Omega$.

4. Karush-Kuhn-Tucker Conditions

4.1. Explicit Electricity Virtual Bidder

$$\frac{\partial L}{\partial v_{r,t}^{\mathrm{DA,E}}} = \hat{\lambda}_t^{\mathrm{E}} - \rho_{r,t} = 0, \;\; \forall r, t, \tag{26a}$$

$$\frac{\partial L}{\partial v_{r,t}^{\mathrm{RT,E}}} = \sum_{\omega \in \Omega} \tilde{\lambda}_{t,\omega}^{\mathrm{E}} - \rho_{r,t} = 0, \;\; \forall r, t, \tag{26b}$$

$$v_{r,t}^{\mathrm{DA,E}} + v_{r,t}^{\mathrm{RT,E}} = 0 : \rho_{r,t}, \;\; \forall r, t. \tag{26c}$$

4.2. Day-Ahead Electricity Market

$$\frac{\partial L}{\partial p_{i,t}^{\mathrm{DA}}} = C_i^{\mathrm{E}} - \hat{\lambda}_t^{\mathrm{E}} + \overline{\mu}_{i,t}^{\mathrm{P}} - \underline{\mu}_{i,t}^{\mathrm{P}} + \overline{\mu}_{i,t}^{\mathrm{R}} - \overline{\mu}_{i,(t+1)}^{\mathrm{R}} - \underline{\mu}_{i,t}^{\mathrm{R}} + \underline{\mu}_{i,(t+1)}^{\mathrm{R}} = 0, \ \ \forall i \in \mathcal{C} \setminus \mathcal{SS}, t < |\mathcal{T}|, \tag{27a}$$

$$\frac{\partial L}{\partial p_{i,t}^{\mathrm{DA}}} = C_i^{\mathrm{E}} - \hat{\lambda}_t^{\mathrm{E}} + \overline{\mu}_{i,t}^{\mathrm{P}} - \underline{\mu}_{i,t}^{\mathrm{P}} + \overline{\mu}_{i,t}^{\mathrm{R}} - \underline{\mu}_{i,t}^{\mathrm{R}} = 0, \ \ \forall i \in \mathcal{C} \setminus \mathcal{SS}, t = |\mathcal{T}|, \tag{27b}$$

$$\frac{\partial L}{\partial p_{i,t}^{\mathrm{DA}}} = \hat{\lambda}_t^{\mathrm{G}} \phi_i - \hat{\lambda}_t^{\mathrm{E}} + \overline{\mu}_{i,t}^{\mathrm{P}} - \underline{\mu}_{i,t}^{\mathrm{P}} + \overline{\mu}_{i,t}^{\mathrm{R}} - \overline{\mu}_{i,(t+1)}^{\mathrm{R}} - \underline{\mu}_{i,t}^{\mathrm{R}} + \underline{\mu}_{i,(t+1)}^{\mathrm{R}} = 0, \ \ \forall i \in \mathcal{G} \setminus \mathcal{SS}, t < |\mathcal{T}|, \tag{27c}$$

$$\frac{\partial L}{\partial p_{i,t}^{\mathrm{DA}}} = \hat{\lambda}_t^{\mathrm{G}} \phi_i - \hat{\lambda}_t^{\mathrm{E}} + \overline{\mu}_{i,t}^{\mathrm{P}} - \underline{\mu}_{i,t}^{\mathrm{P}} + \overline{\mu}_{i,t}^{\mathrm{R}} - \underline{\mu}_{i,t}^{\mathrm{R}} = 0, \ \ \forall i \in \mathcal{G} \setminus \mathcal{SS}, t = |\mathcal{T}|, \tag{27d}$$

$$\frac{\partial L}{\partial u_{i,t}^{\mathrm{DA}}} = -P_i^{\max} \overline{\mu}_{i,t}^{\mathrm{P}} + P_i^{\min} \underline{\mu}_{i,t}^{\mathrm{P}} - R_i \overline{\mu}_{i,t}^{\mathrm{R}} - R_i \underline{\mu}_{i,(t+1)}^{\mathrm{R}} + C_i^{\mathrm{SU}} (\overline{\mu}_{i,t}^{\mathrm{SU}} - \overline{\mu}_{i,(t+1)}^{\mathrm{SU}}) + \overline{\mu}_{i,t}^{\mathrm{B}} - \underline{\mu}_{i,t}^{\mathrm{B}} = 0,$$
$$\forall i \in \mathcal{I} \setminus \mathcal{SS}, t < |\mathcal{T}|, \tag{27e}$$

$$\frac{\partial L}{\partial u_{i,t}^{\mathrm{DA}}} = -P_i^{\max} \overline{\mu}_{i,t}^{\mathrm{P}} + P_i^{\min} \underline{\mu}_{i,t}^{\mathrm{P}} - R_i \overline{\mu}_{i,t}^{\mathrm{R}} + C_i^{\mathrm{SU}} \overline{\mu}_{i,t}^{\mathrm{SU}} + \overline{\mu}_{i,t}^{\mathrm{B}} - \underline{\mu}_{i,t}^{\mathrm{B}} = 0, \ \ \forall i \in \mathcal{I} \setminus \mathcal{SS}, t = |\mathcal{T}|, \tag{27f}$$

$$\frac{\partial L}{\partial w_{j,t}^{\mathrm{DA}}} = -\hat{\lambda}_t^{\mathrm{E}} \overline{\mu}_{j,t}^{\mathrm{W}} - \underline{\mu}_{j,t}^{\mathrm{W}} = 0, \ \ \forall j, t \tag{27g}$$

$$\frac{\partial L}{\partial c_{i,t}^{\mathrm{DA}}} = 1 - \overline{\mu}_{i,t}^{\mathrm{SU}} - \underline{\mu}_{i,t}^{\mathrm{SU}} = 0, \ \ \forall i \in \mathcal{I} \setminus \mathcal{SS}, t \tag{27h}$$

$$0 \leq (p_{i,t}^{\mathrm{DA}} - u_{i,t}^{\mathrm{DA}} P_i^{\min}) \perp \underline{\mu}_{i,t}^{\mathrm{P}} \geq 0 \ \ \forall i \in \mathcal{I} \setminus \mathcal{SS}, t, \tag{27i}$$

$$0 \leq (u_{i,t}^{\mathrm{DA}} P_i^{\max} - p_{i,t}^{\mathrm{DA}}) \perp \overline{\mu}_{i,t}^{\mathrm{P}} \geq 0 \ \ \forall i \in \mathcal{I} \setminus \mathcal{SS}, t, \tag{27j}$$

$$0 \leq w_{j,t}^{\mathrm{DA}} \perp \underline{\mu}_{j,t}^{\mathrm{W}} \geq 0, \ \ \forall j, t \tag{27k}$$

$$0 \leq (W_{j,t}^{\mathrm{DA}} - w_{j,t}^{\mathrm{DA}}) \perp \overline{\mu}_{j,t}^{\mathrm{W}} \geq 0, \ \ \forall j, t, \tag{27l}$$

$$0 \leq \left[(p_{i,t}^{\mathrm{DA}} - p_{i,(t-1)}^{\mathrm{DA}}) + u_{i,(t-1)}^{\mathrm{DA}} R_i \right] \perp \underline{\mu}_{i,t}^{\mathrm{R}} \geq 0, \ \ \forall i \in \mathcal{I} \setminus \mathcal{SS}, t > 1, \tag{27m}$$

$$0 \leq \left[u_{i,t}^{\mathrm{DA}} R_i - (p_{i,t}^{\mathrm{DA}} - p_{i,(t-1)}^{\mathrm{DA}}) \right] \perp \overline{\mu}_{i,t}^{\mathrm{R}} \geq 0, \ \ \forall i \in \mathcal{I} \setminus \mathcal{SS}, t > 1, \tag{27n}$$

$$0 \leq \left[(p_{i,t}^{\mathrm{DA}} - P_i^{\mathrm{ini}}) + U_i^{\mathrm{ini}} R_i \right] \perp \underline{\mu}_{i,t}^{\mathrm{R}} \geq 0, \ \ \forall i \in \mathcal{I} \setminus \mathcal{SS}, t = 1, \tag{27o}$$

$$0 \leq \left[u_{i,t}^{\mathrm{DA}} R_i - (p_{i,t}^{\mathrm{DA}} - P_i^{\mathrm{ini}}) \right] \perp \overline{\mu}_{i,t}^{\mathrm{R}} \geq 0, \ \ \forall i \in \mathcal{I} \setminus \mathcal{SS}, t = 1, \tag{27p}$$

$$0 \leq \left[c_{i,t}^{\mathrm{DA}} - C_i^{\mathrm{SU}} (u_{i,t}^{\mathrm{DA}} - u_{i,(t-1)}^{\mathrm{DA}}) \right] \perp \overline{\mu}_{i,t}^{\mathrm{SU}} \geq 0, \ \ \forall i \in \mathcal{I} \setminus \mathcal{SS}, t > 1, \tag{27q}$$

$$0 \leq \left[c_{i,t}^{\mathrm{DA}} - C_i^{\mathrm{SU}} (u_{i,t}^{\mathrm{DA}} - U_i^{\mathrm{ini}}) \right] \perp \overline{\mu}_{i,t}^{\mathrm{SU}} \geq 0, \ \ \forall i \in \mathcal{I} \setminus \mathcal{SS}, t = 1, \tag{27r}$$

$$0 \leq c_{i,t}^{\mathrm{DA}} \perp \underline{\mu}_{i,t}^{\mathrm{SU}} \geq 0, \ \ \forall i \in \mathcal{I} \setminus \mathcal{SS}, t, \tag{27s}$$

$$0 \leq u_{i,t}^{\mathrm{DA}} \perp \underline{\mu}_{i,t}^{\mathrm{B}} \geq 0, \ \ \forall i \in \mathcal{I} \setminus \mathcal{SS}, t, \tag{27t}$$

$$0 \leq (1 - u_{i,t}^{\mathrm{DA}}) \perp \overline{\mu}_{i,t}^{\mathrm{B}} \geq 0, \ \ \forall i \in \mathcal{I} \setminus \mathcal{SS}, t, \tag{27u}$$

$$\sum_{i \in \mathcal{I}} p_{i,t}^{\mathrm{DA}} + \sum_{j \in \mathcal{J}} w_{j,t}^{\mathrm{DA}} - D_t^{\mathrm{E}} + \sum_{r \in \mathcal{R}} v_{r,t}^{\mathrm{DA,E}} = 0 : \hat{\lambda}_t^{\mathrm{E}}, \forall t. \tag{27v}$$

$$\tag{27w}$$

4.3. Real-Time Electricity Market

$$\frac{\partial L}{\partial p_{i,t,\omega}^{\mathrm{RT}}} = \pi_\omega C_i^{\mathrm{E}} - \tilde{\lambda}_{t,\omega}^{\mathrm{E}} + \overline{\nu}_{i,t,\omega}^{\mathrm{P}} - \underline{\nu}_{i,t,\omega}^{\mathrm{P}} + \overline{\nu}_{i,t,\omega}^{\mathrm{R}} - \overline{\nu}_{i,(t+1),\omega}^{\mathrm{R}} - \underline{\nu}_{i,t,\omega}^{\mathrm{R}} + \underline{\nu}_{i,(t+1),\omega}^{\mathrm{R}} = 0,$$

$$\forall i \in \mathcal{C} \setminus \mathcal{SS}, t < |\mathcal{T}|, \omega, \tag{28a}$$

$$\frac{\partial L}{\partial p^{\mathrm{RT}}_{i,t,\omega}} = \pi_\omega C^{\mathrm{E}}_i - \tilde{\lambda}^{\mathrm{E}}_{t,\omega} + \overline{\nu}^{\mathrm{P}}_{i,t,\omega} - \underline{\nu}^{\mathrm{P}}_{i,t,\omega} + \overline{\nu}^{\mathrm{R}}_{i,t,\omega} - \underline{\nu}^{\mathrm{R}}_{i,t,\omega} = 0, \;\; \forall i \in \mathcal{C} \setminus \mathcal{SS}, t = |\mathcal{T}|, \omega, \tag{28b}$$

$$\frac{\partial L}{\partial p^{\mathrm{RT}}_{i,t,\omega}} = \tilde{\lambda}^{\mathrm{G}}_{t} \phi_i - \tilde{\lambda}^{\mathrm{E}}_{t,\omega} + \overline{\nu}^{\mathrm{P}}_{i,t,\omega} - \underline{\nu}^{\mathrm{P}}_{i,t,\omega} + \overline{\nu}^{\mathrm{R}}_{i,t,\omega} - \overline{\nu}^{\mathrm{R}}_{i,(t+1),\omega} - \underline{\nu}^{\mathrm{R}}_{i,t,\omega} + \underline{\nu}^{\mathrm{R}}_{i,(t+1),\omega} = 0,$$
$$\forall i \in \mathcal{G} \setminus \mathcal{SS}, t < |\mathcal{T}|, \omega, \tag{28c}$$

$$\frac{\partial L}{\partial p^{\mathrm{RT}}_{i,t,\omega}} = \tilde{\lambda}^{\mathrm{G}}_{t} \phi_i - \tilde{\lambda}^{\mathrm{E}}_{t,\omega} + \overline{\nu}^{\mathrm{P}}_{i,t,\omega} - \underline{\nu}^{\mathrm{P}}_{i,t,\omega} + \overline{\nu}^{\mathrm{R}}_{i,t,\omega} - \underline{\nu}^{\mathrm{R}}_{i,t,\omega} = 0, \;\; \forall i \in \mathcal{G} \setminus \mathcal{SS}, t = |\mathcal{T}|, \omega, \tag{28d}$$

$$\frac{\partial L}{\partial w^{\mathrm{RT}}_{j,t,\omega}} = -\tilde{\lambda}^{\mathrm{E}}_{t,\omega} \overline{\nu}^{\mathrm{W}}_{j,t,\omega} - \underline{\nu}^{\mathrm{W}}_{j,t,\omega} = 0, \;\; \forall j, t, \omega, \tag{28e}$$

$$\frac{\partial L}{\partial l^{\mathrm{sh,E}}_{t,\omega}} = \pi_\omega \; C^{\mathrm{sh,E}} - \tilde{\lambda}^{\mathrm{E}}_{t,\omega} + \overline{\nu}^{\mathrm{DE}}_{t,\omega} - \underline{\nu}^{\mathrm{DE}}_{t,\omega} = 0, \;\; \forall t, \omega, \tag{28f}$$

$$\frac{\partial L}{\partial u^{\mathrm{RT}}_{i,t,\omega}} = -P^{\max}_i \overline{\nu}^{\mathrm{P}}_{i,t,\omega} + P^{\min}_i \underline{\nu}^{\mathrm{P}}_{i,t,\omega} - R_i \overline{\nu}^{\mathrm{R}}_{i,t,\omega} - R_i \underline{\nu}^{\mathrm{R}}_{i,(t+1),\omega} + C^{\mathrm{SU}}_i (\overline{\nu}^{\mathrm{SU}}_{i,t,\omega} - \overline{\nu}^{\mathrm{SU}}_{i,(t+1),\omega})$$
$$+ \overline{\nu}^{\mathrm{B}}_{i,t,\omega} - \underline{\nu}^{\mathrm{B}}_{i,t,\omega} = 0, \;\; \forall i \in \mathcal{F}, t < \mathcal{T}, \omega, \tag{28g}$$

$$\frac{\partial L}{\partial u^{\mathrm{RT}}_{i,t,\omega}} = -P^{\max}_i \overline{\nu}^{\mathrm{P}}_{i,t,\omega} + P^{\min}_i \underline{\nu}^{\mathrm{P}}_{i,t,\omega} - R_i \overline{\nu}^{\mathrm{R}}_{i,t,\omega} + C^{\mathrm{SU}}_i \overline{\nu}^{\mathrm{SU}}_{i,t,\omega} + \overline{\nu}^{\mathrm{B}}_{i,t,\omega} - \underline{\nu}^{\mathrm{B}}_{i,t,\omega} = 0, \;\; \forall i \in \mathcal{F}, t = |\mathcal{T}|, \omega, \tag{28h}$$

$$\frac{\partial L}{\partial c^{\mathrm{RT}}_{i,t,\omega}} = \pi_\omega - \overline{\nu}^{\mathrm{SU}}_{i,t,\omega} - \underline{\nu}^{\mathrm{SU}}_{i,t,\omega} = 0, \;\; \forall i \in \mathcal{F}, t, \omega, \tag{28i}$$

$$0 \leq \left[(p^{\mathrm{DA}}_{i,t} + p^{\mathrm{RT}}_{i,t,\omega}) - u^{\mathrm{DA}}_{i,t} P^{\min}_i \right] \perp \underline{\nu}^{\mathrm{P}}_{i,t,\omega} \geq 0, \;\; \forall i \in \mathcal{S}, t, \omega, \tag{28j}$$

$$0 \leq \left[u^{\mathrm{DA}}_{i,t} P^{\max}_i - (p^{\mathrm{DA}}_{i,t} + p^{\mathrm{RT}}_{i,t,\omega}) \right] \perp \overline{\nu}^{\mathrm{P}}_{i,t,\omega} \geq 0, \;\; \forall i \in \mathcal{S}, t, \omega, \tag{28k}$$

$$0 \leq \left[(p^{\mathrm{DA}}_{i,t} + p^{\mathrm{RT}}_{i,t,\omega}) - (u^{\mathrm{DA}}_{i,t} + u^{\mathrm{RT}}_{i,t,\omega}) P^{\min}_i \right] \perp \underline{\nu}^{\mathrm{P}}_{i,t,\omega} \geq 0, \forall i \in \mathcal{F}, t, \omega, \tag{28l}$$

$$0 \leq \left[(u^{\mathrm{DA}}_{i,t} + u^{\mathrm{RT}}_{i,t,\omega}) P^{\max}_i - (p^{\mathrm{DA}}_{i,t} + p^{\mathrm{RT}}_{i,t,\omega}) \right] \perp \overline{\nu}^{\mathrm{P}}_{i,t,\omega} \geq 0, \forall i \in \mathcal{F}, t, \omega, \tag{28m}$$

$$0 \leq (w^{\mathrm{DA}}_{j,t} + w^{\mathrm{RT}}_{j,t,\omega}) \perp \underline{\nu}^{\mathrm{W}}_{j,t,\omega} \geq 0, \;\; \forall j, t, \omega, \tag{28n}$$

$$0 \leq \left[W_{j,t,\omega} - (w^{\mathrm{DA}}_{j,t} + w^{\mathrm{RT}}_{j,t,\omega}) \right] \perp \overline{\nu}^{\mathrm{W}}_{j,t,\omega} \geq 0, \;\; \forall j, t, \omega, \tag{28o}$$

$$0 \leq l^{\mathrm{sh,E}}_{t,\omega} \perp \underline{\nu}^{\mathrm{DE}}_{t,\omega} \geq 0, \;\; \forall t, \omega, \tag{28p}$$

$$0 \leq D^{\mathrm{E}}_t - l^{\mathrm{sh,E}}_{t,\omega} \perp \overline{\nu}^{\mathrm{DE}}_{t,\omega} \geq 0, \;\; \forall t, \omega, \tag{28q}$$

$$0 \leq \left[(p^{\mathrm{DA}}_{i,t} + p^{\mathrm{RT}}_{i,t,\omega} - p^{\mathrm{DA}}_{i,(t-1)} - p^{\mathrm{RT}}_{i,(t-1),\omega}) + u^{\mathrm{DA}}_{i,(t-1)} R_i \right] \perp \underline{\nu}^{\mathrm{R}}_{i,t,\omega} \geq 0, \;\; \forall i \in \mathcal{S}, t > 1, \omega, \tag{28r}$$

$$0 \leq \left[u^{\mathrm{DA}}_{i,t} R_i - (p^{\mathrm{DA}}_{i,t} + p^{\mathrm{RT}}_{i,t,\omega} - p^{\mathrm{DA}}_{i,(t-1)} - p^{\mathrm{RT}}_{i,(t-1),\omega}) \right] \perp \overline{\nu}^{\mathrm{R}}_{i,t,\omega} \geq 0, \forall i \in \mathcal{S}, t > 1, \omega, \tag{28s}$$

$$0 \leq \left[(p^{\mathrm{DA}}_{i,t} + p^{\mathrm{RT}}_{i,t,\omega} - P^{\mathrm{ini}}_i) + U^{\mathrm{ini}}_i R_i \right] \perp \underline{\nu}^{\mathrm{R}}_{i,t,\omega} \geq 0, \forall i \in \mathcal{S}, t{=}1, \omega, \tag{28t}$$

$$0 \leq \left[u^{\mathrm{DA}}_{i,t} R_i - (p^{\mathrm{DA}}_{i,t} + p^{\mathrm{RT}}_{i,t,\omega} - P^{\mathrm{ini}}_i) \right] \perp \overline{\nu}^{\mathrm{R}}_{i,t,\omega} \geq 0, \forall i \in \mathcal{S}, t{=}1, \omega, \tag{28u}$$

$$0 \leq \left[(p^{\mathrm{DA}}_{i,t} + p^{\mathrm{RT}}_{i,t,\omega} - p^{\mathrm{DA}}_{i,(t-1)} - p^{\mathrm{RT}}_{i,(t-1),\omega}) + (u^{\mathrm{DA}}_{i,(t-1)} + u^{\mathrm{RT}}_{i,(t-1)}) R_i \right] \perp \underline{\nu}^{\mathrm{R}}_{i,t,\omega} \geq 0, \;\; \forall i \in \mathcal{F}, t > 1, \omega, \tag{28v}$$

$$0 \leq \left[(u^{\mathrm{DA}}_{i,t} + u^{\mathrm{RT}}_{i,t}) R_i - (p^{\mathrm{DA}}_{i,t} + p^{\mathrm{RT}}_{i,t,\omega} - p^{\mathrm{DA}}_{i,(t-1)} - p^{\mathrm{RT}}_{i,(t-1),\omega}) \right] \perp \overline{\nu}^{\mathrm{R}}_{i,t,\omega} \geq 0, \;\; \forall i \in \mathcal{F}, t > 1, \omega, \tag{28w}$$

$$0 \leq \left[p^{\mathrm{DA}}_{i,t} + p^{\mathrm{RT}}_{i,t,\omega} - P^{\mathrm{ini}}_i + U^{\mathrm{ini}}_i R_i \right] \perp \underline{\nu}^{\mathrm{R}}_{i,t,\omega} \geq 0, \forall i \in \mathcal{F}, t{=}1, \omega, \tag{28x}$$

$$0 \leq \left[(u^{\mathrm{DA}}_{i,t} + u^{\mathrm{RT}}_{i,t}) R_i - (p^{\mathrm{DA}}_{i,t} + p^{\mathrm{RT}}_{i,t,\omega} - P^{\mathrm{ini}}_i) \right] \perp \overline{\nu}^{\mathrm{R}}_{i,t,\omega} \geq 0, \forall i \in \mathcal{F}, t{=}1, \omega, \tag{28y}$$

$$0 \leq \left[(c^{\mathrm{DA}}_{i,t} + c^{\mathrm{RT}}_{i,t,\omega}) - C^{\mathrm{SU}}_{i}(u^{\mathrm{DA}}_{i,t} + u^{\mathrm{RT}}_{i,t,\omega} - u^{\mathrm{DA}}_{i,(t-1)} - u^{\mathrm{RT}}_{i,(t-1),\omega})\right] \perp \overline{\nu}^{\mathrm{SU}}_{i,t,\omega} \geq 0, \ \ \forall i \in \mathcal{F}, t > 1, \omega, \tag{28z}$$

$$0 \leq \left[(c^{\mathrm{DA}}_{i,t} + c^{\mathrm{RT}}_{i,t,\omega}) - C^{\mathrm{SU}}_{i}(u^{\mathrm{DA}}_{i,t} + u^{\mathrm{RT}}_{i,t,\omega} - U^{\mathrm{ini}}_{i})\right] \perp \overline{\nu}^{\mathrm{SU}}_{i,t,\omega} \geq 0, \ \ \forall i \in \mathcal{F}, t{=}1, \omega, \tag{28aa}$$

$$0 \leq \left(c^{\mathrm{DA}}_{i,t} + c^{\mathrm{RT}}_{i,t,\omega}\right) \perp \underline{\nu}^{\mathrm{SU}}_{i,t,\omega} \geq 0, \ \ \forall i \in \mathcal{F}, t, \omega, \tag{28ab}$$

$$0 \leq \left(u^{\mathrm{DA}}_{i,t} + u^{\mathrm{RT}}_{i,t,\omega}\right) \perp \underline{\nu}^{\mathrm{B}}_{i,t,\omega} \geq 0, \ \ \forall i \in \mathcal{F}, t, \omega, \tag{28ac}$$

$$0 \leq \left[1 - (u^{\mathrm{DA}}_{i,t} + u^{\mathrm{RT}}_{i,t,\omega})\right] \perp \overline{\nu}^{\mathrm{B}}_{i,t,\omega} \geq 0, \ \ \forall i \in \mathcal{F}, t, \omega, \tag{28ad}$$

$$\sum_{i \in \mathcal{I}} p^{\mathrm{RT}}_{i,t,\omega} + l^{\mathrm{sh,E}}_{t,\omega} + \sum_{r \in \mathcal{R}} v^{\mathrm{RT,E}}_{r,t} + \sum_{j \in \mathcal{J}} w^{\mathrm{RT}}_{j,t,\omega} = 0 : \tilde{\lambda}^{\mathrm{E}}_{t,\omega}, \forall t. \tag{28ae}$$

4.4. Explicit Natural Gas Virtual Bidder

$$\frac{\partial L}{\partial v^{\mathrm{DA,G}}_{q,t}} = \hat{\lambda}^{\mathrm{G}}_{t} - \psi_{q,t} = 0, \ \ \forall q, t, \tag{29a}$$

$$\frac{\partial L}{\partial v^{\mathrm{RT,G}}_{q,t}} = \sum_{\omega \in \Omega} \tilde{\lambda}^{\mathrm{G}}_{t,\omega} - \psi_{q,t} = 0, \ \ \forall q, t, \tag{29b}$$

$$v^{\mathrm{DA,G}}_{q,t} + v^{\mathrm{RT,G}}_{q,t} = 0 : \psi_{q,t}, \ \ \forall q, t. \tag{29c}$$

4.5. Day-Ahead Natural Gas Market

$$\frac{\partial L}{\partial g^{\mathrm{DA}}_{k,t}} = C^{\mathrm{G}}_{k} - \hat{\lambda}^{\mathrm{G}}_{t} + \overline{\mu}^{\mathrm{G}}_{k,t} - \underline{\mu}^{\mathrm{G}}_{k,t} = 0 \ \ \forall k, t, \tag{30a}$$

$$0 \leq g^{\mathrm{DA}}_{k,t} \perp \underline{\mu}^{\mathrm{G}}_{k,t} \geq 0 \ \ \forall k, t, \tag{30b}$$

$$0 \leq (G^{\max}_{k} - g^{\mathrm{DA}}_{k,t}) \perp \overline{\mu}^{\mathrm{G}}_{k,t} \geq 0 \ \ \forall k, t, \tag{30c}$$

$$\sum_{k \in \mathcal{K}} g^{\mathrm{DA}}_{k,t} - \sum_{i \in \mathcal{G}} \phi_i \ p^{\mathrm{DA}}_{i,t} - D^{\mathrm{G}}_{t} + \sum_{q \in \mathcal{Q}} v^{\mathrm{DA,G}}_{q,t} = 0 : \hat{\lambda}^{\mathrm{G}}_{t}, \ \ \forall t. \tag{30d}$$

4.6. Real-Time Natural Gas Market

$$\frac{\partial L}{\partial g^{\mathrm{RT}}_{k,t,\omega}} = \pi_{\omega} C^{\mathrm{G}}_{k} - \tilde{\lambda}^{\mathrm{G}}_{t,\omega} + \overline{\nu}^{\mathrm{G}}_{k,t,\omega} - \underline{\nu}^{\mathrm{G}}_{k,t,\omega} + \overline{\nu}^{\mathrm{GR}}_{k,t,\omega} = 0, \ \ \forall k, t, \omega, \tag{31a}$$

$$\frac{\partial L}{\partial l^{\mathrm{sh,G}}_{t,\omega}} = \pi_{\omega} C^{\mathrm{sh,G}} - \tilde{\lambda}^{\mathrm{G}}_{t,\omega} + \overline{\nu}^{\mathrm{DG}}_{t,\omega} - \underline{\nu}^{\mathrm{DG}}_{t,\omega} = 0, \ \ \forall t, \omega, \tag{31b}$$

$$0 \leq (g^{\mathrm{DA}}_{k,t} + g^{\mathrm{RT}}_{k,t,\omega}) \perp \underline{\nu}^{\mathrm{G}}_{k,t,\omega} \geq 0, \ \ \forall k, t, \omega, \tag{31c}$$

$$0 \leq \left[G^{\max}_{k} - (g^{\mathrm{DA}}_{k,t} + g^{\mathrm{RT}}_{k,t,\omega})\right] \perp \overline{\nu}^{\mathrm{G}}_{k,t,\omega} \geq 0, \ \ \forall k, t, \omega, \tag{31d}$$

$$0 \leq (G^{\mathrm{adj}}_{k} - g^{\mathrm{RT}}_{k,t,\omega}) \perp \overline{\nu}^{\mathrm{GR}}_{t,\omega} \geq 0, \ \ \forall k, t, \omega, \tag{31e}$$

$$0 \leq l^{\mathrm{sh,G}}_{t,\omega} \perp \underline{\nu}^{\mathrm{DG}}_{t,\omega} \geq 0, \ \ \forall t, \omega, \tag{31f}$$

$$0 \leq (D^{\mathrm{G}}_{t} - l^{\mathrm{sh,G}}_{t,\omega}) \perp \overline{\nu}^{\mathrm{DG}}_{t,\omega} \geq 0, \ \ \forall t, \omega, \tag{31g}$$

$$\sum_{k \in \mathcal{K}} g^{\mathrm{RT}}_{k,t,\omega} - \sum_{i \in \mathcal{G}} \phi_i \ p^{\mathrm{RT}}_{i,t,\omega} + l^{\mathrm{sh,G}}_{t,\omega} + \sum_{q \in \mathcal{Q}} v^{\mathrm{RT,G}}_{q,t} = 0 : \tilde{\lambda}^{\mathrm{G}}_{t,\omega}, \forall t, \omega. \tag{31h}$$

4.7. Self-Scheduling Slow-Starting Gas-Fired Generator

$$\begin{cases} \frac{\partial L}{\partial p_{i,t}^{\mathrm{DA}}} = -\hat{\lambda}_t^{\mathrm{E}} + \hat{\lambda}_t^{\mathrm{G}}\phi_i + \overline{\mu}_{i,t}^{\mathrm{P}} - \underline{\mu}_{i,t}^{\mathrm{P}} + \overline{\mu}_{i,t}^{\mathrm{R}} - \overline{\mu}_{i,(t+1)}^{\mathrm{R}} - \underline{\mu}_{i,t}^{\mathrm{R}} + \underline{\mu}_{i,(t+1)}^{\mathrm{R}} \\ \qquad + \sum_{\omega\in\Omega}\left[\overline{\nu}_{i,t,\omega}^{\mathrm{P}} - \underline{\nu}_{i,t,\omega}^{\mathrm{P}} + \overline{\nu}_{i,t,\omega}^{\mathrm{R}} - \overline{\nu}_{i,(t+1),\omega}^{\mathrm{R}} - \underline{\nu}_{i,t,\omega}^{\mathrm{R}} + \underline{\nu}_{i,(t+1),\omega}^{\mathrm{R}}\right] = 0, \ \ \forall t < |\mathcal{T}|, \end{cases} \tag{32a}$$

$$\frac{\partial L}{\partial p_{i,t}^{\mathrm{DA}}} = -\hat{\lambda}_t^{\mathrm{E}} + \hat{\lambda}_t^{\mathrm{G}}\phi_i + \overline{\mu}_{i,t}^{\mathrm{P}} - \underline{\mu}_{i,t}^{\mathrm{P}} + \overline{\mu}_{i,t}^{\mathrm{R}} - \underline{\mu}_{i,t}^{\mathrm{R}} + \sum_{\omega\in\Omega}\left[\overline{\nu}_{i,t,\omega}^{\mathrm{P}} - \underline{\nu}_{i,t,\omega}^{\mathrm{P}} + \overline{\nu}_{i,t,\omega}^{\mathrm{R}} - \underline{\nu}_{i,t,\omega}^{\mathrm{R}}\right] = 0, t = |\mathcal{T}|, \tag{32b}$$

$$\frac{\partial L}{\partial u_{i,t}^{\mathrm{DA}}} = -P_i^{\max}\overline{\mu}_{i,t}^{\mathrm{P}} + P_i^{\min}\underline{\mu}_{i,t}^{\mathrm{P}} - R_i\overline{\mu}_{i,t}^{\mathrm{R}} - R_i\underline{\mu}_{i,(t+1)}^{\mathrm{R}} + C_i^{\mathrm{SU}}(\overline{\mu}_{i,t}^{\mathrm{SU}} - \overline{\mu}_{i,(t+1)}^{\mathrm{SU}}) + \overline{\mu}_{i,t}^{\mathrm{B}} - \underline{\mu}_{i,t}^{\mathrm{B}}$$
$$+ \sum_{\omega\in\Omega}\left(-P_i^{\max}\overline{\nu}_{i,t,\omega}^{\mathrm{P}} + P_i^{\min}\underline{\nu}_{i,t,\omega}^{\mathrm{P}} - R_i\overline{\nu}_{i,t,\omega}^{\mathrm{R}} - R_i\underline{\nu}_{i,(t+1),\omega}^{\mathrm{R}}\right) = 0, \ \ \forall t < |\mathcal{T}|, \tag{32c}$$

$$\frac{\partial L}{\partial u_{i,t}^{\mathrm{DA}}} = -P_i^{\max}\overline{\mu}_{i,t}^{\mathrm{P}} + P_i^{\min}\underline{\mu}_{i,t}^{\mathrm{P}} - R_i\overline{\mu}_{i,t}^{\mathrm{R}} + C_i^{\mathrm{SU}}\overline{\mu}_{i,t}^{\mathrm{SU}} + \overline{\mu}_{i,t}^{\mathrm{B}} - \underline{\mu}_{i,t}^{\mathrm{B}}$$
$$+ \sum_{\omega\in\Omega}\left(-P_i^{\max}\overline{\nu}_{i,t,\omega}^{\mathrm{P}} + P_i^{\min}\underline{\nu}_{i,t,\omega}^{\mathrm{P}} - R_i\overline{\nu}_{i,t,\omega}^{\mathrm{R}}\right) = 0, \ \ t = |\mathcal{T}|, \tag{32d}$$

$$\frac{\partial L}{\partial c_{i,t}^{\mathrm{DA}}} = 1 - \overline{\mu}_{i,t}^{\mathrm{SU}} - \underline{\mu}_{i,t}^{\mathrm{SU}} = 0, \ \ \forall t, \tag{32e}$$

$$\frac{\partial L}{\partial p_{i,t,\omega}^{\mathrm{RT}}} = -\tilde{\lambda}_{t,\omega}^{\mathrm{E}} + \phi_i\tilde{\lambda}_{t,\omega}^{\mathrm{G}} + \overline{\nu}_{i,t,\omega}^{\mathrm{P}} - \underline{\nu}_{i,t,\omega}^{\mathrm{P}} + \overline{\nu}_{i,t,\omega}^{\mathrm{R}} - \overline{\nu}_{i,(t+1),\omega}^{\mathrm{R}} - \underline{\nu}_{i,t,\omega}^{\mathrm{R}} + \underline{\nu}_{i,(t+1),\omega}^{\mathrm{R}} = 0,$$
$$\forall t < |\mathcal{T}|, \omega, \tag{32f}$$

$$\frac{\partial L}{\partial p_{i,t,\omega}^{\mathrm{RT}}} = -\tilde{\lambda}_{t,\omega}^{\mathrm{E}} + \phi_i\tilde{\lambda}_{t,\omega}^{\mathrm{G}} + \overline{\nu}_{i,t,\omega}^{\mathrm{P}} - \underline{\nu}_{i,t,\omega}^{\mathrm{P}} + \overline{\nu}_{i,t,\omega}^{\mathrm{R}} - \underline{\nu}_{i,t,\omega}^{\mathrm{R}} = 0, \ \ t = |\mathcal{T}|, \omega, \tag{32g}$$

$$0 \le (p_{i,t}^{\mathrm{DA}} - u_{i,t}^{\mathrm{DA}}P_i^{\min}) \perp \underline{\mu}_{i,t}^{\mathrm{P}} \ge 0 \ \ \forall t, \tag{32h}$$

$$0 \le (u_{i,t}^{\mathrm{DA}}P_i^{\max} - p_{i,t}^{\mathrm{DA}}) \perp \overline{\mu}_{i,t}^{\mathrm{P}} \ge 0 \ \ \forall t, \tag{32i}$$

$$0 \le \left[(p_{i,t}^{\mathrm{DA}} - p_{i,(t-1)}^{\mathrm{DA}}) + u_{i,(t-1)}^{\mathrm{DA}}R_i\right] \perp \underline{\mu}_{i,t}^{\mathrm{R}} \ge 0, \ \ \forall t > 1, \tag{32j}$$

$$0 \le \left[u_{i,t}^{\mathrm{DA}}R_i - (p_{i,t}^{\mathrm{DA}} - p_{i,(t-1)}^{\mathrm{DA}})\right] \perp \overline{\mu}_{i,t}^{\mathrm{R}} \ge 0, \ \ \forall t > 1, \tag{32k}$$

$$0 \le \left[(p_{i,t}^{\mathrm{DA}} - P_i^{\mathrm{ini}}) + U_i^{\mathrm{ini}}R_i\right] \perp \underline{\mu}_{i,t}^{\mathrm{R}} \ge 0, \ \ \forall t = 1, \tag{32l}$$

$$0 \le \left[u_{i,t}^{\mathrm{DA}}R_i - (p_{i,t}^{\mathrm{DA}} - P_i^{\mathrm{ini}})\right] \perp \overline{\mu}_{i,t}^{\mathrm{R}} \ge 0, \ \ \forall t = 1, \tag{32m}$$

$$0 \le \left[c_{i,t}^{\mathrm{DA}} - C_i^{\mathrm{SU}}(u_{i,t}^{\mathrm{DA}} - u_{i,(t-1)}^{\mathrm{DA}})\right] \perp \overline{\mu}_{i,t}^{\mathrm{SU}} \ge 0, \ \ \forall t > 1, \tag{32n}$$

$$0 \le \left[c_{i,t}^{\mathrm{DA}} - C_i^{\mathrm{SU}}(u_{i,t}^{\mathrm{DA}} - U_i^{\mathrm{ini}})\right] \perp \overline{\mu}_{i,t}^{\mathrm{SU}} \ge 0, \ \ \forall t = 1, \tag{32o}$$

$$0 \le c_{i,t}^{\mathrm{DA}} \perp \underline{\mu}_{i,t}^{\mathrm{SU}} \ge 0, \ \ \forall t, \tag{32p}$$

$$0 \le u_{i,t}^{\mathrm{DA}} \perp \underline{\mu}_{i,t}^{\mathrm{B}} \ge 0, \ \ \forall t, \tag{32q}$$

$$0 \le (1 - u_{i,t}^{\mathrm{DA}}) \perp \overline{\mu}_{i,t}^{\mathrm{B}} \ge 0, \ \ \forall t, \tag{32r}$$

$$0 \le \left[(p_{i,t}^{\mathrm{DA}} + p_{i,t,\omega}^{\mathrm{RT}}) - u_{i,t}^{\mathrm{DA}}P_i^{\min}\right] \perp \underline{\nu}_{i,t,\omega}^{\mathrm{P}} \ge 0, \ \ \forall t, \omega, \tag{32s}$$

$$0 \le \left[u_{i,t}^{\mathrm{DA}}P_i^{\max} - (p_{i,t}^{\mathrm{DA}} + p_{i,t,\omega}^{\mathrm{RT}})\right] \perp \overline{\nu}_{i,t,\omega}^{\mathrm{P}} \ge 0, \ \ \forall t, \omega, \tag{32t}$$

$$0 \le \left[(p_{i,t}^{\mathrm{DA}} + p_{i,t,\omega}^{\mathrm{RT}} - p_{i,(t-1)}^{\mathrm{DA}} - p_{i,(t-1),\omega}^{\mathrm{RT}}) + u_{i,(t-1)}^{\mathrm{DA}}R_i\right] \perp \underline{\nu}_{i,t,\omega}^{\mathrm{R}} \ge 0, \ \ \forall t > 1, \omega, \tag{32u}$$

$$0 \leq \left[u_{i,t}^{\mathrm{DA}} R_i - (p_{i,t}^{\mathrm{DA}} + p_{i,t,\omega}^{\mathrm{RT}} - p_{i,(t-1)}^{\mathrm{DA}} - p_{i,(t-1),\omega}^{\mathrm{RT}})\right] \perp \overline{\nu}_{i,t,\omega}^{\mathrm{R}} \geq 0, \forall t > 1, \omega, \tag{32v}$$

$$0 \leq \left[(p_{i,t}^{\mathrm{DA}} + p_{i,t,\omega}^{\mathrm{RT}} - P_i^{\mathrm{ini}}) + U_i^{\mathrm{ini}} R_i\right] \perp \underline{\nu}_{i,t,\omega}^{\mathrm{R}} \geq 0, \forall t{=}1, \omega, \tag{32w}$$

$$\left.\begin{aligned} 0 \leq \left[u_{i,t}^{\mathrm{DA}} R_i - (p_{i,t}^{\mathrm{DA}} + p_{i,t,\omega}^{\mathrm{RT}} - P_i^{\mathrm{ini}})\right] \perp \overline{\nu}_{i,t,\omega}^{\mathrm{R}} \geq 0, \forall t{=}1, \omega \end{aligned}\right\} \ \forall i \in (\mathcal{G} \cap \mathcal{SS}) \tag{32x}$$

5. Proof of Proposition 1

The KKT optimality conditions of each self-scheduling gas-fired generator, whose day-ahead dispatch is restricted by operational bounds, enforce

$$\left\{\begin{aligned} &\frac{\partial L}{\partial p_{i,t}^{\mathrm{DA}}} = -\hat{\lambda}_t^{\mathrm{E}} + \hat{\lambda}_t^{\mathrm{G}} \phi_i + \overline{\mu}_{i,t}^{\mathrm{P}} - \underline{\mu}_{i,t}^{\mathrm{P}} + \overline{\mu}_{i,t}^{\mathrm{R}} - \overline{\mu}_{i,(t+1)}^{\mathrm{R}} - \underline{\mu}_{i,t}^{\mathrm{R}} + \underline{\mu}_{i,(t+1)}^{\mathrm{R}} \\ &\quad + \sum_{\omega \in \Omega} \left[\overline{\nu}_{i,t,\omega}^{\mathrm{P}} - \underline{\nu}_{i,t,\omega}^{\mathrm{P}} + \overline{\nu}_{i,t,\omega}^{\mathrm{R}} - \overline{\nu}_{i,(t+1),\omega}^{\mathrm{R}} - \underline{\nu}_{i,t,\omega}^{\mathrm{R}} + \underline{\nu}_{i,(t+1),\omega}^{\mathrm{R}}\right] = 0, \ \ \forall t < T, \end{aligned}\right. \tag{33a}$$

and

$$\left.\begin{aligned} &\frac{\partial L}{\partial p_{i,t,\omega}^{\mathrm{RT}}} = -\pi_\omega \left(\frac{\tilde{\lambda}_{t,\omega}^{\mathrm{E}}}{\pi_\omega} - \phi_i \frac{\tilde{\lambda}_{t,\omega}^{\mathrm{G}}}{\pi_\omega}\right) + \overline{\nu}_{i,t,\omega}^{\mathrm{P}} - \underline{\nu}_{i,t,\omega}^{\mathrm{P}} + \overline{\nu}_{i,t,\omega}^{\mathrm{R}} - \overline{\nu}_{i,(t+1),\omega}^{\mathrm{R}} - \underline{\nu}_{i,t,\omega}^{\mathrm{R}} + \underline{\nu}_{i,(t+1),\omega}^{\mathrm{R}} = 0, \\ &\quad \forall t < T, \omega, \end{aligned}\right\} \ \forall i \in (\mathcal{G} \cap \mathcal{SS}). \tag{33b}$$

The summation of condition (33b) over all scenarios, i.e., $\sum_\omega$(33b), shows that when virtual bidders in electricity and natural gas markets enforce price convergence in expectation, i.e., $\hat{\lambda}_t^{\mathrm{E}} = \sum_\omega \tilde{\lambda}_{t,\omega}^{\mathrm{E}}$ and $\hat{\lambda}_t^{\mathrm{G}} = \sum_\omega \tilde{\lambda}_{t,\omega}^{\mathrm{G}}$, the problem is feasible if only if $\overline{\mu}_{i,t}^{\mathrm{P}} - \underline{\mu}_{i,t}^{\mathrm{P}} + \overline{\mu}_{i,t}^{\mathrm{R}} - \overline{\mu}_{i,(t+1)}^{\mathrm{R}} - \underline{\mu}_{i,t}^{\mathrm{R}} + \underline{\mu}_{i,(t+1)}^{\mathrm{R}} = 0, \ \ \forall i, t$, e.g., for the case when day-ahead operational bounds are non-binding.

6. Proof of Proposition 2

The KKT optimality conditions of the stochastic two-stage optimization problem (25) and those of the equilibrium problem (1), (2), (7), (15), (16), (19), (23), (24) with all gas-fired units as implicit virtual bidders are identical under the conditions that day-ahead operational bounds on $p_{i,t}^{\mathrm{DA}}$, $w_{j,t}^{\mathrm{DA}}$, $c_{i,t}^{\mathrm{DA}}$, $u_{i,t}^{\mathrm{DA}}$, and $g_{k,t}^{\mathrm{DA}}$ are non-binding (e.g., $\overline{\mu}_{i,t}^{\mathrm{P}} - \underline{\mu}_{i,t}^{\mathrm{P}} + \overline{\mu}_{i,t}^{\mathrm{R}} - \overline{\mu}_{i,(t+1)}^{\mathrm{R}} - \underline{\mu}_{i,t}^{\mathrm{R}} + \underline{\mu}_{i,(t+1)}^{\mathrm{R}} = 0, \ \ \forall i, t$ and $\overline{\mu}_{k,t}^{\mathrm{G}} - \underline{\mu}_{k,t}^{\mathrm{G}} = 0, \ \ \forall k, t$) so that day-ahead and real-time prices converge in expectation (i.e., $\hat{\lambda}_t^{\mathrm{E}} = \sum_\omega \tilde{\lambda}_{t,\omega}^{\mathrm{E}}$ and $\hat{\lambda}_t^{\mathrm{G}} = \sum_\omega \tilde{\lambda}_{t,\omega}^{\mathrm{G}}$), see (26)-(32) .

Generator $i \in \mathcal{I}$ in sequential setup:

$$\frac{\partial L}{\partial p_{i,t}^{\mathrm{DA}}} = C_i^{\mathrm{E}} - \hat{\lambda}_t^{\mathrm{E}} + \overline{\mu}_{i,t}^{\mathrm{P}} - \underline{\mu}_{i,t}^{\mathrm{P}} + \overline{\mu}_{i,t}^{\mathrm{R}} - \overline{\mu}_{i,(t+1)}^{\mathrm{R}} - \underline{\mu}_{i,t}^{\mathrm{R}} + \underline{\mu}_{i,(t+1)}^{\mathrm{R}} = 0, \ \ \forall t, \tag{34a}$$

$$\frac{\partial L}{\partial p_{i,t,\omega}^{\mathrm{RT}}} = \pi_\omega C_i^{\mathrm{E}} - \tilde{\lambda}_{t,\omega}^{\mathrm{E}} + \overline{\nu}_{i,t,\omega}^{\mathrm{P}} - \underline{\nu}_{i,t,\omega}^{\mathrm{P}} + \overline{\nu}_{i,t,\omega}^{\mathrm{R}} - \overline{\nu}_{i,(t+1),\omega}^{\mathrm{R}} - \underline{\nu}_{i,t,\omega}^{\mathrm{R}} + \underline{\nu}_{i,(t+1),\omega}^{\mathrm{R}} = 0, \ \ \forall t. \tag{34b}$$

Generator $i \in \mathcal{I}$ in two-stage stochastic setup:

$$\frac{\partial L}{\partial p^{\mathrm{DA}}_{i,t}} = C^{\mathrm{E}}_i - \hat{\lambda}^{\mathrm{E}}_t + \overline{\mu}^{\mathrm{P}}_{i,t} - \underline{\mu}^{\mathrm{P}}_{i,t} + \overline{\mu}^{\mathrm{R}}_{i,t} - \overline{\mu}^{\mathrm{R}}_{i,(t+1)} - \underline{\mu}^{\mathrm{R}}_{i,t} + \underline{\mu}^{\mathrm{R}}_{i,(t+1)} + \sum_{\omega\in\Omega}\left[\overline{\nu}^{\mathrm{P}}_{i,t,\omega} - \underline{\nu}^{\mathrm{P}}_{i,t,\omega} + \overline{\nu}^{\mathrm{R}}_{i,t,\omega} - \overline{\nu}^{\mathrm{R}}_{i,(t+1),\omega} - \underline{\nu}^{\mathrm{R}}_{i,t,\omega} + \underline{\nu}^{\mathrm{R}}_{i,(t+1),\omega}\right] = 0, \ \ \forall t, \tag{34c}$$

$$\frac{\partial L}{\partial p^{\mathrm{RT}}_{i,t,\omega}} = \pi_\omega \ C^{\mathrm{E}}_i - \tilde{\lambda}^{\mathrm{E}}_{t,\omega} + \overline{\nu}^{\mathrm{P}}_{i,t,\omega} - \underline{\nu}^{\mathrm{P}}_{i,t,\omega} + \overline{\nu}^{\mathrm{R}}_{i,t,\omega} - \overline{\nu}^{\mathrm{R}}_{i,(t+1),\omega} - \underline{\nu}^{\mathrm{R}}_{i,t,\omega} + \underline{\nu}^{\mathrm{R}}_{i,(t+1),\omega} = 0, \ \ \forall t,\omega. \tag{34d}$$

Gas supplier $k \in \mathcal{K}$ in sequential setup:

$$\frac{\partial L}{\partial g^{\mathrm{DA}}_{k,t}} = C^{\mathrm{G}}_k - \hat{\lambda}^{\mathrm{G}}_t + \overline{\mu}^{\mathrm{G}}_{k,t} - \underline{\mu}^{\mathrm{G}}_{k,t} = 0 \ \ \forall t, \tag{34e}$$

$$\frac{\partial L}{\partial g^{\mathrm{RT}}_{k,t,\omega}} = \pi_\omega C^{\mathrm{G}}_k - \tilde{\lambda}^{\mathrm{G}}_{t,\omega} + \overline{\nu}^{\mathrm{G}}_{k,t,\omega} - \underline{\nu}^{\mathrm{G}}_{k,t,\omega} + \overline{\nu}^{\mathrm{GR}}_{k,t,\omega} = 0, \ \ \forall t,\omega. \tag{34f}$$

Gas supplier $k \in \mathcal{K}$ in two-stage stochastic setup:

$$\frac{\partial L}{\partial g^{\mathrm{DA}}_{k,t}} = C^{\mathrm{G}}_k - \hat{\lambda}^{\mathrm{G}}_t + \overline{\mu}^{\mathrm{G}}_{k,t} - \underline{\mu}^{\mathrm{G}}_{k,t} + \sum_{\omega\in\Omega}\left[\overline{\nu}^{\mathrm{G}}_{k,t,\omega} - \underline{\nu}^{\mathrm{G}}_{k,t,\omega} + \overline{\nu}^{\mathrm{GR}}_{k,t,\omega}\right] = 0 \ \ \forall t, \tag{34g}$$

$$\frac{\partial L}{\partial g^{\mathrm{RT}}_{k,t,\omega}} = \pi_\omega C^{\mathrm{G}}_k - \tilde{\lambda}^{\mathrm{G}}_{t,\omega} + \overline{\nu}^{\mathrm{G}}_{k,t,\omega} - \underline{\nu}^{\mathrm{G}}_{k,t,\omega} + \overline{\nu}^{\mathrm{GR}}_{k,t,\omega} = 0, \ \ \forall t,\omega. \tag{34h}$$

(34i)

7. Computational Performance

Model	Postsolved residual	Computational time [s]
Seq	-	0.142
Seq+eVB	2.46E-09 & 5.03E-8	13.99 + 0.20
Seq+iVB	0.64	863.97
Seq+VB	3.80E-09	251.7
Ideal	-	0.19

Table 4 Computational performance

Department of Electrical Engineering
Center for Electric Power and Energy (CEE)
Technical University of Denmark
Elektrovej, Building 325
DK-2800 Kgs. Lyngby
Denmark

www.elektro.dtu.dk/cee
Tel: (+45) 45 25 35 00
Fax: (+45) 45 88 61 11
E-mail: cee@elektro.dtu.dk